ÁNALISIS FUNCIONAL DE FOTOPROTEÍNAS EN *FUSARIUM*

FUNCTIONAL ANALYSIS OF PHOTOPROTEINS IN *FUSARIUM*

Marta Castrillo Jiménez

Departamento de Genética

Universidad de Sevilla

MARTA CASTRILLO JIMÉNEZ

RESUMEN DE TESIS DOCTORAL

ANÁLISIS FUNCIONAL DE FOTOPROTEÍNAS EN *FUSARIUM*

FUNCTIONAL ANALYSIS OF PHOTOPROTEINS IN *FUSARIUM*

The ascomycete *Fusarium fujikuroi* stands out for its capacity to produce a wide array of secondary metabolites. These compounds exhibit a large chemical diversity and very different biological properties, ranging from pernicious to beneficial for human or animals health, in some cases with biotechnological applications. For this reason, the regulation of secondary metabolism is currently an active area of research. The group of the University of Sevilla where this Thesis has been carried out focuses its attention on the study of the production of *F. fujikuroi* metabolites, such as carotenoids, gibberellins, bikaverins and fusarins. Their syntheses are controlled by different environmental cues, with light and nitrogen among the most relevant ones. In this Thesis we have analyzed the molecular basis of the regulation by light of carotenoid biosynthesis. Carotenoids are terpenoid pigments that provide colors or exert other biological functions in living beings. As relevant examples, in plants they serve as antenna pigments for photosynthesis, and in animals they are used as signaling and vision molecules. Their role in fungi is under discussion, but in some cases they serve as precursor of other relevant compounds and in others they seem to protect against oxidative stress.

Carotenoid photoinduction is a well-characterized response in many fungi, such as *Neurospora crassa*, *Phycomyces blakesleeanus* or *Mucor circinelloides,* where it is performed at transcriptional level of the biosynthetic genes. As found in these fungi, light produces in *F. fujikuroi* a rapid but transient induction of the expression of the structural genes, in this case *carRA, carB*, and *carT*. Former studies with another *Fusarium* species showed that carotenoid photoinduction is particularly effective with blue light and that the action spectrum of the response suggests the mediation of a photoreceptror with a flavin chromophore. Blue-light responses are coordinated in other fungi by LOV-domain flavin proteins of the WC-1 family. Previous studies in *F. fujikuroi* revealed that the mutants of the *wc-1* orthologous gene *wcoA* conserve the photoinduction of carotenogenesis, thus involving another photoreceptor(s) in this photoresponse.

This Thesis has investigated the biological role of other photoreceptors in the photobiology of this fungus. The genome of *F. fujikuroi* contains several genes coding for blue light

photoreceptors in addition to WcoA. The list includes a small LOV protein (VvdA), a DASH-cryptochrome (CryD), a plant-related cryptochrome (Phr1) and a photolyase (PhlA). This Thesis has been dedicated to the study of the CryD and VvdA photoreceptors in *F. fujikuroi*, and its possible functional relation with the photoreceptor WcoA, formerly studied by the same group.

Regarding the role of CryD, the Thesis shows that the gene is strongly induced by light and that WcoA mediates this induction. Targeted mutation experiments showed that CryD produce similar amounts of carotenoids than the wild type in the light. Unexpectedly, they are affected in the production of other secondary metabolites, such as bikaverins or gibberellins under light and nitrogen starvation. However, no correlation was found with the mRNA levels for the biosynthetic genes, indicating that CryD functions at other regulatory levels. The Δ*cryD* mutants also exhibit developmental alterations, such as production of macroconidia, rarely observed in the wild type strain of *F. fujikuroi*, and defects in the formation of aerial mycelia. Furthermore we have investigated the biochemical properties of CryD, and the results revealed that CryD binds the expected chromophore molecules, FAD and MTHF. Moreover it was found to be a functional photoprotein able to bind nucleic acids and to photorepair UV-induced DNA damages *in vitro*.

In *N. crassa*, carotenoid biosynthesis is negatively regulated by VVD, a photoreceptor that counteracts the activity of the light-induced White Collar complex, a process known as photoadaptation. Consequently, the mutants of the *vvd* gene of this fungus produce more carotenoid under light than the wild type. As found for *cryD*, the expression of the *vvd* orthologous gene of *F. fujikuroi*, *vvdA*, is induced by light through the activity of the WcoA photoreceptor. In contrast to the *N. crassa vvd* mutants, the Δ*vvdA* mutants of *F. fujikuroi* accumulate less carotenoids than the wild type, but the transcription pattern of the carotenoid genes is not affected. These results indicate that in *F. fujikuroi* VvdA does not mediate the photoadapation of carotenogenesis. However our phenotypic studies revealed that VvdA is also involved in development, with noticeable effects of its mutation on conidiation and mycelia organization.

Finally, this Thesis has studied the roles of the investigated photoreceptors in the induction kinetics of carotenoid biosynthesis upon illumination of dark-grown mycelia. We found that the induction of carotenogenesis of wild type *F. fujikuroi* is achieved in two steps, a fast one lasting up to 6 hours, and a slower second one starting after 12 hours. The mutant phenotypes show that the rapid initial activation (1st step) is transcriptionally achieved by the WcoA

photoreceptor, which exhibits a high light sensitivity, while the slower delayed activation (2nd step), possibly pot-transcriptional, is mediated by the CryD photoreceptor, which exhibits a low light sensitivity. Both steps are separated by a pause of several hours. Finally, VvdA plays a modulating role, achieving a negative regulation on WcoA in the first stage and a positive regulation on CryD in the second stage. Further analyses of WcoA revealed that it regulates the synthesis of carotenoids in the dark, as already found for bikaverin biosynthesis, a function achieved at transcription level.

In summary, we have determined that the *F. fujikuroi* photoreceptors CryD and VvdA play coordinated roles with WcoA in the photoregulation of carotenoid biosynthesis, and additionally they play light-dependent regulatory functions in different developmental processes. On the other hand, WcoA plays a central role in the regulation of carotenoid biosynthesis, since it is required for the expression of the structural genes in the dark, and for their photoinduction in the first hours of light; additionally WcoA controls the expression of the photoreceptor genes *cryD* and *vvdA*.

INDICE

INTRODUCCIÓN

1.El organismo

Fusarium fujikuroi es un hongo filamentoso de la clase de los ascomicetos. Como es habitual en las especies del género *Fusarium*, *F. fujikuroi* es un patógeno de plantas, mostrando una alta especificidad por su hospedador *Oryza sativa* (arroz). Las pérdidas que produce en el sector agrícola, especialmente en China como primer productor de arroz mundial, proporcionan especial interés al estudio de esta especie.

1.1. Clasificación

El género *Fusarium* fue definido por Link en 1908, [citado en (Booth C., 1971)] y engloba un conjunto de especies imperfectas o anamorfas (sin ciclo sexual) cuya característica principal es la formación de conidios fusiformes. La nomenclatura de este grupo de especies ha cambiado a lo largo de los años a medida que se ha observado su ciclo sexual, estado perfecto o teleomorfo (Wollenweber and Reinking, 1935) en condiciones de laboratorio. Así, las estirpes de *Fusarium* capaces de desarrollar una fase sexual durante su ciclo de vida y que habían escapado a la nomenclatura tradicional por carecer de estructuras sexuales identificables, se incluyeron en el género *Giberella*. Un ejemplo fue *Fusarium moniliforme* que se denominó a partir de entonces *Giberella Fujikuroi*.

Aunque tiene su origen en una sola especie, estudios sucesivos identificaron en *Giberella Fujikuroi* diferentes grupos de cruzamiento, formados por estirpes haploides y heterotálicas fértiles entre sí, descritos en número creciente a lo largo de los años hasta alcanzar un total de 11 (Tabla 1). Cada grupo de cruzamiento, designado con letras desde la A a la K, constituye una especie diferente, renombrada posteriormente como tal dentro del género *Fusarium* (O'Donnell et al., 1998). Como se observa en la tabla 1, *Fusarium fujikuroi* corresponde al grupo de cruzamiento C. Los individuos de distinto sexo se denominan (+) y (-), que serían el equivalente a los sexos macho y hembra en el reino animal. Dentro de cada grupo de cruzamiento, o para identificar uno nuevo, cada estirpe debe ser fértil actuando tanto de macho como de hembra frente a otra estirpe de esa misma población. Este sistema sexual está basado en un

locus con dos alelos *MAT-1* y *MAT-2*, con secuencias de ADN y proteínas diferentes, y específicas para cada grupo (Steenkamp et al., 2000).

Grupo de cruzamiento	Especie de *Fusarium*	Referencia
A	*verticillioides*	(O'Donnell et al., 1998)
B	*sacchari*	(O'Donnell et al., 1998)
C	*fujikuroi*	(O'Donnell et al., 1998)
D	*proliferatum*	(O'Donnell et al., 1998)
E	*subglutinans*	(O'Donnell et al., 1998)
F	*thapsinum*	(O'Donnell et al., 1998)
G	*nygamai*	(O'Donnell et al., 1998)
H	*circinatum*	(Britz et al., 1999)
I	*konzum*	(Zeller et al., 2003)
J	*gaditjirrii*	(Phan et al., 2004)
K	*xylarioides*	(Lepoint et al., 2005)

Tabla 1. Grupos de cruzamiento del complejo de especies *Giberella fujikuroi* y su equivalencia actual como especie de *Fusarium*.

Cada uno de estos grupos es patógeno preferente de una planta (Kuhlman, 1983; Leslie, 1991; Voigt et al., 1995), como son por ejemplo *F. fujikuroi* del arroz o *F. vertocilliodes* y *F. proliferatum* del maíz. En algunas especies que no se han podido cruzar aún en el laboratorio, como es el caso de *F. oxysporum*, se distinguen como "formas especiales" estirpes o grupos de estirpes con alta especificidad patógenica sobre especies vegetales diferentes. Así, las *formae speciales lycopersici* o *phaseoli* infectan respectivamente plantas de tomate o de judía. La comparación de los genomas de distintas "formas especiales" de *F. oxysporum* indica que éstas constituyen realmente especies diferentes. Las enfermedades producidas por estos hongos reciben genéricamente el nombre de fusariosis, aunque según los efectos que produzca en la planta reciben nombres más específicos y conocidos por los agricultores, como son la roya del trigo, el tizón de la cebada, o la podredumbre del maíz. Las especies del género *Fusarium* pueden infectar esporádicamente a la especie humana, sin consecuencias relevante en individuos sanos pero no así en individuos inmunodeprimidos (Austwick, 1984).

1.2. Ciclo de vida de *Fusarium*

F. fujikuroi se reproduce asexualmente mediante esporas llamadas conidios. Éstas pueden ser de dos tipos: microconidios o macroconidios (Fig.1). Sus nombres hacen referencia a su tamaño, siendo los primeros pequeños, fusiformes y uninucleados, y

los segundos, de mayor tamaño, con forma de media luna, multinucleados y septados (Avalos et al., 1985b; Kuhlman, 1983; Leslie and Summerell, 2006). Cuando las condiciones ambientales son propicias, los conidios germinan formando hifas, estructuras filamentosas que se desarrollan y ramifican para formar una densa red denominada micelio.

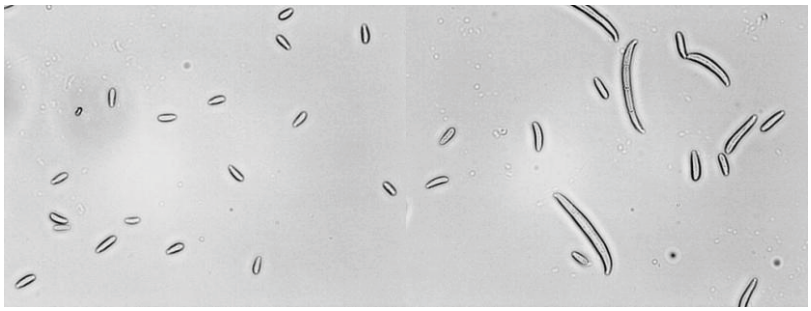

Fig. 1. Imagen al microscopio óptico de conidios de *F. fujikuroi*. A la izquierda se muestran microconidios, A la derecha aparecen algunos macroconidios..

En condiciones de laboratorio, el ciclo sexual se induce sembrando conidios de la estirpe (+), producidos en condiciones desfavorables de cultivo, sobre micelio previamente crecido de la estirpe (-) en un medio adecuado. Es especialmente propicio para este fin un medio cuyo componente principal es un extracto de zanahoria. Tras varias semanas de incubación bajo luz blanca y radiación ultravioleta cercana alternando con oscuridad en fotoperiodos de 12 horas (Klittich and Leslie, 1988; Sidhu, 1983), (Leslie et al., 2005), se desarrollan los peritecios, estructuras globulares y negras que contienen en su interior ascosporas formando tétradas desordenadas. Dada su complejidad este tipo de reproducción, resulta fácil entender que este tipo de reproducción no se observe habitualmente en la naturaleza.

Las estirpes de *Fusarium* presentan también un ciclo de vida infectivo. Como ya se ha mencionado *F. fujikuroi* infecta plantas de arroz (Amoah et al., 1995; Desjardins et al., 2000) produciendo una enfermedad conocida como “bakanae”, que en japonés significa “plántulas locas”. La enfermedad consiste en una hiperelongación de los tallos de la planta, que se vuelven más delgados, frágiles y quebradizos. A su vez, en las hojas aparecen manchas cloróticas, correspondientes a tejido que pierde la capacidad de realizar la fotosíntesis (Amoah et al., 1995; Ou, 10987).

La infección se produce principalmente en primavera. Las esporas, dispersadas por el viento o insectos, pueden encontrarse en las semillas o en el suelo y penetran por pequeños espacios o lesiones presentes en las raíces. El micelio se desarrolla por el interior de la planta, hasta que ésta muere en verano. Finalmente el micelio sale al exterior y esporula, contaminando la superficie del arrozal y las semillas durante la recolección invernal. De este modo las esporas se propagan y pueden contaminar nuevos cultivos sembrados (Ou, 10987). Las etapas se resumen en la Fig. 2.

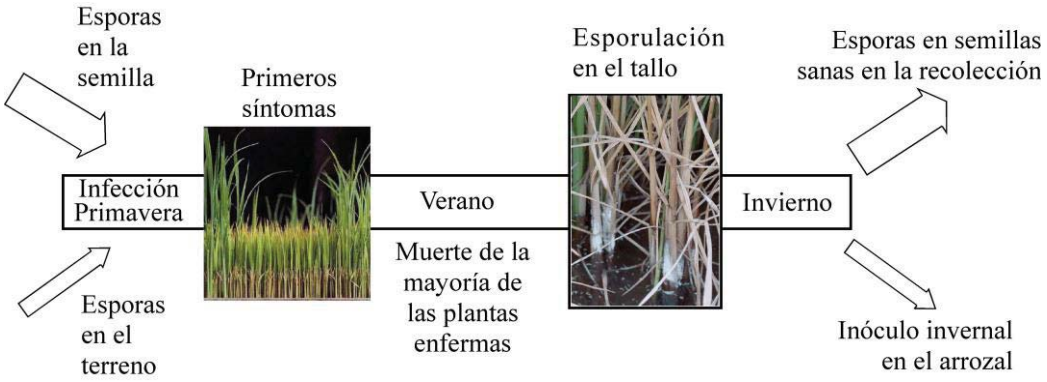

Fig.2. Etapas del ciclo infectivo de *F. fujikuroi* en las plantas de arroz.

1.3. Características para su utilización en el laboratorio

F. fujikuroi presenta varias características que propician su uso como organismo de trabajo en el laboratorio. Junto a sus cortos tiempos de crecimiento, 2-4 días, se disponen de medios sencillos, bien definidos y asequibles económicamente. Sus colonias producen mayoritariamente conidios uninucleados que permiten aislar fácilmente mutaciones recesivas. Por otro lado, presenta altas tasas de mutación frente a agentes químicos o físicos (Koelblin et al., 1990; Puhalla and Spieth, 1983, 1985), favoreciendo la búsqueda de mutantes en mutagénesis.

En la actualidad, la disponibilidad de la secuencia del genoma del organismo objeto de estudio constituye una de las herramientas más necesarias en estudios de biología molecular. En el momento de inicio de esta Tesis no se disponía del genoma de *F.*

fujikuroi, usándose como referencia los genomas publicados de otras especies de *Fusarium* (*F. verticilliodes*, *F. graminearum* y *F. oxysporum*). Por su alto grado de similitud, el análisis comparativo de estos genomas fue una herramienta muy útil para identificar secuencias conservadas en *F. fujikuroi*. Las secuencias de estos genomas, así como las correspondientes herramientas de búsqueda y análisis, están disponibles en el servidor del Broad Institute (www.broadinstitute.org/annotation/genome/fusarium_group/MultiHome.html). En 2010, el grupo de investigación donde se ha realizado esta Tesis obtuvo un borrador del genoma de la estirpe silvestre IMI58289. Aunque altamente fragmentado, este borrador permitió la identificación de secuencias citadas en varias publicaciones (Díaz-Sánchez et al., 2012; Díaz-Sánchez et al., 2011a). Posteriormente otros grupos de investigación llevaron a cabo una secuenciación más completa, disponible ahora en las bases de datos públicas, y realizaron un detallado análisis de la secuencia y del correspondiente proteoma (Wiemann et al., 2013).

2. Metabolismo secundario de hongos filamentosos

Los hongos filamentosos poseen un metabolismo muy activo y complejo que produce moléculas de distinta naturaleza, en muchos casos con impacto sobre la vida humana. Muchos de estos compuestos no son esenciales para la vida del hongo (metabolitos secundarios), y su producción puede estar restringida a algunas etapas de crecimiento, estructuras de desarrollo, o incluso condiciones ambientales (Calvo et al., 2002). En algunos casos se ha determinado el papel que desempeñan, con ejemplos como compuestos defensivos (Rohlfs et al., 2007; Rohlfs and Churchill, 2011) o moléculas señalizadoras (Bohnert et al., 2004; Dufour and Rao, 2011; Rodrigues et al., 2011), pero en otros la función es aún desconocida. Algunas de estas sustancias tienen propiedades beneficiosas y tienen aplicaciones en la industria médica y farmacológica, mientras que otras son tóxicas. Tanto por sus posibles aplicaciones como por sus potenciales efectos perjudiciales, sus rutas metabólicas y sus mecanismos de regulación son objeto de numerosos estudios. En el primer caso, un ejemplos paradigmático es la producción de antibióticos por las estirpes del género Penicillium o Aspergillus {Fleming, 1929 #25; van den Berg, 2011)

2.1. Regulación de rutas biosintéticas

Las rutas metabólicas de estos compuestos son llevadas a cabo por conjuntos de enzimas cuyos genes se encuentran con frecuencia agrupados en el genoma formando *clusters* (Keller and Hohn, 1997). Estos agrupamientos contienen genes para proteínas con distintas funciones. Además de la(s) enzima(s) principal(es) para la síntesis del metabolito, suelen contener enzimas modificadoras, proteínas transportadoras y uno o más factores de transcripción que regula la expresión de los genes del *cluster* (Hoffmeister and Keller, 2007; Osbourn, 2010). Se conocen diferentes mecanismos implicados en la co-regulación de estos genes a nivel transcripcional, esquematizados en la Fig. 3: a) factores de transcripción específicos de la ruta, b) factores de transcripción de amplio espectro, o c) complejos heteroméricos globales (Yin and Keller, 2011).

a) Entre los factores de transcripción específicos de la ruta, los más comunes son las proteínas con "dedos" de Zinc binucleares del tipo $Zn(II)_2Cys_6$, como Fum21 en el *cluster* de biosíntesis de fumonisinas en *F. verticillioides* (Brown et al., 2007), o las proteínas de "dedo" de Zinc Cys_2His_2, como Tri6 en el *cluster* de biosíntesis de tricotecenos en algunas especies de *Fusarium* (Trapp et al., 1998).

b) Los hongos suele integrar diferentes señales ambientales, como la luz, el pH o la disponibilidad de nutrientes, para activar o reprimir la expresión de los *clusters* en función de sus necesidades. La síntesis de metabolitos secundarios es un proceso costoso energéticamente, por lo que sólo se producen cuando el entorno y el estado fisiológico son favorables. Son conocidos los casos de regulación por fuente de carbono, nitrógeno o pH que se llevan a cabo por medio de factores de transcripción globales del tipo Zinc Cys_2His_2, denominados respectivamente CreA (Dowzer and Kelly, 1989), AreA (Hynes, 1975) y PacC (Tilburn et al., 1995).

c) Otras proteínas reguladoras ejercen su acción formando complejos, como el denominado HAP, que participa en la regulación por medio de la unión a promotores con secuencias consenso CCAAT (Brakhage, 1998). Este tipo de proteínas son muy frecuentes en los organismos eucariotas y aproximadamente el 30% de los promotores contienen sus secuencias consenso (Kato, 2005).

En la regulación de los genes del metabolismo secundario desempeña un papel importante el control a nivel de estructura de cromatina. Algunas proteínas reguladoras actúan a nivel de modificación de la estructura de la cromatina, bien añadiendo o quitando marcas activadoras o represoras en las histonas. Entre ellas cabe destacar la metiltransferasa de histonas LaeA, inicialmente descubierta en *Aspergillus nidulans*, que interacciona con las proteínas *velvet* VeA y VeB (Bok and Keller, 2004; Yin and Keller, 2011). Estas proteínas se han identificado en varios géneros de hongos filamentosos además de *Aspergillus*, como *Penicillium* o *Fusarium* (Bok and Keller, 2004; Butchko et al., 1999; Kale et al., 2008; Kosalkova et al., 2009; Wiemann et al., 2010).

Se ha postulado que el origen evolutivo de estos agrupamientos génicos es la transferencia horizontal de juegos completos de genes entre especies. En apoyo de esta hipótesis, los *clusters* del metabolismo secundario se encuentran con frecuencia en las regiones subteloméricas de los cromosomas, para las que se ha descrito una alta tasa de recombinación (Palmer and Keller, 2010).

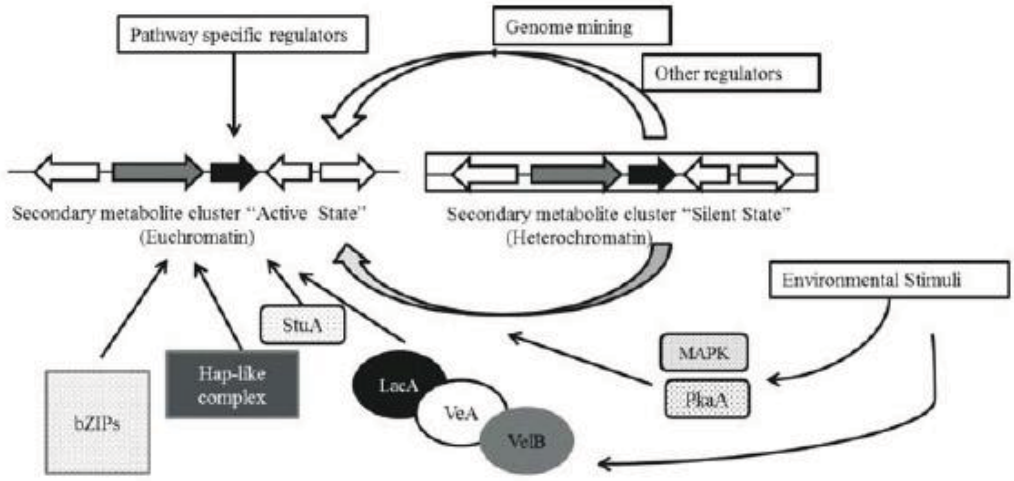

Fig. 3. Niveles de regulación transcripcional del metabolismo secundario en hongos. Los reguladores específicos de la ruta, los globales y los estímulos externos desencadenan una señal que activa la transcripción de los genes por remodelación de la cromatina (Yin and Keller, 2011).

2.2 Metabolismo secundario *en Fusarium*

Dentro de los hongos, las especies del género *Fusarium* son especialmente relevantes en cuanto a la complejidad de su metabolismo secundario. Entre las numerosas sustancias producidas destacan muchas por su toxicidad o potencial dañino tanto sobre la especie humana como sobre animales domésticos o ganadería (Čonková et al., 2003; Jestoi, 2008). Estas sustancias, que se conocen genéricamente como micotoxinas, son incorporadas al organismo a través de la ingesta de plantas de consumo cotidiano en la población. Entre ellas figuran las fumonisinas (Desjardins et al., 1993; Gelderblom et al., 1988), fusarinas (Barrero et al., 1991), ácido fusárico (Bacon et al., 1996), moniliformina (Desjardins et al., 1997; Marasas et al., 1986), tricotecenos (Desjardins et al., 1993), zearalenona (Caldwell et al., 1970), fusaproliferina (Moretti et al., 2007), bicaverinas (Giordano et al., 1999; Limón et al., 2010), y aurofusarinas (Malz et al., 2005; Shibata et al., 1966).

Sin embargo, entre los compuestos producidos por especies del género *Fusarium* figuran también algunos de interés biotecnológico, como los carotenoides (Avalos et

al., 2014) y las giberelinas (Tudzynski, 2005). Los primeros son pigmentos que proporcionan colores amarillos, anaranjados o rojizos a frutos, flores, o incluso animales. Las giberelinas por su parte son hormonas vegetales promotoras del crecimiento, producidas casi exclusivamente por el grupo de cruzamiento C del complejo de especies *Gibberella fujikuroi* (Troncoso et al., 2010); es decir, por la especie objeto de atención en esta Tesis.

En el caso de *F. fujikuroi,* además de los carotenoides y las giberelinas, de naturaleza terpenoide, ha sido objeto de atención la producción de bicaverinas, fusarinas, fumonisinas, ácido fusárico y fusarrubinas (Studt et al., 2012), todos ellos de naturaleza policétida. Por las implicaciones en este trabajo, únicamente se detallan aquí las rutas de síntesis y regulación de carotenoides, giberelinas, bicaverinas y fusarinas (Fig. 4).

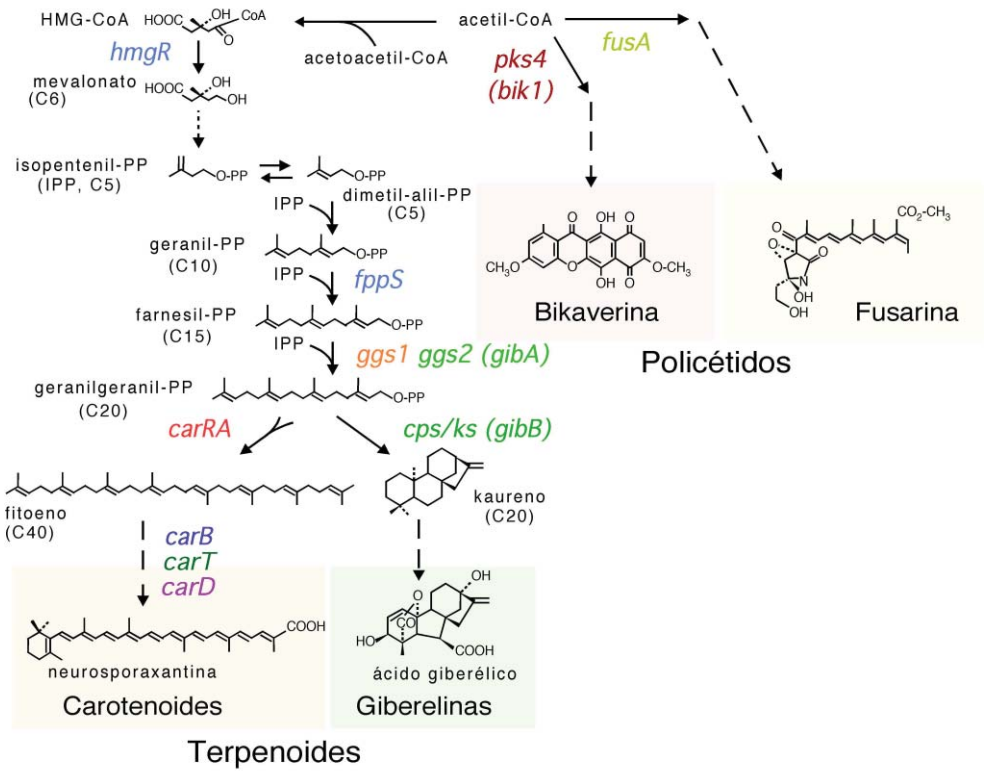

Fig. 4. Esquema de las rutas y metabolitos secundarios de la especie *Fusarium fujikuroi* relevantes en esta Tesis. Los dos grupos principales, policétido y terpenoides ,se sintetizan a partir del precursor Acetil-CoaA. Los terpenoides comparten los primeros pasos de la ruta, mientras que los policétidos se originan por la acción de enzimas diferentes. Las flechas discontinuas indican varias reacciones hasta obtener ese producto.

2.2.1 Policétidos

Los policétidos son un grupo de metabolitos secundarios muy diversos y extendidos en hongos (Keller et al., 2005), sintetizados por enzimas multimodulares denominadas sintetasas de policétidos (PKSs) (Menzella et al., 2005; Staunton and Weissman, 2001). Las PKSs de hongos pertenecen a la clase PKS I y comprenden varios dominios conservados que actúan como una única unidad para generar un esqueleto carbonado, procedente de la adición secuencial de varias moléculas (Chiang et al., 2010). Los dominios mínimos presentes en estas enzimas son una sintasa de β-cetoacil-coA (KS), un transportador de acilo (ACP) y una transferasa de acilo (AT), así como un dominio tioesterasa (TE) que libera el producto del centro catalítico de la enzima (Fig.5). Recientemente también se han identificado dos nuevos dominios: una unidad iniciadora de la transferasa de acilo (SAT) y un dominio aldo ciclasa de especies β-ceto (PT) (Crawford et al., 2006; Crawford et al., 2009).

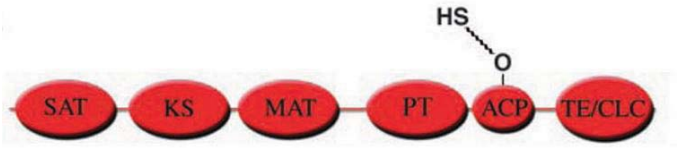

Fig. 5. Organización estructural de una sintetasa de policétidos de tipo PKS I típica de hongos. La acción conjunta de estas actividades enzimáticas sintetiza un policétido precursor que podrá sufrir otras reacciones y modificaciones hasta llegar a su forma final.

2.2.1.1. Bicaverinas

Las bicaverinas son pigmentos rojizos con actividad antibiótica frente a distintos organismos, como protozoos (Balan et al., 1970), nematodos (Kwon et al., 2007) u otros hongos filamentosos (Cornforth et al., 1971; Son et al., 2008). Se distinguen dos tipos de bicaverina según su estructura (Fig. 6): la bicaverina y la nor-bicaverina.

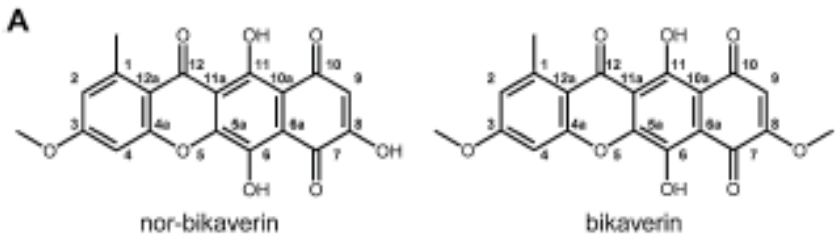

Fig. 6. Estructura química de la bicaverina y nor-bicaverina (Wiemann et al., 2009).

Las enzimas de la ruta biosintética han sido objeto de estudio durante varios años. Inicialmente se identificó una sintasa de policétido, producto del gen *pks4* (Linnemannstöns et al., 2002), posteriormente renombrado *bik1* (Wiemann et al., 2009), cuyos dominios enzimáticos son similares a los descritos para otras PKSs fúngicas (ver Fig. 7).

Fig. 7. Dominios estructurales de la Pks4 responsable de la síntesis de bicaverina en la estirpe IMI58289 de *F. fujikuroi* (Studt et al., 2012).

El gen *bik1* se encuentra agrupado en el genoma formando un *cluster* co-regulado con otros cinco genes *bik* (Fig. 8). De éstos, *bik2* determina una monooxigenasa dependiente de FAD, *bik3* una O-metiltransferasa, *bik5* un factor de transcripción específico de ruta de tipo Zn(II)2Cys6, *bik4* un potenciador del factor de transcripción y *bik6* una bomba de antiporte de H^+ que excreta bicaverina al medio.

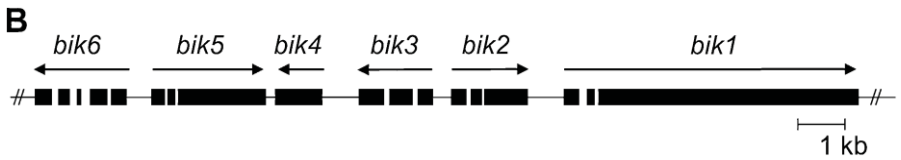

Fig. 8. Esquema del agrupamiento génico para la biosíntesis de bicaverinas. Los huecos dentro de los genes representan intrones, y las flechas la dirección de la transcripción (Wiemann et al., 2009).

Se ha postulado que la actividad de Bik1 origina un compuesto llamado pre-bicaverina que es posteriormente oxidado en los carbonos C6 y C7 por Bik2 y metilado por Bik3 en C3 para producir nor-bikaverina y posteriormente en C8 para dar bicaverina. La diferente abundancia relativa de nor-bicaverina y bicaverina en varias estirpes de *F. fujikuroi* sugiere diferentes funciones para estos dos compuestos (Wiemann et al., 2009).

El principal factor ambiental que regula la síntesis de bicaverinas es el nitrógeno. La ausencia de nitrógeno estimula su producción y altas concentraciones de este elemento inhiben su síntesis (Giordano et al., 1999). Como se muestra en la Fig. 9, esta regulación ocurre a nivel transcripcional, de forma que la expresión de todos los genes *bik* es mucho mayor cuando el hongo se cultiva en un medio con bajo nitrógeno. Los promotores de los genes *bik* presentan sitios de unión para el factor de transcripción AreA, una proteína reguladora que se une a los promotores de los genes regulados por nitrógeno (Marzluf, 1997). Sin embargo, a

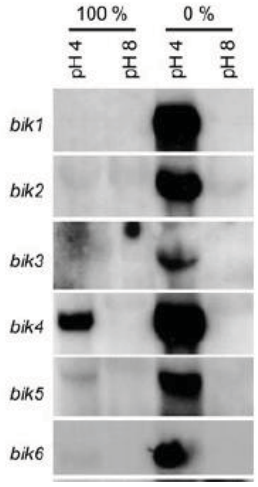

Fig. 9. Análisis en Northern de la expresión de los genes del *cluster bik*. Los porcentajes indican el contenido en nitrógeno de los medios empleados. Los resultados muestran que la expresión en bajo nitrógeno depende del pH (Wiemann et al., 2009).

diferencia de la regulación de los genes de otros metabolitos (veáse la sección 2.2.2.1. sobre las giberelinas), no se ha podido establecer aún una relación directa entre la proteína AreA y la expresión de los genes del *cluster bik* (Wiemann et al., 2009).

La síntesis de bicaverinas está influida también por el pH, siendo favorables las condiciones de pH ácido (Fig. 9) (Balan et al., 1970; Bell et al., 2003; Giordano et al., 1999). El promotor del gen *bik1* presenta tres posibles sitios de unión a PacC (Espeso et al., 1997), un factor de transcripción que regula la expresión de genes por pH en otros hongos (Brakhage et al., 2004; Espeso et al., 1993; Flaherty et al., 2003). La proteína PacC de *F. fujikuroi* reprime la síntesis de bicaverinas a pH neutro y alcalino (Wiemann et al., 2009).

Existen otras proteínas implicadas en la regulación de la síntesis de bicaverinas. Entre ellas figuran proteínas relacionadas con el metabolismo del nitrógeno, como la glutamina sintetasa GlnA (Teichert et al., 2004), las permeasas de amonio MepB y MepC (Teichert et al., 2008) o la quinasa TOR (Teichert et al., 2006).

La disponibilidad de fuentes para otros nutrientes, como el carbono, el fósforo o el azufre, también influye en los niveles de producción de bicaverinas. En condiciones de hambre de nitrógeno, la sacarosa es una fuente de carbono especialmente eficaz para su síntesis comparada con otras fuentes de carbono, como la glucosa u otros azúcares simples. Por otro lado, la escasez de sales de fosfato y/o sulfato también estimula notablemente la síntesis (Rodríguez-Ortiz et al., 2010).

Como ya se ha mencionado, el complejo VeA/VeB/LaeA participa en la regulación del desarrollo y metabolismo secundario en hongos. En *F. fujikuroi* la mutación de los genes ortológos *vel1* y *vel2* produce una desrepresión en la producción de bicaverinas, mientras que los mutantes *laeA1* reducen parcialmente su producción (Wiemann et al., 2010).

2.2.1.2. Fusarinas

F. fujikuroi produce fusarina C (Barrero et al., 1991; Wiebe and Bjeldanes, 1981), una micotoxina con actividad mutagénica (Gelderblom, 1983 #93} que afecta también al ser humano (Cheng et al., 1985; Dong and Zhan, 1987). Se ha descrito su estructura química (Fig. 10) (Barrero et al., 1991) y se ha atribuido su capacidad mutagénica al grupo epóxido presente en los carbonos C13 y C14. La fusarina C es inestable por exposición a radiación UV e isomeriza rápidamente (Gelderblom et al., 1983). Su máximo de absorción se encuentra en la región UV-A del espectro, pero una leve absorbencia en la región visible le confiere al hongo una caracteristica pigmentación amarillenta cuando produce el compuesto a elevadas concentraciones.

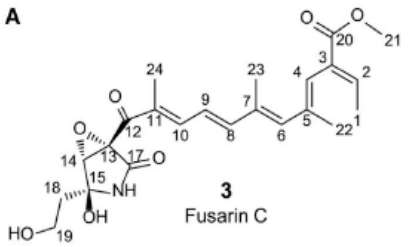

Fig. 10. Estructura química de la fusarina C (Niehaus et al., 2013).

La enzima responsable de la síntesis de fusarina es una PKS determinada por el gen *fusA* (Díaz-Sánchez et al., 2012), también llamado *fus1* (Niehaus et al., 2013). Esta enzima presenta la particularidad de incluir dominios de síntesis de péptidos no ribosomales (Fig. 11A), normalmente ausentes en las PKSs. Las enzimas de esta subfamilia se conocen como PKSs híbridas PKS/NRPS.

El gen *fusA*/*fus1* se localiza en el genoma en un *cluster* con ocho genes que participan en la síntesis de fusarina C y con los que comparte la regulación (Fig. 11B). Se ha investigado la función de cada uno de ellos y se ha propuesto una ruta de síntesis (Niehaus et al., 2013). Así, *fus2* determina una proteína similar a las α/β hidrolasas, *fus3* una transferasa de glutatión, *fus4* una péptidasa A1, *fus5* una hidrolasa de serina, *fus6* una proteína transportadora de la familia MFS, *fus7* una aldehído deshidrogenasa, *fus8* una mono-oxigena P450 y *fus9* una metiltransferasa. De todas las enzimas determinadas por estos genes, sólo parecen ser esenciales para la síntesis de fusarina C Fus1, Fus2, Fus8 y Fus9.

A

B

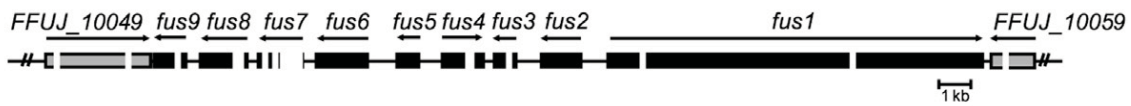

Fig. 11. Estructura de la PKS Fus1 y organización de los genes de la ruta biosintética. (A) Dominio encontrados en la PKS Fus1 en *F. graminearum*. (B) Esquema de la organización en el genoma de los nueve genes implicados en la síntesis de fusarina C en *F. fujikuroi* y los genes que flanquean el clúster en gris (Niehaus et al., 2013).

La regulación de la producción de fusarina ha sido objeto de especial atención en los últimos años. La síntesis se estimula en medios de cultivo con exceso de nitrógeno, siendo preferible su presencia en forma de fuentes orgánicas. La estimulación de la producción es acompañada por un aumento transitorio en la transcripción de los genes *fus*, indicando un control a nivel transcripcional (Díaz-Sánchez et al., 2012; Niehaus et al., 2013). El complejo Vel1/Vel2/Lae1 parece estar implicado en la mencionada activación transcripcional a través de mecanismos epigenéticos (Niehaus et al., 2013; Wiemann et al., 2010).

Las condiciones de cultivo también afectan a la síntesis de este metabolito. Así, la síntesis se ve favorecida por altas temperaturas, 30°C en vez de 22°C (Barrero et al., 1991) y una buena aireación {Giordano, 1999 #98).

2.2.2. Terpenoides

Los terpenoides son sustancias con importantes funciones en todos los seres vivos. Entre ellas cabe citar como ejemplos el papel de los esteroles como constituyentes necesarios para la integridad de las membranas celulares {Accoceberry, 2006 #99} o la actividad de las giberelinas y el ácido abscísico como hormonas vegetales. Todos los terpenoides comparten su síntesis a partir de un único precursor, el pirofosfato de isopentenilo (IPP). Sucesivas condensaciones de esta unidad de cinco átomos de carbono originan terpenoides de complejidad creciente, que se clasifican según su número de átomos de carbono. De este modo obtenemos monoterpenos de 10 átomos de C, derivados del pirofosfato de geranilo (GPP), sesquiterpenos de 15

átomos de C, derivados del pirofosfato de farnesilo (FPP), y diterpenos de 20 átomos de C, derivados del pirofosfato de geranilgeranilo (GGPP), y así sucesivamente. Como se muestra en la ruta de la Fig. 12, en hongos el IPP se sintetiza a partir de mevalonato (Goodwin and Lijinski, 1952). En otros organismos existe una ruta alternativa para síntesis de IPP que utiliza gliceraldehido-3-fosfato como precursor (Rohmer et al., 1993). Por su ausencia en hongos, no se le dedica aquí más atención.

2.2.2.1 Giberelinas

Atendiendo a la terminología descrita en el apartado anterior, las giberelinas (GAs) son diterpenos. Estas moléculas poseen estructura tetracíclica y actúan como hormonas vegetales estimuladoras del crecimiento y el desarrollo en las plantas. Se conocen numerosas GAs, muchas de ellas implicadas en diferentes procesos de desarrollo y diferenciación vegetal, como la germinación, elongación del tallo, floración, fructificación y senescencia (Yamaguchi, 2008). Las GAs deben su nombre al primer organismo en el que se identificaron, *Giberella fujikuroi* (Kawaide, 2006), en particular al grupo de cruzamiento C de este complejo. Además se ha descrito su producción en algunas especies del grupo de cruzamiento G (Troncoso et al., 2010) y pocos hongos más (Kawaide et al., 1997{Bomke, 2009 #105), estando ausente su ruta biosintética en la gran mayoría de los hongos. Por sus posibles aplicaciones biotecnológicas, la ruta de síntesis y sus mecanismos de regulación han sido objeto de estudio detallado en los últimos años en *F. fujikuroi*. Estos estudios han revelado diferencias bioquímicas con la ruta de síntesis de GAs en plantas, sugiriendo orígenes evolutivos independientes (Hedden et al., 2001; MacMillan, 1997; Yamaguchi, 2008).

Los genes de *F. fujikuroi* necesarios para la síntesis de GAs han sido identificados (Fig. 13) y, al igual que ocurre con los de otros metabolitos secundarios, están agrupados en el genoma formando un *cluster* (Tudzynski, 2005) (Fig. 13B). Los genes fueron denominados por sus descubridores en función de la naturaleza bioquímica del producto sin atender criterios de terminología genética. Aunque en una revisión

posterior se renombraron con una terminología más lógica (Demerec et al., 1966) como *gibA-G* (Avalos et al., 2007), conservamos aquí los nombres originales por coherencia con las correspondientes publicaciones.

La síntesis de GAs comparte los pasos iniciales, hasta GGPP, con los de la síntesis de carotenoides, pero ambos procesos se llevan a cabo en compartimentos celulares diferentes (Domenech et al., 1996). En *F. fujikuroi* hay dos genes de prenil transferasas para síntesis de GGPP a partir de FFPP, *ggs1* (Mende et al., 1997) y *ggs2*. La enzima determinada por este segundo gen, ubicado en el *cluster* de la síntesis de GAs (Tudzynski and Holter, 1998a), es presuntamente responsable de la síntesis de GPP para la producción de GAs. Una enzima bifuncional, la copalil difosfato/ent-kaureno sintasa CPS/KS (Tudzynski et al., 1998b), introduce cuatro ciclaciones en la molécula de GGPP para dar ent-kaureno, que es posteriormente oxidado por una monooxigenasa

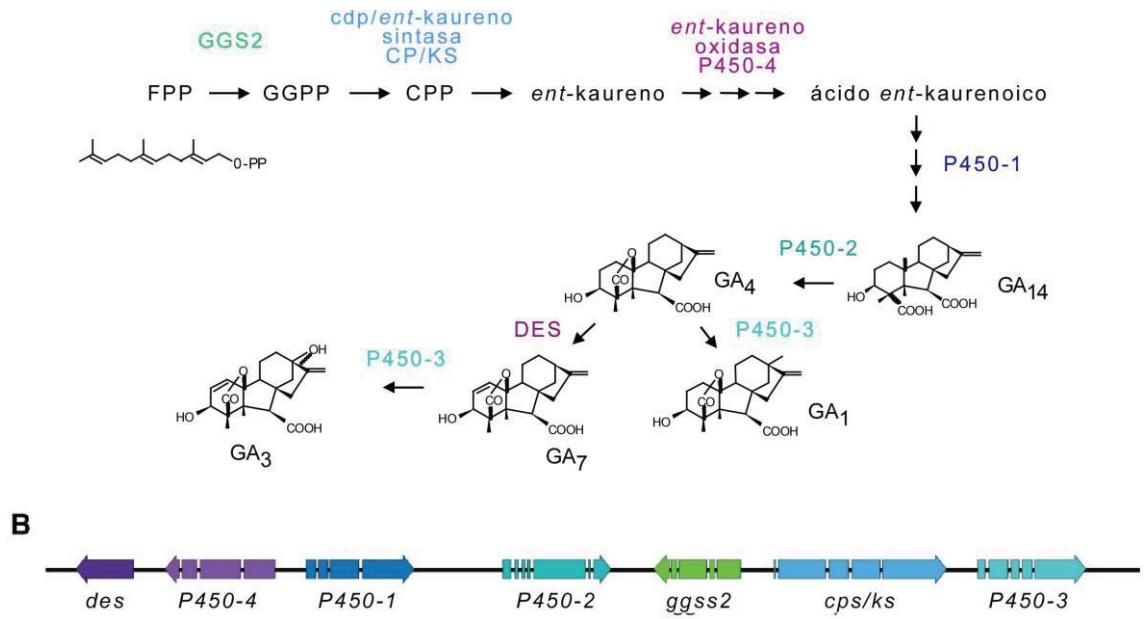

Fig. 13. Síntesis de GAs en *F. fujikuroi.* (A) Principales pasos y enzimas de la síntesis de GA3, producto mayoritario de la ruta en este hongo. Se omiten las reacciones e intermediarios concretos entre del precursor ent-kaurenoico y la GA_{14}. (B) Esquema de la organización de los genes en el genoma. La dirección de la flecha indica la dirección de la transcripción, y los huecos internos se corresponden con los intrones de los genes [adaptado de (Rodríguez-Ortiz, 2012)].

de la familia P450, denominada P450-4. Las enzimas P450-1, P450-3 y Des llevan a cabo oxidaciones, hidroxilaciones y desaturaciones (Hedden et al., 1974; MacMillan, 1997; Urrutia et al., 2001) para producir GAs con diferentes grupos químicos (hidroxilaciones en distintas posiciones y presencia/ausencia de desaturaciones). La ruta resumida se muestra en la Fig. 13.

Como ocurre con las bicaverinas, las giberelinas se producen preferentemente en condiciones limitantes de nitrógeno, de forma que la presencia de fuentes de nitrógeno, tanto orgánicas como inorgánicas, reprimen su producción (Borrow et al., 1964; Muñoz and Agosín, 1993). Este aumento de producción va acompañado de una activación de los genes del *cluster* que es dependiente de la proteína AreA (Mihlan et al., 2003). En este caso AreA actúa como un regulador positivo que se une directamente a los promotores de los genes *gib*, de forma que un mutante carente de AreA no activa su expresión y por tanto no sintetiza giberelinas (Tudzynski, 1999). Una excepción es el gen P450-3, que no es regulado por nitrógeno. La enzima P450-3 participa en reacciones tardías de la ruta, por lo que su diferente regulación no influye sobre el requerimiento de la ausencia de nitrógeno para la síntesis de GAs.

Se han descubierto otros genes involucrados en la regulación de la síntesis de GAs, también relacionados con el metabolismo del nitrógeno. Es el caso de *nmr*, que determina un inhibidor de la actividad de AreA (Mihlan et al., 2003; Schönig et al., 2008), así como *meaB* (Wagner et al., 2010) o *glnA* (Schönig et al., 2009; Teichert et al., 2004). Una vez más, en este grupo se encuentra también el complejo Vel1/Vel2/Lae1 que es necesario para activar los genes de la ruta (Wiemann et al., 2010).

El papel que desempeñan las giberelinas en el hongo es aún incierto. Se postula que puedan suponer una ventaja durante el proceso infectivo de la planta, pero hasta ahora existen pocos datos sobre ésta u otras funciones. Las estirpes no productoras de GAs pueden penetrar en la planta y crecer en su interior, sin embargo parece que son incapaces de llevar a cabo la invasión completa (Wiemann et al., 2013).

2.2.2.2. Carotenoides

Los carotenoides son sustancias por lo general coloreadas que presentan distintas funciones en los seres vivos. En plantas son esenciales, ya que actúan como pigmentos antena de la fotosíntesis, pero también intervienen en la fotomorfogénesis y ejercen efectos beneficiosos por detoxificiación de especies reactivas de oxígeno, como el oxígeno “singlete” (Cuttriss and Pogson, 2006). Además confieren colores llamativos a flores y frutos, haciéndolos más atractivos y facilitando así la polinización y dispersión de las semillas. Por ello todas las plantas poseen rutas biosintéticas de carotenoides

(Edge et al., 1997). También se han descrito rutas de síntesis de estos compuestos en hongos (Sandmann and Misawa, 2002) y bacterias (Armstrong, 1997). Con muy raras excepciones, explicadas por transmisión génica horizontal (Moran and Jarvik, 2010), los animales carecen de la capacidad de sintetizar carotenoides y necesitan ingerirlos en la dieta. Las funciones que desempeñan en animales son igualmente variadas, pero tienen especial importancia el ácido retinoico en desarrollo celular y diferenciación en cordados (Kam et al., 2012; Rhinn and Dolle, 2012), y el retinal como grupo prostético de las opsinas en la visión (Britton et al., 1998; von Lintig, 2010). Además, las propiedades antioxidantes de los carotenoides pueden proporcionar ventajas a los seres humanos disminuyendo la incidencia de algunas enfermedades, como cáncer o enfermedades cardiovasculares y del sistema inmunológico (Hadley et al., 2002; Jyonouchi et al., 1993).

Además de sus funciones en la naturaleza, las propiedades beneficiosas de los carotenoides para la salud hacen que sean productos muy atractivos para la industria biotecnológica. Además, sus llamativos colores les proporciona aplicaciones como colorantes en la industria cosmética y alimentaria (Castillo et al., 2005; Mapari et al., 2005). Aunque los carotenoides se pueden obtener por síntesis química, el creciente rechazo social al uso de aditivos químicos ha estimulado el desarrollo de métodos de producción biológica, figurando los hongos entre los organismos preferentes para su producción industrial (Avalos and Cerdá-Olmedo, 2004).

Estructuralmente, los carotenoides son tetraterpenos procedentes de la condensación de dos moléculas de GGPP, que da lugar a una cadena alifática de 40 átomos de carbono a la que se acaba introduciendo dobles enlaces conjugados alternos, responsables de su capacidad de absorber luz visible. El esqueleto principal es un hidrocarburo, del cual se diferencian dos clases según las sustituciones que incorpore: carotenos y xantofilas (Olson and Krinsky, 1995). Los primeros se componen únicamente de átomos de carbono e hidrógeno (β-caroteno, γ-caroteno y licopeno entre otros), mientras que las segundas incorporan al menos un átomo de oxígeno (zeaxantina, luteína, α- y β- criptoxantina y astaxantina, entre los más conocidos).

2.2.2.2.1 Carotenoides en hongos

La síntesis de carotenoides es un rasgo muy extendido en hongos, con ejemplos en los grupos taxonómicos más conocidos, zigomicetos, basidiomicetos y ascomicetos. Las rutas biosintéticas son similares en todos ellos en sus primeros pasos, difieren con frecuencias en los últimos pasos, dando lugar a carotenoides distintos en varios casos bien investigados.

Como ya se ha indicado, la ruta biosintética comienza con la condensación de dos moléculas de GGPP para dar fitoeno, un carotenoide incoloro. A continuación esta molécula de 40 átomos de carbono es desaturada varias veces en posiciones simétricas, originando moléculas con dobles enlaces conjugados que absorben la luz visible y proporcionan la característica coloración amarilla, naranja y rojiza a estos pigmentos. La introducción de cuatro desaturaciones da lugar al licopeno, de color rojo. El siguiente paso suele ser la ciclación de uno o los dos extremos de la cadena, originando anillos tipo α, β, o γ. La ciclación β de un extremo produce γ-caroteno, y la del segundo extremo β-caroteno. La serie de cuatro desaturaciones y dos ciclaciones para producir β-caroteno se conoce como ruta de Porter y Lincoln (Porter and Lincoln, 1950). En otros hongos, como *Neurospora* y *Fusarium*, la desaturasa lleva a cabo cinco desaturaciones y la ciclasa una sola ciclación. Son responsables de estos pasos una enzima bifuncional con actividad sintasa de fitoeno y ciclasa, y una desaturasa. Los genes responsables de ambas enzimas se han identificado en zigomicetos, como *Phycomyces blakesleeanus* (Arrach et al., 2001; Ruiz-Hidalgo et al., 1997) y *Mucor circinelloides* (Velayos et al., 2000b; Velayos et al., 2000a), en ascomicetos, como *Neurospora crassa* (Schmidhauser et al., 1990; Schmidhauser et al., 1994) y *Fusarium fujikuroi* (Fernández-Martín et al., 2000; Linnemannstöns et al., 2002b), y en basidiomicetos, como *Xantophyllomyces dendrorhous* (Verdoes et al., 1999b); (Verdoes et al., 1999a) y *Ustilago Maydis* (Estrada et al., 2009b).

Como se ha mencionado, el producto final de la ruta difiere de un grupo a otro. En zigomicetos y *U. maydis* el producto final es el β-caroteno, usándose el hongo *Blakeslea trispora* para su producción industrial (Avalos and Cerdá-Olmedo, 2004). En el basidiomiceto *X. dendrorohous*, se produce astaxantina, una xantofila procedente de

la acción de la introducción de grupos ceto e hidroxilos en los anillos del β-caroteno (Álvarez et al., 2006; Ojima et al., 2006). Su uso en la industria está ampliamente extendido en el ámbito de los colorantes alimenticios (Johnson 2003). Sin embargo, en los ascomicetos *N. crassa* y *F. fujikuroi*, el resultado final es la síntesis de una xantofila ácida, con cinco átomos menos de carbono, denominada neurosporaxantina. Para su síntesis son necesarios pasos adicionales de rotura oxidativa y oxidación (Estrada et al., 2008b; Prado-Cabrero et al., 2007b; Saelices et al., 2007), descritos en la siguiente sección.

Los carotenoides no son esenciales en los hongos y se sabe poco acerca de sus funciones en estos organismos. Se ha postulado que su síntesis puede conferir protección frente al estrés oxidativo, ya que la exposición a compuestos con capacidad oxidante provoca un aumento en la síntesis de carotenoides en hongos como *X. dendrorhou*s (Schroeder and Johnson, 1995) o *Cercospora spp* (Daub et al., 2005; Daub and Payne, 1989). En muchas especies de hongos la síntesis de carotenoides es estimulada por la luz, lo cual se puede deber al estrés oxidativo ocasionado por la misma (Avalos et al., 1993). En otros, como es el caso de los mucorales *P. blakesleeanus* o *B. trispora*, el β-caroteno desempeñan un papel importante en el ciclo sexual como precursor de las hormonas sexuales, los ácidos trispóricos (Austin et al., 1970; Polaino et al., 2010), necesarios para la comunicación entre las estirpes de sexo opuesto (Sutter, 1975).

2.2.2.2.2. Carotenogénesis en *F. fujikuroi*

Los primeros pasos de la síntesis de carotenoides en *F. fujikuroi* se ajustan al patrón habitual, ya mencionado en la sección anterior (Fig. 14). La condensación de dos moléculas de GGPP para dar fitoeno la realiza la enzima bifuncional CarRA (Linnemannstöns et al., 2002b). El orden del resto de las reacciones se ha deducido del análisis de intermediarios en mutantes superproductores (Avalos and Cerdá-Olmedo, 1987). A partir del fitoeno, la desaturasa CarB (Fernández-Martín et al., 2000; Prado-Cabrero et al., 2009) realiza tres desaturaciones consecutivas que originan fitoflueno, ζ-caroteno y neurosporeno. A continuación la actividad ciclasa de CarRA introduce un anillo β en un extremo para producir β-zeacaroteno. Este compuesto es objeto de dos

nuevas desaturaciones por CarB, dando lugar sucesivamente a γ-caroteno y toruleno. Este último es un caroteno rojizo que es reconocido por la oxigenasa CarT (Prado-Cabrero et al., 2007b) para producir un corte oxidativo, y dar lugar a β-apo-4'-carotenal, de 35 átomos de carbono. El grupo aldehído de este apocarotenoide es oxidado por la deshidrogenasa de aldehído CarD (Díaz-Sánchez et al., 2011a) para dar el producto final, la neurosporaxantina. A nivel del γ-caroteno arranca una segunda rama que origina β-caroteno por la acción de CarRA, que cicla el otro extremo libre de la molécula. Este caroteno se encuentra en pequeñas cantidades (Avalos and Cerdá-Olmedo, 1987), probablemente por tratarse de un intermediario, ya que es cortado simétricamente por la oxigenasa CarX para producir dos moléculas de retinal (Prado-Cabrero et al., 2007a; Thewes et al., 2005).

Los genes necesarios para la síntesis de retinal, *carRA*, *carB* y *carX*, están agrupados en el genoma y comparten la misma regulación (Fig. 15). El *cluster* incluye también un cuarto gen, *carO,* que determina una rodopsina (Prado et al., 2004). Como se mencionará más adelante, las rodopsinas son fotoreceptores que utilizan retinal como cromóforo. Por su parte, los genes *carT* y *carD,* que determinan la oxigenasa y la deshidrogenasa de aldehído necesarias para la síntesis de neurosporaxantina, se localizan en otras regiones del genoma.

Fig. 15. Organización en el genoma de los genes para la biosíntesis de carotenoides. En la región central aparecen los genes que forman el *cluster* co-regulado, y en los extremos los genes que se encuentran en otras regiones del genoma (*carT* y *carD*).

En *F. fujikuroi*, con excepción de *carO* y *carX*, las pérdidas de función de estos genes da lugar a fenotipos muy característicos, fácilmente distinguibles de la estirpe silvestre por el cambio de color del micelio como consecuencia de la acumulación de un intermediario coloreado. Así los mutantes *ΔcarB* acumulan fitoeno y son albinos por ser este caroteno incoloro. También son albinos los mutantes *ΔcarRA*, en este caso por carencia total de caroteno. No se han descrito, sin embargo, mutantes afectados exclusivamente en la actividad ciclasa de la enzima bifuncional, supuestamente por su

parecida pigmentación a la estirpe silvestre. Los mutantes *ΔcarT* acumulan toruleno confiriendo un color rojizo al micelio (Prado-Cabrero et al., 2007b). Por último, los mutantes *ΔcarD* son inicialmente anaranjados por acumulación de β-apo-carotenal, y difíciles de distinguir por tanto de la estirpe silvestre. Por esta razón, tampoco se han identificado por mutagénesis química. Sin embargo, su pigmentación se vuelve amarillenta al envejecer el micelio por la inestabilidad de este intermediario, que da lugar a carotenoides derivados (Díaz-Sánchez et al., 2011a).

Tanto los genes *car* como su regulación están muy conservados en otras especies de *Fusarium* investigadas, como *F. verticillioides* (Díaz-Sánchez, 2013) y *F. oxysporum* (Rodríguez-Ortiz et al., 2012). Recientemente se ha identificado otro gen en *F. verticilloides*, *carY,* que determina una aldehído deshidrogenasa capaz de oxidar retinal en ácido retinoico (Díaz-Sánchez, 2013). Dados los bajos niveles de retinal en el hongo, es plausible que la fracción de retinal no usada por las rodopsinas sea convertida en ácido retinoico, el cual a su vez podría desempeñar funciones como señal en morfogénesis y desarrollo sexual (Díaz-Sánchez, 2013).

Como ocurre en la mayoría de los hongos, el principal factor estimulador de la síntesis de carotenoides es la luz (Avalos and Schrott, 1990), proceso conocido como fotocarotenogénesis. Los niveles de carotenoides producidos en *F. fujikuroi* en oscuridad son bajos, pudiendo variar según las condiciones de cultivo (Avalos and Cerdá-Olmedo, 1987), y aumentan significativamente al ser expuestos a la luz al menos 1 hora (Avalos et al., 1993). En cultivos sumergidos y sometidos a aireación, la respuesta máxima se alcanza tras 24h de iluminación (Avalos and Schrott, 1990). Este aumento es consecuencia de una acumulación progresiva de transcritos de ARNm para los genes del *cluster*, que presentan sus niveles máximos tras aproximadamente una

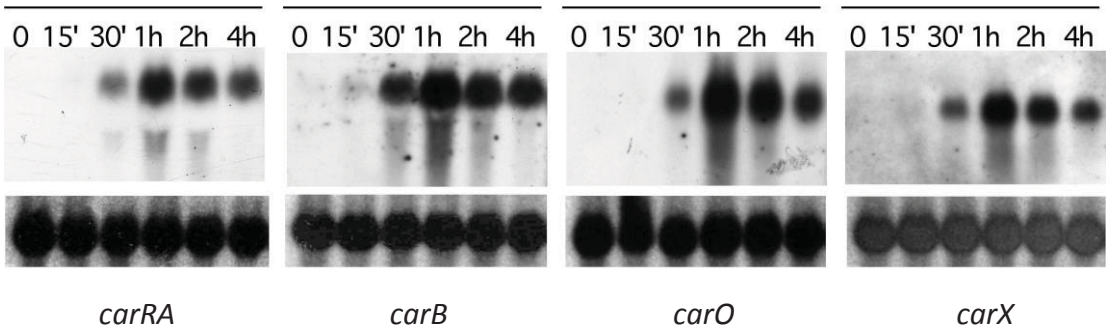

Fig. 16. Regulación por luz de la expresión de los genes del *cluster car* en *F. fujikuroi*. Cada recuadro muestra el resultado de la hibridación en Northern con la sonda del gen indicado abajo. Los tiempos de iluminación se indican arriba. El panel inferior muestra un ARNr como control de carga.

hora de exposición a luz para decaer posteriormente (Fig. 16) (Linnemannstöns et al., 2002b), (Prado et al., 2004), (Thewes et al., 2005). La transitoriedad de la respuesta apunta a la existencia de un mecanismo de fotoadaptación similar al observado en otros hongos. Este fenómeno ha sido objeto de especial atención en *N. crassa* (Arpaia et al., 1999; Schrott et al., 1982) y su base molecular será objeto de atención en una sección posterior. Los genes *carT* y *carD*, no ligados genéticamente al *cluster car* en el genoma, presentan niveles de fotoinducción más bajos que los arriba mencionados en el primer caso (Prado-Cabrero et al., 2007b), e inexistentes en el segundo caso (Díaz-Sánchez et al., 2011a).

Como se ha visto en los mecanismos regulatorios para otros metabolitos, la disponibilidad de nitrógeno desempeña también un papel en la regulación de la carotenogénesis en *Fusarium*. Las condiciones limitantes de este nutriente favorecen la producción de carotenoides, tanto en luz como en oscuridad (Rodríguez-Ortiz et al., 2009).

A diferencia de lo que ocurre en los hongos mucorales, como *P. blakesleeanus* o *B. trispora* (Barnett et al., 1956; Govind and Cerda-Olmedo, 1986; Kuzina and Cerdá-Olmedo, 2007), en *Fusarium* no se ha observado estimulación sexual de la síntesis de carotenoides.

Entre los mutantes de la pigmentación de *F. fujikuroi*, merecen especial atención los de fenotipo *carS* (**S**obreproductor de **car**otenoides). Este fenotipo, consistente en la sobreproducción de carotenoides en cualquier condición de cultivo, tanto en luz como en oscuridad, es especialmente llamativo y sus mutantes figuran entre los primeros descritos en este hongo (Avalos and Cerdá-Olmedo, 1987). Esta sobreproducción, principalmente de neurosporaxantina, tiene su causa en una desregulación de la expresión de los genes *carB*, *carRA*, *carX* y *carT*, cuyos niveles de ARNm son mucho más elevados que los de la estirpe silvestre (Prado-Cabrero et al., 2007b; Prado-Cabrero et al., 2007a; Thewes et al., 2005). El gen afectado en estos mutantes, denominado *carS*, se ha identificado recientemente en *F. fujikuroi* y *F. oxysporum* (Rodríguez-Ortiz et al., 2013; Rodríguez-Ortiz et al., 2012). De acuerdo con el fenotipo de los mutantes, la proteína CarS actuaría como un represor de la ruta, pero su

mecanismo molecular de acción es aún desconocido. De forma similar a los propios genes de la carotenogénesis, la expresión del gen *carS* es estimulada por luz, aunque los valores máximos de inducción son bastante más bajos. La secuencia proteica presenta similitud con la de la proteína CrgA de *M. circinelloides*, cuyos mutantes tienen un fenotipo similar (Lorca-Pascual et al., 2004; Nicolas-Molina et al., 2008; Silva et al., 2008). CarS y CrgA comparten varios dominios estructurales, entre ellos uno relacionado con ligasas de ubiquitina (Fang et al., 2003). Además, tienen en común un dominio de tipo RING finger, un dominio LON, regiones ricas en glutamina y un dominio de isoprenilación. La identificación del gen *carS* tuvo su origen en el análisis de mutantes insercionales por ADN-T en *F. oxysporum* capaces de producir carotenoides en oscuridad. En dos mutantes investigados, las inserciones no afectaron al marco de lectura del gen *carS*, sino a una larga región intergénica situada aguas arriba. Se sospecha que estas mutaciones pueden guardar relación con elementos reguladores de ARN no codificantes, actualmente bajo estudio.

3. Fotorrecepción

En la naturaleza, la luz no solo es una fuente primaria de energía (fotosíntesis), sino también una importante fuente de información. Entre los procesos no fotosintéticos en los que interviene la luz se encuentra la generación de calor, la visión, el desarrollo o la fisiología de los organismos. La integración de las señales externas ayuda a los organismos a mejorar su competitividad en su medio ambiente (Tisch and Schmoll, 2010). Por todo ello, la gran mayoría de los seres vivos han desarrollado sistemas para detectar la luz y adaptar su actividad según las condiciones.

Los primeros indicios de mecanismos específicos de respuesta a la luz datan de la época de Darwin (1881), cuyas observaciones apuntaba a la existencia de fototropismo en plantas, es decir, de crecimiento dirigido hacia una fuente de luz, aunque también puede darse fototropismo negativo, es decir, en dirección contraria a ella. Hasta la fecha se han estudiado fotorrespuestas en todos los reinos. Se han encontrado ejemplos de empleo de la luz en muy diversos procesos, como son los mecanismos de defensa frente a especies reactivas de oxígeno, la reparación de ADN, la fototaxis, el

desarrollo, la virulencia, el metabolismo (como el ejemplo ya citado de la síntesis de carotenoides), o el ritmo circadiano (Rockwell et al., 2006b). En las plantas, la luz regula procesos tales como el fototropismo, las transiciones entre distintas fases de desarrollo (germinación y floración), la de-etiolación, la apertura y cierre de los estomas, el desarrollo de cloroplastos y otras estructuras de la planta, o sus respuestas defensivas (Kami et al., 2010). En animales, la señal lumínica es especialmente importante en el proceso de visión (Kelber and Lind, 2010) y en el ritmo circadiano (Huang et al., 2011).

Las proteínas encargadas de detectar la luz y transmitir la señal a otras moléculas se conocen como fotorreceptores. Estas proteínas se unen a pequeñas moléculas llamadas cromóforos, que son las que realmente absorben la luz y provocan un cambio conformacional en la proteína que desencadena una respuesta (Briggs and Spudich,

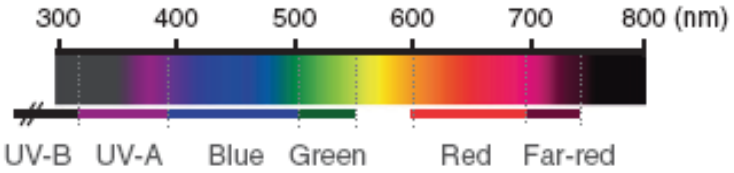

Fig. 17. Espectro de luz visible y radiaciones de longitudes de onda próximas (Kami et al., 2010).

2005). Los fotorreceptores discriminan dos componentes de la señal lumínica: la intensidad y la composición espectral. El espectro de la radiación emitida por el sol se separa en varios segmentos (Fig. 17): radiación ultravioleta (UV-A y UV-B en función de la proximidad de la longitud de onda a la de la luz violeta), luz azul, luz verde, luz roja y radiación infrarroja. En función de la naturaleza de su cromóforo, los fotorreceptores son capaces de detectar luz o radiación de un rango concreto de longitudes de onda. Así, se distinguen fotorreceptores de UV, luz azul/UV, luz verde o luz roja.

3.1. Fotorrespuestas en hongos

Los hongos no son una excepción en la utilización de la señal luminosa como fuente de información. Procesos tan importantes de su desarrollo como la germinación, la esporulación o la formación de estructuras reproductoras, son regulados por la luz (Corrochano, 2007; Idnurm et al., 2010). Es especialmente llamativa la respuesta

fototrópica de los Mucorales, cuyas estructuras de reproducción asexual conocidas como esporangióforos al crecen curvándose hacia la luz (Idnurm et al., 2006). Por otro lado, la luz puede producir estrés oxidativo y daños en el ADN, que explica la frecuente acumulación de pigmentos protectores, como los carotenoides o la melaninas (Moline et al., 2009).

La mayoría de las respuestas estudiadas en hongos se activan por luz azul (revisado en (Herrera-Estrella and Horwitz, 2007; Idnurm et al., 2010; Purschwitz et al., 2006)), aunque se han descrito respuestas reguladas para otros tipos de luz (Herrera-Estrella and Horwitz, 2007; Purschwitz et al., 2006). Algunos ejemplos relevantes son la regulación por luz roja de la esporulación en *A. nidulans* (Mooney and Yager, 1990a), por radiación UV-A en *Alternaria tomato* (Kumagai, 1989), o por luz verde en *Tricometasphaeria turcica* y *Alternaria solani* (Klein, 1992).

La regulación por luz de los procesos se suele producir a nivel de transcripción de los genes implicados (Tisch and Schmoll, 2010). En los últimos se años se han realizado análisis de expresión a nivel genómico (*microarray*) para identificar genes regulados por luz en diferentes organismos. El número de genes objeto de fotoregulación varía entre diferentes especies de hongos, siendo 0,25% en *C. neoformans* (Idnurm and Heitman, 2010), 2,5% en *A. nidulans* (Rodríguez-Romero et al., 2010; Ruger-Herreros et al., 2011), 2,8% en *Trichoderma atroviride* (Rosales-Saavedra et al., 2006) y 3-7% en *N. crassa* (Chen et al., 2009a; Dong et al., 2008; Lewis et al., 2002; Smith et al., 2010). Estos valores confirman la importancia de la luz como señal reguladora en los hongos y su uso para adaptarse y anticiparse a los cambios que ocurran en el medio.

Los primeros estudios moleculares de genes regulados por luz azul se realizaron en *N. crassa* (Crosthwaite et al., 1995; Linden and Macino, 1997; Sommer et al., 1989). En este hongo, algunos genes son capaces de iniciar su activación trascurridos sólo 2 minutos desde la exposición a la luz, lo que implica la existencia de una maquinaria preparada en la célula para responder a esta señal en el menor tiempo posible. Estudios más recientes han demostrado la existencia de genes de respuesta temprana (early light-responsive genes, ELRGs) con niveles máximos de expresión entre 15-45 minutos, y genes de respuesta tardía (late light-responsive genes, LLRGs) con inducción

máxima hasta 90 minutos después del pulso de luz (Chen et al., 2009a). Los ELRGs están relacionados con la necesidad de responder rápido a efectos dañinos de la luz, como la síntesis de pigmentos protectores, mientras que los LLRGs se asocian a ajustes de procesos metabólicos.

A lo largo del día, la intensidad de luz sufre variaciones que pueden afectar a la temperatura y a la disponibilidad de agua. Sin embargo, durante la noche las condiciones son más estables. Los hongos, como la mayoría de los organismos (Bunning and Moser, 1973), han desarrollado sistemas para adaptar su actividad a los ciclos luz/oscuridad del día conocidos como ritmos circadianos. Estos son comparables a un reloj interno que establece la fase del día y la duración de los periodos luz/oscuridad (Heintzen and Liu, 2007). En hongos, se han estudiado en detalles estos mecanismos en *N. crassa* (Brunner and Kaldi, 2008; Dunlap et al., 2007; Tan et al., 2004) y *Aspergillus spp* (Devlin, 2002; Greene et al., 2003; Heintzen and Liu, 2007).

3.2 Fotorreceptores

Como ya se ha mencionado, los fotorreceptores son proteínas capaces de absorber luz a través de un cofactor llamado cromóforo. La proteína sin el cofactor recibe el nombre de apoproteína. Existen pocos tipos de cromóforos (Delbrück et al., 1976), y sirven para clasificar los fotorreceptores en familias:

- Las opsinas unen retinal y absorben luz verde.

- Los fitocromos unen tetrapirroles, como la fitocromobilina o biliverdina, y absorben luz roja.

- Las fotoliasas y criptocromos unen flavinas (FAD o FMN) y absorben radiación UV-A (ultravioleta cercano) y luz azul respectivamente.

- Las proteínas con dominios LOV/PAS unen flavinas (FAD) y absorben luz azul.

3.2.1. Proteínas con dominios LOV/PAS

3.2.1.1. Proteínas White collar

La existencia de mutantes carentes de fotoinducción de la carotenogénesis en *N. crassa* permitió identificar el gen para el primer fotorreceptor, *white collar-1* o *wc-1* (Degli-Innocenti and Russo, 1984a). El nombre del gen se debe al peculiar fenotipo de los mutantes, con carotenoides en la masa aérea de esporas pero no en el micelio, que forma un anillo blanco en la base de los tubos de agar inclinado ("collar blanco"). Esta diferencia se debe a la regulación de la síntesis de carotenoides por luz en el micelio y por desarrollo en los conidios de este hongo, siendo ambos mecanismos de regulación independientes. El análisis genético de los mutantes de fenotipo "white collar" mostró la existencia de un segundo gen, denominado *white collar-2* o *wc-2*. Los mutantes de los genes estructurales de la ruta biosintética de carotenoides se distinguen fácilmente de los mutantes *wc-1* y *wc-2*, ya que producen tanto micelio como conidios albinos.

La riqueza de las fotorrespuestas de *N. crassa* y los numerosos estudios moleculares de los que ha sido objeto han convertido esta especie en un modelo de referencia en fotobiología de hongos y los estudios sobre sus mecanismo de acción han dado lugar a numerosos artículos y revisiones (Corrochano, 2007; Herrera-Estrella and Horwitz, 2007; Liu et al., 2003; Purschwitz et al., 2006). Además de la fotocarotenogénesis (Harding and Turner, 1981), las proteínas WC-1 y WC-2 controlan la regulación por luz azul de la esporulación, el desarrollo de protoperitecios y la orientación de sus picos a la luz, y el ritmo circadiano (Ballario et al., 1996; Degli-Innocenti et al., 1984b; Harding and Melles, 1983; Sargent and Briggs, 1967).

La clonación de los dos genes *white collar* de *N. crassa* (Ballario and Macino, 1997; Linden and Macino, 1997) constituyó un hito en la fotobiología de los hongos, ya que fue el primer sistema fotorreceptor identificado a nivel molecular. El análisis de sus

Fig. 18. Esquema de la organización estructural de la proteína WC-1. Presenta tres dominios PAS (marcados en naranja), de los cuales uno es un dominio LOV sensible a luz (dominio más próximo al extremo amino). El dominio dedo de Zinc (en verde) está situado en el extremo C-terminal (Rodríguez-Romero et al., 2010).

secuencias reveló que WC-1 y WC-2 son factores de transcripción del tipo "dedo de zinc", capaces de unirse al ADN y regular la transcripción de genes diana en el núcleo (Ballario et al., 1996). Estructuralmente, la proteína WC-1 es semejante a las fototropinas de plantas (Fig. 18). Su secuencia polipeptídica contiene un dominio LOV (de "Light, Oxygen, Voltage") sensible a la luz, ya que une el cromóforo (FAD), varios dominios PAS (de "Per-Ant-Sim") relacionados con la interacción entre proteínas, y un dominio "dedo de zinc" de unión a ADN. El dominio LOV es a su vez un dominio PAS de interacción, y está ausente en WC-2, lo que indica que éste último no funciona realmente como un fotorreceptor. El mecanismo de acción por el que el dominio LOV de WC-1 detecta la luz es similar al de las fototropinas (Cheng et al., 2003a; Kennis et al., 2003). Estos dominios presentan una cisteína muy conservada que forma un aducto con la flavina y produce un cambio conformacional en la proteína.

Las proteínas WC-1 y WC-2 interaccionan a través de sus dominios PAS y forman un complejo heterodimérico nuclear denominado "White collar complex" (WCC) o complejo WC, que activa la transcripción de los genes regulados por luz (Cheng et al., 2002; Froehlich et al., 2002; Talora et al., 1999). Muchos de estos genes diana determinan factores de transcripción para otros fines, lo que explica que el complejo WC centralice las distintas fotorrespuestas de *N. crassa*. El complejo WC reconoce específicamente secuencias reguladoras conservadas en los promotores de aquellos genes que responden a luz azul, que se denominan LREs ("Light Responsive Elements") (He and Liu, 2005). En el complejo WC cada proteína lleva a cabo un papel: WC-1 es el elemento fotosensible del complejo y WC-2 estabiliza WC-1 y es responsable de la activación transcripcional de los genes diana a través de su dominio de unión a ADN (Cheng et al., 2002; Cheng et al., 2003b).

Se han encontrado genes ortólogos a *wc-1* en los genomas de muchas especies de hongos pertenecientes a grupos taxómicos muy distantes, lo que sugiere un origen evolutivo común en un antepasado ancestral de estos organismos. En los ascomicetos se ha descrito en *Trichoderma aoroviridae* (Casas-Flores et al., 2004) y *Trichoderma reesei* (Castellanos et al., 2010), *Magnaporte* oryzae (Lee et al., 2006), *Fusarium spp* (Estrada and Avalos, 2008; Kim et al., 2013b; Ruiz-Roldán et al., 2008), *A. nidulans* (Purschwitz et al., 2008) o *Botrytis cinerea* (Canessa et al., 2013). En los basidiomicetos

se ha estudiado en *C. neoformans* (Idnurm and Heitman, 2005) y *Coprinus cinerea* (Terashima et al., 2005), aunque el gen está presente en otros géneros, como *Ustilago*, *Puccinia* o *Sprobolomyces* (Idnurm et al., 2010). También se han identificado genes de tipo *wc-1* en algunos quítridos, como *Allomyces macrogynus* y *Spizellomyces Punctatus* (revisado en (Idnurm et al., 2010). En los zigomicetos se ha encontrado más de una copia para este gen (Fig. 19), hasta tres en el caso de *P. blakeasleeanus* (Idnurm et al., 2006) y *M. circinelloides* (Silva et al., 2008; Silva et al., 2006) y también varias copias de genes ortólogos a *wc-2* (Sanz et al., 2009). Las diferentes copias de genes tipo *wc* en estas especies parecen haber surgido por duplicación y posteriormente cada una de ellas se ha especializado en diferentes funciones. En el caso de *P. blakeasleeanus* uno de los genes *wc-1* se denomina *madA* (Idnurm et al., 2006), y su producto regula tanto la fotocarotenogénesis como la fotomorfogénesis y el fototropismo de los esporangióforos. En *M. circinelloides* se ha investigado en detalle las funciones de sus tres genes tipo *wc-1: mcwc-1a* regula el fototropismo, *mcwc-1c* regula la fotocarotenogénesis y *mcwc-1b* es un regulador adicional de la carotenogénesis (Silva et al., 2006).

Tanto en *N. crassa* como en los mucorales *P. blakeasleeanus* y *M. circinelloides*, la fotocarotenogénesis es mediada por proteínas de tipo WC. Ese no es el caso, sin embargo, de *F. fujikuroi* (Estrada and Avalos, 2008) y *F .oxysporum* (Ruiz-Roldán et al., 2008), cuyos mutantes del gen tipo *wc-1* mantienen la capacidad de inducir la carotenogénesis por la luz. Estos mutantes muestran sin embargo otros fenotipos, como son alteraciones en el metabolismo secundario, la virulencia, la resistencia a UV o la hidrofobicidad.

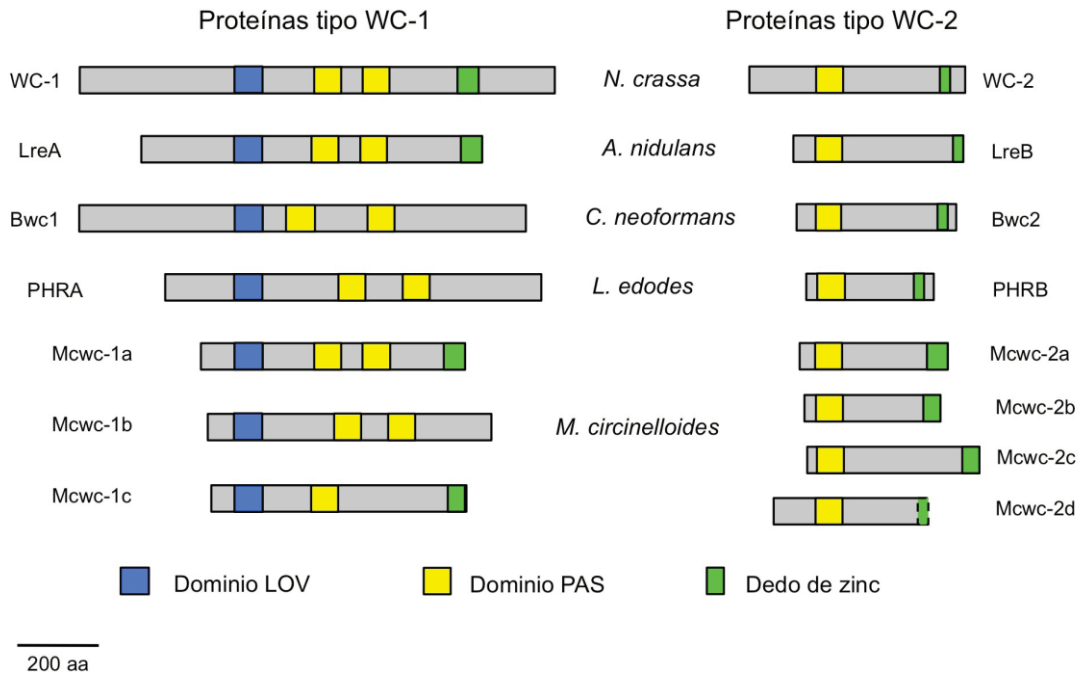

Fig. 19. Proteínas ortólogas de WC-1 y WC-2 en los genomas de hongos ascomicetos (*N. crassa* y *A. nidulans*), basidiomicetos (*C. neoformans y L. edodes*) y zigomicetos *(M. circinelloides*). Los genomas de zigomicetos contienen varias copias de genes tipo *wc-1* y *wc-2*. El tamaño de ambas proteínas es variable entre especies. Las proteínas WC-2 no presentan dominio LOV, y contienen un solo dominio PAS.

3.2.1.2. VIVID

VIVID (VVD) es una proteína de *N. crassa* de pequeño tamaño que consiste únicamente en un dominio LOV/PAS que une FAD no covalentemente (Heintzen et al., 2001) (Fig. 20). Este dominio puede mediar su interacción con el complejo WC (Chen et

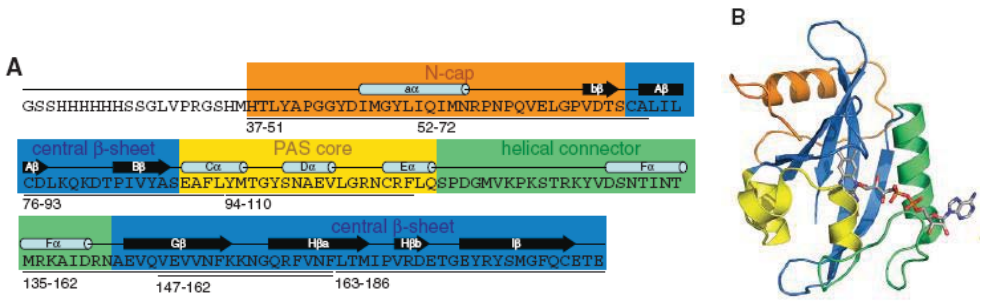

Fig. 20. Estructura de la proteína VVD. (A) Secuencia, dominios y elementos de su estructura secundaria. (B) Modelado de su estructura terciaria. Los colores de las láminas y hélices se corresponden con los colores de la secuencia en A. El esquema incluye la flavina unida a la proteína [Obtenido de (Lee et al., 2014)].

al., 2010; Hunt et al., 2010).

Los datos disponibles indican que VVD es un elemento regulador clave en el mecanismo de fotoadaptación de los genes fotoinducibles en *N. crassa*, participando también en la modulación del ritmo circadiano (Elvin et al., 2005; Schwerdtfeger and Linden, 2003). Su implicación en la fotoadaptación se manifiesta por la pigmentación más anaranjada de los mutantes *vvd*, debida a una fotoinducción de los genes de la carotenogénesis más sostenida en el tiempo. Por otro lado, la adaptación a la luz le permite al hongo responder a cambios en el estímulo luminoso, lo cual explica que los mutantes Δ*vvd* sean insensibles a pulsos de luz de mayor intensidad tras un periodo de iluminación a menor intensidad. VVD se induce a su vez rápidamente por luz a través del complejo WC (Heintzen et al., 2001) y actúa como represor de los genes fotoinducibles, incluso del propio *vvd*, para modular su expresión y en consecuencia la respuesta. El mecanismo molecular por el que actúa es similar al descrito anteriormente para WC-1. Una cisteína (Cys108) de la proteína VVD forma una unión covalente con una flavina (aducto), lo que induce un cambio conformacional en el dominio N-terminal que parece ser esencial para la función represora (Chen et al., 2010; Schwerdtfeger and Linden, 2003).

En *Trichoderma reesei* se ha descrito la proteína ENVOY, ortóloga de VVD y compuesta también solo por un dominio LOV/PAS. Esta proteína juega un papel más importante en este hongo, como demuestra el pobre crecimiento en la luz del mutante nulo del gen (Schmoll et al., 2005b). Además, está implicada en procesos diferentes, como la regulación de la producción de celulasas (Schmoll et al., 2004) o la conidiación. Estudios más recientes han revelado que ENVOY también participa en cascadas de señalización a través de la regulación de proteínas G-triméricas y de los niveles de AMPc (Schmoll, 2011; Schmoll et al., 2009; Seibel et al., 2009) y desempeña un papel importante en el desarrollo sexual (Seibel et al., 2012). Aunque aún no está confirmado su papel como fotorreceptor, los mutantes Δ*env1* presentan alteradas algunas respuestas dependientes de luz y mantienen activa la expresión de genes fotoinducibles más tiempo. Este efecto parece indicar que Env1 actúa como represor de Blr1 y Blr2 (Castellanos et al., 2010), ortólogos de Wc-1 y Wc-2. A pesar de la similitud de secuencias entre ambas proteínas, y otras características regulatorias,

ENVOY no complementa la mutación Δ*vvd* de *N. crassa*, lo que indica que los mecanismos de transmisión de la señal son diferentes en ambas especies.

3.2.1.3. Regulación por el complejo WC

En los últimos años se ha dedicado especial atención al mecanismo molecular por el cual el complejo WC lleva a cabo su regulación. El proceso muestra una notable complejidad, jugando diferentes papeles la fosforilación de las proteínas del complejo, la expresión de genes diana de WCC, y la disociación del aducto Cys/FAD inducido por luz (Gin et al., 2013).

En oscuridad existen niveles basales de las proteínas WC-1 y WC-2 (Talora et al., 1999), siendo más abundantes los de WC-2. WC-1 es una proteína nuclear y WC-2 se encuentra tanto en el núcleo como en el citoplasma (Schafmeier et al., 2006). Al recibir la luz, WC-1 se fosforila progresivamente por medio de una quinasa desconocida. Durante el proceso de fosforilación, primero pasa por un estado poco fosforilado en el que es competente para la activación transcripcional de los genes diana (Franchi et al., 2005; Lee et al., 2000; Schwerdtfeger and Linden, 2000; Talora et al., 1999). Posteriormente alcanza un grado hiperfosforilado que promueve la degradación del propio complejo WC (He and Liu, 2005; Schwerdtfeger and Linden, 2001).

3.2.1.3.1. Proceso de fotoadaptación

En el mecanismo de fotoadapatción participan al menos dos proteínas: VVD y una quinasa (PKC). La información disponible sobre PKC es muy limitada (Arpaia et al., 1999), pero se sabe que ejerce un efecto negativo sobre la transcripción de *wc-1*. Se dispone sin embargo, de mucha más información sobre la función de VVD, que se describe a continuación.

En presencia de un estímulo lumínico, el complejo WC se activa (WC*) por la formación del fotoaducto y se une a las secuencias LRE (Froehlich et al., 2002) de los promotores de los genes de fotoinducción temprana, como *frq*, *vvd y* el propio *wc-1* (ver Fig. 21) (Haldi et al., 2006; Linden and Macino, 1997; Liu et al., 2003). El dímero unido a ADN es inestable y se degradada rápidamente (Schafmeier et al., 2006; Talora et al., 1999). A medida que VVD se acumula y activa por luz, forma homodímeros

(Zoltowski and Crane, 2008) y se une a las subunidades WC-1 del complejo WC* interaccionando a través de los dominos LOV/PAS de ambas proteínas. Así, VVD actúa como represor impidiendo el mantenimiento del complejo WC y por tanto, deteniendo la expresión de sus genes dianas (Chen et al., 2010; Heintzen et al., 2001; Hunt et al., 2010; Malzahn et al., 2010). El complejo WC*/VVD no es transcripcionalmente funcional pero sí muy estable. Sin embargo, el complejo WC-VVD conserva la capacidad de responder a nuevos estímulos de luz de mayor intensidad, a la vez que lo protege de la degradación, convirtiéndose así este "estado adaptado" en un reservorio de complejo WC que se puede liberar lentamente (Gin et al., 2013). Hay que reseñar, sin embargo, que en el estado adaptado los niveles de inducción de los genes genes fotoinducibles son más bajos aún aplicando un pulso de luz de mayor intensidad (Arpaia et al., 1999; Schwerdtfeger and Linden, 2001, 2003).

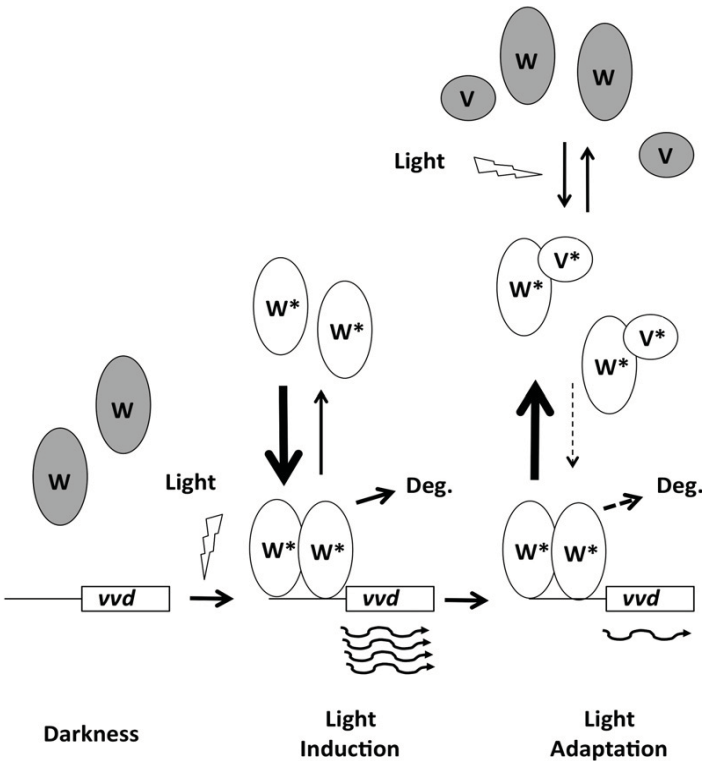

Fig. 21. Modelo del mecanismo molecular de la fotoinducción mediada por el complejo WC y la adaptación. En oscuridad (gris), la proteína WC-1 se activa por luz (blanco*) y dimeriza con WC-2 para formar el complejo WC. Éste se une a los promotores de genes de respuesta a luz temprana, como *vvd* (recuadro blanco) e induce su transcripción. El complejo WC activo es degradado rápidamente. La nueva proteína VVD se activa por luz (*) y heterodimeriza con WC-1 activo (*), bloqueando así la función del complejo WC (Malzahn et al., 2010).

3.2.2.Criptocromos/Fotoliasas

3.2.2.1. Características y clasificación

Los criptocromos y fotoliasas son fotorreceptores capaces de absorber luz azul y radiación UV cercana (UV-A, $\lambda > 315$ nm) y están presentes en todos los reinos, desde arqueas hasta bacterias y eucariotas (Cashmore et al., 1999; Sancar, 1994; Todo et al., 1996). La radiación UV de alta energía, especialmente la UV-C ($\lambda < 280$ nm), induce daños en el ADN, entre los que destacan por su frecuencia los dímeros de timina. Las fotoliasas utilizan la energía procedente de la luz azul y la radiación UV-A para reparar los daños inducidos en el ADN, proceso que se conoce como fotorreactivación (Alejandre-Durán et al., 2003; Berrocal-Tito et al., 1999; Kihara et al., 2004; Sancar, 2003). Los criptocromos poseen similitud de secuencia con las fotoliasas, y presuntamente evolucionaron a partir de éstas. Sin embargo, a diferencia de las fotoliasas, no poseen la capacidad de reparar lesiones en el ADN pero poseen funciones sensoriales (Chaves et al., 2011). Así, a los criptocromos se les han atribuido funciones en regulación del crecimiento, desarrollo, señalización celular, ritmo circadiano y magnetorrecepción (Liedvogel and Mouritsen, 2010).

Filogenéticamente se distinguen seis clases en esta familia: criptocromos de plantas, criptocromos de animales, criptocromos DASH, CPD fotoliasas de clase I, CPD fotoliasas de clase II y 6-4 fotoliasas. Se cree que todas las CPD de clase I y II, criptocromos DASH y criptocromos de plantas proceden de un mismo ancestro CPD. Más tarde, a partir de las CPD I se originaron las 6-4 fotoliasas, que son las más similares a los criptorcomos de animales (Chaves et al., 2011). Los criptocromos DASH (llamados así por su presencia en *Drosophila*, *Arabidopsis*, *Synechocystis*, y *Homo*) fueron descubiertos en 2003 (Brudler et al., 2003) y sus secuencias son más próximas a las 6-4 fotoliasas y a los criptocromos de plantas. Se diferencian sin embargo de los criptocromos de plantas en que poseen actividad de reparación de ADN, aunque con características diferentes a las fotoliasas (Pokorny et al., 2008; Selby and Sancar, 2006). Recientemente se describió una tercera clase de fotoliasas, llamadas CPD III (Oztürk et al., 2008), de las que presuntamente surgieron los criptocromos de plantas (Müller and Carell, 2009). Posteriormente se ha descrito una nueva clase de fotoliasas en bacterias, llamadas FeS-BCPs (Oberpichler et al., 2011). Estas fotoliasas presentan como

cromóforos FAD y un *cluster* de hierro y azufre (Fe-S) y su capacidad para reparar dímeros de timina es muy baja.

Los criptocromos y fotoliasas comparten una región estructuralmente similar (Lin and Todo, 2005). El dominio N-terminal llamado PHR (de "Photolyase-Related-Region") está muy conservado y une dos cromóforos, 5-10 meteniltetrahidrofolato (MTHF) y FAD. Como se muestra en la Fig. 22, el cofactor FAD se une en una cavidad próxima al extremo C-terminal del dominio mientras que el MTHF se localiza en la región N-distal. Además, los criptocromos poseen un dominio C-terminal ausente en fotoliasas y muy variable entre diferentes criptocromos. La estructura terciaria de la proteína se ha estudiado en detalle (Brautigam et al., 2004; Brudler et al., 2003; Park et al., 1995), y consiste en un dominio α/β formado por 5 láminas-β flanqueadas por dos hélices-α, conectado por una región variable a un dominio helicoidal. La región C-terminal está

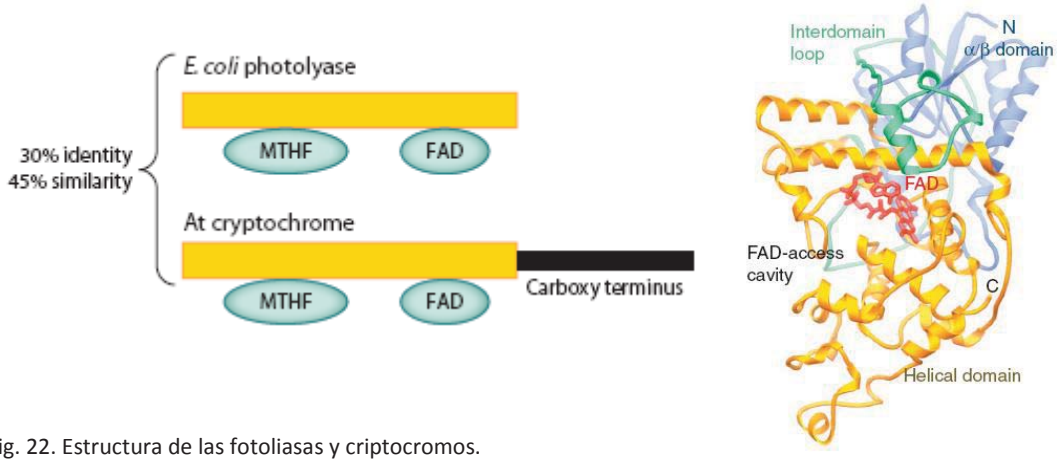

Fig. 22. Estructura de las fotoliasas y criptocromos.
(A) Comparación de la organización de dominios de la fotoliasa de *E.coli* y el criptocromo *cry1* de *A.thaliana*. El dominio N-terminal une MTHF y el C-terminal FAD. Los criptocromos presentan una extensión en el extremo C-terminal (barra negra). (B) Estructura plegada del criptocromo DASH de *Synechosystis* (Lin and Todo, 2005).

poco estructurada y no se han identificado patrones definidos de organización.

3.2.2.2. Mecanismo de acción

Las fotoliasas y criptocromos DASH reparan los dímeros de timinas en el ADN mediante una cadena de transporte de electrones cedidos desde el cromóforo FAD (Lin and Todo, 2005). Para ello es necesario que la proteína se una a la molécula de ADN, "voltee" el dímero de timina y lo deje accesible para el sitio catalítico de unión a

FAD. Las fotoliasas y criptocromos DASH presentan un bolsillo de unión cargado positivamente que facilita la interacción con la doble hélice de ADN y su estabilización una vez "volteado" el dímero de timinas (Müller and Carell, 2009). Para que la cadena de electrones funcione, es necesario que el cromóforo se encuentre en su forma reducida FADH, que es su estado habitual en las células. Se distinguen de esta forma dos etapas en el proceso: fotoactivación y fotorreparación.

- Fotoactivación: La fotoexcitación de la forma no reducida del FAD hace que tome un electrón de un residuo de triptófano cercano al cromóforo para reducirlo totalmente. El electrón cedido es posteriormente regenerado (Aubert et al., 2000).

- Fotorreparación: La energía de excitación del primer cromóforo antena se transmite a la forma reducida ($FADH^-$ → $FADH^{-*}$). Esta molécula puede ceder directamente el electrón al dímero de timinas rompiéndolo en dos monómeros. Una vez reparado, el electrón vuelve a la forma semirreducida FADH° para regenerar FADH. Para los criptocromos DASH, esta reacción sólo se ha descrito en moléculas dañadas de cadena simple (Selby and Sancar, 2006).

En los criptocromos de plantas y animales no se ha esclarecido aún el mecanismo de transducción, pero se cree que el dominio C-terminal puede disparar respuesta por luz azul independientemente del dominio PHR (Wang et al., 2001; Yang et al., 2000).

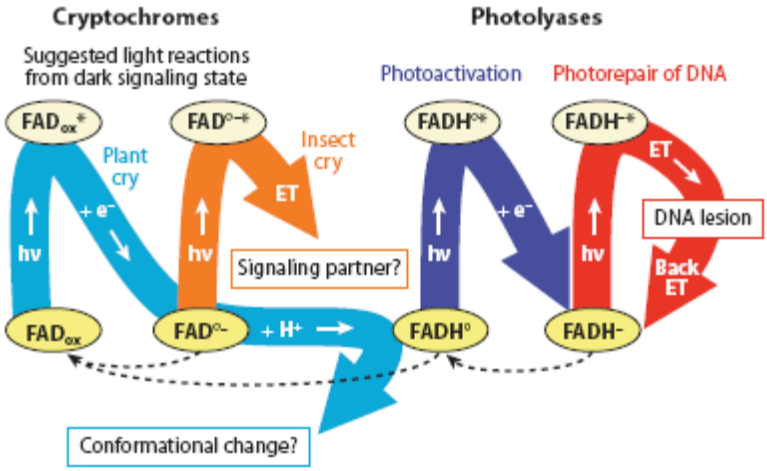

Fig. 23. Mecanismo de fotoactivación y fotorreparación en criptocromos y fotoliasas. En los criptocromos, el estado activo excitable es la forma semirreducida FAD°, que capta un fotón y cede electrones a otra molécula que puede desencadenar una cascada de señalización. En las fotoliasas el estado activo es la forma reducida FADH, que una vez excitada cede electrones al dímero de timina y lo rompe. Para obtener el estado activo de la molécula, se reduce el cromóforo con electrones cedidos desde residuos de aminoácidos cercanos. Las reacciones entre círculos amarillos indican el proceso de fotoactivación (fotorreducción), y la reacción entre círculos amarillos y beig, la excitación del cromóforo (Chaves et al., 2011).

De las reacciones anteriores, los criptocromos sólo llevan a cabo la fotoactivación pero su funcionamiento es sustancialmente diferente. En primer lugar el estado del cromóforo en la célula suele ser oxidado (FAD_{ox}) y la forma activa señalizadora es la semirreducida (FAD°) (Balland et al., 2009; Banerjee et al., 2007). En la Fig. 23 se resumen ambos procesos en criptocromos y fotoliasas.

3.2.2.3. Criptocromos DASH

Los criptocromos DASH se han encontrado en bacterias, plantas, hongos, y animales, incluyendo vertebrados como peces y anfibios (Daiyasu et al., 2004), pero hasta la fecha no se han podido identificar en pájaros o mamíferos. Tampoco se han podido relacionar con ninguna función biológica concreta. En esta Tesis se ha prestado especial atención al único criptocromo DASH presente en el genoma de *F. fujikuroi*, por lo que se describen a continuación en más detalle las características de estas proteínas.

Los criptocromos DASH de *A. thaliana* y *Synechocystis* se unen inespecíficamente a moléculas de ADN de cadena doble y sencilla no dañadas (Brudler et al., 2003; Kleine et al., 2003). Este hecho, junto con la observación de desregulación en *Synechocystis* de los patrones de expresión de ciertos genes en mutantes carentes del criptocromo DASH, o la copurificación en *Vibrio cholerae* y *Ostreococcus tauri* (Heijde et al., 2010; Worthington et al., 2003) de la proteína con ARN, plantean las hipótesis de funciones regulatorias postranscripcionales o de reparación de lesiones en ARN. Sin embargo, estas funciones no concuerdan con la localización observada (cloroplastos y/o mitocondrias) o predicha para algunos de ellos (Chaves et al., 2011). También se ha postulado que estén regulados y relacionados con ritmo circadiano (Facella et al., 2006; Heijde et al., 2010).

Como se ha descrito anteriormente, la organización estructural y el mecanismo de acción por el que los criptocromos DASH actúan es similar al de las fotoliasas. En los casos en los que no actúan como fotoproteínas reparadoras, su función podría ser iniciar una cascada de señalización. *In vivo*, los criptocromos DASH no complementan la actividad de las fotoliasas (Froehlich et al., 2010; Worthington et al., 2003), posiblemente porque son incapaces de unirse a ADN dañado de cadena doble (Hitomi

et al., 2000; Selby and Sancar, 2006). Actualmente, los criptocromos DASH se consideran proteínas con actividad fotoliasa sobre dímeros de timina en moléculas de ADN de cadena sencilla (Selby and Sancar, 2006), aunque en algunos casos concretos también se ha demostrado que son capaces de unirse y reparar dímeros de timina localizados en una cadena doble si ésta presenta un bucle unicatenario (Pokorny et al., 2008). Ello indica que los criptocromos DASH son deficientes en el proceso de volteo del dímero para unirse al sitio catalítico.

3.2.2.4 Fotoliasas y criptocromos en hongos

En comparación con otros grupos taxonómicos, se dispone de poca información sobre los criptocromos y fotoliasas de hongos. Los primeros indicios de funciones sensoriales por proteínas de esta familia en hongos provienen de los estudios de la fotoliasa Phr1 de *T. atroviride* (Berrocal-Tito et al., 2007). En esta especie la fotoliasa es responsable de la reparación de lesiones inducidas por radiación UV, pero también regula su propia expresión, posiblemente por inhibición del complejo WC (llamado aquí LR), y la de otros cuatro genes dependientes de luz azul.

En *A. nidulans* se ha identificado una única proteína bifuncional de esta familia, CryA, con actividad fotoliasa y criptocromo (Bayram et al., 2008a). CryA reprime en presencia de luz el desarrollo sexual, y los mutantes presentan mayores niveles de expresión para genes relacionados con este proceso. Además la mutación dirigida del gen también produce fenotipos no dependientes de luz, como defectos en el crecimiento y biosíntesis de toxinas.

Un caso distinto lo encontramos en *Cercospora zeae-maydis*, que posee dos genes para fotoliasas. El gen *phl1* determina una 6-4 fotoliasa y el gen *cpd1* otra fotoliasa. La mutación de *phl1* elimina la fotorreactivación y desregula la expresión de *cpd1*, así como la de otros genes implicados en reparación de daños en el ADN. Las funciones reguladoras de Phl1 están relacionadas también con la conidiación y con la inducción por luz de la síntesis de cercosporina (Bluhm and Dunkle, 2008a).

En hongos se ha estudiado el papel de los criptocromos-DASH en dos especies, *Sclerotinia sclerotiorium* y *N. crassa* (Froehlich et al., 2010; Olmedo et al., 2010;

Veluchamy and Rollins, 2008). En el primero es el producto del gen *cry1* y participa en la producción de los esclerocios y en algunos aspectos del desarrollo de los apotecios, pero no es la proteína principal en la fotorreactivación. Su gen ortólogo en *N. crassa*, llamado *cry*, está regulado por ritmo circadiano, y su mutación apenas tiene efectos fenotípicos en este hongo, salvo un leve retraso en la entrada en dicho ritmo.

3.2.3. Fitocromos

Los primeros fitocromos se descubrieron en plantas y durante un tiempo se consideraron fotorreceptores exclusivos de este grupo filogenético. La presencia de fitocromos en hongos se propuso en 1979 (Valadon et al., 1979) y en 1990 se asoció por primera vez una respuesta dependiente de luz roja a este tipo de fotorreceptor en *A. nidulans* (Mooney and Yager, 1990a). Los fitocromos son proteínas solubles sensibles a luz roja y radiació infrarroja (Rockwell and Lagarias, 2006a; Rockwell et al., 2006b) y se estructuran en dos módulos esquematizados en la Fig. 24. La señal lumínica es captada por el módulo N-terminal, formado por dominios GAF, PAS (P2) y PHY, el último de los cuales es responsable de la unión del cromóforo. El módulo C-terminal es el responsable de la transducción de la señal y en hongos se compone de un dominio HDK histidina quinasa y un dominio regulador RRD (Purschwitz et al., 2006; Rodríguez-Romero et al., 2010).

Los fitocromos se encuentran en la célula en dos estados interconvertibles: la forma sintetizada, Pr, es sensible a luz roja (600 nm) y su absorción produce un cambio conformacional en el cromóforo que se transmite a la proteína, originando la forma Pfr. Ésta a su vez absorbe radiación infrarroja (730 nm) y devuelve a la proteína a su conformación Pr.

La respuesta a luz roja mejor estudiada en hongos es la represión del desarrollo sexual y activación de la conidiación en *A. nidulans* (Blumenstein et al., 2005; Brandt et al., 2008; Mooney and Yager, 1990a). En esta respuesta no sólo interviene el fitocromo, sino receptores de luz azul (proteínas WC, LreA y LreB) y la proteína reguladora del desarrollo y metabolismo VeA, con quienes interacciona en el núcleo (Purschwitz et al., 2008). En *N. crassa* y *C. neoformans* se han identificado genes para fitocromos, pero sus mutaciones no producen fenotipos detectables en condiciones de

laboratorio (Froehlich et al., 2005; Idnurm and Heitman, 2005). Sin embargo, en *T. reseei* la luz roja induce la expresión de algunos genes, por lo que se sospecha la participación de un fitocromo (Rosales-Saavedra et al., 2006). Cabe deducir, por tanto, que la regulación por luz roja no es un fenómeno inusual en los hongos, aunque hacen falta más estudios para conocer mejor su relevancia.

3.2.4.Opsinas

Las opsinas son un grupo de proteínas de membrana formadas por siete dominios α-hélice transmembranales, que unen el cromóforo retinal a través de un residuo de lisina muy conservado en la séptima hélice (Fig. 25). La absorción de luz verde conlleva la isomerización del retinal de su forma *trans* a *cis,* generando un intermediario que absorbe radiación UV-A. Las opsinas utilizan la luz con fines sensoriales, como ocurre con las rodopsinas visuales de animales (Menon et al., 2001), o bien funcionan como bombas de iones H+ o Cl- impulsadas por la energía obtenida de la luz, siendo el ejemplo mejor conocido la bacteriorrodopsina de arqueas [Revisado por (Spudich et al., 2000b)]. Las opsinas que desempeñan su función como bomba de protones realizan esta reacción muy rápidamente, mientras que en las opsinas sensoriales la reacción es más lenta (Purschwitz et al., 2006).

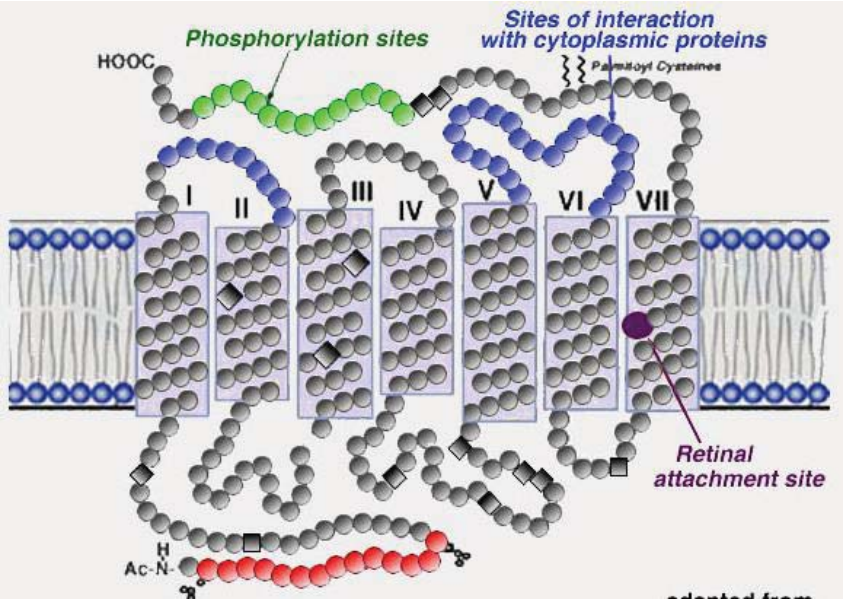

Fig. 25. Estructura secundaria de las opsinas. Los siete dominios transmembrana dejan extremos libres a ambos lados de la membrana. En color se muestran las regiones importantes para su funcionamiento. El sitio de unión al cromóforo, el retinal, se encuentra en la séptima hélice (círculo morado) (adaptado de (Hargrave et al., 1984)).

Numerosos hongos poseen genes para opsinas en sus genomas (Brown, 2004). Los análisis filogenéticos de algunas de ellas revelan un posible origen por transferencia horizontal y un papel más relacionado con bombeo de iones que con respuestas fotosensoriales (Sharma et al., 2006). Además de genes para opsinas fotorreactivas propiamente dichas ("opsin-like proteins" o OLPs), se han encontrado genes para proteínas relacionadas con las opsinas ("opsin-related proteins" o OPRs). Las proteínas de esta subfamilia se caracterizan por carecer del residuo de lisina para la unión del cofactor y se consideran no fotorreactivas (Brown, 2004; Spudich et al., 2000b).

Hasta la fecha se han estudiado pocos genes de opsinas en hongos y sus funciones no ha podido aún ser esclarecidas. Destaca por los varios trabajos publicados la opsina NOP-1 de *N. crassa*, cuya ausencia por mutación dirigida no produce ningún cambio fenotípico detectable alguno bajo las condiciones habituales de cultivo, en luz o en oscuridad (Bieszke et al., 1999). La única alteración fenotípica observada tras un detallado escrutinio fue un aspecto distinto del micelio cuando el mutante Δ*nop-1* crece en un medio de cultivo con inhibidores de bombas de protones mitocondriales en condiciones de iluminación (Bieszke et al., 1999; Bieszke et al., 2007). Además, se ha detectado en el mutante una leve alteración en los niveles de ARNm de los genes implicados en conidiación y carotenogénesis (Bieszke et al., 2007), lo que lleva a su consideración como opsina de tipo sensorial. Por otro lado, la opsina del hongo *Leptosphaeria maculans* está relacionada con bombeo de protones y su actividad es dependiente de pH (Idnurm and Howlett, 2001; Waschuk et al., 2005).

En el genoma de *F. fujikuroi* se encuentran dos genes para opsinas supuestamente fotoactivas, *carO*, situado en el *cluster* biosintético de carotenoides (Prado et al., 2004), y *opsA,* independiente del *cluster* y con una regulación diferente (Estrada and Avalos, 2009a). Además, posee un tercer gen para una ORP, *hspA,* que determina una presunta proteína de choque térmico. La comparación de secuencias indica que *opsA* es ortólogo de *nop-1* de *N. crassa*, careciendo este hongo de un equivalente de *carO*. Desde el punto de vista de sus funciones, ni la mutación dirigida de *carO* (Prado et al., 2004) ni la de *opsA* (Estrada and Avalos, 2009a) produce alteraciones fenotípicas externas en *F. fujikuroi*. Los análisis comparativos de sus secuencias asocian OpsA a una opsina sensorial y CarO a una bomba de protones. Actualmente el grupo de

investigación donde se ha realizado esta Tesis investiga la actividad de ambas proteínas como transportadores de iones (J. García-Martínez, colaboración con U. Terpitz, Universidad de Würzburg, Alemania). Los resultados, aún no publicados, indican que CarO bombea protones activamente a través de la membrana en respuesta a luz verde, mientras que OpsA, por el contrario, es incapaz de desempeñar esta acción.

3.3. Regulación por luz en *Fusarium*

La respuesta dependiente de luz mejor caracterizada en *Fusarium* es la estimulación de la síntesis de carotenoides (Fig. 26B) (revisado en (Avalos and Estrada, 2010)). Esta fotorrespuesta se conoce desde hace muchos años en la especie *Fusarium aquaeductuum*, donde se determinó tanto su cinética de inducción como su espectro de acción (Fig. 26A). Este último muestra que se trata de una respuesta de luz azul, correspondiente al espectro de absorción de una flavoproteína (Rau, 1967a). En congruencia con este dato, la carotenogénesis no es inducida en este hongo por luz roja (Schrott et al., 1982). La fotorrespuesta requiere condiciones aeróbicas para que el fotorreceptor esté en un estado oxidado activo (Rau, 1969). De hecho, la carotenogénesis de *F. aquaeductuum* puede activarse en oscuridad añadiendo agentes oxidantes, como el peróxido de hidrógeno, y se reprime en luz por agentes reductores, como el ditionito o la hidroxilamina (Theimer and Rau, 1970).

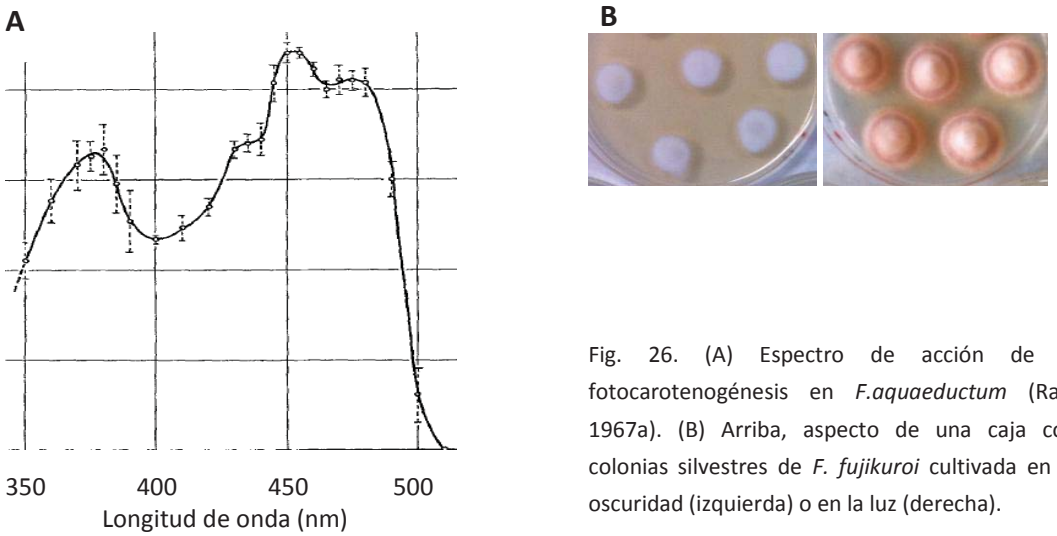

Fig. 26. (A) Espectro de acción de la fotocarotenogénesis en *F.aquaeductum* (Rau, 1967a). (B) Arriba, aspecto de una caja con colonias silvestres de *F. fujikuroi* cultivada en la oscuridad (izquierda) o en la luz (derecha).

Como ya se indicó en el apartado 2.2.2.2.2, la identificación de los genes estructurales de la carotenogénesis en *F. fujikuroi* en los últimos años ha permitido estudiar la fotoinducción de esta ruta a nivel transcripcional. Sin embargo, se desconoce la base molecular de esta fotorrespuesta, y en particular la identidad del fotorreceptor. En el genoma de *F. fujikuroi* se han identificado genes para fotorreceptores pertenecientes a los grupos descritos en los apartados anteriores (Avalos and Estrada, 2010). Así su proteoma incluye un fitocromo, dos opsinas, dos proteínas White collar (tipo 1 y 2), una proteína VVD, una fotoliasa y dos criptocromos.

En *N. crassa* la inducción por la luz de la carotenogénesis, tanto a nivel de expresión de los genes estructurales como de síntesis de carotenoides, se pierde totalmente en los mutantes *wc-1* y *wc-2* (Harding and Turner, 1981) por lo que dicho proceso es mediado por el complejo WC. Además, como ya se ha indicado anteriormente, la proteína VVD participa en la fotoadaptación de esta fotorrespuesta. En *F. fujikuroi* y *F. oxysporum*, sin embargo, los mutantes de su único gen *white collar* conservan la fotoinducción de la síntesis de carotenoides (Fig. 27A)(Estrada and Avalos, 2008; Ruiz-Roldán et al., 2008), por lo que se espera la participación de otros fotorreceptores. A pesar del alto grado de similitud estructural entre las proteínas WC-1 de *N. crassa* y su ortólogo WcoA de *F. fujikuroi,* hay diferencias destacables en cuanto a su regulación, ya que el gen *wc-1* es fotoinducible y su expresión está autorregulada por el compejo WC (Ballario et al., 1996), mientras que los niveles de ARNm para *wcoA* no varían significativamente de oscuridad a luz (Estrada and Avalos, 2008). Además, la mutación del gen *wcoA* elimina la fotoactivación de los dos genes de las opsinas, pero afecta solo parcialmente a la de los genes estructurales de la carotenogénesis(Fig. 27B) [revisado en (Avalos and Estrada, 2010)].

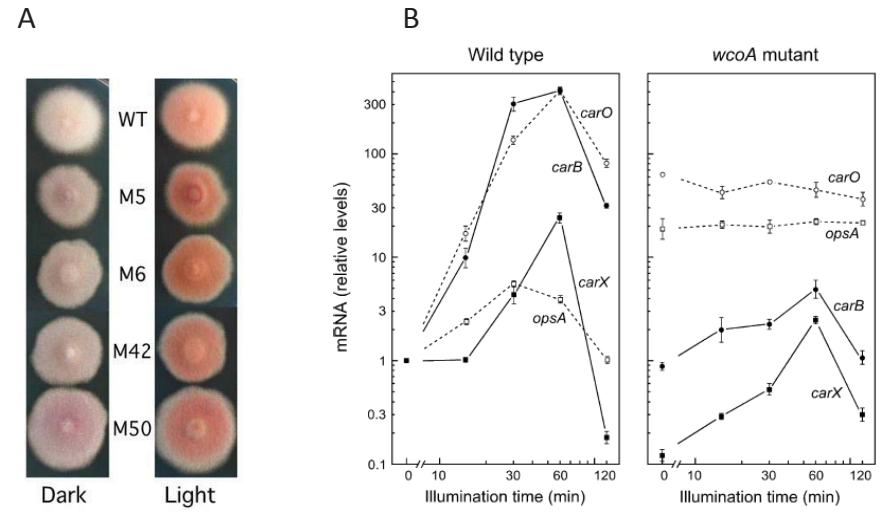

Fig. 27. Regulación por WcoA en *F. fuikuroi*. (A) Fenotipo de cuatro mutantes ΔwcoA en comparación con el silvestre. A los 4-5 días de crecimiento en luz, los mutantes adquieren la pigmentación anaranjada característica de los carotenoides (Estrada 2008). (B) Regulación de la expresión. WcoA es responsable de la fotoinducción observada en las opsinas, y parcialmente de los genes de la carotenogénesis (Avalos and Estrada, 2010).

En *N. crassa*, el complejo WC está involucrado en otras fotorespuestas, incluyendo la regulación del ritmo circadiano (Dunlap and Loros, 2004; Heintzen and Liu, 2007), pero este fenómeno regulado por luz no se ha demostrado aún en las especies del género *Fusarium*. Por otro lado, se sabe poco aún del papel de la proteína WcoB de *F. fujikuroi* ortóloga a Wc-2, aunque se asume que interacciona con WcoA para formar un complejo WC. Datos no publicados (Wiemann 2011, 26ª Conferencia de Genética de hongos) sugieren que tanto WcoA como WcoB son responsables de la inducción inmediata de la síntesis de carotenoides tras cortos impulsos de luz.

Los estudios realizados en este grupo (Estrada and Avalos, 2008) han aportado nueva información relacionada con las funciones de WcoA en *F. fujikuroi*. WcoA regula procesos independientemente de la luz, como la hidrofobicidad del micelio o la conidiación. Además esta proteína está implicada en la regulación del metabolismo secundario, como indica las alteraciones en los mutantes *wcoA* en la síntesis de giberelinas y bicaverinas.

Otros fotorreceptores estudiados en *F. fujikuroi* son las opsinas, ya mencionadas en el apartado 3.2.4, y la fotoliasa de tipo CPD Phr1, estudiada por el grupo de la Dra. Bettina Tudzinsky (Universidad de Münster, Alemania). Los resultados, aún no

publicados (Wiemann 2013, 27ª Conferencia de Genética de Hongos), indican que esta proteína es responsable de la fotorreactivación y que está regulada por el complejo WC. Otro criptocromo, Phl1, similar al estudiado en *C. zeae-maydis,* podría estar implicado en la expresión de los genes de la carotenogénesis, pero tampoco hay resultados definitivos. En cuanto a las opsinas, CarO y *OpsA* (Estrada and Avalos, 2009a; Prado et al., 2004), sus genes son fotoinducibles, especialmente *carO*, y su expresión es totalmente dependiente de WcoA. Los niveles de inducción de *carO* son similares a los del *cluster* de la carotenogénesis, pero los de *opsA* son significativamente menores, aunque los niveles de ARNm en oscuridad son más elevados. El diferente papel de WcoA en la expresión de las opsinas y los genes estructurales de la carotenogénesis sugiere diferencias regulatorias en la expresión de los genes de la opsinas y los de la síntesis de su cromóforo, el retinal (Estrada and Avalos, 2009a).

En conclusión, los trabajos realizados hasta la fecha han proporcionado información interesante pero parcial sobre las funciones de los fotorreceptores de *Fusarium*, y de momento han dejado sin resolver la identidad del fotorreceptor(es) responsable(s) de la respuesta a la luz mejor conocida de este hongo, la fotoinducción de la carotenogénesis. A pesar de los paralelismos encontrados con *N. crassa* en la síntesis de carotenoides, las diferencias en la regulación de *F. fujikuroi* y sus posibles implicaciones en su complejo metabolismo secundario proporcionan especial interés a la fotobiología de éste hongo, objeto de esta Tesis.

OBJETIVOS/AIMS

OBJETIVOS

1. Estudiar del papel biológico del criptocromo DASH CryD y de la flavoproteína VvdA en *F. fujikuroi* y sus posibles funciones en la regulación por luz en este organismo.

2. Determinar el grado de participación de estas fotoproteínas en el sistema sensorial que media la regulación por luz de la carotenogénesis en *F. fujikuroi*, y su posible relación con el fotorreceptor de la familia White Collar WcoA.

AIMS

1. To study the biological role of the DASH cryptochrome CryD and the flavoprotein VvdA in F. fujikuroi and their possible roles in the regulation by light in this organism.

2. To determine the degree of involvement of these photoproteins in the sensory system that mediates the regulation of carotenogenesis by light in *F. fujikuroi* and its possible relationship with the White Collar photoreceptor WcoA.

CHAPTER I

Light-dependent functions of the *Fusarium fujikuroi* CryD DASH cryptochrome in development and secondary metabolism.

Published in Applied Environmental Microbiology 2013

INTRODUCTION

Filamentous fungi are a natural source for a large diversity of chemical compounds (Hoffmeister and Keller, 2007). Among them stand out many species of the genus *Fusarium*, a wide group of phytopathogenic fungi able to produce an extense array of metabolites and mycotoxins (Desjardins and Proctor, 2007a). A representative example is *Fusarium fujikuroi,* well known for its capacity to produce gibberellins (GAs), growth-promoting plant hormones with biotechnological applications (Rademacher, 1997). This fungus produces many other compounds (Avalos et al., 2007), including pigments that provide characteristic colors to the mycelia. Under certain conditions the *F. fujikuroi* cultures become reddish due to the synthesis of bikaverin, a polyketide pigment with antibiotic properties against protozoa and other organisms (Limón et al., 2010). When grown in the light, surface-grown mycelia acquire a characteristic orange pigmentation due to the synthesis of carotenoids, with the xanthophyll neurosporaxanthin as major component (Avalos and Cerdá-Olmedo, 1987). The enzymatic genes for the synthesis of GAs [reviewed in (Tudzynski, 2005)], bikaverin (Wiemann et al., 2009) and carotenoids (Avalos and Estrada, 2010) have been identified, and, with the exception of some genes of the carotenoid pathway, they are organized in transcriptionally co-regulated clusters.

Productions of GAs, bikaverins and carotenoids are modulated in *F. fujikuroi* by diverse environmental cues. Nitrogen availability is a major key regulatory signal in the control of secondary metabolism by this fungus, in which the three mentioned pathways are transcriptionally induced by nitrogen starvation (Rodríguez-Ortiz et al., 2009; Tudzynski, 2005; Wiemann et al., 2009). Considerable efforts have been devoted to identify the proteins involved in the regulation of GA and bikaverin biosynthesis. In the case of GA production, a central role is played by the transcription factor AreA, needed for the expression of the structural genes (Mihlan et al., 2003; Schönig et al., 2008; Tudzynski, 2005). AreA activity is modulated by ammonium availability, probably through the detection of its assimilation product glutamine (Muñoz and Agosín, 1993).

Mutations of other genes involved in nitrogen assimilation, the glutamine synthetase gene *glnA* (Teichert et al., 2004) and the major ammonium permease gene *mepB* (Teichert et al., 2008), produce down and up regulation of the GA genes, respectively, demonstrating their participation in the nitrogen regulatory mechanism. In contrast, bikaverin production is repressed by nitrogen in an AreA-independent manner, and it is modulated by other regulatory proteins, including those encoded by two genes present in the *bik* cluster (Wiemann et al., 2009). The biosynthesis requires acidic pH (Giordano et al., 1999), indicating the participation of the pH regulatory protein PacC, whose deletion results in up-regulation of the *bik* genes (Wiemann et al., 2009). Functional loss of the bZIP transcription factor MeaB results in a mild upregulation of the bikaverin genes in high nitrogen conditions, and this effect is significantly enhanced in the absence of AreA (Wagner et al., 2010), reflecting the complexity of the regulatory network governing this pathway.

Light is an environmental signal widely used by fungi to modulate developmental and metabolic processes (Corrochano and Garre, 2010; Idnurm et al., 2010). As indicated above, light induces the synthesis of carotenoids in *F. fujikuroi* (Avalos and Cerdá-Olmedo, 1987), a response similar to that observed in other fungi, as *Neurospora crassa* (Navarro-Sampedro et al., 2008) or *Phycomyces blakesleeanus* (Salgado et al., 1991). Additionally, light stimulates gibberellin biosynthesis in some *F. fujikuroi* strains (Avalos and Estrada, 2010), but this response is of a lesser magnitude compared to photocarotenogenesis and has barely been investigated. In *N. crassa*, a well-known photobiology model, most photoresponses are mediated by the White Collar (WC) complex (Chen et al., 2010), a heterodimer formed by the proteins WC-1 and WC-2 (Ballario and Macino, 1997). Upon illumination, the WC complex binds upstream promoter sequences of light-regulated genes, including those of the carotenoid pathway, to induce their transcription. The photoreception function in the complex is played by WC-1 through its LOV flavin-binding domain (He et al., 2002). Similar WC complexes were found to play diverse photoreception roles in other fungi (Corrochano, 2007). Contrary to what was expected, the mutants of the only WC-1 like gene of *F. fujikuroi* [*wcoA,* (Estrada and Avalos, 2008)] or *Fusarium oxysporum*, [*wc1*, (Ruiz-Roldán et al., 2008)] conserved the photoinduction of the carotenoid pathway,

pointing to the participation of a different photoreceptor system. However, the *wcoA* mutation led to unexpected changes in the production of different metabolites of *F. fujikuroi*, including a sharp decline in the production of GAs irrespective of light (Estrada and Avalos, 2008), preventing conclusions to be drawn about the possible role of the WcoA protein on GAs photostimulation.

No information is available on the photoreceptors involved in the known Fusarium photoresponses. The analysis of the freely accessible *Fusarium* genomes reveals the presence of several genes for presumed photoreceptors. These include a DASH-cryptochrome (Avalos and Estrada, 2010) and a second cryptochrome gene related to plant cryptochromes, currently under investigation (P. Wiemann and B. Tudzysnki, unpublished). Cryptochromes are blue/UV-A light photoreceptors which probably evolved from photolyases, enzymes able to use light as an energy source to repair UV-B-induced lesions (Chaves et al., 2011; Sancar, 2003). Cryptochromes typically have a N-terminal photolyase-related domain able to bind two chromophores, FAD and 5,10-methenyltetrahydrofolate (MTHF)/pterin, followed by a long C-terminal domain absent in photolyases, reported to play regulatory roles related to light control of growth, development, cell signaling and circadian rhythm in different taxonomic groups (Chaves et al., 2011).. The DASH-cryptochromes (abbreviated hereafter as cry-DASH) are a subgroup in this family, which differs from cryptochromes in the ability to repair single stranded DNA [reviewed by Chaves et al. (Chaves et al., 2011).] and the lack of the long carboxy extension. The unexpected role of WcoA on secondary metabolism (Estrada and Avalos, 2008) and the lack of knowledge on the functions of cryptochromes in fungi has led us to perform a functional analysis of the *F. fujikuroi* cry-DASH gene, that we called *cryD*. Expression of *cryD* was induced by light in the wild type but not in *wcoA* mutants, and lack of a functional *cryD* allele led to several light-dependent effects, such as morphological alterations, macroconidia production under nitrogen starvation, and enhanced bikaverin biosynthesis. As formerly found with the *wcoA* mutation, the *cryD* mutants kept the induction of the synthesis of carotenoids in the light, but they did not exhibit photo-stimulation of GA production. Our results provide new insights into the biological functions of DASH cryptochromes in fungi with the first example of a role in the regulation of secondary metabolism.

RESULTS

1. Sequence analysis of fungal cry-DASHs genes

Genes encoding putative cry-DASHs are found in different taxonomic groups, from filamentous fungi to animals, plants, algae, bacteria and archaea. The analysis of the three publicly available *Fusarium* genome databases indicated the occurrence of a single cry-DASH encoding gene in this genus, that we named *cryD*. A Clustal comparison of the predicted CryD from *Fusarium verticillioides* with representative cry-DASHs from different origins showed the conservation of the characteristic photolyase domain (Fig. I-1A). Irrespective of this overall domain structure, different cry-DASH sequence patterns were observed, with evident divergences between the various considered fungal taxonomic groups, ascomycetes, basidiomycetes and zygomycetes. These differences were further supported by a phylogenetic analysis of these and other cry-DASHs from different phyla. The tree displayed in Fig. I-1B shows that cry-DASHs from ascomycete fungi differ in their phylogenetic origin from those of other taxonomic groups, including the basidiomycete and zygomycete fungi. A more detailed analysis of ascomycete CRY-DASh sequence is shown in Fig. I-2A . This difference would be compatible either with a single ancestral separation or with an independent origin of ascomycete cry-DASHs from those found in other species.

Comparison of fungal cry-DASHs showed the occurrence of a carboxy-terminal extension in ascomycetes, mostly absent in the analyzed cry-DASHs from other fungal phyla. Comparison of eight of such extensions from different ascomycetes revealed that they are variable in sequence and length, from 44 to 115 amino acids in the cases investigated compared to the *Mucor circinelloides* (156465) and *Ustilago maydis* (UM05917) orthologues. These extensions showed low sequence conservation, except for a preference for glycine in several positions (Fig. I-2B).

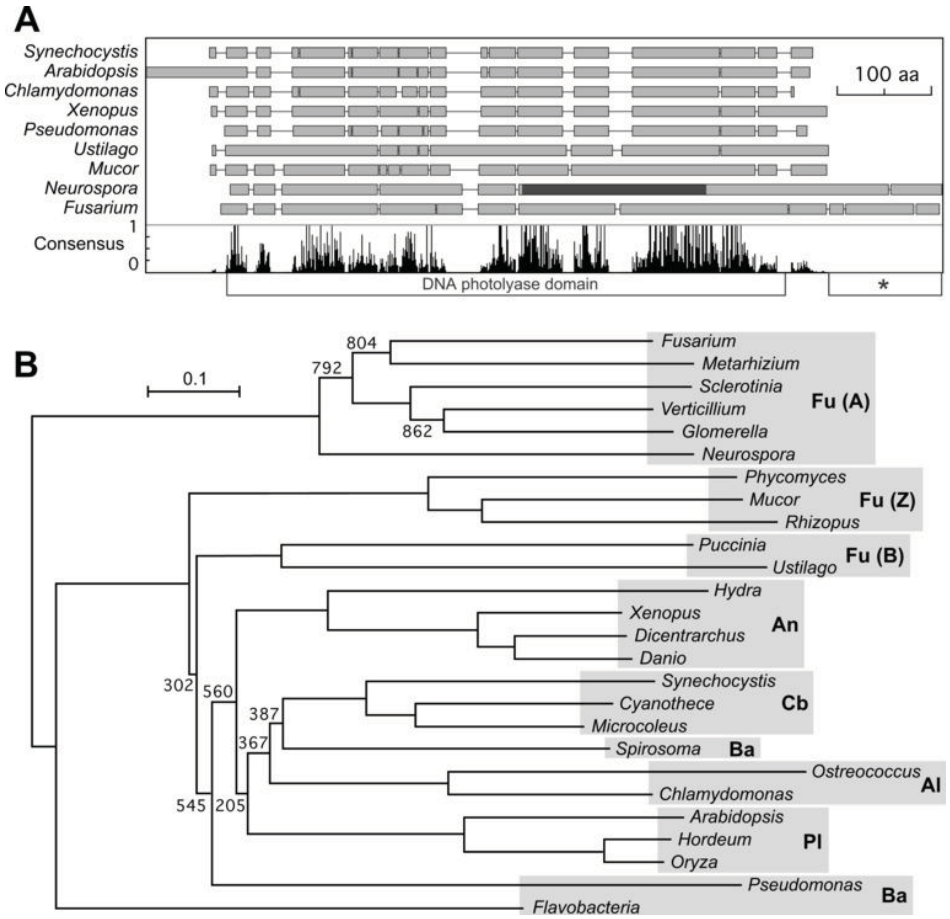

Fig. I-1. Sequence analysis of cry-DASH proteins. (A) Simplified representation of the Clustal comparison between cry-DASH proteins from *F. verticillioides* and eight species from representative taxonomic groups. Breaks between the boxes represent gaps introduced by the Clustal program to facilitate alignment. The diagram below plots the presence of the consensus amino acids as given by the Clustal analysis. The photolyase domain is represented below the plot. The asterisk indicates the carboxy extension displayed in Fig. S2 of supplemental material. (B) Neighbor-Joining phylogram of 26 representative cry-DASH proteins. Reliability of clusters was evaluated by bootstrapping with 1000 replicates (bootstrap values are indicated). Genus names stand for the following species and protein accession numbers: *Fusarium verticillioides* (FVEG 02442), *Metarhizium anisopliae* (EFZ01174), *Sclerotinia sclerotium* (SS1G 05163), *Verticillium albo-atrum* (VDBG 00705.1), *Glomerella graminicola* (EFQ26657), *Neurospora crassa* (NCU 00582), *Phycomyces blakesleeanus* (85761), *Mucor circinelloides* (156465), *Rhizopus oryzae* (RO3G_16297.3), *Puccinia graminis* (XP 003326630), *Ustilago maydis* (UM05917), *Hydra magnipapillata* (XP 002166544), *Xenopus laevis* (NP 001084438), *Dicentrarchus labrax* (CBN81995), *Danio rerio* (NP 991249), *Synechocystis sp.* (P77967), *Cyanothece sp.* (YP 002375679), *Microcoleus chthonoplastes* (ZP 05026729), *Spirosoma linguale* (YP 003390944), *Ostreococcus tauri* (Q5IFN2), *Chlamydomonas reinhardtii* (XP 001701871), *Arabidopsis thaliana* (Q84KJ5), *Hordeum vulgare* (BAK06380), *Oryza sativa* (NP 001058278), *Pseudomonas fulva* (YP 004472278), and *Flavobacteria bacterium* (ZP 03701378). The shaded areas group the species by taxonomic categories. The labels stand for fungi (Fu, in which ascomycetes [A], basidiomycetes [B] and zygomycetes [Z] are distinguished), cyanobacteria (Cb), bacteria (Ba), algae (Al), animals (An) and plants (Pl).

A

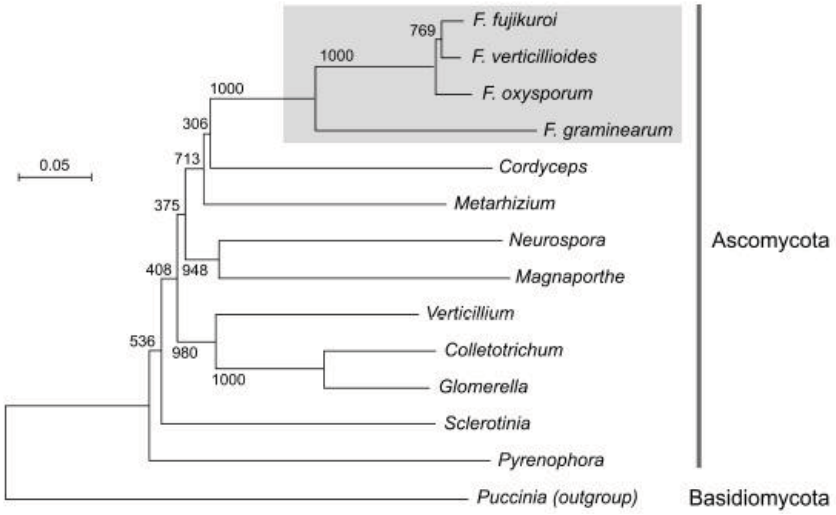

B

Fig. I-2. (A) Phylogram of 13 cry-DASH proteins from ascomycete species. The three cry-DASH sequences available from *Fusarium* genomes and CryD from *F. fujikuroi* are also included (grey box). Genus names stand for the following species and protein accession numbers: *Fusarium* group: *F. fujikuroi* (HE650104, this work), *F. verticillioides* (FVEG_02442), *F. oxysporum* (FOXG_03570), *F. graminearum* (FOXG_03570). Other ascomycetes: *Cordyceps militaris* (EGX96119), *Metarhizium anisopliae* (EFZ01174), *Neurospora crassa* (NCU 00582), *Magnaporthe oryzae* (XP_366926), *Verticillium albo-atrum* (VDBG 00705), *Colletotrichum higginsianum* (CCF46101), *Glomerella graminicola* (EFQ26657), *Sclerotinia sclerotium* (SS1G 05163), *Pyrenophora tritici-repentis* (XP_001936482). The sequence from a cry-DASH protein of the basidiomycete *Puccinia graminis* (XP_003326630) was used as an outgroup. (B) Clustal comparison of the carboxy-terminal extension in the cry-DASH protein from *F. verticillioides* and seven additional ascomycete species. Amino acids present in at least six of the eight protein segments are shaded in black, and those present at least in three of them are shaded in grey. The number of residues of each carboxy-terminal extension is indicated at the right end. Starting point of the extension was arbitrarily defined as the end of the homologous sequence of the *U. maydis* protein UM05917 (Fig. 1A)

2. Identification and expression of the *F. fujikuroi cryD* gene

The predicted proteins encoded by the *cryD* genes of *F. verticillioides* (FVEG_02442) and *F. oxysporum* (FOXG_03570) show a high degree of identity (94%), but the one encoded by the orthologous gene in *F. graminearum* (FGSG_08852) exhibits an unexpectedly high degree of divergence (68% conserved positions along its 678 aa compared to the 715 aa of FVEG_02442 and FOXG_03570). Based on the high sequence conservation between the two cry-DASH genes and the 5' and 3' neighbor genes in *F. verticilli*oides and *F. oxysporum*, two primer sets were designed from sequence alignments and used to amplify by PCR 1.60 kb and 1.28 kb products of *F. fujikuroi* DNA, located upstream and downstream of the *cryD* coding sequence, respectively. Once their sequence analyses confirmed the cloning of the correct DNA segments, two new primers were designed to amplify by PCR and clone the *cryD* coding sequence. Assembly of the obtained sequences led to define the whole *F. fujikuroi cryD* gene sequence, including upstream and downstream non-coding sequences, which was deposited at the EMBL gene database with accession number HE650104. As expected, the *F. fujikuroi cryD* gene was highly similar to those of *F. verticilli*oides and *F. oxysporum*, with that of *F. verticillioides* as its closest relative (93.5 % and 95 % identity at coding DNA and protein sequence, respectively; Fig. I-3)

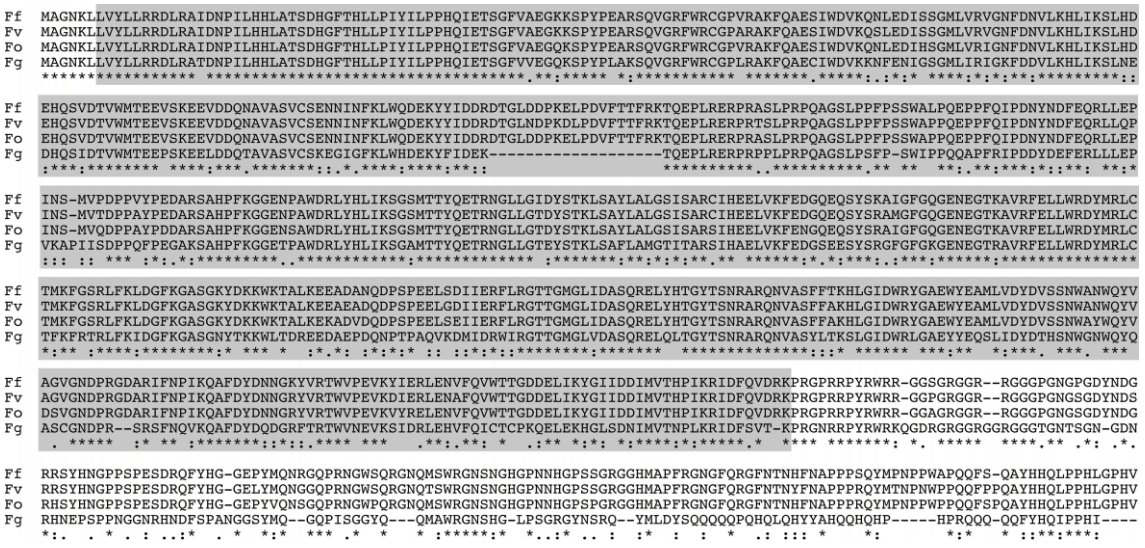

Fig. I-3. CLUSTAL alignment of CryD of *F. fujikuroi* and the three cry-DASH sequences from the available *Fusarium* enomes. Ff: *F. fujikuroi* (HE650104, this work), Fv: *F. verticillioides* (FVEG_02442), Fo: *F. oxysporum* (FOXG_03570), Fg: *F. graminearum* (FGSG_08852). The DNA photolyase domain is indicated in grey.

The availability of the *cryD* sequence allowed design of primers for qRT-PCR expression analyses. In contrast to the lack of significant light-induction formerly reported for the White Collar gene *wcoA* (Estrada and Avalos, 2008), the *cryD* mRNA levels increased rapidly following illumination, reaching nearly 100-fold induction after 1h of light treatment, and declining slowly afterwards (Fig. I-4A). In contrast, no significant *cryD* photoinduction was recognizeded in *ΔwcoA* mutants, pointing to WcoA as a key photoreceptor in *cryD* photoregulation. Furthermore, *cryD* mRNA levels in the dark were about ten-fold lower in the *ΔwcoA* mutants than in the wild-type, indicating a more general role of WcoA as a positive regulator of *cryD* expression (Fig. I-4B).

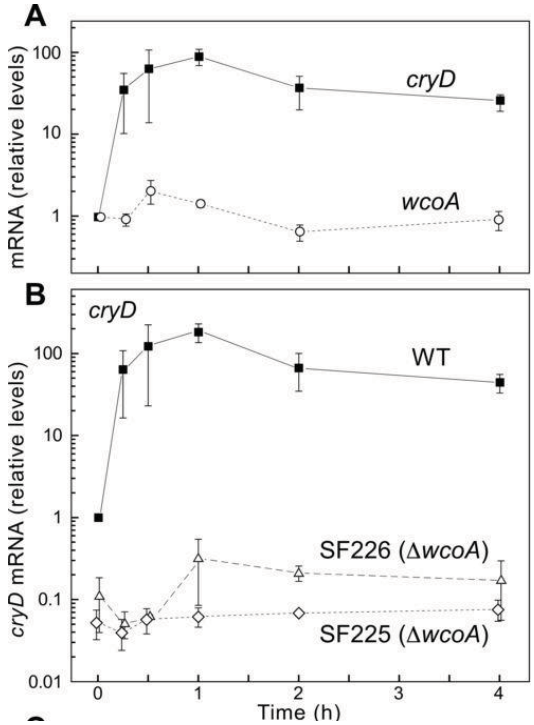

Fig. I-4-Expression of the *cryD* gene. (A) Effect of light on *cryD* and *wcoA* mRNA levels in wild type *F. fujikuroi*. The data show real-time RT-PCR analyses of total RNA samples from the wild type grown in the dark or exposed for 15 min, 30 min, 1 h, 2 h or 4 h to 7 W m^{-2} white light. Relative levels are referred to the values for each gene in the dark. All data show means and standard deviations for three measurements from three independent experiments. (B) Relative levels of mRNAs upon same time of illuminatio for gene *cryD* in two white collar mutants mutants (*SF226 y SF225S*) compared to the wild type. The mRNA levels were referred to those of the wild type in the dark.

The *cryD* photoinduction resembled that of the genes coding for enzymes in the carotenoid pathway, such as *carRA* or *carB* (Estrada and Avalos, 2009a). These genes are also upregulated in the dark in *carS* carotenoid-overproducing mutants (Díaz-Sánchez et al., 2011a; Prado et al., 2004). However, four independent *carS* mutants contained similar *cryD* mRNA levels in the dark to those of the wild-type (Fig. I-5), indicating that *cryD* gene expression is not under control of the CarS-mediated repressing mechanism.

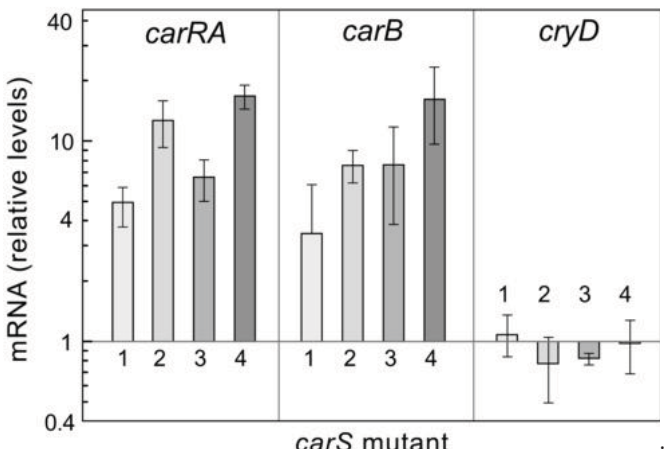

Fig. I-5. *cryD* expression in carotenoid overproducing mutants (*carS*).Relative levels of mRNAs for genes *carRA*, *carB* and *cryD* in four *carS* mutants grown in the dark, numbered 1-4 (1: SF114; 2: SF115; 3: SF116; 4:SF134). The mRNA levels were referred to those of the wild type under the same conditions.

3. Generation of *ΔcryD* mutants

The 1.60 kb and 1.28 kb DNA segments that included sequences upstream and downstream of the *cryD* coding region were used to construct a *cryD* deletion plasmid in which 1.3 kb of the *cryD* coding sequence was replaced by a Hyg^r cassette (Fig. I-6A). Incubation of wild-type *F. fujikuroi* protoplasts with this plasmid led to the isolation of five transformants, denominated T1 to T5, which were subcultured from uninucleate microconidia under selective conditions to ensure homokaryosis. Two of them, T1 and T3, exhibited a different phenotype than wild type when grown at 30°C under light but not in the dark (Fig. I-7A). Accordingly, they were suspected to have undergone a replacement of the wild type-*cryD* gene. To check the occurrence of the wild type *cryD* allele, genomic DNA of the wild-type, T1, T3, and one of the transformants exhibiting a wild-type phenotype, T5, were digested with different restriction enzymes and hybridized by Southern-blot with the *cryD* DNA segment absent in the deletion plasmid. The film showed clear signals in the wild type and in T5, but no signals in T1 and T3 (Fig. I-6B). PCR analyses confirmed the presence of the hyg_r cassette and the replacement of the wild type *cryD* gene in the transformants T1 and T3 (Fig. I-6*C*). The latter is shown by the size of the PCR product obtained with DNA from transformants T1 and T3 with primer set 5 (see Table I-1 in matherials and methods,; see the gray triangles in Fig. I-6A and the result in the bottom graph of Fig.I-6C), which coincides

with the 5,4-kb size expected from the replacement. We conclude that T1 and T3 lack a functional *cryD* gene, and therefore were subjected to a detailed phenotypic analysis. They are referred hereafter as Δ*cryD* mutants SF236 and SF237.

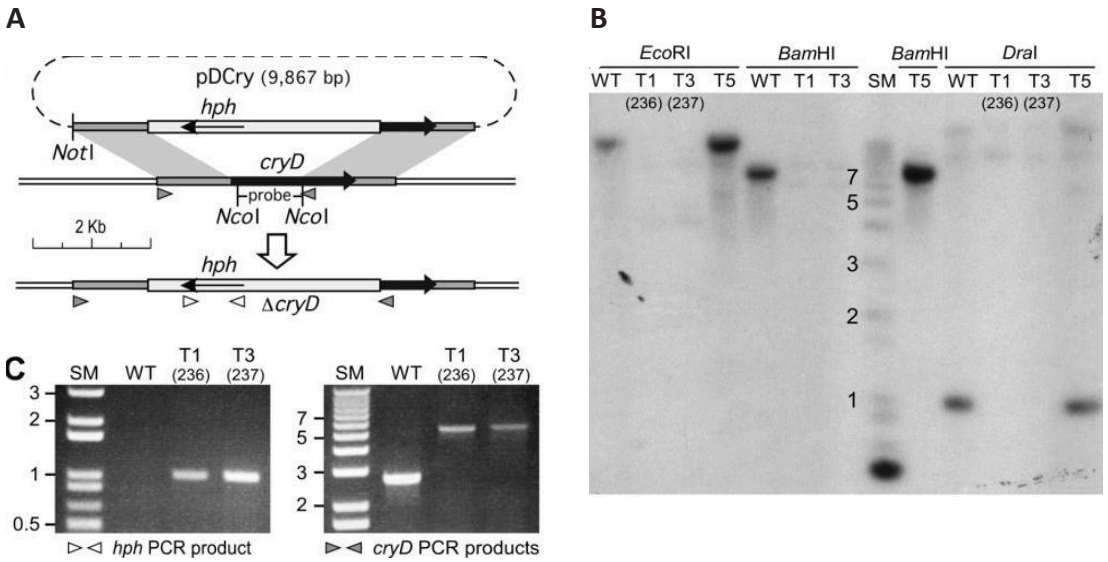

Fig. I-6. Generation of targeted Δ*cryD* mutants. (A) Schematic representation of the gene replacement event leading to the generation of hygR Δ*cryD* transformants. The black arrow represents the *cryD* coding sequence. Plasmid pDCry contains the hygR cassette with the *hph* gene (pale grey box) surrounded by upstream and downstream *cryD* sequences. The recombination events leading to *cryD* disruption and the resulting physical map in the generated Δ*cryD* mutants occur in the shaded DNA segments. The *Not*I and *Nco*I restriction sites used to linearize pDCry and to obtain the probe for the Southern blot, respectively, are indicated. (B) Southern blot of genomic DNA from the wild type (WT) and transformants T1, T3 and T5 digested with the indicated restriction enzymes and hybridized with the *cryD* probe indicated above. SM indicates size markers (relevant sizes in kb are shown). (C) Agarose gel electrophoresis of PCR amplification products obtained from DNA samples from the wild type and transformants T1 and T3 with the primer sets indicated below (see primer locations on panel A). Left: Result with *hph* primer set (hygR resistance, primer set 4 in Table I). The expected PCR product (1 kb) indicates the presence of the *hph* gene. Right: Result with *cryD* primer set for sequences surrounding the deleted DNA segment in plasmid pDCry (primer set 5 in Table I). The analysis allows detecting the correct gene replacement event. The wild type allele gives a band of 2.7 kb, while the hygR replacement results in a 5.3 kb PCR product. Lack of the 2.7 kb band in T1 and T3 confirms this replacement.

4. Developmental phenotype of *ΔcryD* mutants

The colonies of the Δ*cryD* mutants exhibited the same appearance as the wild-type in the dark, but differences in morphology and pigmentation were appreciated under constant illumination (Fig. I-7A). The differences were more pronounced at 30°C than at 22°C: at the higher temperature the mutants were deeply pigmented, and exhibited rougher surface and marked morphological alterations (Fig. I-7B). In contrast to the *wcoA* gene mutants (Estrada and Avalos, 2008), no apparent difference was

detected in surface hydrophobicity of Δ*cryD* mycelia upon water addition, and the amounts of microconidia (small ellipsoidal uninucleated spores) were similar to those produced by the wild type (Fig. I-8A). As formerly found (Estrada and Avalos, 2008), conidiation was not induced by light in any of the strains tested, either in DG-asn or low-N DGasn medium (Fig. I-8A, left panel).

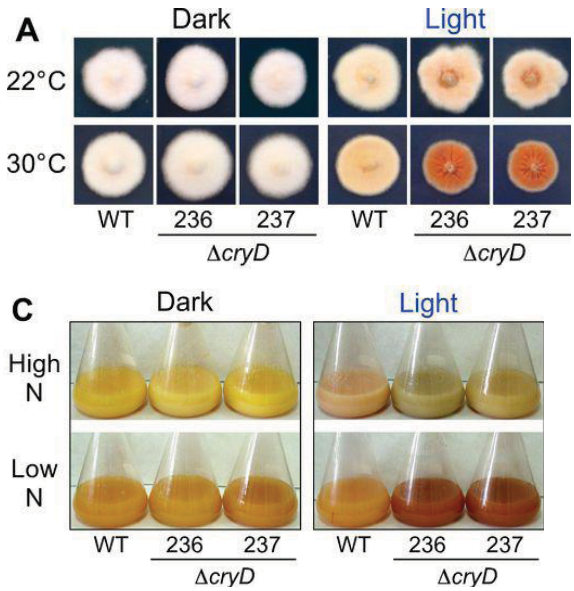

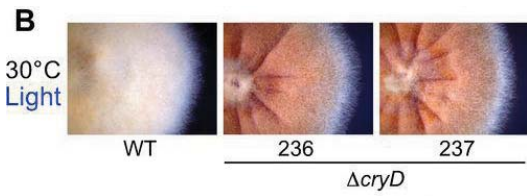

Fig. I-7. Visual phenotype of Δ*cryD* mutants. (A) Colonies of the wild type and Δ*cryD* mutants T1 and T3 grown for 6 days at 22°C or 30°C on minimal medium in the dark or under constant illumination (5 W m^{-2}). (B) Partial magnification of the colonies grown in the light at 30°C. (C) Representative shake cultures of the wild type and the Δ*cryD* mutants T1 and T3 grown for 7 days at 30°C in high nitrogen or low-N media in the dark or under constant illumination (3 Wm^{-2}).

As typically found in *F. fujikuroi* cultures, microconidia were the only class of spores found in most of the samples. However, macroconidia, long falciform septated cells, were also observed in the spore preparations from Δ*cryD* mutant colonies grown under nitrogen-limiting conditions in the light (Fig. I-8B and right panel in Fig. I-8A,). Interestingly, no macroconidia were detected under any other tested conditions, including submerged cultures of the wild type or the mutants irrespective of light or nitrogen availability. Formation of macroconida is a widespread trait in other *Fusarium* species (Leslie and Summerell, 2006). This result suggests that CryD acts in *F. fujikuroi* as a nitrogen-dependent repressor of macroconidiation in surface cultures under illumination.

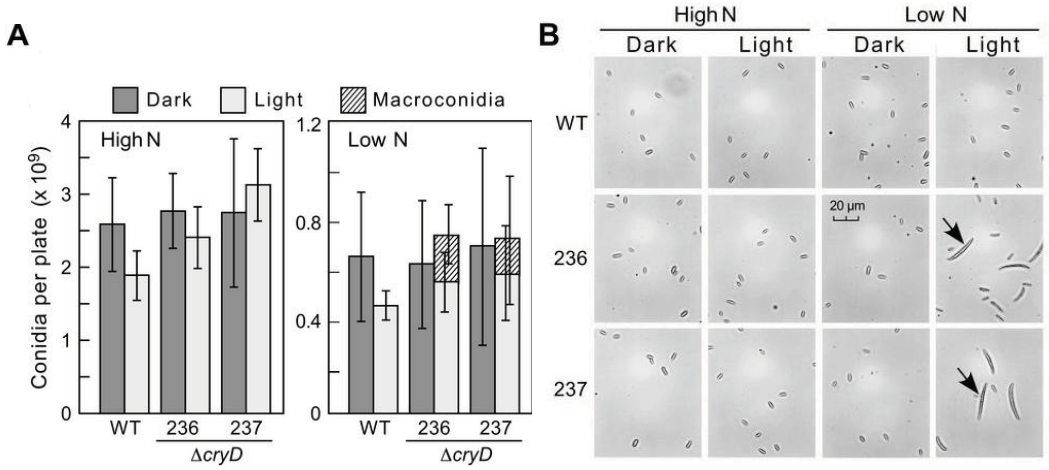

Fig. I-8. Effect of the Δ*cryD* mutation on conidiation. (A) Numbers of conidia produced by the wild type and the Δ*cryD* mutants T1 and T3 grown for 7 days under white light (5 W m^{-2}) in DGasn and DGasn low-N medium (High N and Low N on the graph, respectively). The data show average and standard deviations from six biological replicates. (B) Conidia samples from representative examples of the data shown above. The pictures were taken under microscope (400x).

5. Effect of the *ΔcryD* mutation on pigment production

The mycelia of either the wild type or the Δ*cryD* mutants were weakly pigmented in the dark and contained low amounts of carotenoids. As expected, the wild type acquired a pale orange pigmentation when grown under constant illumination (Fig. I-7A), which was accompanied by a 10-fold increase in the carotenoid content (Fig. I-9). Despite the visible differences in pigmentation compared to the wild type, the Δ*cryD* mutants exhibited the same increase in carotenoid content (see Fig. S4), indicating that carotenoid photoinduction is not prevented by the absence of a functional CryD cryptochrome. Therefore, the reddish pigmentation of the Δ*cryD* mutants in the light must be attributed to the accumulation of carotenoid-unrelated pigments, absent in the wild

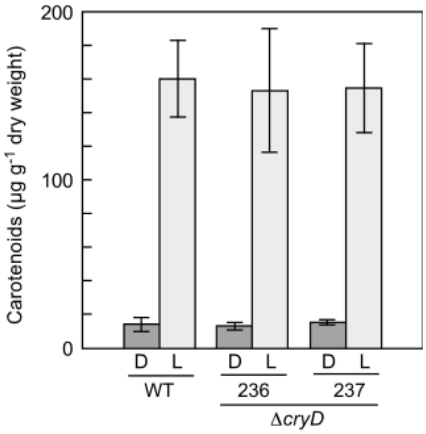

Fig. I-9. Effect of light on carotenoid biosynthesis of the wild type and Δ*cryD* mutants. Concentrations of carotenoids in the mycelia of the wild type and the *cryD* mutants T1 and T3 grown for 7 days at 30°C on inimal medium in the dark (D) or under constant hite light illumination (L). The data show average and tandard deviations from 3 independent determinations.

type.

6. Complementation of the *ΔcryD* mutation

To confirm that the alterations in pigmentation and morphology are produced by the loss of a functional *cryD* gene, the mutant SF236 was transformed with a plasmid with a wild-type *cryD* allele. Since SF236 contains the *hph* gene, a geneticin-resistance gene (*nptII*) was used in this case as selective marker. After incubation of the protoplasts with the plasmid, six geneticin-resistant colonies were obtained. Upon subculture from uninucleate microconidia, the six transformants were subjected to molecular and phenotypic characterization. PCR experiments (Fig. I-10A) confirmed the presence of the *hph* gene in all the strains except in the wild type, and the *nptII* gene in the six SF236-derived transformants, called here C1-C6 (Fig. I-10B). As expected, the SF236 Δ*cryD* mutant did not contain the entire *cryD* sequence (3.3 kb PCR product) or its 5' region (2.1 kb product), found in the wild type. These *cryD* sequences were detected in the transformants C1, C2, C3, C5 and C6, but not in C4. The absence of the 5' *cryD* sequence in C4 suggests the disruption of the gene by ectopic integration of the plasmid through this DNA region. Expression of the *cryD* gene in C1, C2, C3, C5 and C6, but not in C4, was confirmed by PCR amplification of an internal cryD segment on cDNA samples from illuminated mycelia, and by a RT-PCR analyses (Fig. I-10D).

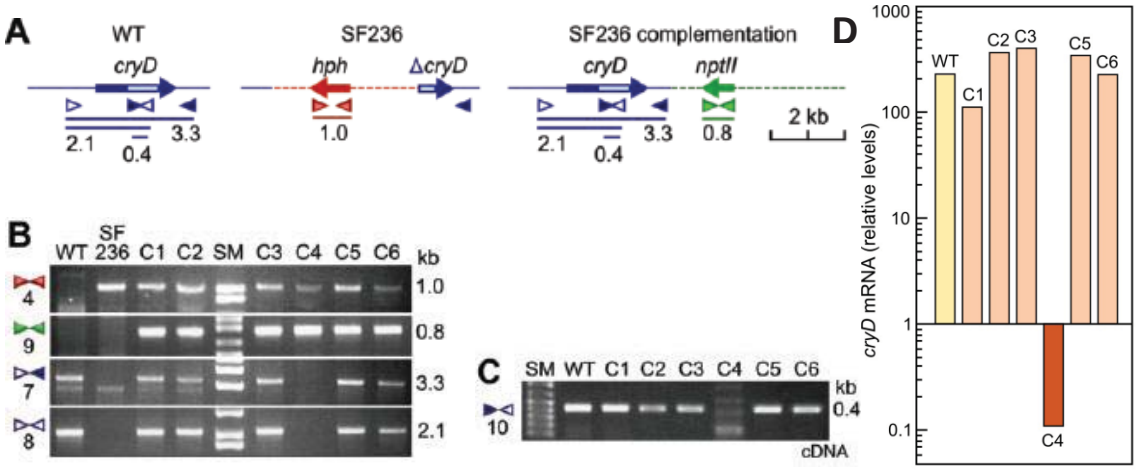

Fig. I-10. Complementation of the Δ*cryD* mutants. (A) Schematic representation of primer locations and PCR products (sizes in kb) for the *cryD* gene in the wild type (WT), the *hph*-disrupted allele in the Δ*cryD* mutant SF236, and the construct added to SF236 in the transformation experiment. The light box in the *cryD* gene represents the FAD binding domain. (B) Agarose gel electrophoresis of PCR amplification products obtained from genomic DNA samples of the wild type (WT), the Δ*cryD* mutant SF236, and the complementation transformants C1-C6. Primer sets are numbered on the left according to Table I. Expected PCR products are indicated on the right. The 1 kb band (primer set 4) and the 0.8 kb band (primer set 9) indicate the presence of the *hph* and *nptII* genes, respectively. The 2.1 and 3.2 kb bands indicate the presence of the 5' *cryD* sequence or the entire *cryD* sequence, respectively. (C) Agarose gel electrophoresis of the PCR amplification products obtained with primer set 10 from cDNA samples of the wild type (WT) and the complementation transformants C1-C6 after 1 h exposure to light. The 0.4 kb product indicates the presence of *cryD* transcript. (D) RT-PCR nalyses of relative *cryD* mRNA levels in the wild type (WT) and the complementation transformants C1-C6 after 1 h exposure to light. The values are referred to the mRNA content of the wild type in the dark (data are verage of three RT-PCR values from a single experiment).

The morphology and pigmentation of the colonies of transformants C1, C2, C3, C5 and C6 were similar to those of the wild type under white light (Fig. I-11B;). However, transformant C4 conserved the characteristic phenotypic alterations of the Δ*cryD* mutants (Fig. I-11B). The same result was obtained upon illumination with blue light, but not with red light, under which the Δ*cryD* mutants exhibited no major phenotypic changes. This result contrast with the exhibition of a clear mutant phenotype by the Δ*wcoA* strain under red light (Fig. I-11B). Taken together, the results strongly support that the loss of a functional *cryD* gene is responsible for the phenotypic alterations exhibited by the Δ*cryD* mutants, and that this effect requires the participation of a blue-light photoreceptor.

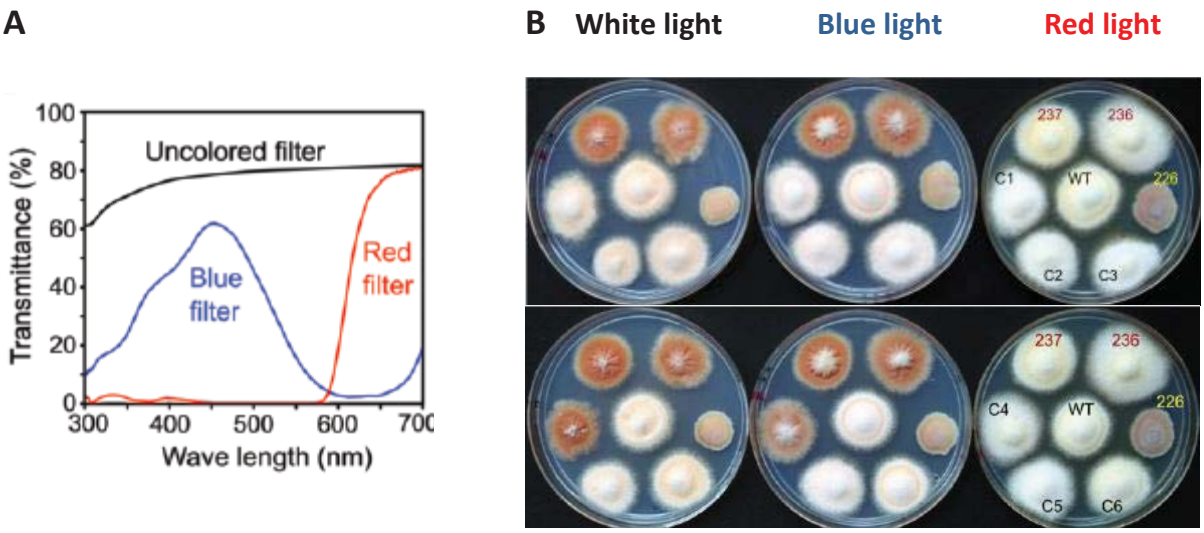

Fig. I-11. Phenotype of complemented strains. (A)Transmittance spectra of cellophane sheets used as filters for illumination with white light (uncolored filter), blue light (blue filter) and red light (red filter). (B) Visual phenotype of the wild type (WT), the Δ*cryD* mutants SF236 and SF237, the Δ*wcoA* mutant SF226 and the transformants C1-C6 grown upon illumination with white, blue or red lights (see transmittance spectra).

7. Effect of the *ΔcryD* mutation on bikaverin production

As already mentioned, bikaverin is a well-known reddish secondary metabolite produced by this fungus (Fig. I-12A). To check the possible role of CryD on the production of this pigment, the wild type and the Δ*cryD* mutant strains were grown in high-N and low-N media, in the dark or under constant illumination. Under these

culture conditions, the illuminated cultures of the Δ*cryD* mutants exhibited a different hue in high nitrogen medium and a deep reddish color in low-N medium, not apparent in the wild type (Fig. I-7C). The reddish pigments extracted from these strains showed the typical bikaverin absorption spectrum, with a maximum at 521 nm (Fig. I-12B). Bikaverin concentrations were determined for all the tested culture conditions, either in the mycelium or in the culture filtrates. Bikaverin was also found in low amounts in the cultures in high-nitrogen medium, where its color was likely masked by other pigments (Fig. I-7C). However, the bikaverin levels were significantly enhanced in the mycelia of the Δ*cryD* strains upon illumination (Fig. I-12C). This effect was particularly outstanding in low-N medium, where the illuminated cultures of the mutants accumulated much larger amounts of bikaverin either in the mycelium or in the medium. No relevant differences were observed however in the dark, indicating a

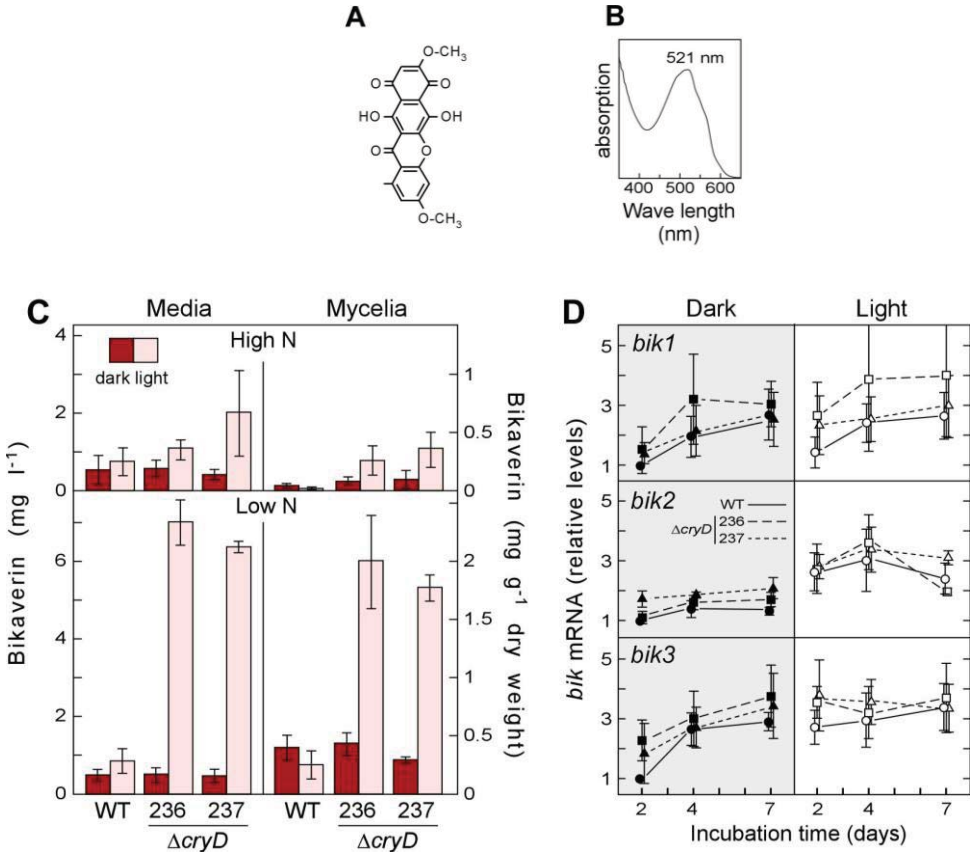

Fig. I-12. Effect of the Δ*cryD* mutation on bikaverin production. (A) Chemical structure of bikaverin. (B) Representative example of absorption spectrum of the red pigment isolated from the shake cultures of the Δ*cryD* mutants T1 and T3 grown in low-N medium in the light (see Fig. I-7C). (C) Bikaverin concentrations in the mycelia and the filtrates of shake cultures of the same strains grown for 7 days at 30°C in high-N or low-N media in the dark or under constant illumination (3 Wm^{-2}). (D) Real-time RT-PCR analyses for genes *bik1*, *bik2* and *bik3* in RNA samples from the mycelia of cultures after 2, 4 and 7 days incubation in low-N medium. Relative expression was referred to the value of the wild type in the dark. The data on bikaverin and *bik* mRNA levels show average and standard errors from three independent experiments.

light-dependent role of CryD in the nitrogen regulation of bikaverin biosynthesis.

To check if the Δ*cryD* mutation exerts its effect on gene expression of enzymatic genes for the bikaverin pathway, qRT-PCR analyses were achieved to determine transcript levels in wild type and Δ*cryD* mutants after 2, 4 and 7 days incubation in low-N medium. In agreement with former results (Wiemann et al., 2009), mRNA levels for the polyketide synthetase gene *bik1* [*pks4*, (Linnemannstöns et al., 2002)] showed a tendency to increase in the wild type during incubation in this medium, but the mRNA pattern was not affected by light. A similar tendency was exhibited by *bik3* in the dark but not by *bik2*, although a minor light induction was apparent for both genes in this case. The results were very similar in the Δ*cryD* mutants, except that a propensity for larger mRNA amounts was apparent in most cases. Overall, the differences of *bik1, bik2 and bik3* mRNA levels between wild type and *cryD* mutants were too minor to explain the large differences in bikaverin production, suggesting the participation of CryD in a nontranscriptional regulatory mechanism.

8. Effect of the *ΔcryD* mutation on gibberellin production

Because of their similar nitrogen regulation, the effect of the Δ*cryD* mutation on bikaverin biosynthesis led us to investigate its effect on GA production in the same experiments. The filtrates of the wild type and Δ*cryD* cultures contained similar amounts of gibberellic acid in the dark, but a *ca.* 40% increase was found in those of the wild type when grown under light (Fig. I-13A). However, this light induction was not apparent in the cultures of the Δ*cryD* mutants.

The light-induced increase in the GA content of the wild type cultures was too limited to expect significant changes in expression of the structural genes of the gibberellin pathway. However, the mRNA levels for three GA genes were analyzed in the same RNA samples described in the experiments of Fig. I-12D. The genes chosen for this assay were *gibB,* coding for ent-kaurene synthase or ent-copalyl diphosphate synthase, in turn the first specific enzyme of GA biosynthesis, *gibD*, coding for the P450-1 enzyme, and *gibG*, coding for the desaturase responsible of the last reaction of the pathway. These three genes were originally called *cps/ks*, *P450-1* and *des*, respectively (Tudzynski, 2005). As expected, the mRNA content for the three genes

was low in the early stage of the cultures (2 days) and augmented in later stages (4 and 7 days) (Fig. 7B), when nitrogen is exhausted (Candau et al., 1992). However, in contrast to the GA3 amounts found in the cultures, mRNA contents in the wild type reached higher levels in the dark than under illumination, suggesting that CryD facilitates a more efficient translation of *gib* transcripts in the light, possibly linked to enhanced mRNA degradation. Interestingly, the Δ*cryD* mutants exhibited a delayed time-course of mRNA accumulation for the three genes compared to the wild type, suggesting also the implication of CryD in the rapid response to nitrogen starvation.

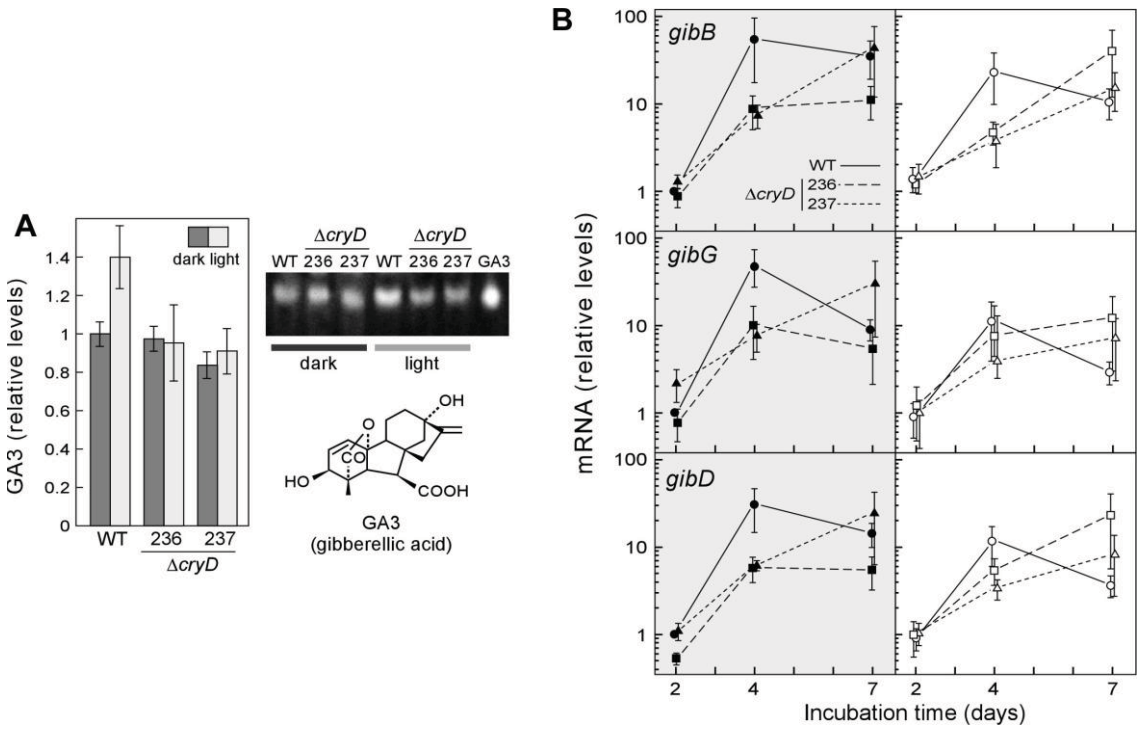

Fig. I-13 Effect of the Δ*cryD* mutation on GA production. (A) GA3 amounts in the filtrates of the wild type and the Δ*cryD* mutants T1 and T3 grown for 7 days at 22°C or 30°C in low-N medium in the dark or under constant illumination. The right picture shows a representative example of the fluorescent spots on the TLC separation of gibberellin samples from the three strains, used for GA3 densitometry quantification. GA3 indicates gibberellic acid run as a control on the same TLC (chemical formula shown below). (B) Real-time RT-PCR analyses for genes *gibB*, *gibD* and *gibG* in RNA samples from the mycelia after 2, 4 and 7 days incubation in low-N medium. Relative expression was referred to the value of the wild type in the dark. The data on GA3 production and *gib* mRNA levels show average and standard errors from three independent experiments.

DISCUSSION

Cryptochromes were defined as photolyase-like proteins with no DNA repair activity but with known or presumed blue-light photoreceptor functions (Chaves et al., 2011; Sancar, 2004). The functional diversity of these photoreceptors became more evident when new members of this protein family were described in recent years, and cryptochromes are currently divided into at least seven subfamilies (Oberpichler et al., 2011). One of the subfamilies comprises the cry-DASHs (Brudler et al., 2003), widespread in photosynthetic organisms, but also found in some non-photosynthetic bacteria, archaea, animals and fungi. In the latter, genes for cry-DASHs have been found in ascomycete, basidiomycete, and zygomycete genomes. Our analyses showed high sequence divergence between cry-DASHs of the three fungal groups, indicating distant evolutionary origins. The difference is further emphasized by a carboxy-terminal extension usually found in cry-DASHs of ascomycetes, but rarely present in those of basidiomycetes and zygomycetes or other phyla compared in our analyses. Whether these extensions play a specific biological role needs to be addressed in future studies.

The functions of two ascomycete cry-DASH proteins were recently investigated *in vivo* through the generation of targeted mutations: *cry* in *N. crassa* (Froehlich et al., 2010) and *cry1* in *Sclerotinia sclerotiorum* (Veluchamy and Rollins, 2008). In *N. crassa*, the white collar system centralizes the light detection of all its known photoresponses (Chen and Loros, 2009b). Hence, the role of the genes for other putative photoreceptors found in its genome, including one for a cry-DASH, remains a challenging task. The mutations of some of them result in weak light-related phenotypic effects, but in most cases there is no apparent change in any light-controlled phenomenon (Chen and Loros, 2009b). In the case of the cry-DASH gene of *N. crassa*, the mutation caused no phenotypic alterations except a slight but detectable phase delay of circadian entrainment. This cry-DASH may be a relevant piece of the complex regulatory mechanism governing circadian rhythmicity in *N. crassa*, and the subtle phenotypic change that its loss has under laboratory conditions could have an impact on fitness of this fungus in nature. As found for *cryD*, the

expression of the *cry* gene in *N. crassa* is strongly induced by light through the white collar complex. This complex plays a central role in the control of circadian rhythmicity (Dunlap and Loros, 2004), a phenomenon whose occurrence of in *F. fujikuroi* has not been investigated.

A different biological role is noticeably played by the cry-DASH of *S. sclerotiorum,* Cry1. The expression of the *cry1* gene exhibits a tissue-specific regulation: its mRNA levels are low in vegetative mycelia and increase during development of apothecia, sexual reproduction structures formed during the life cycle of this fungus (Veluchamy and Rollins, 2008). In contrast to the cry-DASH genes of *F. fujikuroi* or *N. crassa*, exposure to visible light hardly affects the expression of *cry1* in *S. sclerotiorum*. However, it is strongly stimulated by exposure to UV-A wavebands, which also induce the maturation of apothecial stipes. The mutants carrying a *cry1* deletion exhibited minor developmental alterations, but still were able to produce normal apothecia, indicating that Cry1 plays a secondary role in the completion of the normal life cycle of *S. sclerotiorum* under laboratory conditions (Veluchamy and Rollins, 2008). In comparison, *N. crassa* protoperithecia formation and phototropism of perithecial beaks are induced by blue light through the WC system (Degli-Innocenti and Russo, 1984a; Harding and Melles, 1983), and none of these responses was apparently altered in the *cry* mutant (Froehlich et al., 2010).

The phenotypic alterations produced by the Δ*cryD* mutation in *F. fujikuroi* are different from those described for the counterpart mutants of *N. crassa* and *S. sclerotiorum.* The phenotypic changes of the *F. fujikuroi* mutants were only exhibited under blue light, in agreement with the wcoA-dependent expression of the *cryD* gene. Furthermore, the noticeable changes in pigmentation patterns, affecting more than one colored metabolite, indicate an unexpected participation of CryD in light regulation of secondary metabolism. This effect was quite manifest in the case of bikaverin production, derepressed under light in the Δ*cryD* mutants. The up-regulation was particularly noticeable under nitrogen starvation, a major inducing signal for bikaverin biosynthesis in this fungus (Wiemann et al., 2009). This result involves CryD in the complex regulatory network governing nitrogen regulation of secondary metabolism in *F. fujikuroi*, and provides a link between nitrogen and light regulations.

The regulatory role of CryD affects also the synthesis of other metabolites, as suggest the different pigmentation of the Δ*cryD* cultures in the light, due to unidentified pigments.

Our data implicate also CryD in the decision to make macroconidia. Little is known on the regulatory mechanisms governing this developmental process in *Fusarium.* Macroconidia are usually formed in large quantities by other *Fusarium* species (Leslie and Summerell, 2006), but they are rarely found in the cultures of our wild type strain, which produces mostly microconidia as asexual spores. Our data suggest a role for CryD as a negative regulator of macroconida production in *F. fujikuroi*, and associates this regulatory function to nitrogen availability. However, the light-dependent repressing roles of CryD in macroconidia and bikaverin production are not easy to interpret. Since functional CryD is only expected under illumination, the absence of macroconidia and the low bikaverin production in the dark suggests different repressing systems operating in the dark and in the light for both processes.

Light induction on gibberellin production was formerly reported for two *F. fujikuroi* wild-type strains. In contrast to the 10 to 50-fold photoinduction of carotenoid biosynthesis, depending on strain and culture conditions [see, e.g., (Avalos and Cerdá-Olmedo, 1987; Estrada and Avalos, 2009a)], the induction levels for gibberellin production were only of 2-fold (Mertz and Henson, 1967), and 1.4 fold (Johnson and Coolbaugh, 1990). Our data showed about 1.4 fold increase in GA3 production in the light compared to the dark, in good agreement with the reported stimulations and with our former data with the same wild type-strain (Estrada and Avalos, 2008). The induction was not apparent in the Δ*cryD* mutants, suggesting the mediation of the CryD photoreceptor in this photoresponse. The transcript analyses for three enzymatic genes of the pathway suggest that this regulation is not achieved on mRNA levels. Actually, mRNA contents for the three genes investigated reached higher levels in the dark than in the light, indicating the participation of CryD in other regulatory mechanism, possibly associated to mRNA translation or stability. A similar conclusion may be inferred from the lack of significant effect of the Δ*cryD* mutation on the mRNA levels of the structural *bik* genes. Taken together, our data point to CryD as a putative

photoreceptor involved in posttranscriptional regulatory mechanisms of secondary metabolism in *F. fujikuroi*.

In addition to cry-DASHs, some cryptochrome or photolyase-like proteins were found to play regulatory functions in fungi. PHR1 from *Trichoderma atroviride* was found to regulate its own transcription, possibly modulating the activity of the white collar BLR1/BLR2 complex (Berrocal-Tito et al., 2007). Targeted mutation of *phl1* from *Cercospora zeae-maydis* alters the expression of other genes involved in DNA damage repair, including the putative photolyase gene *cpd1*, and causes abnormalities in development and secondary metabolism (Bluhm and Dunkle, 2008a). Finally, deletion of *cryA* from *Aspergillus nidulans* causes the induction of regulatory genes of the sexual cycle and stimulates sexual fruiting body formation (Bayram et al., 2008a). CryA may be also involved in other light-regulated processes, as indicated the induction of the *veA* gene in the *cryA* mutant (Bayram et al., 2008a). VeA is a component of the VelB/VeA/LaeA complex, which participates in the control of asexual development and secondary metabolism in *A. nidulans* Bayram, 2008b #486}. Interestingly, a similar velvet-like complex affects conidiation and secondary metabolism in *F. fujikuroi* (Wiemann et al., 2010), suggesting a possible regulatory connection with CryD.

The participation of cry-DASH proteins in circadian rhythmicity in *N. crassa*, apothecia development in *S. sclerotiorum*, and secondary metabolism and macroconidia formation in *F. fujikuroi*, points to a considerable functional diversification of these predicted photoreceptors in ascomycete fungi. Not by chance, these fungi are model systems in the study of the aforementioned biological processes, and some degree of functional conservation might still exist. For example a role of the *F. fujikuroi* or *S. sclerotiorum* cry-DASHs in circadian rhythmicity would be easily disregarded, since this process has not been investigated in these fungi. In the case of *F. fujikuroi*, the light-dependent effects of the *cryD* mutation may be explained by the light-dependent expression of the gene, but a direct photoreceptor activity is not discarded. New experiments will be needed to investigate the photo-biochemical properties of this protein. So far, our experiments, together with those of the formerly reported fungal cry-DASHs, demonstrate the functional versatility of these proteins in

fungi, irrespective of their possible photoreceptor roles, and should aim to extend these studies to new examples in other fungal species.

CHAPTER II

Biochemical characterization of the DASH-cryptochrome CryD of *Fusarium fujikuroi*

INTRODUCTION

Light is a key environmental signal used by organisms from all taxonomic groups as a source of energy or information. Light is detected by photoreceptor proteins, which use different chromophores for light absorbance. Cryptochromes are blue/UV-A light photoreceptors most likely evolved from DNA-repair enzymes called DNA photolyases, which use light energy to repair two major UV-B lesions, cyclobutane pyrimidine dimers (CPD) and 6-4 photoproducts. Photolyases and cryptochromes form a huge family which comprises at least 7 subfamilies: CPD photolyases of class I (Sancar, 1994; Sancar, 1990; Yasui et al., 1994) and II (Kato et al., 1994; Todo et al., 1994), 6-4 photolyases (Todo, 1999), plant cryptochromes (Ahmad and Cashmore, 1993), animal cryptochromes (Hsu et al., 1996) and the latest discovered DASH-cryptochromes (Brudler et al., 2003) and CPD photolyases of class III (Oztürk et al., 2008). Most cryptochromes are unable to repair UV-B lesions in DNA (Chaves et al., 2011; Sancar, 2003; Todo, 1999) and typically exhibit an N-terminal photolyase-related domain able to bind non-covalently two chromophores, flavin adenine dinucleotide (FAD) and, as an antenna cofactor, the pterin N^5,N^{10}-methenyl-tetrahydrofolate (MTHF). The three-dimensional structure of the N-region in photolyases and cryptochromes is also conserved. Both present a α/β domain and a helical domain, which binds FAD, connnected by an internal loop (Brautigam et al., 2004; Brudler et al., 2003; Park et al., 1995).

Most cryptochromes have poorly structured extensions at the C-terminus (Partch et al., 2005), absent in photolyases. These extensions play regulatory roles related to light control of growth, development, signaling and circadian rhythm in different taxonomic groups (Chaves et al., 2011). The DASH-cryptochromes (abbreviated hereafter as cry-DASHs) are a subgroup in this family, and differ from conventional cryptochromes in their ability to repair cyclobutane pyrimidine dimer (CPD) lesions in single-stranded DNA (Selby and Sancar, 2006) or in loop-structures of duplex DNA (Pokorny et al., 2008). Cry-DASHs have been identified in bacteria (Brudler et al., 2003; Hitomi et al.,

2000), plants (Kleine et al., 2003), fungi (Froehlich et al., 2010) and vertebrates (Daiyasu et al., 2004), except birds and mammals.

The oxidation state of the flavin cromophore plays a critical role in the function of cryptochromes/photolyases. The reduced state is photoexcitable and capable to transfer energy, while the oxidized states are catalytically inactive. Irrespective of the prevailing state under physiological conditions, both types of photoproteins undergo a specific photoactivation reaction, consisting of the light-dependent reduction of the flavin via electron transfer through three conserved tryptophan residues (Trp-triad). In photolyases and cry-DASHs, the active form is the fully reduced deprotonated FADH (Sancar, 2003). In contrast, cryptochromes use the semireduced radical form FAD°/FADH° (Giovani et al., 2003). The mechanism used by photolyases to repair DNA is well understood (revised in (Chaves et al., 2011)). However, despite its similarities with photolyases, it remains unclear how the excited flavin activates a signaling pathway in cryptochromes.

Because of experimental amenability, microorganisms have been extensively used as research subjects in photobiology. Some filamentous fungi stand out because of their ability to use light to modulate different biochemical and developmental processes (Idnurm et al., 2010). Additionally, many fungal species exhibit a complex secondary metabolism, regulated by environmental cues, including light. A paradigmatic example is found in the genus *Fusarium*, a widespread group of phytopathogenic fungi able to produce an extensive array of metabolites and mycotoxins (Desjardins and Proctor, 2007a). The genomes of the *Fusarium* species contain genes for different photoreceptors (Avalos and Estrada, 2010) including three members of the cryptochrome/photolyase family: a CPD photolyase, a cry-DASH and a cryptochrome closer to the plant cryptochromes family. Former studies on *F. fujikuori* showed that mutation of the cry-DASH gene *cryD* leads to phenotypic changes under light conditions, including alterations in secondary metabolism, colony development and macroconidia production (Chapter I of this Thesis). The investigation of similar cry-DASH proteins in other fungi revealed an unexpected functional diversity, with roles in

sclerotia production in *Sclerotinia sclerotiorum* (Veluchamy and Rollins, 2008) and circadian rhythmicity in *Neurospora crassa* (Froehlich et al., 2010).

Despite the knowledge on the phenotypic effects of the mutations of the cry-DASH genes in *S. sclerotium*, *N. crassa* and *F. fujikuroi*, no information is available on the mechanisms of action of this class of fungal proteins. Therefore, to obtain more information about cry-DASH functions and mechanism of action we carried out the biochemical characterization of the *F. fujikuroi* cry-DASH protein, CryD. We heterologously expressed this protein and found that recombinant CryD binds FAD and MTHF, the cofactors formerly found attached to other cry-DASH proteins (Chaves et al., 2011). The FAD cofactor in CryD is photoreducible, and CryD binds single and double-stranded DNA without significant discrimination between substrates with or without CPD-lesions. Moreover, CryD repairs CPD lesions in single-stranded DNA, thus having all the characteristics of a DASH-type cryptochrome. These results reinforce its function in *F. fujikuroi* as a photoactive protein with dual photoreceptor and photorepair functions.

RESULTS

1. Sequence analysis of the CryD protein

The CryD protein of *F. fujikuroi* contains the expected FAD binding domain, as revealed by the PFAM domain prediction software, and the typical carboxy extension (C-extension) found in this class of proteins (Fig. II-1A). Considering the presumed evolutionary origin of cryptochromes from photolyases and the biochemical similarities of both classes of protein, we performed a Clustal comparison of the protein sequences of CryD of *F. fujikuroi,* and the photolyases Phr1 of *F. fujikuroi* and Phr of *E. coli* (Fig. II-1B). The alignment revealed a higher similarity between the two photolyases (184 identical positions), despite their distant phylogenetic origins, than between the *F. fujikuroi* photolyase and CryD (only 107 identical positions). The photolyases contain a similar putative FAD binding domain (Fig. II-1A and II-1B), consistent with the use of FAD as a choromophore. The tryptophan triad required for FAD photoreduction in the photolyases (Aubert et al., 2000) is found incomplete in CryD although an alternative tryptophan residue could be used in this case (indicated by an arrow in Fig. II-1B). The occurrence of these conserved residues suggest a similar photoreduction mechanism for CryD.

Taking apart the carboxy extensions, the 568-aa CryD segment depicted in Fig 1B is very similar to the homologous sequences of the other fungal cry-DASH proteins investigated so far, CRY of *N. crassa* and Cry1 of *S. sclerotiorum* (252 conserved positions, i.e., 44% of the protein segment). However, the C-extensions are highly dissimilar between the three proteins (Fig. II-1C), with that of *S. sclerotium* being much shorter than those of CryD and CRY. The three extensions coincide however in the occurrence of several arginine/glycine (RGG) repeats, possibly associated to RNA binding (Godin and Varani, 2007). The differences between these domains in the three proteins suggest highly species-specific regulatory roles for the corresponding cry-DASH proteins.

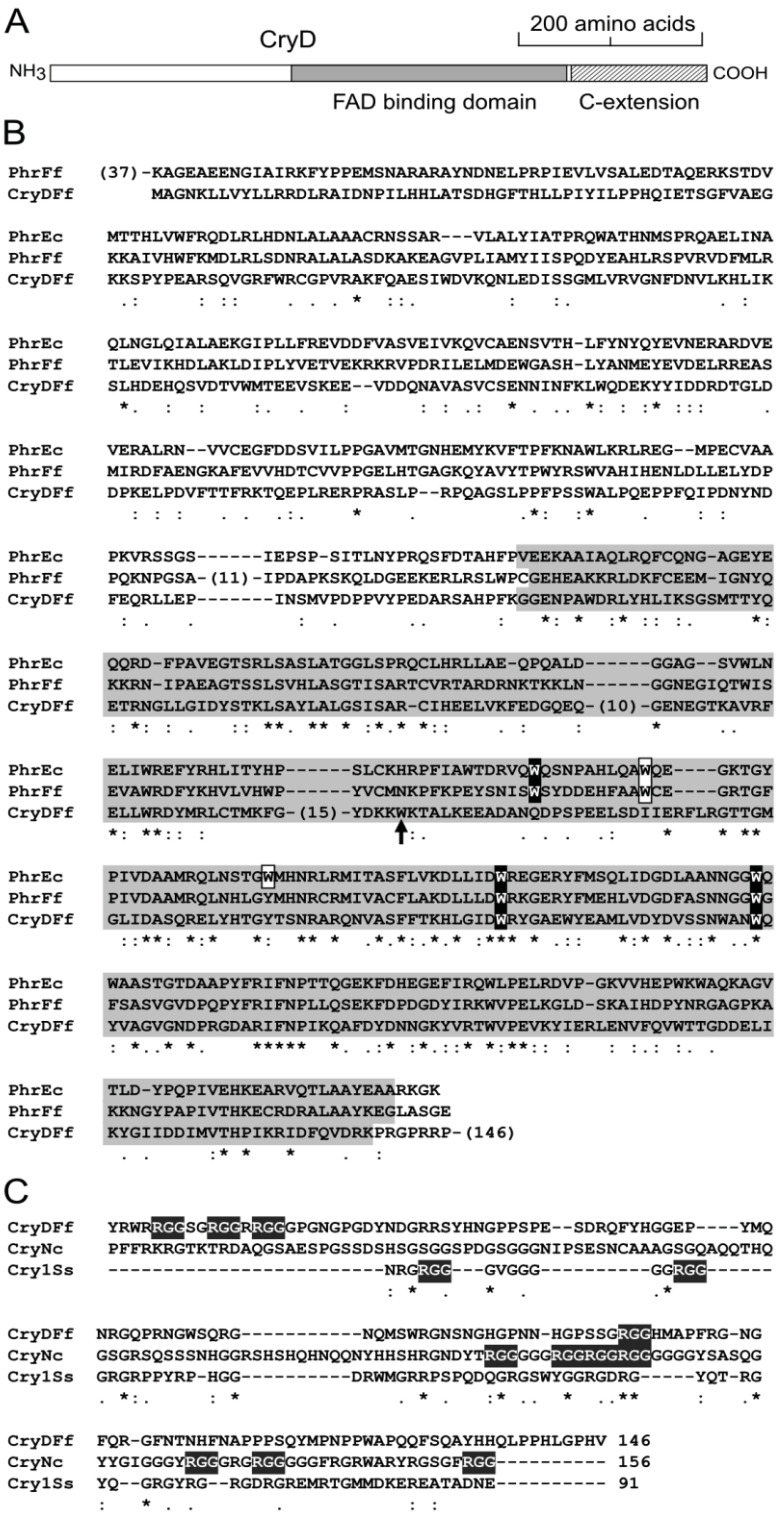

Fig. II-1. Sequence features of CryD. (A) Schematic representation of the cry-DASH protein CryD of *F. fujikuroi* (HE650104). The FAD binding domain and the carboxy extension are indicated. (B) Comparison of protein sequences of CryD (CryDFf), *E. coli* photolyase Phr1 (PhrEc, accession No. AAA24388) and *F. fujikuroi* photolyase Phr1 (PhrFf, FFUJ_00436). The sequences were aligned with the Clustal W2 program. Numbers in parentheses indicate amino acids present only in one of the proteins, not shown in the diagram. The grey shading indicates the predicted FAD binding domains deduced by the PFAM tool for the three proteins. Tryptophan residues conserved among photolyases and cryptochromes (Trp-triad) required for FAD photoreduction (W306, W359 and W382 in *E.coli)* are indicated in black background; other tryptophan residues presumably necessary for structure maintenance are highlighted in white background. (C) Clustal alignment of the carboxy extensions of CryD (CryDFf), and the two other fungal Cry-DASHs investigated so far, Cry from *N. crassa* (CryNC, XP_965722) and Cry1 from *S. sclerotiorum* (Cry1Ss, SS1G_05163). Numbers of amino acids of the extension are indicated at the end of the sequences. Black boxes mark RGG motifs.

2. Characterization of CryD cofactors *in vitro*

For biochemical characterization of the CryD protein, we expressed a tagged cDNA version of *cryD* in *E. coli* and subjected the purified protein to spectroscopic and chromatographic assays. CryD was expressed in *E. coli* BL21 (Studier and Moffatt, 1986) as a fusion protein with a Strep-tag at the N-terminus and a His_{10}-tag at C-terminus. The resulting tagged CryD was obtained as a soluble protein after two purification steps in non-denaturing conditions. The absorbances at 380 and 450 nm were monitored during the process. Ni^{2+}-affinity purification followed by heparin purification resulted in essentially pure CryD, as shown in the denaturing polyacrylamide gel (Fig. II-2A), with a yield of *ca.* 1 mg l^{-1}. According to protein markers, the position of the obtained CryD tagged protein fitted the expected size of 86 kDa (lane 3 in Fig. II-2A).

The purified samples exhibited a yellowish color, consistent with the presence of a flavoprotein. The UV-Vis absorption spectrum of purified CryD (Fig. II-2B) showed a prominent peak at 380 nm. This was indicative of the presence of N^5,N^{10}-methenyl-tetrahydrofolate (MTHF), identified as the antenna cofactor in other cry-DASH proteins and folate-type DNA-photolyases [reviewed in (Chaves et al., 2011)]. The secondary peak at *ca.* 445 nm with a 470 nm shoulder is characteristic of the fully oxidized flavin cofactor bound to the apoprotein (Klar et al., 2007). More detailed spectra in the UV-region allowed us to see a light shift from the expected 280 nm peak to 260 nm, indicating the presence of a nucleic acid in the sample preparation. This nucleic acid was confirmed to be an RNA molecule (data not shown).

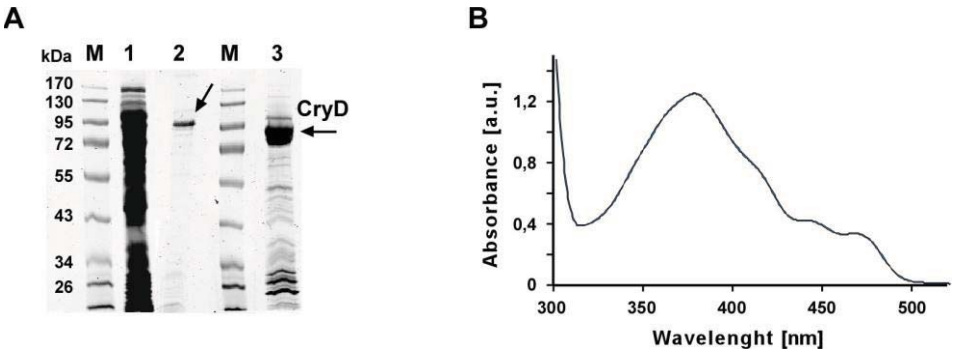

Fig. II-2. Purity and spectral characteristics of *E. coli* expressed CryD. A. Coomassie stained gel of the obtained sample in each purification step. Lanes M are protein markers of the indicated sizes. Lane 1: soluble extract obtained after lysis of *E. coli* cells; lane 2: fraction obtained after His trap column purification and that used for heparin purification; lane 3: eluted peak from the last purification step. 10 µg of purified CryD were obtained and this sample was used for further experiments. Arrows indicate CryD bands of the expected size (86 kDa). B. Absorption spectrum of purified CryD in the range of 300 to 520 nm. The peak at 380 nm is characteristic of MTHF and the peaks at 445 and 470 nm correspond to an oxidized state of FAD.

The flavin cofactor was identified as FAD after the release from CryD by its characteristic pH-dependent fluorescence behavior (Fig. II-3A). When the pH was raised from acidic (*ca.* 2.5) to neutral (*ca.* 7.5), the fluorescence of riboflavin and FMN increased due to the shift in equilibrium of the protonated (less-fluorescent) and neutral fully oxidized isoalloxazine moiety (Drössler et al., 2002; Islam et al., 2003). In FAD, however, additional effects completely reverse this behavior, observing a fluorescence decrease at neutral pH (Islam et al., 2003).

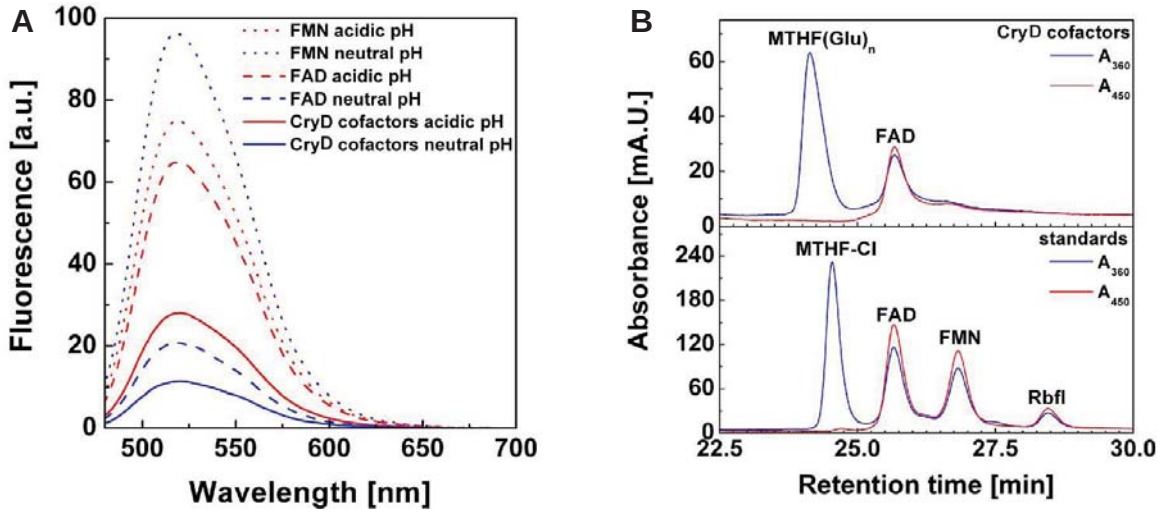

Fig. II-3. Cofactors identification. A. Fluorescence spectra of the released cofactors from CryD. Fluorescence was measure after excitation with a wavelength of 450 nm at acidic (pH 2.5, red line) and neutral (pH 7.5, blue line) conditions. FMN (dotted lines) and FAD (dashed lines) standards were used as controls (full lines). B. Reversed-phase chromatograms of the released CryD cofactors (upper panel) and of the mixture of MTHF-Cl, FAD, FMN and riboflavin (Rbfl) standards (lower panel). The elution was monitored at 360 nm (blue line) and 450 nm (red line). While FAD in the released CryD cofactors has the same elution time as the FAD standard (25.65 min), MTHF released from CryD, due to its polyglutamation, elutes slightly earlier (24.13 min) than the corresponding MTHF-Cl standard (24.53 min).

Reversed-phase chromatography (RPC) of released CryD cofactors performed under acidic conditions revealed a second peak with spectral properties of MTHF but eluting slightly earlier compared to the MTHF-Cl standard (Fig. II-3B). This shift, previously observed for the cry-DASH Cry3 from *Arabidopsis thaliana*, is explained by the polyglutamated nature of the MTHF cofactor of both proteins expressed in *E. coli* while the used MTHF standard is monoglutamated (Moldt et al., 2009). Quantitative analysis

of the chromatograms shown in Fig. II-3B revealed the MTHF:FAD:apoCryD ratio of 0.74:0.93:1. A multicomponent simulation of the CryD absorption cross-section spectrum (Fig. II-2B) provided a similar value of 0.75:0.99:1. However, the best fit of the spectrum included also methylene-THF (a more reduced state of the C1-bridge between N^5 and N^{10}) at a molar fraction of 0.094, whereas this ~10 % of methylene-THF escaped the detection in RPC probably due to its instability in acidic conditions (Moldt et al., 2009). Thus, the occupancy of purified CryD by the FAD cofactor is stoichiometric while the occupancy by the folate antenna is slightly substoichiometric.

3. CryD photoreduction properties

Irradiation of CryD with blue light in the presence of dithiothreitol (DTT), used as external reducing agent, caused bleaching of the fully oxidized FAD (FAD_{ox}), as attested by the continuous decrease in absorbance at 445 nm and 470 nm (Fig. II-4A). This behavior is well known from other members of the cryptochrome/photolyase family and referred to as FAD photoreduction, yet the final accumulated state differs among the family subgroups (Chaves et al., 2011). No transient accumulation of the neutral FAD semiquinone ($FADH^{\bullet}$), with its characteristic absorption in the 550-700 nm region, was detected during FAD photoreduction in CryD under the applied experimental conditions (Fig. II-4A), similar to the majority of cry-DASH proteins (Chaves et al., 2011). The presumption of fully reduced FAD formation was confirmed by multicomponent simulation of each spectrum. The overall change in 450 nm absorption and the changes in molar fractions of each flavin state obtained from spectra simulation followed mono-exponential kinetics (Fig. II-4A, inset) with a half time of 1.6 ± 0.2 min. In contrast, the molar fraction of MTHF remained almost unchanged at ~ 0.75 (green line in Fig. II-4A, inset). The stability of the fully reduced FAD state against reoxidation in the dark was checked in the illuminated probe after the light switch-off (Fig. II-4B). Within the analyzed 5 h time period, only approximately half of the 450 nm change caused by previous blue-light illumination was reversed. This result indicates that CryD stays in an active state for hours.

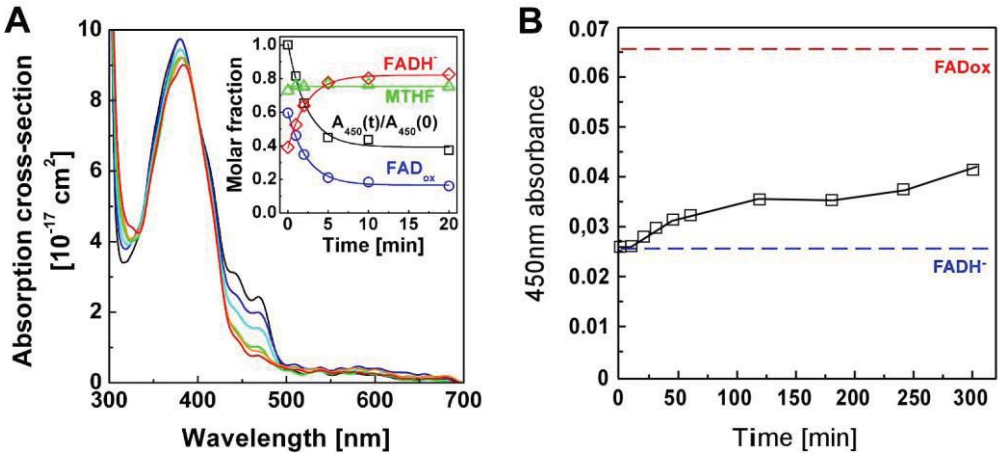

Fig. II-4. Light-dependent flavin reduction and stability. (A) Photoreduction of FAD cofactor in the presence of 10 mM DTT monitored by UV-vis absorption spectroscopy. Absorption cross-section spectra are shown for the isolated CryD (black) and for CryD illuminated with 100 µmol m^{-2} s^{-1} of 450 nm light at time points 1 min (blue), 2 min (cyan), 5 min (green), 10 min (orange) and 20 min (red) after onset of light. The decrease at 450 nm with no change in the 500-700 nm spectral region is indicative for the overall FAD_{ox}-to-$FADH^-$ reduction. *Inset*. Kinetic traces of the relative change in absorbance at 450 nm (squares, black line), and of the changes in molar fraction of FAD_{ox} (circles, blue line), $FADH^-$ (diamonds, red line) and MTHF (triangles, green line) as derived from the multicomponent analysis of the shown spectra. Lines represent monoexponential fits of the data with the resulting half-time of flavin photoconversion $t_{1/2}$ = 1.6 ± 0.2 min in all fits. (B) Dark recovery assay. Absorbance at 450 nm of the photoreduced sample of CryD incubated for the times indicated in the dark. A slow increase in the absorbance is characteristic for a stable reduced state. Blue dashed line represents the absorbance at 450 nm of the fully reduced state, and red dashed line represents the basal absorbance of the physiological flavin state (oxidized) released from purified CryD before blue-light exposure.

4. DNA binding and repair activities of CryD

The hallmark of cry-DASH proteins is the repair of CPD lesions in single-stranded DNA and loop structures of duplex DNA but not in completely double-stranded DNA (Pokorny et al., 2008; Selby and Sancar, 2006). We tested the ability of recombinant and photoreduced CryD to photorepair CPDs in single-stranded $oligo(dT)_{18}$. An increase in 265 nm absorbance of the oligonucleotide is indicative of T<>T repair (Kim and Sancar, 1991a). As expected, no repair of CPDs was observed for the dark sample in contrast to that irradiated with UV-A (Fig. II-5, black circles *vs* blue squares), and CPD repair increased along illumination time. The catalytic turnover number of 0.98 ± 0.04 min^{-1} was derived from the linear part (first 60 min) of the repair kinetics (Fig. II-5, blue fit line). A slight repair was observed in the control reaction in which 10-times lower CryD concentration was used (Fig. II-5, green triangles), demonstrating the CryD-catalyzed nature of the observed repair. Furthermore, it confirmed that the catalytic

turnover number mentioned above was estimated under conditions with a non-saturating protein concentration.

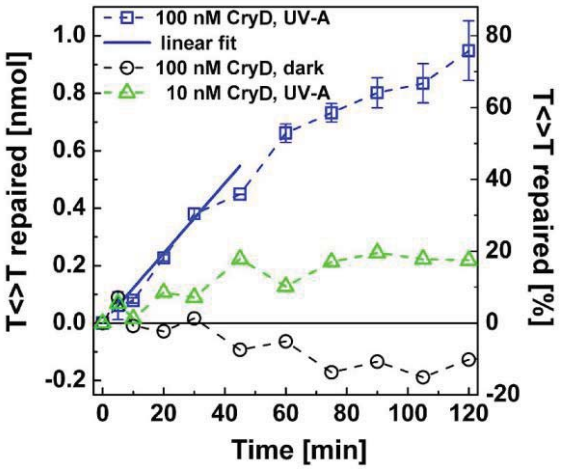

Fig. II-5. Photorepair activity. Photorepair of thymine dimers (T<>Ts) in UV-irradiated oligo(dT)$_{18}$. Prior to repair experiments, CryD was photoreduced with blue light (as shown in graph 4A) and the repair was quantified based on the increase in oligonucleotide absorbance at 265 nm. Samples were irradiated with 75 µmol m^{-2} s^{-1} of 365 nm UV-A (blue squares) or kept in the dark (black circles). The data show mean values of two independent experiments with standard errors (blue bars). The catalytic turnover number of 0.98 ± 0.04 min^{-1} was derived from the linear fit of the 0-60 min data. CryD concentration in these experiments was not saturating, as demonstrated by the control reaction with 10-times less amount of CryD (green triangles).

Although cry-DASH proteins repair CPD-lesions specifically in single-stranded DNA, they also bind to single- and double-stranded DNA with or without CPDs [reviewed in (Chaves et al., 2011)]. We tested by electrophoretic mobility shift assay (EMSA) the capability of purified CryD to bind defined DNA probes, either single-stranded (*ss*) or completely double-stranded (*ds*), that contained none or a single thymine dimer (T<>T) in the middle of one strand (Pokorny et al., 2008). The binding behavior of the isolated CryD to all probes was found to be very similar (Fig. II-6A and II-6B). In all cases, multiple CryD-probe complexes were resolved, and all bands appeared almost simultaneously above a threshold level of about 50-100 nM CryD. This behavior indicates some heterogeneity of the CryD protein, currently under investigation. Further increase in CryD concentration resulted in more pronounced to complete disappearance of unbound probe and progressive concentration of all complexes into a single, highly-retarded strong band (Fig. II-6A and II-6B), which is indicative for multiple CryD-bound units per probe molecule. Accordingly, a precise quantitative binding analysis was hampered. Based on the intensity of the bands and the number of complexes formed, we could calculate the percentage of bound and unbound probe to CryD. The overall dissociation constants in these experiments, obtained by Hill equation fitting, were in a very similar range of around 120-130 nM for the probes with a single T<>T and around 150 nM for undamaged probes (Fig. II-6C and II-6D).

Thus, CryD shows essentially no discrimination between CPD-free and CPD-containing substrates as well as between single stranded and double stranded DNA.

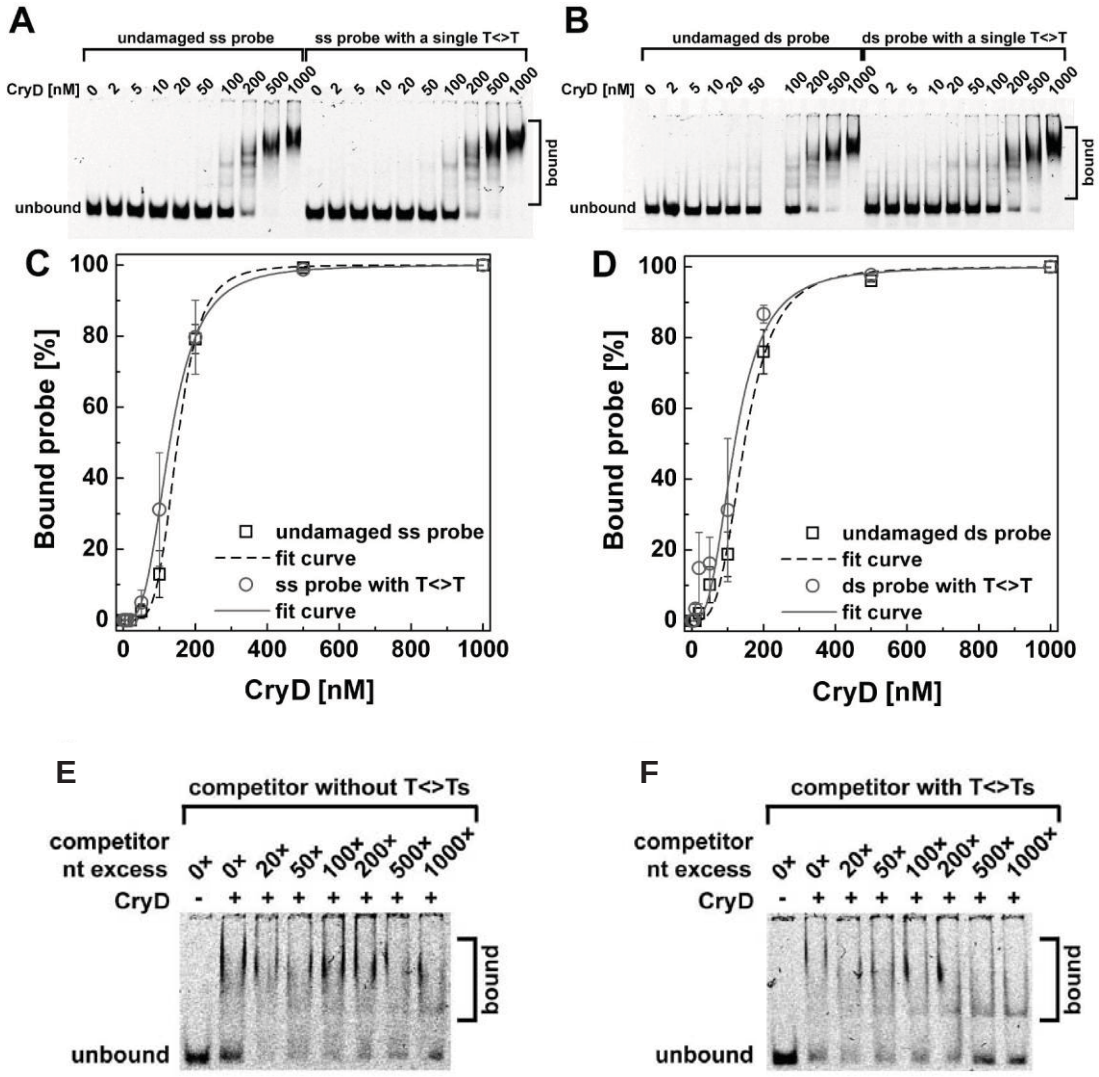

Fig. II-6. Binding of purified CryD to DNA probes. (A) and (B). Electrophoretic mobility shift assays containing a constant concentration of DNA probes (2 nM) and indicated concentrations of CryD. Single-stranded (*ss*, panel A) and double-stranded (*ds*, panel B). DNA probes were either undamaged (left halves of gel pictures) or comprised a single thymine dimer (T<>T) in their centers (right halves of gel pictures). Multiple shifted bands appear simultaneously at a certain CryD concentration in all cases whereas a single gross retarded band is visible at the highest CryD concentrations. (C) and (D) Quantification of the binding data from two independent experiments with representative gels displayed in panels A and B. Data show mean values (symbols) with standard errors (bars). Overall dissociation constants (K_d values) were derived from Hill´s fits of the data (lines): undamaged *ss* probe, K_d = 150 ± 1 nM; *ss* probe with T<>T, K_d = 129 ± 1 nM; undamaged *ds* probe, K_d = 146 ± 6 nM; *ds* probe with T<>T, K_d = 120 ± 10 nM. (E) and (F). Electrophoretic mobility shift assays containing a constant concentration (2 nM) of the labeled 50-mer single-stranded DNA probe with a single thymine dimer (T<>T) and increasing amounts of unlabeled competitor oligo(dT)18 without (E) and with (F) T<>Ts. CryD was present (+) at 120 nM final concentration or absent (-) in the control reactions. Numbers above the lanes represent the molar excess of nucleotides (nt) in competitor oligo(dT)18 molecules over the nucleotides in probe molecules (E and F) and at the same time the molar excess of T<>Ts present in competitor molecules over the T<>Ts in probe molecules (F).

This conclusion was further supported by competition experiments where competitor DNA with or without CPD lesions was added in increasing concentrations in EMSA experiments (Fig. II-6E and II-6F). No significant differences were observed between the two competitors. However, these results must be cautiously interpreted, as this equation is a simplification of the interaction between the two partners. It considers a unique binding site for DNA in the protein and occupancy of the binding site is not evaluated and supposed to be free. The latter point deserves special attention, as purified CryD seemed to be bound to a nucleic acid molecule (results not shown). Identification of this molecule, binding specificity, and whether it binds to the canonical DNA binding site of the cry-DASHs is currently under investigation.

5. UV-sensitivity of *ΔcryD* mutants

The conidia of *F. fujikuroi* are highly sensitive to UV irradiation, but its lethal effects are partially prevented by illumination after UV exposure, indicating efficient photoreactivation of UV damage (Avalos et al., 1985b). To check a possible participation of CryD in the photorepair process *in vivo*, the wild type strain and two Δ*cryD* mutants, SF236 and SF237 (Chapter I), were exposed to different UV doses, and kept in dark or under illumination after the UV treatment. After three days, colonies growing on the plates were counted (Fig. II-7). The data showed higher survival rates when the conidia were incubated under light, indicative of a photorepair process in the fungus. Additionally, very similar dose/survival curves were observed for the wild type and the mutants, irrespective of illumination. This result strongly suggests that CryD plays no relevant function in the repair of UV damage in *F. fujikuroi*, a function presumably accomplished by the Phr1 photolyase ortholog (Alejandre-Durán et al., 2003) also found to be light-inducible (data not shown).

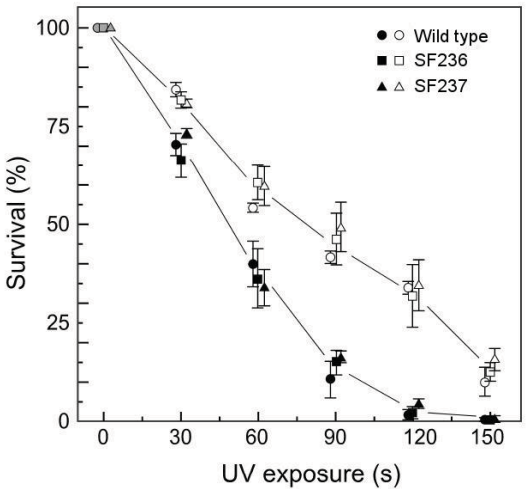

Fig. II-7. Effect of UV irradiation on survival rate of conidia of the wild type and Δ*cryD* mutants. Fresh conidia were exposed to UV irradiation (Philips TUV 15W/G15T8 lamp) for the indicated times, and incubated afterwards in the dark (closed symbols) or under continuous white light illumination (open symbols). The symbols have been slightly separated for clarity. 100% of survival rate corresponds to the number of colonies in non-irradiated samples. Survival rates for each UV exposure was calculated from the total number of colonies referred to those in the non-irradiated samples.

DISCUSSION

Cryptochromes are blue light photoreceptors with high similarity to photolyases but with functions related to signaling roles rather than to photorepair (Chaves et al., 2011; Sancar, 2004). Plant and animal cryptochromes have been widely studied in *A. thaliana*, *D. melanogaster* or mammals. Plants usually have several genes for cryptochromes [reviewed by (Lin, 2002)] with overlapping roles in different light-controlled processes, such as development, flowering or photoperiodicity (Li and Yang, 2007). Despite the lack of photorepair activity, the N-termini of plant cryptochromes undergo flavin photoreduction and the C-terminal extension is critical for their action (Ahmad et al., 1995; Yang et al., 2000). Animals have either of two types of cryptochromes, I and II, with functions related to circadian clock and rhythmicity (Todo, 1999; van der Horst et al., 1999). Both types frequently coexist in insects, albeit not in *D. melanogaster* (Emery et al., 1998), and in vertebrates only type II is present. As those of plants, animal cryptochromes maintain their ability to reduce FAD in a light-dependent manner, but again no CPD photorepair was reported. In contrast to plant and animal cryptochromes, the biological roles of Cry-DASHs are controversial. Although they retain the ability to repair CPD lesions, they cannot complement CPD photolyase mutants (Kleine et al., 2003), and few alterations are observed in cry-DASH mutants investigated in fungi. As mentioned above, in addition to CryD of *F. fujikuroi*, cry-DASH functions have been investigated in *N. crassa* (Froehlich et al., 2010) and *S. sclerotiorum* (Veluchamy and Rollins, 2008). In *N. crassa*, the CRY protein plays a role in the control of circadian rhythmicity, a phenomenon not investigated in *S. sclerotiorum* and *F. fujikuroi*. However, the mutants of the cry-DASH genes have phenotypic alterations in development and morphology in *S. sclerotiorum* (Veluchamy and Rollins, 2008) and *F. fujikuroi* (Chapter I of the Thesis).

As other cry-DASH proteins, such as Atcry3 (Kleine et al., 2003) or Vccry1 (Worthington et al., 2003), CryD contains a predicted FAD binding domain that includes two of the three highly conserved tryptophan residues (trp-triad) responsible for FAD photoreduction. Other tryptophan residues found in the *E. coli* photolyase to

play critical roles for structure maintenance and, consequently, for the activity of cryptochromes and photolyases (revised in(Liu et al., 2010) are also found in CryD. Accordingly, our *in vitro* studies on *E. coli*-expressed and purified CryD showed the ability of this Cry-DASH to bind FAD close to stoichiometry. Moreover, as expected from this family of proteins, CryD bound also MTHF, in this case slightly below stoichiometry (Fig. 3 A and B). Both cofactors were likewise identified in other members of the cryptochrome/photolyase family, and specifically in the members of the cry-DASH subclade (Chaves et al., 2011). A small fraction (~10 %) of the folate antenna in CryD is present in its more reduced methylene-THF form, as revealed by multicomponent spectra simulation. This indicates that photoreduction of folate and its retention as a cofactor (Moldt et al., 2009) is also conserved in fungal cry-DASH proteins.

FAD in its anionic fully reduced form ($FADH^-$), when further excited by direct photon absorption or *via* a Förster-type resonance energy transfer from the antenna cofactor, is the only known active flavin state in the photolyase-catalyzed repair of DNA lesions (Essen, 2006; Sancar, 2003). In cryptochromes, FAD is the chromophore required for light perception. The view that cryptochromes have fully oxidized FAD_{ox} in the ground state and semireduced FAD (either neutral $FADH^\bullet$ or anionic $FAD^{\bullet-}$) in the signaling ("lit") state (Chaves et al., 2011) is currently under debate (Liu et al., 2010; Liu et al., 2011; Oztürk et al., 2011). For CryD, we observed the overall photoreduction of FAD_{ox} to fully-reduced FAD (presumably $FADH^-$) with a half-time of 1.6 $\pm$ 0.2 min (Fig. 4A) under the applied conditions, which is even faster than observed for *e.g.* Cry3 of *A. thaliana* (Klar et al., 2007). However, as recently reported for plants and light-insensitive animal cryptochromes (Kao et al., 2005; Kao et al., 2008; Zhu and Green, 2001) and reviewed in (Liu et al., 2010), CryD photoreduction could be no so relevant *in vivo*.

The photorepair of CPD-lesions in the applied single-stranded $oligo(dT)_{18}$ substrate by photoreduced CryD (Fig. 5) demonstrates that the flavin cofactor in CryD must be, at least at the time of electron injection into the lesion, in the photoexcited $FADH^-$ state. The catalytic turnover number of 0.98 ± 0.04 min^{-1} calculated here for CryD is

~10-times lower compared to the values published for some other cry-DASH proteins (Pokorny et al., 2008; Sokolowsky et al., 2010). However, values between 0.1 and 1 s^{-1} were reported for DNA photolyases under saturating light and they can dramatically increase to 260 s^{-1} with the theoretical limit of ~2 x 10^4 s^{-1} under conditions with a very strong illumination and a high CPD number per substrate molecule (Espagne et al., 2009). Taken together, the FAD cofactor in CryD is active in both, light-induced self-photoreduction and lesion repair *in vitro*. Our UV-sensitivity assays with *ΔcryD* mutants support the hypothesis that CPD photorepair is not the main function of this protein *in vivo*. These results are in agreement with those obtained for *N. crassa* Cry and *S. sclerotiorum* Cry1, whose mutants show no defects in photoreactivation after a UV-light treatment (Froehlich et al., 2010; Veluchamy and Rollins, 2008).

Our EMSA studies showed a gradually increasing retardation of the bound probe band(s) when increasing the CryD concentration, and similar dissociation constants for all the analyzed probes in the range of ~120 - 130 nM for both *ss* and *ds* DNA probes with a single T<>T and ~150 nM for undamaged *ss* and *ds* DNA probes (Fig. 6). A similar behavior was seen before for cryptochromes and/or photolyases from diverse subgroups (Hendrischk et al., 2009; Kiontke et al., 2011; Ozgür and Sancar, 2003). Formation of multiple retarded bands was also reported for *N. crassa* cry-DASH (Froehlich et al., 2010), though CPD-containing probes were not included in this study. These data, however, do not fit the high discrimination ratio between undamaged and CPD-comprising DNA, up to ~10^5, described for the class I CPD photolyases (Sancar, 2003). This indicates that the protein-DNA complexes observed here and in the above mentioned studies could be mostly the DNA interrogation complexes where proteins do essentially not discriminate between undamaged and damaged DNA. However, once the DNA lesion is bound to the active site of a protein, its DNA-binding behavior could change very significantly.

The CryD samples purified from *E. coli* were found to contain RNA (data not shown). The bound *E. coli* RNA molecule was not identified, but its occurrence suggests that CryD is able to bind RNA molecules in a non-specific manner. The RNA-binding ability of CryD is further supported by the presence of RGG motifs in the C-terminal

extension. Such RGG repeats have been described to participate in RNA processing by regulating protein-protein and RNA-protein interactions (Godin and Varani, 2007). CryD is not the only cry-DASH reported to bind RNA. *V. cholerae* Vccry1 was also purified from *E. coli* forming a RNA-complex (Worthington et al., 2003), and *N. crassa* CRY is able to bind either single or double stranded RNA (Froehlich et al., 2010). Therefore, the binding of specific RNA substrates could play a relevant role in the biological function of CryD in *F. fujikuroi*. We formerly described down-regulating roles for CryD in bikaverin biosynthesis and macroconidia production (Chapter I). Transcriptional repression functions have been observed for other cry-DASH (Brudler et al., 2003), but mRNA levels for genes of bikaverin biosynthesis did not change significantly in *F. fujikuroi*. It is a tempting hypothesis that CryD could achieve a repressing activity at a posttranscriptional level, possibly regulating mRNA stability or translation by direct RNA interaction.

In conclusion, we provide data on dual photorepair and photoreceptor functions for another cry-DASH protein. These cryptochromes could represent an intermediate evolutionary step between photolyases and signaling cryptochromes. However, it remains to be elucidated how their ability to bind to DNA and/or to repair DNA-lesions are mechanistically linked with their photoreceptor functions. Further experiments on *F. fujikuroi* CryD and other Cry-DASHs would help to understand the biological meaning of the bifunctionality in this cryptochrome subfamily, since their photoreceptor roles have been poorly investigated and photorepair activity is redundant.

CHAPTER III

Light-dependent role of the VIVID ortholog of *Fusarium fujikuroi* VvdA in pigmentation and development

INTRODUCTION

The species of the genus *Fusarium* are well known for their pathogenic capacity and the complexity of their secondary metabolism, that includes the production of many mycotoxins (Desjardins and Busman, 2006) A paradigmatic example is *Fusarium fujikuroi*, able to produce a large array of compounds (Avalos et al., 2007). This species is the best-known model system for the production gibberellins, growth-promoting plant hormones with agricultural applications. Other metabolic pathways have received also detailed attention in this fungus, as those for the polyketides bikaverin (Wiemann et al., 2009) and fusarin (Niehaus et al., 2013). The recent sequence analysis of the *F. fujikuroi* genome has established the potential of this fungus to produce many others secondary metabolites, some of them potentially novel mycotoxins (Wiemann et al., 2013).

F. fujikuroi is also a well-established research system for the biosynthesis of carotenoids, ubiquitous terpenoid pigments produced by photosynthetic organisms and by many fungi and non-photosynthetic bacteria (Britton et al., 1998). Because of their health-promoting properties and their bright colors, different carotenoids have biotechnological applications as food and feed additives, and some of them are industrially obtained from fungi (Avalos and Cerdá-Olmedo, 2004). *F. fujikuroi* and other *Fusarium* species produce the acidic apocarotenoid neurosporaxanthin (Avalos and Cerdá-Olmedo, 1987). The synthesis of this xanthophyll with varying amounts of carotenoid precursors explains the orange pigmentation of the surface colonies of these species when grown in the light. Neurosporaxanthin is generated from the diterpenoid geranylgeranyl pyrophosphate by the sequential activity of the enzymes encoded by four structural genes, *carRA*, *carB*, *carT*, and *carD* (Avalos et al., 2014. The production of colored carotenoids require CarRA {Linnemannstons, 2002b #78), a bifunctional enzyme with phytoene synthase and cyclase activities, and the desaturase CarB, responsible for the five desaturation steps in this pathway (Prado-Cabrero et al., 2009). The *carT* and *carD* genes are involved in the late steps of neurosporaxanthin production, the oxidative cleavage of torulene by the CarT oxygenase (Prado-Cabrero

et al., 2007b) and the generation of the terminal carboxylic group by the CarD aldehyde dehydrogenase (Díaz-Sánchez et al., 2011a). *carRA* and *carB* are clustered with a gene for a retinal forming oxygenase, *carX* (Thewes et al., 2005) and a rhodopsin gene, *carO* (Prado et al., 2004), while *carT* and *carD* are genetically unlinked.

The photoregulation of carotenoid biosynthesis is achieved transcriptionally, and the four genes of the cluster are strongly induced after illumination(Avalos and Estrada, 2010). The induction reaches a maximum after one hour of light and the mRNA levels decrease afterwards, an effect known as photoadaptation. Carotenoid photoinduction has been investigated in considerable detail in *Neurospora crassa*, where the mutants of the White Collar complex, consisting of the flavin photoreceptor WC-1 and its partner WC-2, are unable to photoinduce the carotenoid biosynthesis (Linden and Macino, 1997). Similarly, WC-1-like proteins mediate the induction of carotenogenesis in mucorales fungi, such as *P. blakesleeanus* or *M. circinelloides* (Corrochano and Garre, 2010). In contrast, mutants of the only WC-1 gene of *F. fujikuroi* (*wcoA*, (Estrada and Avalos, 2008)) and *F. oxysporum* (*wc1,* (Ruiz-Roldán et al., 2008)) conserve a significant carotenoid photoinduction, indicating the participation of other photoreceptors for carotenogenesis in both species. Action spectrum for photocarotenogenesis in *F. aquaeductuum* expands from 400 to 500 nm, with peaks at ca. 450 and 480 nm, consistent with the participation of a favin photoreceptor system (Rau, 1967a). The conservation of photoinduction in albino mutants, such as the phytoene accumulating strain SG43 (Avalos and Cerdá-Olmedo, 1987), or in mutants of the retinal-binding rhodopsins CarO (Prado et al., 2004) and OpsA (Estrada and Avalos, 2009a), discards carotenoids or its derivatives as light absorbing prosthetic groups in the responsible photoreceptor machinery. Moreover, mutants of another putative *F. fujikuroi* photoreceptor, the DASH cryptochrome CryD, also exhibited light-induced carotenogenesis (Chapter I of this Thesis). Therefore, the molecular basis of carotenoid photoinduction in *F. fujikuroi* remains to be elucidated.

The photoadaptation mechanism has been investigated in *N. crassa*, where it involves changes in the activity of the WC complex through interaction with other regulatory proteins (He and Liu, 2005). One of such proteins is VIVID (VVD), a small photoreceptor with a flavin-binding domain required for efficient photoadaptation of

light-regulated genes (Schwerdtfeger and Linden, 2003; Shrode et al., 2001). The *N. crassa vvd* mutants exhibit a deeper pigmentation and accumulate about five-fold more carotenoids than the wild type under light (Youssar et al., 2005) (Navarro-Sampedro et al., 2008), a result explained by the more sustained expression of the structural genes for carotenoid biosynthesis in these strains. Presumably, *vvd* is not the only gene involved in photoadaptation. A specific search for mutants affected in photoadaptation suggested the participation of at least two further genes. The mutant of one of them exhibits a similar phenotype to that of *vvd*, but the implicated gene remains to be identified (Navarro-Sampedro et al., 2008).

We investigate the molecular basis of light regulation in *F. fujikuroi*. Here we describe the identification, regulation and targeted mutation of the gene *vvdA*, ortholog of the *N. crassa vvd* gene. The predicted *F. fujikuroi* VvdA protein is similar to VVD in size and sequence, but its mutational loss results in a significant reduction in pigmentation and carotenoid production instead of the presumed enhanced carotenoid accumulation. As found for *vvd* in *N. crassa*, expression of *vvdA* is strongly stimulated by light in *F. fujikuroi*, an activation that is impaired in the *wcoA* mutants. However, the null *vvdA* mutants exhibit similar patterns of transcriptional photoinduction and photoadaptation of the *car* genes, indicating that VvdA does not play a direct regulatory role on the expression of these genes. Unexpectedly, the *vvdA* mutant colonies exhibit light-dependent developmental alterations, manifest as a more compact formation of aerial mycelia, indicating an unexpected role of this photoprotein in mycelia development.

RESULTS

1. The *F. fujikuroi* genome contains a *vvd* ortholog

A Blast search with the VVD protein of *N. crassa* against *Fusarium* genome databases showed the occurrence of a single *vvd* orthologous gene in the genomes of *F. verticillioides*, *F. graminearum*, *F. oxysporum*, and *F. fujikuroi*. The occurrence of an ortholog was already mentioned for *Gibberella zeae*, teleomorph denomination of *F. graminearum* (Lombardi and Brody, 2005). Following our standard genetic nomenclature, we call this *Fusarium* gene *vvdA*. The predicted VvdA protein has 197 amino acids, 83 of them conserved in the 186 amino acids of the VVD protein of *N. crassa* (Fig. 1A). Similar VvdA proteins are also encoded in the genomes of other ascomycetes, such as ENVOY (Env1) in *Hypocrea jecorina* (anamorph, *Trichoderma reesei*). The VVD protein family consists of very short polypeptides containing a single PAS/LOV domain preceded by a short amino extension (PAS/LOV domain for VvdA indicated in Fig. 1). Such extension is longer in the closer ortholog of *Aspergillus nidulans*, with 366 amino acids, but a more canonical version is found in the *Aspergillus oryzae* genome, similar to those of *Fusarium sp*, *H. jecorina* and *N. crassa* (Fig. 1A).

The Blast search found other proteins in the *Fusarium* genomes with a similar PAS/LOV domain as that found in VvdA, but in all cases they were much larger. One of them is the white collar protein WcoA. 70 aa of the 142 aa segment between positions 322 and 463 in the WcoA protein, are also found in VvdA of *F. fujikuroi*, and include the whole LOV/PAS domain (Fig. III-1B). A similar situation was observed in *N. crassa*, whose VVD protein is highly similar in the equivalent internal segment of WC-1 (68 identical positions along 175 aa).

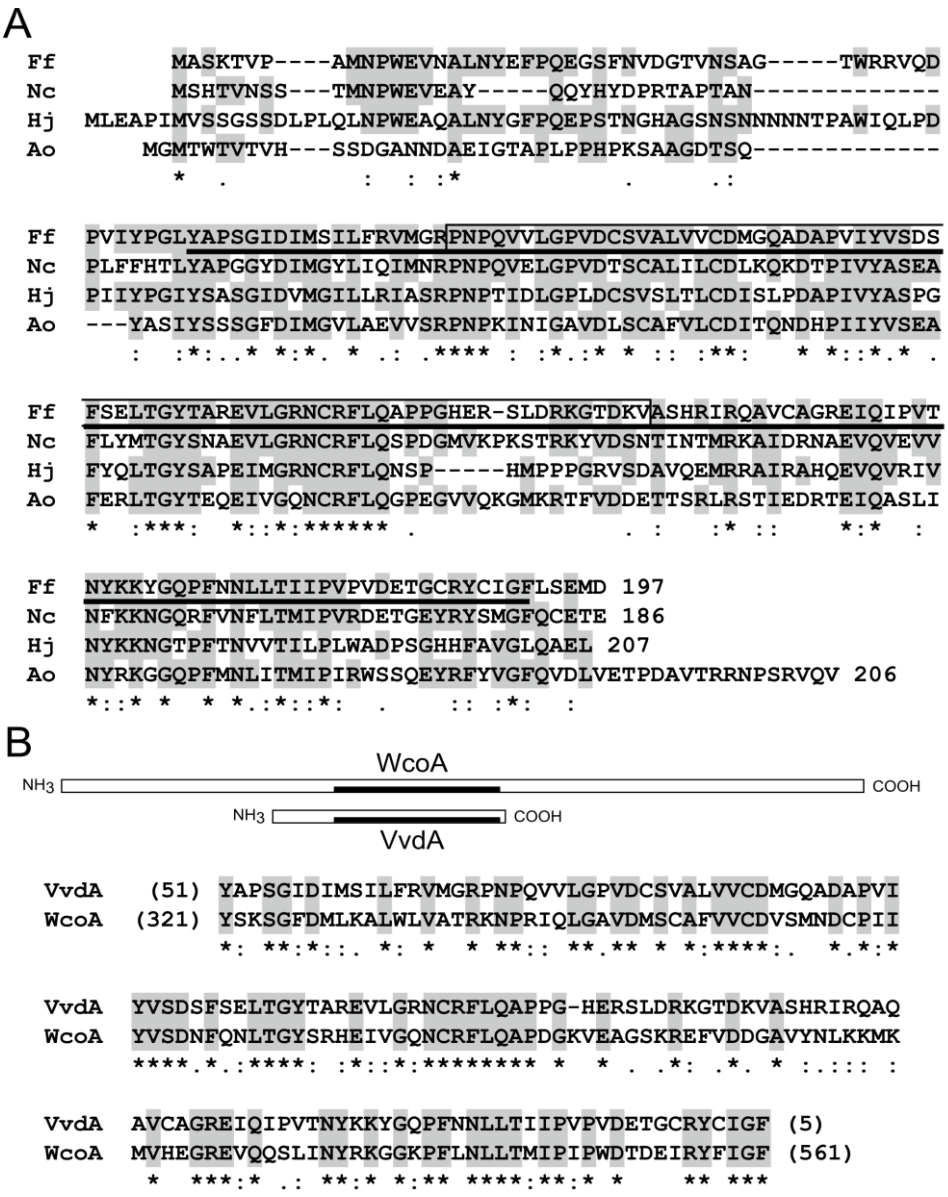

Fig. III-1. Sequence comparisons of VvdA. A. CLUSTALX alignment of VvdA from *F. fujikuroi* (Ff), VVD from *N. crassa* (Nc, Accession No. AF338412_1), Env1 from *H. jecorina* (Hj, AAT40588.1) and the VVD ortholog in *A. oryzae* (Ao, hypothetical protein Ao3042_05945). The LOV/PAS domain is boxed. Amino acids coinciding in at least two of the proteins are shaded in gray. B. Schematic representation of the location of the sequence sharing similarity between VvdA and WcoA of *F. fujikuroi* (thick line, also indicated in panel A). Below: detailed comparison of the CLUSTAL alignment between the thick line segment of both proteins.

2. *vvdA* is regulated by light through the White collar protein WcoA

In *N. crassa*, the *vvd* mRNA is hardly detected in the dark, but its amount increases rapidly under illumination to reach a maximum after 15 min and decreases again to become nearly undetectable after two hours of light (Heintzen et al., 2001). As a first insight on the role of *vvdA* in *F. fujikuroi*, we analyzed the effect of light on its transcript levels. As found in *N. crassa*, the *vvdA* mRNA content was very low in the dark, it increased 500-fold after illumination and it decreased afterwards (Fig. III-2). The induction was not so rapid as in *N. crassa*, with the maximum levels after one hour of light, and the subsequent reduction was not so drastic, conserving about one hundred-fold induction after 4 hours of light.

Photoinduction of *vvd* expression in *N. crassa* requires a functional White Collar Complex (Schwerdtfeger and Linden, 2003). Induction of *vvdA* was mostly lost in the mutants of the WcoA gene (Fig. III-2), indicating the mediation of the equivalent Wc complex of *F. fujikuroi*. Recently we showed that the DASH cryptochrome CryD plays light-dependent functions in *F. fujikuroi*. The Δ*cryD* mutants of this fungus still exhibit a strong photoinduction of *vvdA* (Fig. III-2), but the photoresponse was slightly reduced in these strains, suggesting a secondary role for CryD on *vvdA* regulation.

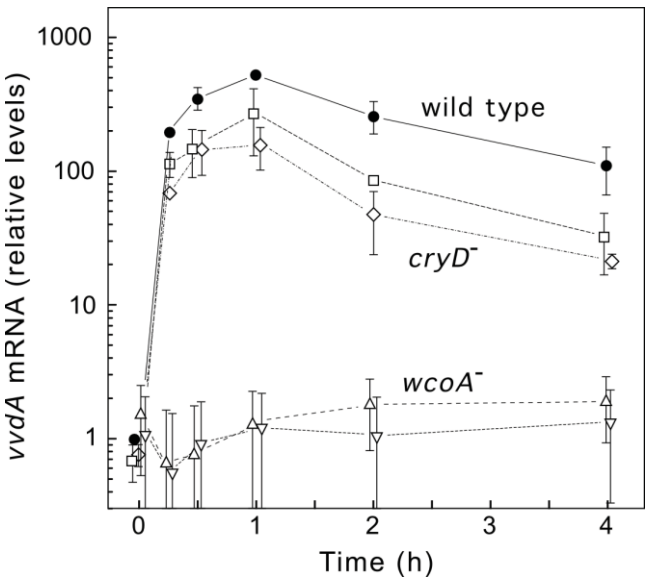

Fig. III-2. Expression of the *vvdA* gene. (A) Effect of light on *vvdA* mRNA levels in wild-type *F. fujikuroi* and in mutants for genes *cryD* (SF236, squares; SF237 rhombs) and *wcoA* (SF226, right way up triangles; SF22, upside down triangles). The data show qRT-PCR analyses of total RNA samples from the strains grown in the dark or exposed for 15 min, 30 min, 1 h, 2 h, or 4 h to 7 W m^{-2} white light. Relative levels are referred to the value of the wild type in the dark. Data show means and standard deviations for 9 measurements from 3 independent experiments.

3. The Δ*vvdA* mutants are affected in morphology and pigmentation

To investigate the function of the *vvdA* gene in *F. fujikuroi*, we generated targeted deletion mutants. For this purpose, we constructed a plasmid with a hygromycin resistance (HygR) cassette flanked by *vvdA* 5' and 3' regions and used it to transform the wild-type strain. The occurrence of two recombination events through the homologous DNA sequences is expected to generate a 2.1 kb deletion that includes the 702 bp *vvdA* coding sequence. Incubation of FKMC1995 protoplasts with the disruption plasmid resulted in the formation of 20 colonies on hygromycin supplemented medium, which were subcultured through single microconidia to ensure homokaryosis. The 20 strains were confirmed for the hygromycin resistant phenotype and analyzed by PCR to check the absence of the *vvdA* gene through its replacement by the hygR resistance cassette. Eight transformants exhibited the Δ*vvdA* pattern, indicated by the failure to detect *vvdA* and the amplification of a PCR product of the expected size from primers surrounding the *vvdA* deleted sequence (Fig. III-3B). Three putative Δ*vvdA* transformants (T1, T3 and T6) were chosen for more detailed

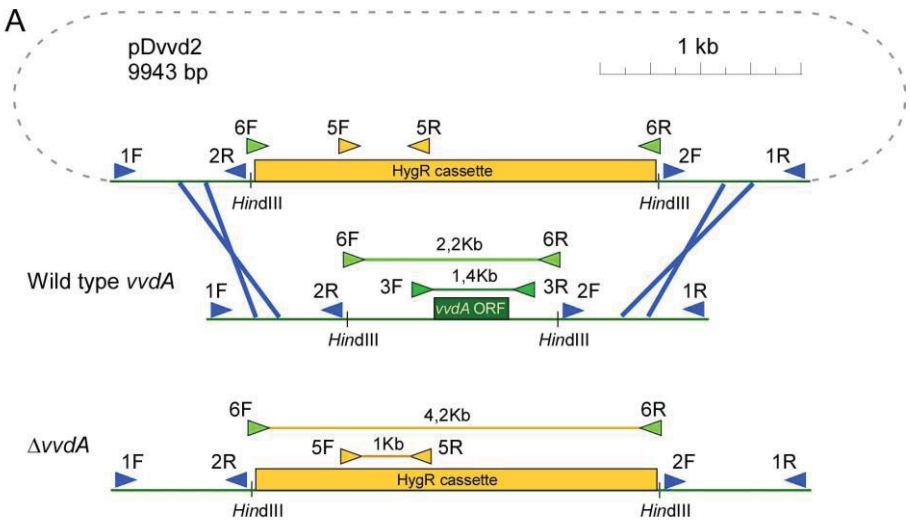

Fig. III-3A. Generation of targeted Δ*vvdA* mutants. A. Schematic representation of the gene replacement event leading to the generation of hygR Δ*vvdA* transformants. Plasmid pDvv2 contains the HygR cassette surrounded by the upstream and downstream *vvdA* sequences delimited by primers 1F-2R and 2F-1R (labeled in blue). The double recombination event (blue lines) results in the replacement of the wild type *vvdA* allele by the HygR cassette, as indicated in the lower scheme. Other primers sets used in the PCR analyses of the transformants are also shown.

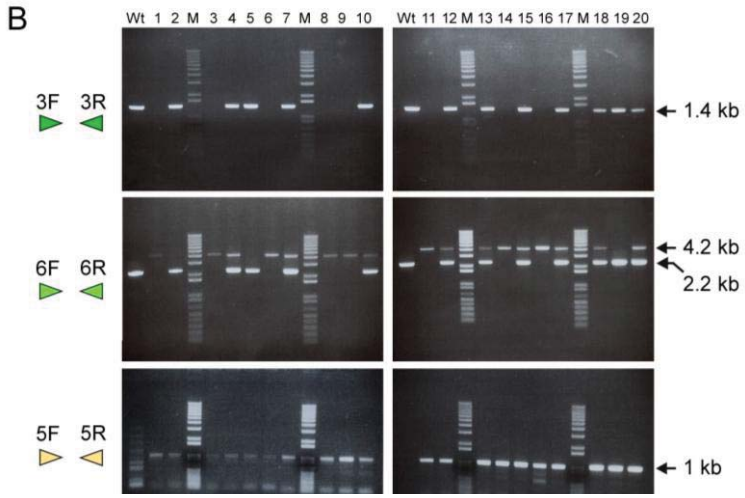

Fig. III-3B. Agarose gel electrophoreses of PCR amplification products obtained from DNA samples of the wild type and transformants T1 to T20 with the primer sets indicated on the left. PCR products and sizes are indicated in the upper scheme. The analysis allows detection of the correct gene by lack of the 3F-3R product, and presence of a 4.2 kb 5F-5R product. The 1 kb 4F-4R product confirms the presence of the HygR cassette in all the transformants but not in the wild type.

phenotypic characterization.

A detailed visual inspection of the three Δ*vvdA* strains revealed differences in the morphology and pigmentation of the colonies when the Petri dishes were incubated in the light on solid minimal medium (Fig. III-4). The assay was done either with inorganic ($NaNO_3$, DG medium) or organic (aparagine, DGasn medium) nitrogen source, which result in different aspects of the colonies. The morphological alterations were more apparent on DG medium, on which the Δ*vvdA* mutants developed colonies with denser mycelia compared to those of the wild type, while the difference was hardly appreciated in the dark (Fig. III-4). The variation in mycelia density was also appreciated under a stereoscopic microscope (Fig. III-4), but no difference was noticed on hyphal branching patterns on slide preparations under a standard microscope.

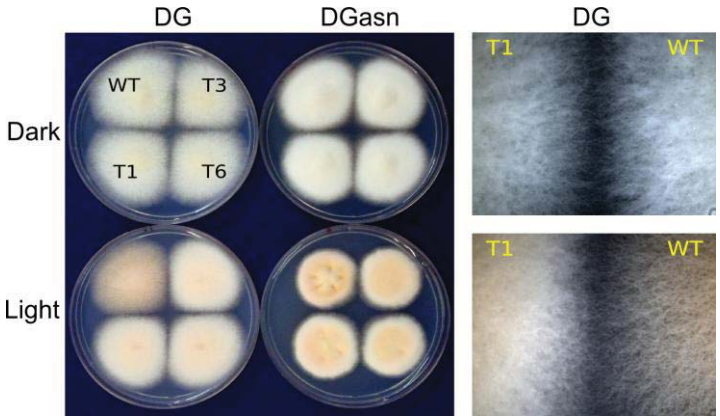

Fig. III-4. Morphological phenotype of ΔvvdA mutants. Colonies of the wild type and ΔvvdA mutants T1, T3 and T6 grown for 7 days at 30°C on DG and DGasn medium in the dark or under constant illumination (7 W m-2)(Left panel). Partial magnification of the border of the colonies of the wild type and the ΔvvdA mutant T1 in DG medium (Right panel).

4. The Δ*vvdA* mutants accumulate less carotenoids in the light and are not affected in photoadaptation

The *vvd* mutants of *N. crassa* accumulate more carotenoids than the wild type in the light (Navarro-Sampedro et al., 2008; Youssar et al., 2005). This phenotype is explained by a defect in photoadaptation of the transcripts for structural genes of the carotenoid pathway, as shown for the *carB* ortholog *al-1* (Schwerdtfeger and Linden, 2001). To check the effect of the Δ*vvdA* mutation on carotenoid photoinduction in *F. fujikuro*i, we analyzed the content of carotenoids of the wild type and the three Δ*vvdA* transformants under the culture conditions shown in Fig. III-5. As expected, the carotenoid content of the wild type was very low in the dark and increased notably under continuous illumination (Fig. III-5A). In accordance with their paler pigmentation, the carotenoid levels of the Δ*vvdA* mutants in the light were significantly reduced compared to the control strain. The carotenoid content of the wild type was higher in medium with asparagine than in medium with nitrate, but the mutants exhibited a similar reduction under any of these culture conditions.

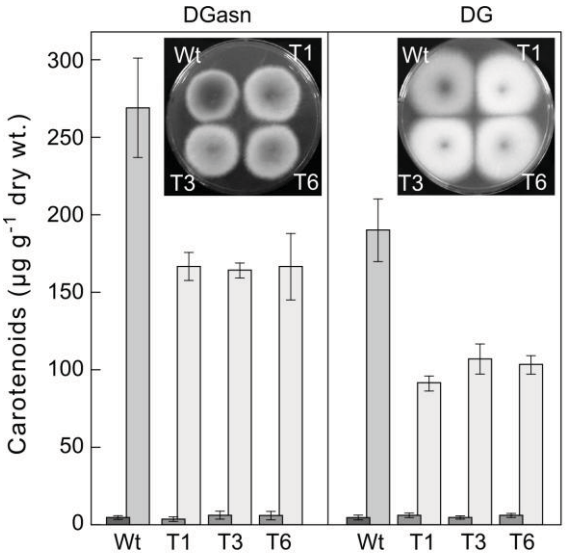

Fig. III-5. Carotenoid production in Δ*vvdA* mutants and effect of light on the expression of structural genes of the carotenoid pathway. Carotenoid content in the mycelia of the wild type and the Δ*vvdA* mutants T1, T3 and T6 in the dark (left obscure bars) or under light (right pale bars). The strains were grown for 7 days either in DGasn medium (left panel) or in DG medium (right panel). Each bar represents the average of 4 determinations. Inner pictures: 7-day-old surface colonies grown in each medium.

To check a possible effect of the Δ*vvdA* mutation on the photoinduction of the genes of the carotenoid pathway, the mRNA levels of the structural genes were investigated in the wild type and in the Δ*vvdA* transformants. The two biosynthetic genes responsible of the formation of colored carotenoids, *carRA* and *carB*, exhibited

the expected photoinduction pattern, with a drastic increase after one hour illumination and a partial reduction in the following hours (Fig. III-6). Despite their different carotenoid contents, the photoinduction patterns of *carRA* and *carB* in the Δ*vvdA* strains were very similar to those of the wild type. Similar results were obtained for other light-regulated genes of the *car* cluster, as *carX* and *carO* (Fig. III-6). The maintenance of the same decrease of mRNA levels in the Δ*vvdA* mutants after one hour illumination suggest that VvdA does not participate in the photoadaptation of this response.

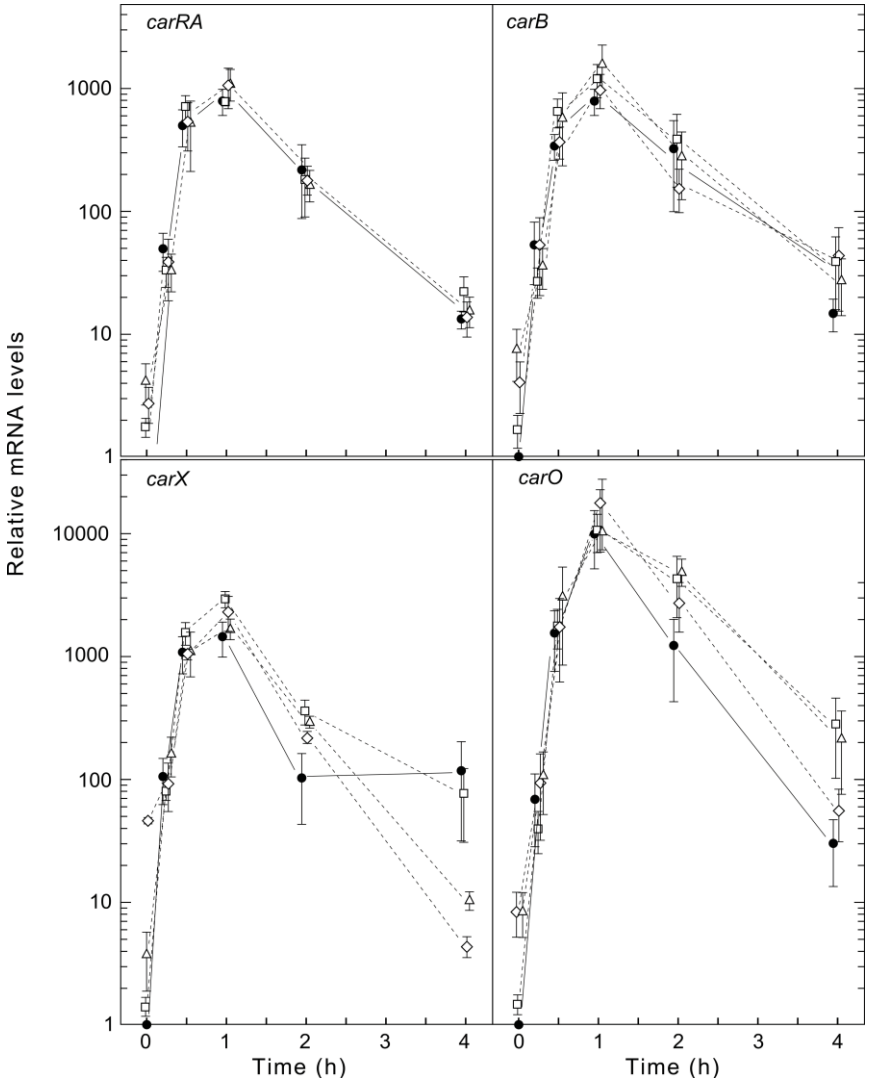

Fig. III-6. Real-time RT-PCR analyses of mRNA levels for the genes *carRA* and *carB* in RNA samples of the wild type and in the three Δ*vvdA* mutants in the dark and exposed to light for the times indicated. Relative expression was referred to the value for each gene in the wild type in the dark. Error bars represent the standard deviation for 9 determinations from 3 independent experiments. Transcript levels were normalized against β-tubulin mRNA.

To confirm that the reduced carotenoid content of the mutants was due to the absence of a functional *vvdA* gene, a wild type *vvdA* allele was introduced by transformation into the Δ*vvdA* mutant T6 using a geneticin resistance marker and 21 transformants were checked by PCR. Ten of the transformants were positive in a screening for the occurrence of a complete *vvdA* gene (Fig. III-7), and three of them were chosen for further phenotypic characterization (Fig. III-7D and III-7E). As expected, *vvdA* transcripts were hardly detected in the Δ*vvdA* mutants, while the complementing strains recovered the ability to produce wild *vvdA* mRNA levels under illumination (Fig. III-7D). Moreover, the three strains increased their carotenoid content under light (Fig. III-7E), confirming that the reduced carotenoid levels of the mutant strains were indeed produced by the deletion of the *vvdA* gene.

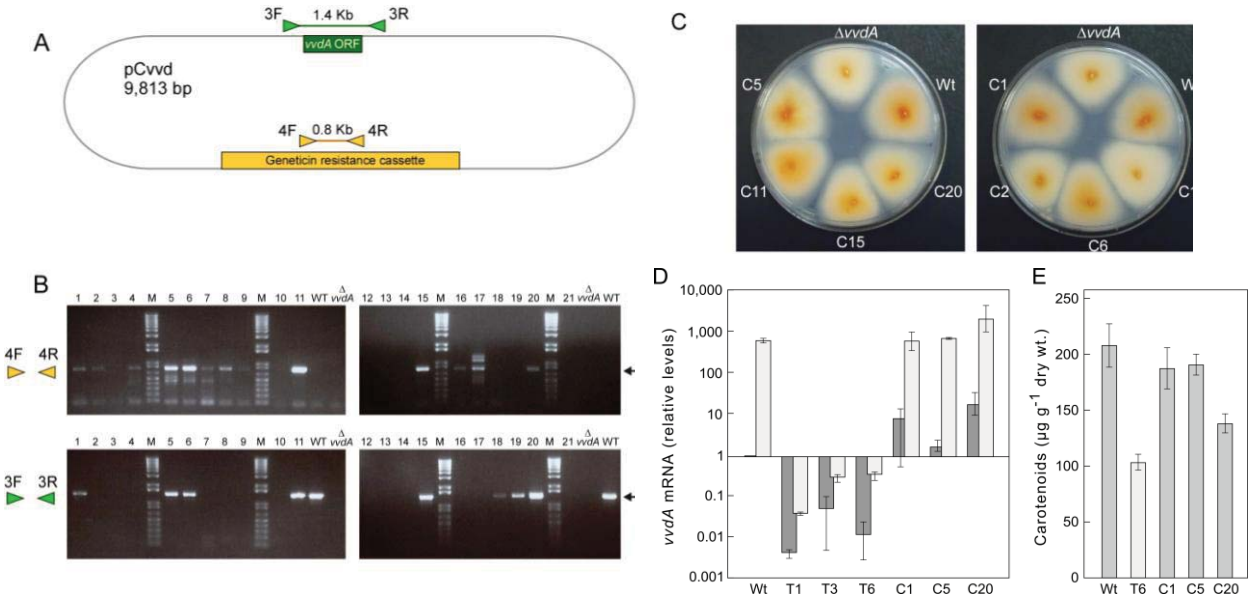

Fig. III-7. Complementation of the Δ*vvdA* mutation. (A) Schematic representation of the plasmid containing the wild type *vvdA* gene (green box) and the geneticin resistance cassette (orange box). Primers sets used in the PCR analyses of the transformants are also shown. (B) Agarose gel electrophoreses of PCR amplification products obtained from DNA samples of the wild type (Wt), the Δ*vvdA* mutant T6, and transformants C1 to C21 with the primer sets indicated on the left. PCR products and sizes are indicated in the upper scheme. The analysis detects the wild type *vvdA* gene by amplification of the 1.4 kb 3F-3R product and the geneticin resistance gene (*nptII*) by amplification of the 0.8 kb 4F-4R product. (C) Pigmentation in 8 transformants with a positive *vvdA* signal in the PCR tests. compared with wild type and Δ*vvdA* colonies. Pictures were taken on the back of the Petri dishes. (D) *vvdA* mRNA levels in wild type, the Δ*vvdA* mutants T1, T3 and T6 and the complementing strains C1, C5 and C20 . The data show qRT-PCR analyses of total RNA samples from the strains grown in the dark (left obscure bars) or after one hour exposure to 7 W m^{-2} white light (right pale bars). Relative levels are referred to the value of the wild type in the dark. All data show means and standard deviations for 6 measurements from 2 independent experiments. E. Carotenoid content in the mycelia of the wild type, the Δ*vvdA* mutant T6 and the complementing strains after 7 days growth in DGasn medium under 7 W m^{-2} white light. Each bar represents the average of 6 determinations from 3 independent experiments.

Two of the complementing strains exhibited higher *vvdA* transcript levels in the dark than the wild type, possibly due to position effects of the inserted plasmid sequence. The transformant exhibiting a *vvdA* expression pattern more similar to that of the wild type, C5, was chosen as an additional control strain for further phenotypic analyses.

5. The *ΔvvdA* mutants are affected in conidiation under light

The mutation of the White collar gene *wcoA* results in a drastic reduction in the production of conidia by *F. fujikuroi* on DG minimal medium (Estrada and Avalos, 2008). We wondered if the morphological alterations exhibited by the Δ*vvdA* strains under light affect their ability to produce conidia. The amounts of conidia produced by the Δ*vvdA* mutants were reduced to about one-half on either DG or DGasn media, while no significant difference was observed in the dark (Fig. III-8A). The complementing strain C5 exhibited a higher conidiation pattern than its preceding

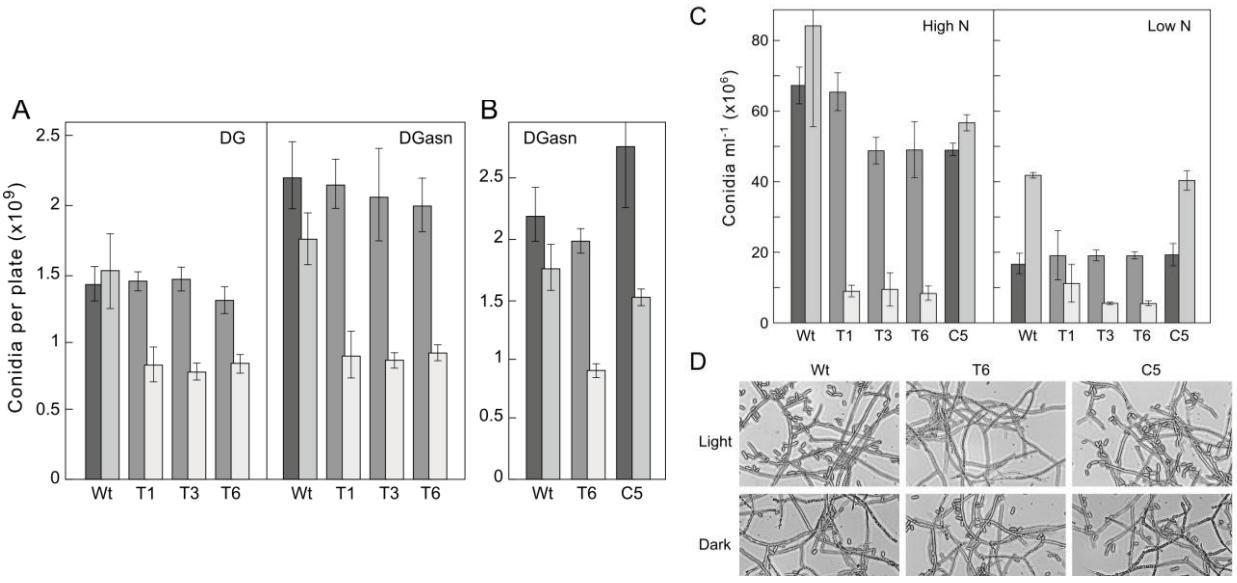

Fig. III-8. Effect of the Δ*vvdA* mutation on conidiatio.(A) Left panel: conidia produced by the wild type (Wt) and the Δ*vvdA* mutants T1, T3 and T6 grown in DG (left panel) or DGasn (right panel) medium in the dark (left obscure bars) or under 5 W m^{-2} white light (right pale bars). (B) Conidia produced by the wild type (Wt), the Δ*vvdA* mutant T6, and the complementing transformant C5 grown in DGasn medium. (C) Conidia produced by the wild type (Wt), the Δ*vvdA* mutants T1, T3 and T6 and the complementing transformant C5 grown in high or low N liquid media. The strains were grown for 7 days in the dark (dark left bars) or under white light (5 W m^{-2}, right paler bars). Data show averages and standard deviations from 2 independent experiments. (D) Representative examples under the microscope (400x) of the cultures on high N medium.

mutant T6 (Fig. III-8B).

The *wcoA* mutation also affects the production of conidia in submerged cultures either with excess or limiting nitrogen concentrations (Estrada and Avalos, 2008), and the mutation of the gene for another photoprotein, the DASH cryptochrome *cryD*, results in an unusual formation of macroconidia under nitrogen starvation and light (Chapter I). The incubation of the Δ*vvdA* mutants under these culture conditions resulted in a drastic decrease in the production of conidia compared to the wild type in the light, but not in the dark (Fig. III-8C). The result was similar irrespective of nitrogen availability, except that conidia were less abundant in low nitrogen conditions. Aside of conidia numbers, no apparent alterations were appreciated in hyphal morphologies in the Δ*vvdA* strains under microscope inspection.

6. The *ΔvvdA* mutants exhibit alterations in mycelia organization under light

The visual inspection of the mycelia produced by the Δ*vvdA* complementing strains showed that the functional *vvdA* gene restored the wild-type morphology under light. This was also visualized through background illumination, which resulted in a denser aspect of the Δ*vvdA* mutant colonies compared to wild-type and complementing strains (Fig. III-9A). A detailed examination under stereoscopic microscope of colony sections revealed a compact mycelial layer on the agar of the Δ*vvdA* mutant, which was less apparent in the wild type or in the complementing strain C5 (Fig. III-9B), or in any of the strains grown in the dark. The magnification of the cross section showed different pigmented layers in the wild type, with the deeper pigmentation in a dense mycelial layer embedded in the agar (Fig. III-9B). However, this layer is less pigmented in the *vvdA* mutant, and it is covered by denser and also less pigmented aerial mycelia. This difference could explain the lower carotenoid content of the Δ*vvdA* mutants. The wild type pattern is essentially recovered in the complementing strain C5.

The protocols for conidia collection from the agar Petri dishes require scraping the surface of the colonies with a spatula after addition of 15% glycerol, followed by washes with water. We noticed that the scraping of the colonies on DG medium totally removed the aerial parts of the colonies in the wild type and the complementing

strains, while a thin mycelial layer was retained on the surface in the case of the Δ*vvdA* mutants, which was partially removed by more persistent scraping (Fig. III-9C). Presumably, this layer corresponds to the denser mycelial coat attached to the agar, as visualized in the Δ*vvdA* mutant in Fig. III-9B. As a general rule, *F. fujikuroi* colonies grown on DGasn medium were more compact than those formed on DG medium. Scraping of DGasn-grown colonies for conidia calculations revealed a softer attachment to the agar surface by the wild type and the complementing strain C5, while the Δ*vvdA* mutants were not detached in this process (Fig. III-9D). That was clearly shown by the aspect of the tubes with scraped samples, in which the mycelial fragments were clearly visible in the tubes of the wild type and complementing strain, but not in those of the Δ*vvdA* mutant (Fig. III-9E). However, the mycelia were not detached from the colonies of any of the strains tested if the same procedure was followed with the Petri dishes incubated in the dark. The difference between Δ*vvdA* mutants and control strains under light was not due to different abilities to absorb water, as formerly described for the hydrophobicity alterations exhibited by the *ΔwcoA* mutants (Estrada and Avalos, 2008).

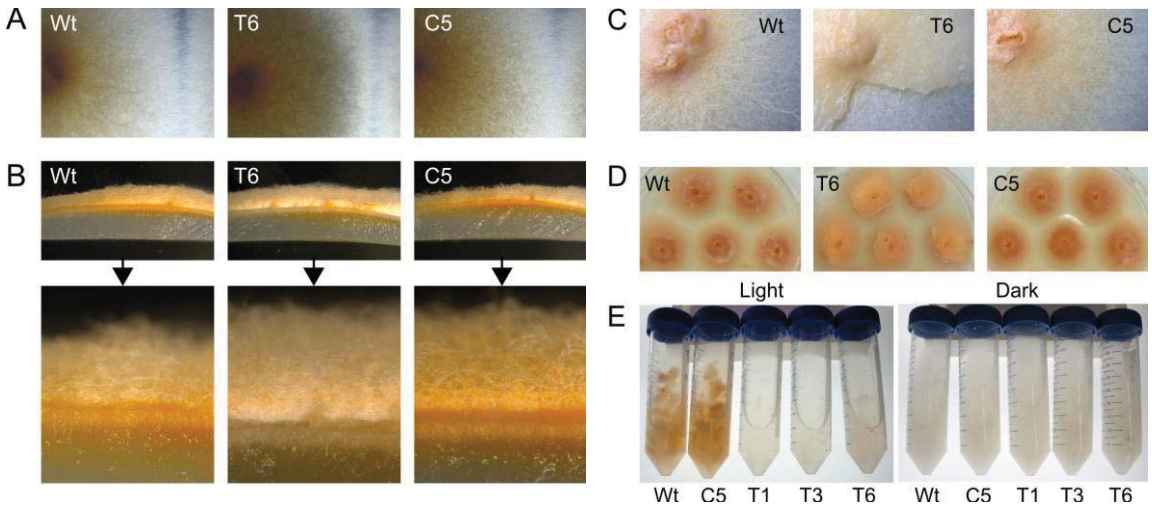

Fig. III-9. Morphological alterations of Δ*vvdA* mutants. (A) Background-illuminated colonies of the wild type (Wt), the Δ*vvdA* mutant T6 and the complementing transformant C5 grown in DG medium for 7 days under constant light. (B) Cross sections of the colonies displayed above. A more detailed magnification is shown in the lower pictures. (C) Surface of the same colonies following scraping and washing in the protocol for conidia determination. (D) Aspect of the surface mycelia after the same conidia extraction protocol applied to colonies of the same strains grown under light on DGasn medium. (E) Left picture: samples collected after washing the colonies displayed on panel B. The aspect of the samples from colonies grown in the dark is shown on the right.

As an alternative culture condition, the strains were grown in top agar cultures. In these conditions, a homogenous mycelial pad is formed from the agar-embedded germinating conidia. Incubation of top agar cultures in the dark resulted in non-pigmented mycelial pads of similar surface texture for the wild type, Δ*vvdA* mutants and complementing strains. However, the texture and pigmentation of the Δ*vvdA* mutant differed in the light, with less rough surface and paler pigmentation compared with the control strains (Fig. III-10).

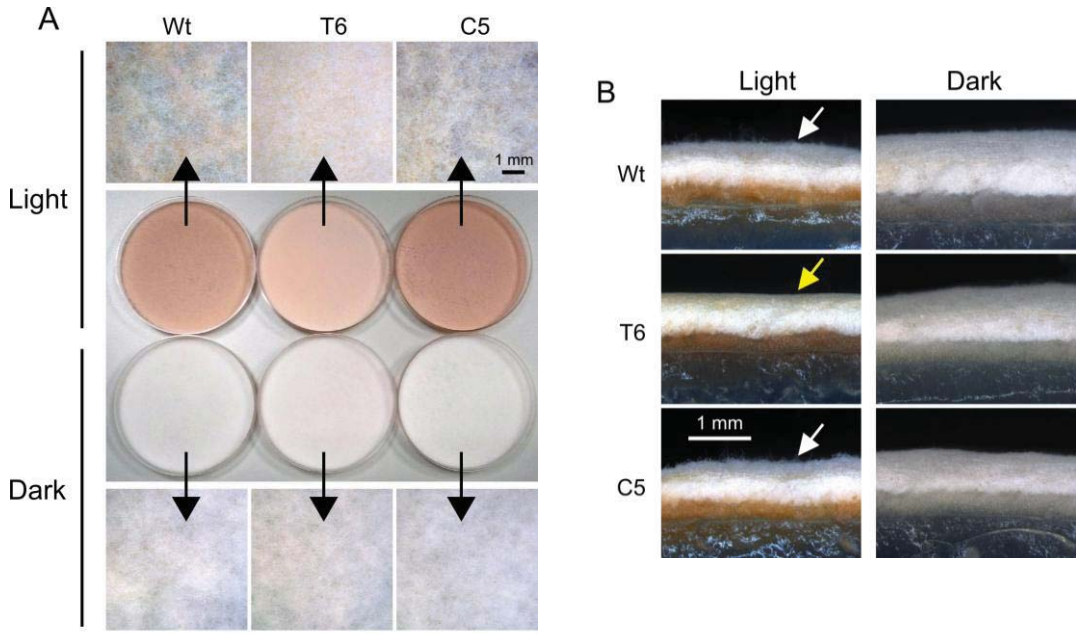

Fig. III-10. Morphological alterations a Δ*vvdA* mutant in top agar cultures. (A) Aspect and pigmentation of top agar pads of the wild type (Wt), the Δ*vvdA* mutant T6 and the complementing transformant C5 grown on DG medium for 7 days under constant light (above) or in darkness (below). The arrows point to magnification pictures under stereoscopic microscope of the surface of the mycelial pads. In the light, the T6 mycelial pad exhibits a smoother surface than those of the wild type and the complementing strain C5. (B) Cross sections of the top agar cultures displayed above. Under light, the surface of the wild type (Wt) and the complementing strain C5 were rougher (white arrows) than that of the Δ*vvdA* mutant T6 (yellow arrow).

DISCUSSION

The genome of *N. crassa* contains genes for several photoreceptor proteins, whose detailed investigation has made this fungus a paradigmatic model in molecular studies of light regulation. Known photoresponses in *N. crassa*, such as photocarotenogenesis, photoinduction of protoperithecia formation, phototropism of perithecial beaks, and circadian rhythmicity, depend on the light-regulated activity of the WC complex, formed by WC-1 and WC-2 (Chen et al., 2010). Therefore other photoreceptors probably only play accessory roles. The *Fusarium* species are appropriate research models for phytopathogenesis and secondary metabolism and have been less frequently used in photobiology studies. An exception is the photoinduction of carotenoid biosynthesis, investigated in detail in *F. aquaeductuum* (Rau, 1967a) and more recently in *F. fujikuroi*. Interestingly, the *Fusarium* genomes contain a set of photoreceptor genes at least as complex as that of *N. crassa* (Avalos and Estrada, 2010), including orthologs for the WC proteins and the small flavoprotein VVD, involved in the transcriptional photoadaptation of light-induced genes in *N. crassa*. However, former results on the *F. fujikuroi* WC gene and those shown in this work on the *vvdA* gene reveal differences in this regulatory mechanism. The mycelia of the WC mutants of *N. crassa* remain albino in the presence of light, but the *wcoA* mutants of *F. fujikuroi* accumulate carotenoids at wild-type levels when grown under constant illumination, even though they are affected in the transcriptional photoinduction of the carotenogenic genes (Estrada and Avalos, 2008). Morevover, in contrast to the light-dependent expression of *wc-1* in *N. crassa*, the transcript levels of *wcoA* of *F. fujikuroi* are hardly affected by light, and its mutation has phenotypic effects not only under light but also in the dark, including changes in the production of different secondary metabolites (Estrada and Avalos, 2008). Taken together, these data show that the WC gene *wcoA* has evolved in *Fusarium* to mediate different regulatory functions than WC-1 in *N. crassa*.

As WC-1, VVD contains a flavin-binding PAS/LOV (from light-oxygen-voltage) domain, a PAS domain variant able to absorb light and mediate protein-protein

interactions (Heintzen et al., 2001; Schwerdtfeger and Linden, 2003). In *N. crassa*, the VVD protein is activated upon illumination, and it is able to form either homodimers (Zoltowski and Crane, 2008) or heterodimers with the WC complex through their PAS/LOV domains (Chen et al., 2010; Malzahn et al., 2010). The formation of VVD-WCC heterodimers interferes with the formation of active WCC homodimers and arrests the WC-mediated activation of light-induced genes (reviewed by (Schafmeier and Diernfellner, 2011)). Since the WC complex transcriptionally induces *vvd*, the result of this negative feed-back regulatory loop is the attenuation of light-induced transcription of WC-regulated genes, a phenomenon known as photoadaptation. VvdA has high sequence conservation with VVD and it exhibits a similar WC-1 dependent transcriptional photoinduction, but it is unknown if the VvdA protein of *F. fujikuroi* is able to interact in a similar way with a light-activated WC complex in this fungus. However, the phenotype of the *vvdA* mutant differs drastically from that of the *vvd* counterpart in *N. crassa*. The most characteristic trait of the *vvd* mutants of *N. crassa*, the higher carotenoid content in the light, is reversed in the *vvdA* mutants of *F. fujikuroi*, which exhibit a lower carotenoid content. In addition, no change was observed in the induction and subsequent photoadaptation of the *car* genes. However, the *vvdA* mutants exhibited light-dependent developmental alterations on agar cultures, manifest as differences in mycelia organization. In contrast to the *vvd* mutants of *N. crassa*, for which no morphological alterations have been reported, a detailed analysis of the Δ*vvdA* colonies under stereoscopic microscope showed a denser mycelial layer on the agar surface, less pigmented that the wild type mycelial counterpart. In other fungi, carotenoid biosynthesis is enhanced by a higher aeration (see, e.g. (Nanou and Roukas, 2011) (Estrada et al., 2009b)). Taking into account the lack of effect of the *vvdA* mutation on the expression of the *car* genes, the reduced carotenoid content might be an indirect effect of a lower oxygenation resulting from a denser mycelia organization. However, the participation of VvdA on light-dependent postranscriptional regulation of carotenogenesis is not discarded.

VvdA is the third VIVID-like protein investigated in filamentous fungi. In addition to *N. crassa*, the VVD ortholog of *Hypocrea jecorina*, Env1, has been also thoroughly analyzed. This fungus exhibits an elaborate photobiology (Schmoll et al., 2010a), with

its WC-1/WC-2 orthologs Blr1/Blr2 playing a central role in the control of its development by light (Casas-Flores et al., 2004; Casas-Flores et al., 2006; Esquivel-Naranjo and Herrera-Estrella, 2007). Env1 was initially detected from a gene lacking expression in a cellulase-negative mutant (Schmoll et al., 2005b) and, as found for *vvd* and *vvdA*, its expression is strongly induced by light through Blr1 and Blr2 (Castellanos et al., 2010). Env1 participates in the control by light of cellulose gene expression. This regulation is achieved on the transcript levels of the G-alpha subunit encoding genes *gna1* and *gna3*, which participate in the heterotrimeric G-protein cascade, thus implicating cAMP through the regulation of a phosphodiesterase activity (Schmoll et al., 2009; Tisch et al., 2011). In our case, the Δ*vvdA* mutants are apparently not affected in their capacity to degrade cellulose, as hint their abilities to grow on cellulose paper as the only carbon source (Fig.III-11). Env1 also participates in the regulation of the sexual cycle of *H. jecorina*, which is up-regulated by light. The strains lacking *env1* exhibit considerable increases under light in transcript levels of genes for peptide pheromone precursors and pheromone receptors, while the crossing phenotype shows that Env1 is essential for female fertility (Seibel et al., 2012). Therefore, Env1 is a key regulator for sexual identity and fruiting body formation in *H. jecorina*. We made attempts to determine if the *vvdA* mutation affects the sexual cycle in *F. fujikuroi*, but fertility of our control strains was too low under our culture conditions to allow any conclusions.

The *H. jecorina* genome lacks structural genes for carotenoid biosynthesis, and a possible role of Env1 on photoadaptation of the carotenogenic genes is therefore out of consideration. However, different results suggest functional similarities between Env1 and VVD. E.g., the *env1* mutants of *T. reesei* show an attenuated photoadaptation of some light-induced genes, such as *blu1* and *blu4* (Castellanos et al., 2010), a feature that reminds the defective photoadaptation of light-regulated genes in the *vvd* mutants of *N. crassa*. In contrast, we did not detect any clear photoadaptation defect in the *vvdA* mutants for any of the four genes of the *car* cluster of *F. fujikuroi*, *carRA*, *carB*; *carX* and *carO*. As an additional Vvd-like feature, a second light exposure did not produce further increments of *blu1* and *blu4* transcripts in the wild type, but they did in the *env1* mutant (Castellanos et al., 2010), suggesting that Env1 participates in the

transient inactivation of the light detecting Blr-1/Blr-2 complex. Nevertheless, Env1 fails to complement the *vvd* mutation in *N. crassa*, suggesting differences in their mechanisms of action.

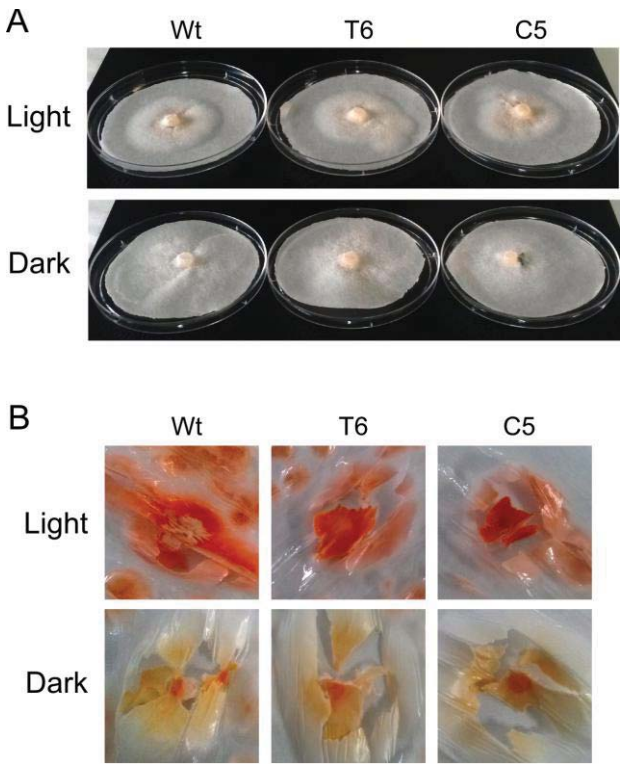

Fig. III-11. Phenotype of Δ*vvdA* mutants on cellulose substrates. (A) Growth of the wild type (Wt), the Δ*vvdA* mutant T6 and the complementing transformant C5 on a cellulose filter in the absence of an alternative carbon source. The strains were incubated for 7 days at 30°C in the dark or under 7 W m^{-2} white light. (B) Aspect of cellophane layers after 7 days growth of the same strains on cellophane-covered DG medium. The mycelia were removed from the cellophane surface, showing its partial degradation.

The phenotypic effects of the *env1* mutation in *H. jecorina* differ from those produced by the *vvdA* mutation in *F. fujikuroi*, but they have in common alterations in development and conidiation. As expected from the light-dependent expression of both genes, the mutants exhibit the alterations especially under illumination. In these conditions, the *env1* mutants are severely impaired in growth and morphology (Schmoll et al., 2005b), possibly because of deleterious effects of the sustained expression of Blr-induced genes in this mutant. These alterations are more severe than the more subtle changes observed in the Δ*vvdA* strains of *F. fujikuroi*. The defective growth of the *env1* mutants indicates a central role for this protein in the control of *H. jecorina* development under light, while *vvdA* apparently plays a less relevant function.

No quantitative analyses have been reported on the impact of the *env1* mutation on conidiation. However, despite the drastic growth defects, an illumination pulse produces in the *env1* mutant conidiation rings very similar to those observed in the wild type (Castellanos et al., 2010), suggesting that Env1 does not participate in the modulation of this photoresponse. Conidiation has a quite different pattern in *F. fujikuroi*, where the conidia are homogeneously produced all through the mycelium in the colonies of our wild type strain, and the conidiation levels are not increased by light. However, under continuous illumination, the mycelia of the *vvdA* mutants produce less conidia than the control strains, specially under submerged conditions. This phenotypic disparity highlights the functional differences between Env1 and VvdA, which adds to those already observed when compared to VVD of *N. crassa*. The results described in this work are the first report on VvdA function in *F. fujikuroi*, and the amount of data are very limited compared with the many reports already available for Vvd and Env1. More experiments will be needed with *vvdA* and with its counterparts in other species to have a wider scope of the diversity of functions of this small photoreceptor in filamentous fungi.

CHAPTER IV

Cooperative functions of WcoA, CryD and VvdA photoreceptors in photoinduction of carotenogenesis in *Fusarium fujikuroi*

INTRODUCTION

Filamentous fungi are a widespread group of lower eukaryotes able to grow in a large diversity of natural habitats, where they use light as a key environmental signal to modulate physiological and developmental processes. Some fungi stand out for their ability to produce a wide range of secondary metabolites (Hoffmeister and Keller, 2007). To this class belong the species of the genus *Fusarium*, an ubiquitous group of phytopathogenic fungi able to produce an extensive array of compounds, many of them mycotoxins (Desjardins and Proctor, 2007a). A representative example is *Fusarium fujikuroi,* well known for its capacity to produce gibberellins (GAs), growth-promoting plant hormones with biotechnological applications (Rademacher, 1997)This fungus produces many other compounds, including pigments that provide characteristic colors to their mycelia (Avalos et al., 2007). When grown in the light, *F. fujikuroi* colonies acquire a characteristic orange pigmentation due to the synthesis of carotenoids (Fig. 1), with the xanthophyll neurosporaxanthin as major component (Avalos et al., 2012). The biosynthetic carotenoid pathway of this fungus has been investigated in detail, and all the enzymatic genes have been identified and characterized (Díaz-Sánchez et al., 2011a; Linnemannstöns et al., 2002b; Prado-Cabrero et al., 2007b; Thewes et al., 2005).

The regulation of carotenoid biosynthesis has been object of special attention in several fungi, including *F. fujikuroi* (Avalos et al., 2014). Light was found to induce the synthesis of carotenoids in different *Fusarium* species (Avalos and Estrada, 2010). This photoinduction was first investigated in *Fusarium aquaeductuum* (Bindl et al., 1970; Rau, 1967a), and later described in *F. fujikuroi* (Avalos and Schrott, 1990), *F. verticillioides* (Adám et al., 2011) and *F. oxysporum* (Rodríguez-Ortiz et al., 2012). A second regulatory signal is nitrogen availability, which plays a central role in the control of secondary metabolism in this fungus (Díaz-Sánchez et al., 2012; Tudzynski, 2005; Wiemann et al., 2009), and it affects negatively the production of carotenoids (Rodríguez-Ortiz et al., 2009). The only regulatory gene identified affecting carotenoid biosynthesis in *Fusarium* is *carS*, whose mutation leads to a strong transcriptional up-

regulation of the structural *car* genes (Prado et al., 2004; Rodríguez-Ortiz et al., 2009), which results in the accumulation of a high amount of carotenoids under different culture conditions (Avalos and Cerdá-Olmedo, 1987; Rodríguez-Ortiz et al., 2009). *carS* encodes a protein of the ring finger family (Rodríguez-Ortiz et al., 2013; Rodríguez-Ortiz et al., 2012), whose molecular mechanism of action remains to be established.

Photoinduction of carotenogenesis has been investigated in detail in *N. crassa,* where it is mediated by the heterodimeric White Collar (WC) complex (Linden and Macino, 1997). Upon illumination, the WC complex is activated through the WC-1 flavin-binding LOV/PAS domain and binds upstream promoter sequences of light-regulated genes to induce their transcription (He and Liu, 2005). Similar WC complexes control diverse photoresponses in other fungi (Corrochano, 2007), including photoinduction of β-carotene production in the mucorales *P. blakesleeanus* and *M. circinelloides*. Against the predictions, the mutation of the WC-1 like protein genes in *F. fujikuroi* (Estrada and Avalos, 2008) and *F. oxysporum* (Ruiz-Roldán et al., 2008) did not impede the photoinduction of the carotenoid pathway, indicating the participation of other photoreceptors. A former action spectrum established for photocarotenogenesis in *F. aquaeductuum* was consistent with the participation of a flavin-based photoreceptor (Rau, 1967a). The *Fusarium* genomes contain several genes coding for other presumptive flavin photoreceptors in addition to the WC-1 like protein (Avalos and Estrada, 2010). The list includes a small *vivid*-like protein, a photolyase, a DASH-cryptochrome and a second cryptochrome-like gene, related to plant cryptochromes and whose function in *Fusarium* is currently under investigation (B. Tudzysnki, unpublished).

Cryptochromes are blue/UV-A light photoreceptors possibly evolved from photolyases, able to bind two chromophores, flavin adenine dinucleotide (FAD) and pterin 5,10-methenyltetrahydrofolate (MTHF) (Chaves et al., 2011; Sancar, 2003). Most cryptochromes have C-terminal extensions absent in photolyases, which play regulatory roles related to light control of growth, development, cell signaling or circadian rhythm in different taxonomic groups (Chaves et al., 2011). DASH-cryptochromes (abbreviated hereafter as cry-DASHs), a subgroup in this family, differ from cryptochromes in their ability to repair DNA lesions in single-stranded DNA (Selby

and Sancar, 2006) or loop-structures of duplex DNA (Pokorny et al., 2008). A recent functional analysis of the *F. fujikuroi* cry-DASH gene, called *cryD*, showed its participation in the regulation by light of the production of secondary metabolites, as the bikaverin and the gibberellins, while it was apparently not involved in carotenoid photoinduction (Chapter I of this Thesis).

Vivid-like photoreceptors are small flavin binding proteins represented by VVD (VIVID) of *N. crassa* and ENV1 (ENVOY) of *Hypocrea jecorina*. In *N. crassa*, VVD participates in photoadaptation of light-regulated genes (Schwerdtfeger and Linden, 2003; Shrode et al., 2001), a function achieved through the modulation of the activity of the WC complex (Malzahn et al., 2010). As a consequence, the Δ*vvd* mutants exhibit a deeper pigmentation and accumulate more carotenoids under light than the wild type (Navarro-Sampedro et al., 2008; Youssar et al., 2005). Env1 plays a more relevant role in *H. jecorina*, as indicates the drastic effect of the *env1* mutation on growth and morphology under light (Schmoll et al., 2005b). Additionally, Env1 was found to participate in the regulation by light of cellulose gene expression (Schmoll et al., 2005b), the sexual cycle (Seibel et al., 2012), and photoadaptation of some light-induced genes (Castellanos et al., 2010). Our recent investigation of the *vvd* gene of *F. fujikuroi*, *vvdA*, revealed significant differences in its function with VVD and Env1: the Δ*vvdA* mutants produce less carotenoids than the control strains and exhibit light-dependent alterations in conidiation and mycelia development (Chapter III of this Thesis). However, no alterations were found in photoinduction or photoadaptation of the *car* genes.

Here we report on the role of the WcoA, CryD and VvdA photoreceptors in the regulation by light of carotenoid biosynthesis in *F. fujikuroi*. We found that this light response has two separate components in this fungus, a fast response in the first hours of illumination and a slower response upon more prolonged light exposure. The kinetics of the photoresponse in the absence of these photoreceptors indicate that WcoA is a major photoreceptor in *F. fujikuroi* carotenoid biosynthesis, but that CryD mediates a slower and less sensitive photoresponse, which explains the photoinduction exhibited by the Δ*wcoA* mutants under continuous illumination. The kinetics of the response is also altered by the loss of VvdA, which seems to play

negative and positive effects on WcoA and CryD functions, respectively. Our results represent the first report on the participation of a cryptochrome in the regulation of carotenoid biosynthesis in any microorganism, and point to a complex organization of the light-detection machinery that controls carotenoid biosynthesis in *Fusarium*.

RESULTS

1. Effect of *wcoA*, *cryD*, and *vvdA* mutations on regulation of carotenogenesis under constant illumination

Formerly, we reported on the effect of the mutations of the WC1-like photoreceptor WcoA (Estrada and Avalos, 2008), the cry-DASH CryD (Chapter I), and the flavoprotein VvdA (Chapter III) on growth and secondary metabolism of *F. fujikuroi*. The strains exhibited different pigmentations, and in some cases the carotenoids produced under illumination were masked by the occurrence of non-carotenoid pigments, such as the bikaverins in the Δ*cryD* mutants (Fig. IV-1). These studies included quantifications of carotenoid contents with independence of other pigments, and showed the occurrence of carotenoid photoinduction in all the mutant strains. Since the accumulation of carotenoids was only marginally investigated in Δ*cryD* mutants (Chapter I) we carried out more detailed analyses, which confirmed that these mutants accumulate under continuous illumination similar amounts of carotenoids than the wild type, either at 22°C or at 30°C (Fig. IV-2A). The relation between polar and neutral carotenoids was apparently altered at 30°C. However, the total amount of carotenoids in the Δ*cryD* mutants remained very similar to those of the wild type, confirming that CryD is not the major photoreceptor of carotenogenesis.

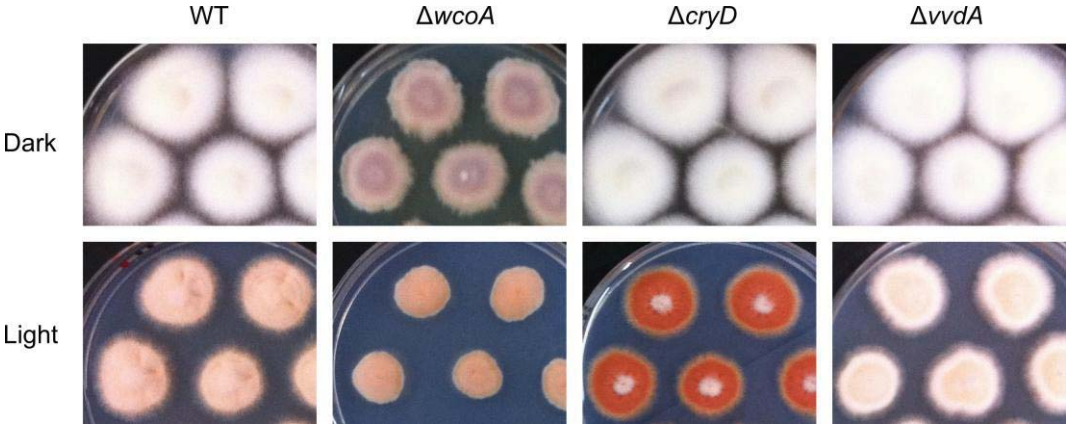

Fig. IV-1.Phenotype of the photoreceptors mutants compared to the wild type.Colonies of the wild type and representative Δ*wcoA* (SF226), Δ*cryD* (SF236) and Δ*vvdA* (SF258) mutants grown for 7 days at 30°C in the dark or under continuous illumination on DGasn medium.

The analyses on the Δ*vvdA* mutants were done at 30°C but those of the *wcoA* mutants were achieved at 22°C. To compare all the strains under the same culture conditions, new experiments were done to determine the amount of carotenoids of two Δ*wcoA* mutants grown either in the dark or under continuous illumination at 30°C (Fig. IV-2B). As recently found for the Δ*vvdA* strains (Chapter III), the Δ*wcoA* colonies produced less carotenoids than those of the wild type, albeit they maintained a clear photoinduction. Interestingly, the amounts of carotenoids in the dark in the Δ*wcoA* mutants were remarkably low compared to those of the wild type, suggesting a regulatory role for WcoA in the dark. To correlate these data with the expression of the genes of the carotenoid pathway, we determined the mRNA levels for the genes *carRA* and *carB* under the same culture conditions (Fig. IV-2C).

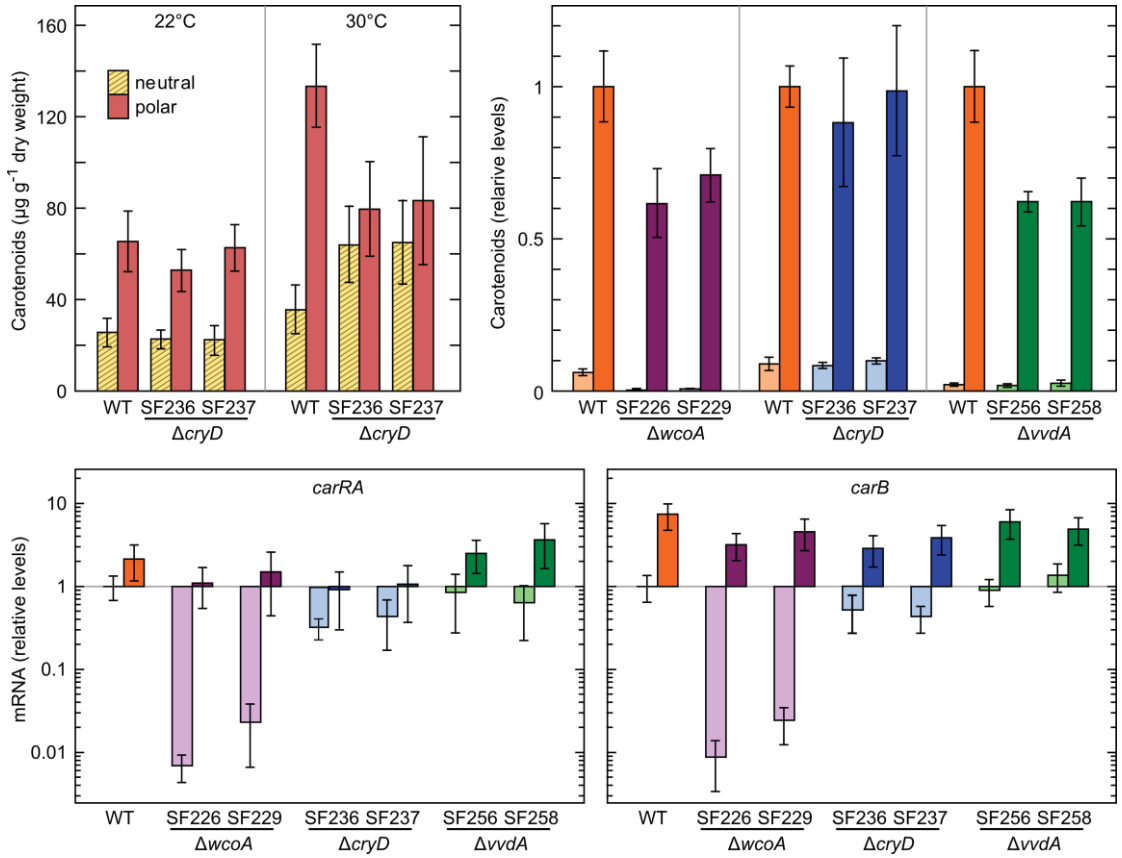

Fig. IV-2. Effect of the mutation of the photoreceptor genes *cryD*, *wcoA* and *vvdA* on the regulation of carotenoid biosynthesis under constant illumination. (A) Concentrations of polar and neutral carotenoids in the mycelia of the wild type and the Δ*cryD* mutants SF236 and SF237 grown for 7 days at 22°C or 30°C on DGasn medium under continuous illumination. The data show the average and standard deviations from 3 independent determinations. (B) Total concentration of carotenoids in the wild type and in parallel cultures of the Δ*wcoA,* Δ*cryD* and Δ*vvdA* mutants grown for 7 days at 30°C on DGasn medium in the dark or under continuous illumination. Data are the average and standard deviation of four determinations from two biological replicates. Data for Δ*vvdA* taken from chapter III. (C) Real-time RT-PCR analyses of the genes *carRA* and *carB* in RNA samples of the wild-type and the indicated strains grown for 7 days at 30°C on DGasn medium in the dark or under continuous illumination. Relative expression for each gene was referred to the value in the wild type grown in the dark. Data are the average and standard deviation of six determinations from two biological replicates.

The results showed a significant downregulation of *carRA* and *carB* mRNA levels in the dark in the Δ*wcoA* mutants, consistent with their lower carotenoid content in vivo. A significant *carB* photoinduction, ranging from 3- to 7-fold compared to wild type dark levels, was observed in all the strains tested. The induction was lower for *carRA* in the wild type and Δ*vvdA* strains, while it was hardly detectable in the Δ*wcoA* and Δ*cryD* mutants. However, because of their lower mRNA levels in the dark, *carRA* photoinduction was also manifest in these strains. In summary these experiments confirm the occurrence of photoinduction of *carRA* and *carB* expression in all the strains, with differences in their relative levels in the light and in the dark in the case of the Δ*wcoA* and Δ*cryD* mutants.

2. Effect of Δ*wcoA*, Δ*cryD*, and Δ*vvdA* mutations on kinetics of carotenoid accumulation upon illumination of dark-grown mycelia

The lower amounts of carotenoids in the light in the Δ*wcoA* and Δ*vvdA* mutants and the differences observed in *carRA* and *carB* mRNA levels in the Δ*wcoA* and Δ*cryD* *mutants* led us to investigate in more detailed the responses to light of these strains. Mutants of each photoreceptor gene were incubated in parallel with the wild type for three days in the dark and the carotenoid content was determined under these conditions or after 3, 6, 12, 24 and 48 h illumination (Fig. IV-3A). Since the colonies grow further during illumination, the analysis was restricted to the central part of the colonies, i.e., the mycelium formed during the three days in the dark. The results showed a biphasic response for the wild-type strain, with a rapid increase in the carotenoid content in the first 6 hours (first stage) followed by arrest of the synthesis (6-12 h), and its resumption after a longer light exposure (12-48 h, second stage). The mutants for the photoreceptor genes showed different alterations of this pattern. Thus, the Δ*cryD* mutants responded to light as fast as the wild type in the first stage and paused the synthesis at the same time, but they exhibited a slow accumulation of carotenoids in the second stage. On the other hand, the response of the Δ*vvdA* mutants was faster in the first stage and slower in the second stage, but not so much as the Δ*cryD* mutants. In contrast with the former strains, the Δ*wcoA* mutants exhibited a much slower monophasic response, resulting after 48 h illumination in about 1/3 of the carotenoids accumulated by the wild type. In congruence with the

data displayed in Fig. IV-2B the carotenoid content of the Δ*wcoA* mutants was much lower than those of the other strains at the start of illumination; so, paradoxically the induction by light was proportionally larger in the Δ*wcoA* strains.

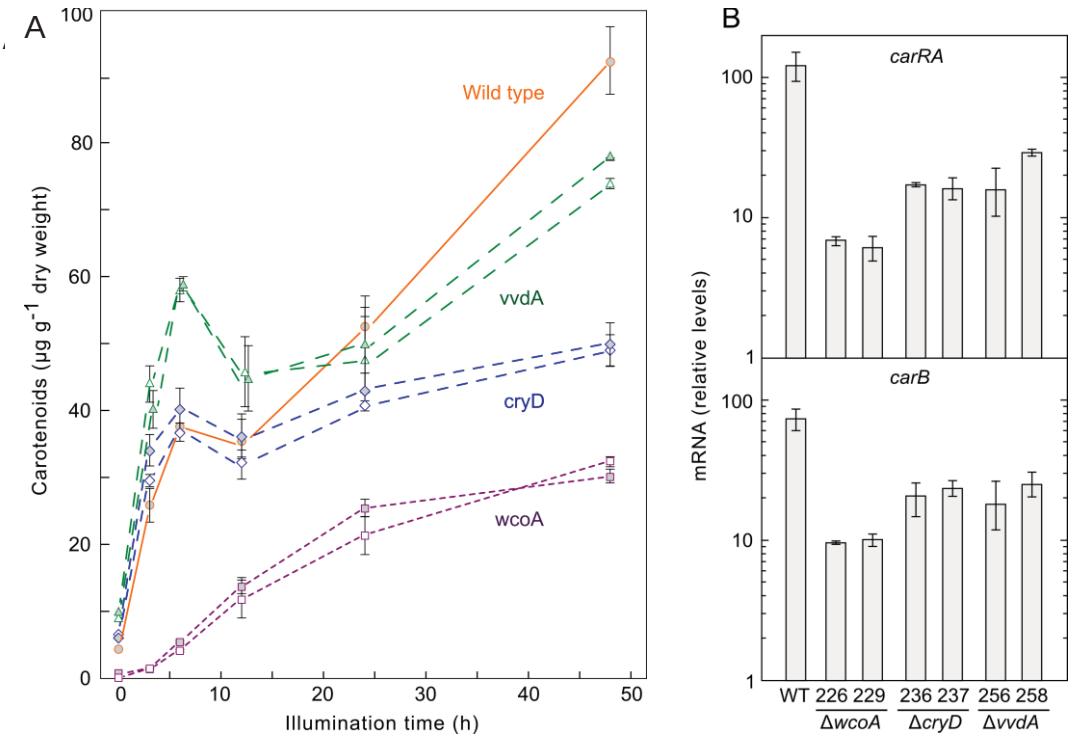

Fig. IV-3. Effect of illumination on carotenogenesis in wild type and mutants of the photoreceptor genes *wcoA, cryD* and *vvdA*. (A) Kinetics of carotenoid accumulation after illumination of the wild type, Δ*wcoA* mutants SF226 and SF229, Δ*cryD* mutants SF236 and SF237, and Δ*vvdA* mutants SF256 and SF258. The strains were incubated for three days in the dark in DGasn agar and exposed to white light for the time indicated in abscissae. Each point is the average and standard deviation of four determinations from two biological replicates. (B) Real-time RT-PCR analyses of the genes *carRA* and *carB* in RNA samples of the same strains under the same culture conditions after 48 h illumination. Relative expression for each gene was referred to the value in the wild type grown in the dark. Data are the average and standard deviation of six determinations from two biological replicates.

To gain more insights on the alterations of carotenoid photoinduction in the mutants, we determined the *carRA* and *carB* mRNA levels in the mycelia of the experiments described above after 48h illumination and the data were referred to the value of the wild-type strain in the dark (Fig. IV-3B). The mutants for the three photoreceptor genes exhibited a significant photoinduction of the transcript levels. However, the amounts were about 4-fold lower in *the* Δ*cryD and* Δ*vvdA* mutants and about 10-fold lower in the Δ*wcoA* mutants when compared to those of the wild type. These data are consistent with the deceleration observed for the different mutants in the later stage of the photoinduction kinetics.

The results described above are consistent with a cooperative participation of the WcoA and CryD photoreceptors in the photoinduction of carotenogenesis in *F. fujikuroi*. To confirm this hypothesis, experiments were done to obtain a double mutant Δ*wcoA* Δ*cryD*. Two plasmids were constructed to obtain the targeted disruption of *wcoA* by homologous recombination in a Δ*cryD* background. In one of them the *wcoA* coding sequence was replaced by the nitrate reductase gene *niaD*, and in the other it was replaced by a geneticin resistance cassette. For *niaD* selection, a *niaD*$^{-}$ mutant was obtained from the Δ*cryD* mutant SF237 by chlorate resistance. After three transformation attempts of the *niaD*$^{-}$ SF237 derivative, none of the transformants obtained either through protoplasts (39 *niaD*$^{+}$ colonies tested from two independent transformations) or through a biolistc approach (7 *niaD*$^{+}$ colonies tested from one transformation), exhibited the expected Δ*wcoA* phenotypic pattern, i.e., purple pigmentation in the dark and reduced mycelial hydrophobicity, and the PCR tests confirmed the presence of an intact *wcoA* gene. Five additional protoplast-mediated transformation experiments achieved upon geneticin resistance selection, in this case using SF236, led to the isolation of 16 transformants. All of them resulted from ectopic plasmid integrations, and no Δ*wcoA* mutants were obtained. As an alternative approach, mutagenesis experiments were done with SF236 and SF237 and a total of 15 mutants with a Δ*wcoA*-like pigmentation were analyzed. The *wcoA* gene from the four mutants exhibiting a phenotype more similar to that of the Δ*wcoA* mutant SF226 was cloned and sequenced, but no mutations were found in their respective *wcoA* coding sequence. Taken together, these results suggest a lack of viability for the double Δ*wcoA* Δ*cryD* mutant.

3. Effect of light intensity on photoinduction of carotenogenesis in Δ*wcoA*, Δ*cryD*, and Δ*vvdA* mutants

The investigated photoreceptors may differ in their sensitivities to light. To obtain more information on the alterations resulting from the loss of the photoreceptors under study we used neutral filters to reduce the light intensity in the photoinduction kinetics experiments. To distinguish the effects on the fast and slow stages of the photoresponse (Fig. IV-3A), we determined the carotenoid content in the mycelia in the dark and after 6 h and 48 h illumination under 0.07, 0.7 and 7 W m^{-2} (Fig. IV-4). The

results confirmed the different responses of the mutants after the first and second kinetics stages. After 6 h illumination, the Δ*cryD* mutants contained similar amounts of carotenoid than the wild type while the Δ*wcoA* mutants produced lower amounts. On the other hand, after 48 h the Δ*cryD* mutants produced less carotenoids than the wild type, but their levels were similar to those of the Δ*wcoA* mutants. Also, the carotenoid content of the Δ*vvdA* strains was higher than those of the wild type after 6 h, and lower after 48 h, indicating that these mutants accumulate less carotenoids than the wild type upon prolonged incubation, as found in the cultures under constant illumination (Fig. IV-2B).

The results also revealed differences in light sensitivity between different photoreceptors. No significant photoinduction was found in the Δ*wcoA* mutants under 0.07 and 0.7 W m^{-2}, indicating that CryD is able to respond only to high light intensities. However, the Δ*cryD* mutants showed a significant photoinduction even at the lower light intensity, indicating a high sensitivity to light of the WcoA photoreceptor. Interestingly, after 6 h illumination the response to low or very low light intensity was enhanced in the Δ*vvdA* mutants compared to the wild type. Thus, these mutants accumulated more carotenoids after this time under 0.7 W m^{-2} than the wild type under 7 W m^{-2}.

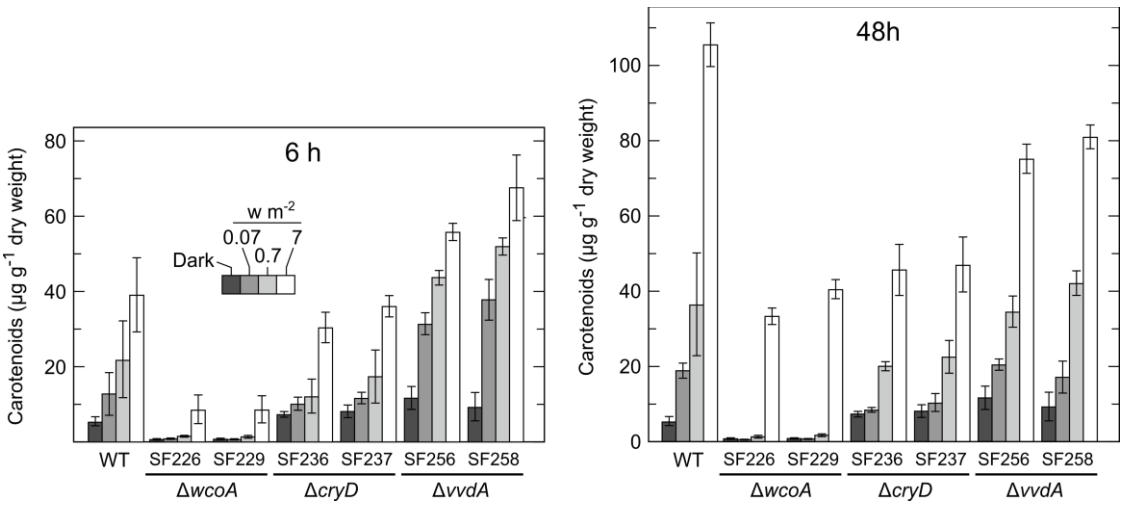

Fig. IV-4. Effect of light intensity on photoinduction of carotenoid accumulation in the wild type and Δ*wcoA* mutants SF226 and SF229, Δ*cryD* mutants SF236 and SF237, and Δ*vvdA* mutants SF256 and SF258. The strains were incubated for three days in the dark in DGasn medium (dark grey bars) and exposed to 0.07 W m^{-2} (grey bars), 0.7 W m^{-2} (pale grey bars) or 7 W m^{-2} (empty bars) white light for 6 hours (above) and 48 h (below). Data show average and standard deviation of four determinations from two biological replicates.

To test if the function of VvdA is performed on transcription of the other photoreceptor genes, we determined the effect of the Δ*vvdA* mutation on *cryD* and *wcoA* mRNA levels. For more complete information, in this case the analysis was done with three independent Δ*vvdA mutants* (Fig. IV-5). The results confirmed the strong photoinduction of *cryD* mRNA, as formerly reported (Chapter I). However, the *cryD* mRNA levels were visibly enhanced in the Δ*vvdA* strains compared to the wild type. As already found for *carRA* and *carB* in Chapter III, the Δ*vvdA* mutants exhibited a similar photoadaptation of *cryD* mRNA levels than the wild type. On the other hand, the minor effect of light on *wcoA* levels was basically unaffected in the Δ*vvdA* mutants. A minor photoinduction was found for *wcoA*, which was not identified in former analysis (Estrada and Avalos, 2008), probably because a higher resolution of the methodology used in this work.

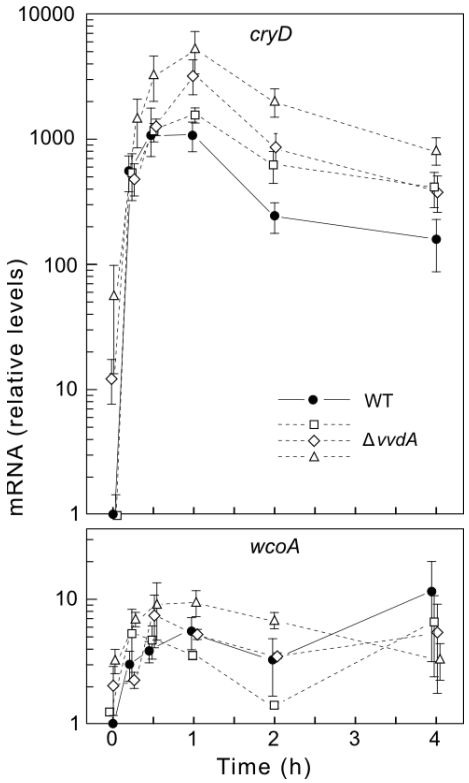

Fig. IV-5. Effect of the *vvdA* mutation on expression of the photoreceptor genes *cryD* and *wcoA*. Real-time RT-PCR analyses of genes *cryD* and *wcoA* in total RNA samples from the wild type (black circles) and the Δ*vvdA* mutants SF256 (squares), SF257 (rhombs) and SF258 (triangles) grown for three days in DGasn medium in the dark or after 15 min, 30 min, 1 h, 2 h, or 4 h exposure to 7 W m^{-2} white light. Relative levels are referred to the value of the wild type in the dark. Data show means and standard deviations for nine measurements from three biological replicates.

4. Effect of the mutation of the *wcoA* and *cryD* genes on expression of photoregulated genes

Recently, it was shown that the mutation of the *vvdA* gene does not affect the photoinduction pattern of the structural genes *carRA* and *carB* (Chapter III). For better understanding of the phenotypic effects of the Δ*wcoA* and Δ*cryD* mutations on the

photoinduction kinetics of carotenoid accumulation, we investigated the effect of light on *carRA*, *carB* and *carT* mRNA levels in these mutants in comparison to the wild type. Formerly, it was reported that the *carB* gene was down-regulated in *wcoA* mutants, while the result was less clear for *carRA* (Estrada and Avalos, 2008). We have analyzed in more detail two Δ*wcoA* mutants, extending the analysis up to 4 h of light exposure (Fig. IV-6). As expected, the RT-PCR data for the wild type showed a strong photoinduction of *carRA* and *carB* transcript levels, exceeding one hundred fold the levels in the dark, and a later decay after one hour of exposure to light. A more modest induction was exhibited by *carT*, which did not reach a ten fold, returning afterwards to background levels. In agreement with the lower carotenoid content of the Δ*wcoA* mutants in the dark (Figs. IV-2 and IV-3), the *car* mRNA levels were much lower in these strains than in the wild type. The photoinduction was also very low, possibly mediated by CryD, but the *carRA*, *carB* and *carT* mRNA levels were still much lower in the Δ*wcoA* mutants after illumination than in the wild type in the dark, indicating that CryD also activates the carotenoid pathway through a posttranscriptional mechanism.

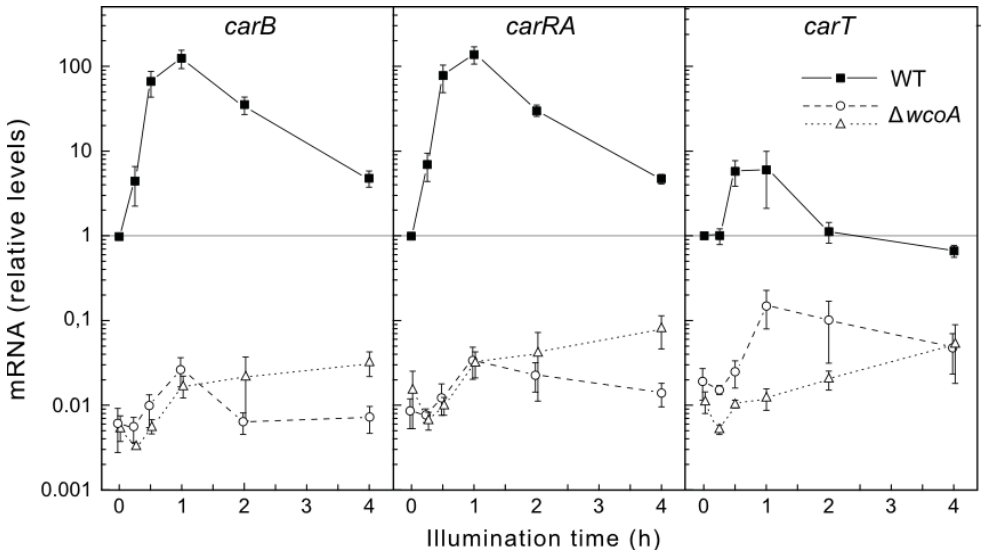

Fig. IV-6. Effect of the *wcoA* mutation on expression of genes of the carotenoid pathway. Real-time RT-PCR analyses of genes *carB, carRA* and *carT* in total RNA samples from the wild type and the Δ*wcoA* mutants SF226 (circles) and SF229 (triangles) grown for three days in DGasn medium in the dark or after 15 min, 30 min, 1 h, 2 h, or 4 h exposure to 7 W m^{-2} white light. Relative levels are referred to the value of the wild type in the dark. Data show means and standard deviations for nine measurements from three biological replicates.

In contrast to the Δ*wcoA* mutants, the expression of the genes *carRA* and *carB* was strongly photoinduced in the Δ*cryD* mutants. However, there was a decrease of at least five-fold in the photoinduction levels of gene *carRA* (Fig. IV-7), but this effect was less manifest on the gene *carB* and hardly detectable for the gene *carT*, that only reached a 4-fold induction in the wild type in this set of experiments. As found for *carB*, the Δ*cryD* mutation produced minor or no effects in the photoinduction of other light-regulated genes, such as *carO*, *carX* and *phr1*, encoding a rhodopsin protein (Prado et al., 2004), a retinal-producing carotenoid oxygenase (Prado-Cabrero et al., 2007a), and a CPD-photolyase (Alejandre-Durán et al., 2003), respectively.

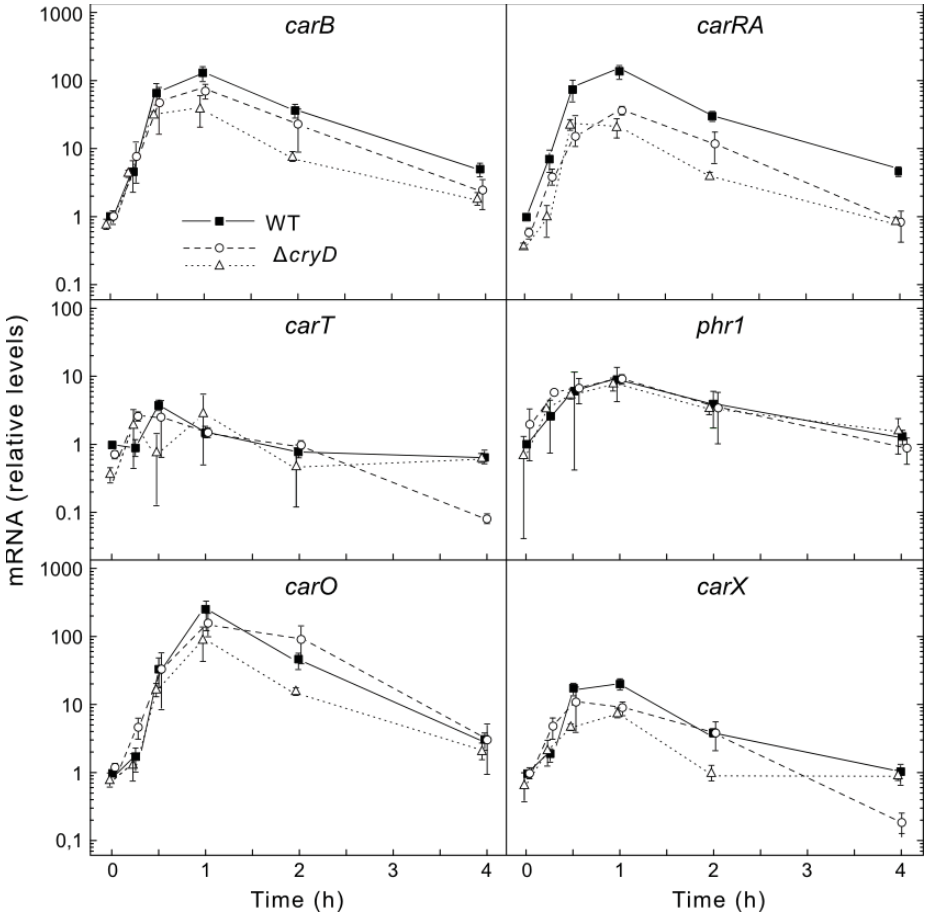

Fig. IV-7. Effect of the *cryD* mutation on expression of genes of the carotenoid pathway and other light-regulated genes of *F. fujikuroi*. Real-time RT-PCR analyses of genes *carB, carRA, carT, carO, carX* and *phr1* in total RNA samples from the wild type and the Δ*cryD* mutants SF2236 (circles) and SF237 (triangles) grown for three days in DGasn medium in the dark or after 15 min, 30 min, 1 h, 2 h, or 4 h exposure to 7 W m^{-2} white light. Relative levels are referred to the value of the wild type in the dark. Data show means and standard deviations for nine measurements from three biological replicates.

5. Effect of blue and red light on expression of *carRA* and photoreceptor genes

The Δ*cryD* mutants exhibit light-dependent alterations in morphology and pigmentation. However, these alterations were not observed under red light (Chapter I). CryD, WcoA and VvdA are blue-light photoreceptors. To check the dependence of photocarotenogenesis on blue light, we compared the effect of blue light, red light and white light on transcript levels of the structural gene *carRA*, and on those of the photoreceptor genes *cryD*, *wcoA* and *vvdA* (Fig. IV-8). As expected blue light was as efficient as white light to induce the expression of the gene *carRA*; however, red light produced a significant photoinduction, with transcript levels reaching about 10% of the induction produced by white or red light. A similar pattern was observed for the gene *vvdA*, with blue light giving the higher efficiency. Surprisingly, red light was particularly efficient to induce *cryD* mRNA levels, being as efficient as white light during the first 30 min of induction. In contrast, the minor induction of *wcoA* was less apparent either with blue or with red light. The mycelia incubated under red light contained about 54 µg g^{-1} dry weight compared to 7 µg g^{-1} dry weight in the dark or 197 µg g^{-1} dry weight under white light. Taken together, these results suggest the participation of a red-light photoreceptor in the transcriptional regulation of the genes for carotenogenesis and in those for the VvdA and CryD photoreceptors.

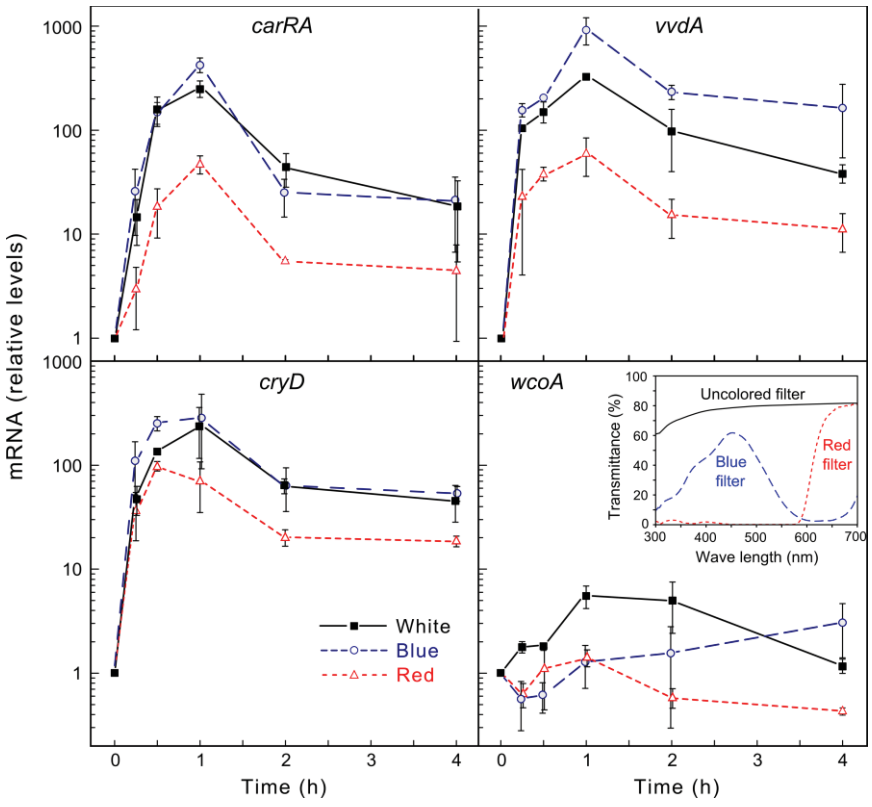

Fig. IV-8. Effect of light wavelength on photoinduced expression of the photoreceptor genes *cryD, wcoA* and *vvdA*, and the carotenogenic gene *carRA*. Real-time RT-PCR analyses of genes *cryD, wcoA, vvdA* and *carRA* in total RNA samples from the wild type grown for three days in DGasn medium in the dark or after 15 min, 30 min, 1 h, 2 h, or 4 h exposure to white light, blue light or red light. Relative levels are referred to the value of the wild type in the dark. Data show means and standard deviations for six measurements from two biological replicates. The inset shows the transmittance spectra of the uncolored, blue and red filters used for illumination in this experiment.

DISCUSSION

Induction of carotenogesis by light is a well-known photoresponse in some filamentous fungi. Our former data indicated that the regulatory mechanism for this photoinduction in *F. fujikuroi* differs from that of other fungal models, such as *N. crassa*, *P. blakesleeanus* and *M. circinelloides*, where photocarotenogenesis is mediated by a White Collar complex ([reviewed by (Corrochano and Garre, 2010)). The persistence of photoinduction of carotenogenesis in the Δ*wcoA* mutants of *F. fujikuroi* (Estrada and Avalos, 2008) led us to investigate other blue-light photoreceptors, as the cry-DASH CryD and the small flavoprotein VvdA. The loss of WcoA has a drastic effect on the ability of the *car* genes to respond to light, but these results contrast with the persistence of photocarotenogenesis in these mutants. We have found that the down-regulatory effect of the *wcoA* mutation is also noticeable in the dark, a result that adds to former data on light-independent functions for this protein (Estrada and Avalos, 2008). The drastic transcriptional effect of the *wcoA* mutation clearly differs from the milder effect of the *cryD* mutation, that produced a significant reduction in the photoinduction of the gene *carRA*, but it did not prevent it. This gene plays a key role in carotenoid biosynthesis, since it encodes the enzyme required for the synthesis of phytoene, the uncolored precursor of all carotenoids. However, the mutants lacking a functional CryD produced only minor effects on other light-regulated genes, including *carB*, and accumulated similar amounts of carotenoids than the wild type upon continuous illumination. The persistence of light induction in the Δ*cryD* and Δ*wcoA* mutants indicates that neither WcoA nor CryD act as single photoreceptor for light regulation of carotenoid biosynthesis.

For a better understanding of the photoinduction mechanism, we investigated the kinetics of carotenoid accumulation resulting from the illumination of young dark-grown colonies from the wild type and mutants of three different photoreceptors. The Δ*wcoA* and Δ*cryD* mutants exhibit alterations in the production of bikaverin (Estrada and Avalos, 2008) (and Chapter I of this Thesis), a red pigment that could interfere with the absorption of blue light by the putative photoreceptors, but the young colonies used in our experiments contain lower concentrations of these pigments. These

experimental conditions led us to identify two different induction stages: a rapid response achieved during the first 6 hours, and a subsequent slower response that lasted at least about 40 h. Former experiments achieved with submerged cultures of *F. fujikuroi* showed simple induction kinetics, with significant increase of the carotenoid content after 3 h illumination and the reach of its maximum levels after 24 h (Avalos and Schrott, 1990). Similar induction curves were described in submerged condition for *F. aquaeductuum* (Rau, 1967a) and *N. crassa* (Rau et al., 1968), although in the latter case a significant photoinduction was detected after one-hour light exposure. A more detailed analysis revealed however a two-step kinetics response in *N. crassa*. Under similar light intensities to those used in our experiment (8 W m^{-2}), the first step occurred in this fungus during the first minute of illumination (Schrott, 1980), a result consistent with the rapid stimulation of activity of an enzymatic set already available in the dark. A simple photoinduction curve of carotene accumulation was also observed in *P. blakesleeanus*, but fluence-response curves achieved with different wavelengths revealed a two step response, suggesting the participation of two photosystems of different sensitivity thresholds (Bejarano et al., 1991). The single mutants of the WC complex MadA/MadB still exhibit photoinduction, but the double mutants become blind (Lopez-Diaz and Cerda-Olmedo, 1980), indicating that this WC complex is responsible for photocarotenogenesis in this fungus.

The alteration in the kinetics curves of carotenoid accumulation in mutants devoid of functional WcoA, CryD or VvdA photoreceptors provide valuable clues on the participation of these photoreceptors in carotenoid photoinduction in *F. fujikuroi*. The results are consistent with the participation of WcoA in a highly sensitive photoinduction mechanism, fast but transient, while CryD is involved in a less sensitive but more sustained photoinduction mechanism. The first mechanism could be involved in the rapid response to sudden changes of light conditions and its subsequent adaption, as indicates the transience of the transcriptional photoinduction of the structural *car* genes. On the other hand, the latter mechanism could be involved in the response to persistent sun-light illumination conditions. Both mechanisms seem to operate simultaneously under long standing illumination, as indicates the low but detectable increase in *carB* mRNA levels of the *car* genes in 7-day-old colonies of either

the wild type or the Δ*wcoA*, Δ*cryD* or Δ*vvdA* mutants incubated under constant light. The low mRNA levels under these conditions suggest the operation of an efficient long-standing adaptation mechanism, in which VvdA apparently does not participate.

The phenotypic effect of the *cryD* mutation on transcriptional regulation of the *car* genes and carotene accumulation in *F. fujikuroi* is the first report on the participation of a cryptochrome on light regulation of carotenogenesis in any microorganism. In the case of *N. crassa*, the regulation by light of carotenogenesis seems under exclusive control of the WC complex, and no effect was reported on this photoresponse by the mutant of the *N. crassa* cryptochrome *cry-1* (Froehlich et al., 2010). Another cryptochrome, Cry1, was investigated in *Sclerotinia sclerotium*. In this fungus, the *cry1* transcripts accumulate at higher levels in the light-exposed stages of apothecia development (Veluchamy and Rollins, 2008), but the mutation had only minor effect in this developmental process. Interestingly, *S. sclerotium* produces β-carotene and its production is induced by light coupled to sclerotia formation (Georgiou et al., 2001). However, the consequences of the *cry1* mutation on light-induced β-carotene production in this fungus have not been reported.

The results in this work support the participation of VvdA in the regulation of photocarotenogenesis of *F. fujikuroi*. As already mentioned, the *vvdA* mutants are not affected in the transcriptional photoinduction and subsequent photoadaptation of mRNA levels of the *car* genes, but they accumulate less carotenoids than the wild type under constant illumination (Chapter III). As the wild type, the Δ*vvdA* mutants exhibit a biphasic photoresponse; however, in these mutants the first stage of the response is enhanced and the second stage is attenuated. Moreover, the Δ*vvdA* mutants become more sensitive than the wild type to a ten-fold reduction of light intensity. This result would be consistent with the function of VvdA as a negative modulator of the activity of the WcoA photoreceptor, a regulatory scenario that reminds the down-regulation of WC-1 by VVD in *N. crassa* (Malzahn et al., 2010). However, the lack of effect of the *vvdA* mutation on light induction of the mRNA levels of the *car* genes (Chapter III) apparently contradicts this hypothesis. On the other hand, the slower response of the Δ*vvdA* mutants in the second stage of the induction kinetics, exhibited only at high light intensity, suggests a function for VvdA as a positive modulator of CryD activity.

This is not achieved at transcription level, since the lack of VvdA does not negatively affect the WcoA-mediated transcriptional photoinduction of the *cryD* gene, which is actually more efficient in the Δ*vvdA* mutants. Taken together, the phenotypic effects of the *vvdA* mutation suggest that the participation of VvdA in carotenoid photoinduction is mainly achieved affecting positively or negatively the functions of the WcoA and CryD photoreceptors.

Our hypotheses of the function of the three photoreceptors must take into account the regulation of their respective genes. The *wcoA* gene is expressed in the dark (Estrada and Avalos, 2008), and its transcript levels are only mildly affected by light. In contrast, the expression of the *cryD* and *vvdA* genes are strongly induced by light through WcoA (Chapters I and III), implying a lag phase after illumination onset before full function. This fits the participation of CryD in a later stage of the photoinduction kinetics, but makes more difficult to interpret the early effect of the *vvdA* mutation. Moreover, our analyses were restricted to three photoreceptors, but the involvement of other photoreceptors cannot be discarded. The significant induction by red-light of *cryD*, *vvdA* and *carRA* transcripts suggest the participation of a red-light absorbing photoreceptor, which could play a secondary accessory role. In support, a minor but detectable induction in the carotenoid content was observed upon incubation of *F. fujik*uroi under red light. The *F. fujikuroi* genome contains a gene for a phytochrome (Avalos and Estrada, 2010), which could account for this red-light photoresponse. The possible participation of this or other additional photoreceptors in photocarotenogenesis of this fungus remains to be investigated.

GENERAL DISCUSSION

Vision, understood as the mechanism to detect and interpret images, is a highly advanced sensorial feature developed in evolution by complex animals. However, most organisms, from bacteria to humans, possess different systems to detect light irrespective of their ability to see. In fungi and other sessile organisms, light sensing is an important trait to adapt to changes in environmental conditions. Light intensity and quality serve as an information source and provides clues about the physical environment, including temperature, day phase and duration.

The ascomycete *F. fujikuroi* stands out for the complexity of its secondary metabolism, and not for the richness of its photoresponses, at least for those visually detected in the laboratory. This is not the case of the well-known photobiology models *N. crassa*, *P. blakesleeanus* and *M. circinelloides*, the first one especially fruitful in the investigation of circadian rhythmicity, and the others in studies of photomorphogenesis. All these fungi coincide however in the photoinduction of carotenogenesis, a biochemical response very amenable for research purposes because of the easy detection of the carotenoid pigments. Following the trail of the early works of the group of Werner Rau (University of Munich, Germany) on photoinduction of carotenogenesis in *F. aquaeductuum* (Rau, 1967a, 1967b, 1969; Rau et al., 1967c), the photoinduction of the pathway was soon also described in *F. fujikuroi* (Avalos et al., 1993; Avalos and Cerdá-Olmedo, 1986). In later years, the identification of the structural genes for carotenoid metabolism in this fungus extended the regulation to transcriptional studies, revealing a strong and transient light induction of mRNA levels of the structural genes, similar to those found in *N. crassa* (Baima et al., 1991; Schmidhauser et al., 1990; Schmidhauser et al., 1994), *P. blakesleeanus* (Arrach et al., 2001; Ruiz-Hidalgo et al., 1997) or *M. circinelloides* (Velayos et al., 2000b; Velayos et al., 2000a). A major goal of this Thesis was to identify and characterize the photoreceptors responsible for this photoresponse.

The mechanism underlying the activation of carotenoid biosynthesis by light was first elucidated in *N. crassa,* where the protein WC-1 and its partner WC-2(Cheng et al., 2003b) centralize all the blue light photoresponses (Ballario et al., 1996; Chen and Loros, 2009b; Cheng et al., 2002), including photocarotenogenesis. Despite the evolutionary distance with zygomycetes, similar WC proteins were found to mediate

this photoresponse in *P. blakesleeanus* and *M. circinelloides* (Corrochano and Garre, 2010; Silva et al., 2006). For this reason, the conservation of carotenoid photoinduction in the mutants of the WC-like genes *wcoA* of *F. fujikuroi* (Estrada and Avalos, 2008) and *wc1* of *F. oxysporum* (Ruiz-Roldán et al., 2008) was a surprising finding, especially considering the closer taxonomic proximity of these fungi with *N. crassa* and that these are the only *wc-1*-like genes found in their genomes. Therefore, the investigation of the *F. fujikuroi* photoreceptors became an interesting field of research and the reason for the present work.

The results described in this Thesis reveal an unexpected complexity in *F. fujikuroi* photobiology, confirming the direct or indirect participation in carotenoid photoinduction of the three photoreceptors investigated, the WC protein WcoA, the VVD ortholog VvdA and the DASH cyptochrome CryD. In overall, despite the high degree of conservation of their protein sequences and domain organization with other orthologs, the results reveal noticeable divergences in function and regulation with their fungal counterparts. Furthermore, we have found that the mentioned photoreceptors regulate very different aspects of the biology of *F. fujikuroi*, in some cases affecting such diverse processes as metabolism, conidiation, mycelia development or the properties of the colony surface. To understand how signal inputs from each photoreceptor are integrated and coordinated to regulate such diverse aspects of cell activity is a complex task. We summarize below some general conclusions.

1. CryD

Few proteins of the photolyase/cryptochrome family have been characterized in fungi (Bayram et al., 2008a; Bluhm and Dunkle, 2008a; Froehlich et al., 2010; Veluchamy and Rollins, 2008), among them only two DASH cryptochromes (Froehlich et al., 2010; Veluchamy and Rollins, 2008). The analysis of its mutations provided some clues on their possible biological roles, none of them related to carotenoid biosynthesis. Because of the poor knowledge of the role of DASH cryptochromes in fungi, we first focused the attention on the protein from this family in *F. fujikuroi*, that we called CryD.

The phenotype of the Δ*cryD* mutants of *F. fujikuroi* described in this Thesis indicates that CryD acts as a repressor of bikaverin and macroconidia production, but this regulatory role is only manifest under light and nitrogen starvation, indicating that it is a functional photoreceptor. Consequently, a CryD-independent mechanism must function in the dark to down-regulate these processes. Additionally, CryD is a positive regulator of light induction of carotenoid biosynthesis under long-term light exposure. None of the metabolic effects was accompanied by parallel changes in transcription of structural genes of either the bikaverin or the carotenoid pathways. Thus, CryD must operate at other regulatory level. The presence in the CryD C-terminal extension of several RGG motifs, formerly associated to RNA binding (Godin and Varani, 2007), is suggestive of a possible role in the regulation of stability or translation of the mRNA from *car* and *bik* genes. This could be a special feature of DASH cryptochromes of ascomycetes, since the C-extensions are apparently absent in this class of proteins in other fungal groups. As further evidence, the tagged CryD protein purified from *E. coli* was bound to a RNA molecule. The molecular nature of this RNA remains to be investigated, but it is evidently an *E. coli* RNA, and therefore the binding should be unspecific. Experiments to express the same-tagged CryD protein in *F. fujikuroi* to identify its *in vivo* RNA target have been unsuccessful so far, possibly because of instability of the tagged protein version in the fungus. Further experiments are required to find out the ability of CryD to bind *F. fujikuroi* mRNA targets.

The biochemical assays described in Chapter II, and the fact that the Δ*cryD* mutants were not more sensitive than the wild type to UV exposure, suggest that DNA repair is not a major CryD function *in vivo*. It must be noted that *F. fujikuroi* has a specific photolyase to deal with UV-induced damages, which could mask a possible contribution of CryD in DNA repair. It has been recently proposed that photolyases and cryptochromes use the same catalytic sites, one binding CDP lesion and the other binding ATP (Brautigam et al., 2004). So, if both classes of protein possess different mechanisms of action, it is biochemically puzzling how CryD is able to attain both biological roles. The differences lie on the subsequent actions when the CPD or ATP receive an electron, either breaking a T<>T dimer or allowing phosphorylation and conformational changes of the protein. Thus, as a tentative hypothesis, a single protein

such as CryD could act either as photolyase or as photoreceptor depending on the substrate bound at each moment. The capacity of ancestral DASH cryptochromes to bind a nucleic acid might have been used in the evolution by ascomycetes to gain regulatory functions for these proteins, with the ability to discriminate different mRNA species residing in the subsequently acquired C-extensions. This would also fit the considerable sequence diversity of these C-extensions in different ascomycete species.

2. VvdA

This VVD ortholog of *F. fujikuroi*, VvdA, was included in the research described in this Thesis because of its implication in the regulation of *N. crassa* photocarotenogenesis. In this fungus, VVD mediates photoadaptation by modulating the duration of light-induced transcriptional responses (Heintzen et al., 2001; Schwerdtfeger and Linden, 2003). This protein shuts off the inducing activity of the WC complex on carotenogenic genes as well as on other light-regulated genes and its mutational loss leads to a sustained carotenoid biosynthesis in *N. crassa*. The function of VVD orthologs has not been investigated in other carotenogenic fungi, and therefore there is no evidence for conservation of the regulatory role observed in *N. crassa*. Actually, the data available on another VVD-like protein, ENVOY (ENV1) of *T. reesei*, showed a considerable functional variation (Castellanos et al., 2010; Schmoll et al., 2005b; Seibel et al., 2012), with roles in development (conidiation, colony growth and sexual reproduction) and cellulose-degrading activity. In contrast, *N. crassa Δvvd* mutants show no morphological or developmental alterations. However, some coinciding functions have been reported. The up-regulation of light-induced genes in *Δenv1* mutants (Castellanos et al., 2010) resembles that of the carotenogenic genes in *N. crassa*. Moreover, VVD and Env1 participate in the detection of further increases in light intensity. However, ENV1 was unable to replace VVD functions in *N. crassa* (Schmoll et al., 2005b).

The data on VvdA function of *F. fujikuroi*, displayed in Chapter III, reinforce the functional variability of the VVD-like photoreceptors in fungi. This protein seems to play no role in transcriptional photoadaptation of light-regulated genes, as shown at least for those of the carotenoid pathway. Moreover, the Δ*vvdA* mutants are less

pigmented in the light than the wild type, with a patent reduction in the carotenoid content. Hoewever, the faster accumulation of carotenoids in an early stage of the photoinduction kinetics indicates that VvdA acts negatively on WcoA, reminding the role of VVD in *N. crassa*. In contrast, it apparently plays a positive regulatory role on CryD, which explains the lower carotenoid content of the Δ*vvdA* mutants upon prolonged illumination. Interestingly, the VvdA protein also plays a role in development, although the effects of the Δ*vvdA* mutation are not so drastic under light as those exhibited by the Δ*env1* mutants of *T. reesei*. The phenotypic alterations of the *ΔvvdA* mutants are less severe, with subtle modifications on the hyphal organization of the mycelia attached to the agar. On the other hand, at variance with *T. reesei* Δ*env-1* mutants, those of Δ*vvdA* are apparently not affected in the capacity to degrade cellulose, as indicates their ability to degrade cellophane or to grow on cellulose paper without an alternative carbon source. Additionally, ENV1 exerts functions independently of light (Schuster et al., 2007), while we only detected phenotypic changes in the Δ*vvdA* mutants under light. Taken together, the available data indicate that different fungi have adapted their VVD-like proteins to different regulatory purposes, usually relying in the ability of these photoreceptors to detect light.

3. WcoA

Of the three photoreceptors investigated, WcoA was the only one previously analyzed. The experiments described in Chapter IV provide new pieces of information on the biological function of WcoA: (1) This protein is a major photoreceptor for this photoresponse, probably as a WC complex in cooperation with the WC-2-like partner WcoB; however, it is not the only photoreceptor involved, what explains the persistence of photocarotenogenesis in the Δ*wcoA* mutants. (2) WcoA controls the production of carotenoids also in the dark, as indicates the strong reduction in the carotenoid content and in transcript levels of the structural *car* genes in the dark in the Δ*wcoA* mutants. This effect was not detected in the previous analysis (Estrada and Avalos, 2008), presumably because of a lower sensitivity of the methodology used in those experiments. WcoA is the primary photoreceptor, since it is also in charge of the transctiptional activation of the genes for the other two photoreceptors, CryD and VvdA. It is plausible that, upon illumination, a fraction of the WcoA protein interacts

with VvdA, presumably in low amounts considering the low *vvdA* transcript levels in the dark. This may explain why the Δ*vvdA* mutants respond more rapidly to light in the first hours after light onset. This is apparently contradicted by the lack of effect of the Δ*vvdA* mutation on the photoinduction of *carRA* and *carB* levels. However, the latter experiment was achieved on submerge cultures while the carotenoid kinetics experiment were achieved on surface colonies. The explanation to this contradiction might reside in a difference in VvdA levels in the dark between both culture conditions.

4. Photocarotenogenesis as a series of regulatory events

Our illumination experiments on young colonies of *F. fujikuroi* on solid medium were especially informative, since they uncovered an unexpected biphasic response of carotenoid accumulation. Two-steps responses of photocarotengenesis were formerly described for *N. crassa* (Schrott, 1980) and *P. blakesleeanus* (Bejarano et al., 1991), but they were obtained in fluence-response experiments, while here the two-step response was found in a time course analysis of carotenoid accumulation. The strength of our approach derives from the finding of specific alterations of the carotenoid-accumulating kinetics in mutants of the different photoreceptos under study. These results not only associate these photoreceptors to carotenoid photoinduction but also assign them distinct roles and different sensitivities in the two-stage kinetics response. Each stage mainly relies on one photoreceptor, the first one on WcoA and the second one on CryD, while the activity of both photoreceptors is influenced by the third investigated photoreceptor, VvdA. Interestingly, both stages are separated by a lapse in which the carotenoid content not only pauses but decreases, consistent with a down-regulation of WcoA induction before the second photoreceptor starts its up-regulating effect. The transient decrease in the carotenoid content suggests the occurrence of degradation by light exposure, indicating that an active synthesis must be operating under continuous illumination to keep the carotenoid levels.

The experimental conditions used to investigate the effect of light in our kinetics experiments, i.e., a sudden change from total darkness to strong illumination, are difficult to translate to the real life conditions of the fungus in its natural habitats. This could happen when mycelia developing on the soil emerges to the surface by some

accidental circumstance, but this is probably an infrequent event. We can speculate that it could also happen when mycelia or conidia are liberated from infected plants, but the infection is probably not achieved in total darkness if we consider the thin structures of the rice plants. On the other hand, the liberation from the plant is probably progressive, and not sudden. Therefore, abrupt changes of light intensity are probably unusual in nature. Rather, light changes are expected to be gradual and normally associated to dawn and sunset. We can speculate that the high sensitivity of WcoA allows the fungus to respond to the first rises of light intensity resulting from daybreak or from getting out from the soil or from an infected plant, and that the less sensitive and plausibly more sustained role of CryD allows keeping an appropriate induction level at open daylight. Such maintenance levels do not imply large transcriptional increments, as indicate the minor difference in mRNA amounts for the *car* genes in 7-day-old cultures incubated in the dark or under continuous illumination. Thus, once the carotenoids are accumulated at appropriate amounts, it is only needed a basal synhtesis to replace the degraded carotenoids.

The results found with red light introduce another factor: the convenience to detect different light wavelengths in different moments of the day. Lights of dawn and sunset are enriched in red wavelengths. Thus, the participation of a phytochrome in signal input under these conditions is a tempting hypothesis. The response found to red light required functional *wcoA* gene. Our red light filter absorbed the vast majority of blue light, making very unlikely that it is a side WcoA-mediated effect. More plausibly, as found for *cryD* and *vvdA,* WcoA could control the expression of the only phytochrome gene of *F. fujikuroi*. Another possibility is that the phytochrome exerts its function as an accessory photoreceptor, transferring the light energy to WcoA. The participation of a phytochrome could be specific of *F. fujikuroi*, as suggests the lack of effect of red light in *N. crassa* (Schrott et al., 1982) or even in *F. aquaeductuum* (Schrott et al., 1982). Further studies will be needed to confirm the participation of the *F. fujikuroi* phytochrome in this response.

5. A model for carotenoid regulation by light in *F. fujikuroi*

Collectively, the data provided in this Thesis suggest a global model for carotenoid photoinduction. In this model, WcoA modulates the synthesis of carotenoids in the dark keeping a basal transcription rate for the structural genes *carB, caRA and carT.* A sudden light stimulus produces a rapid response in which WcoA promotes the expression of the structural *car* genes, together with that of *cryD* and *vvdA*. Then, VvdA negatively regulates WcoA and restrains its activity. This scenario changes with the persistence of the light stimulus in the following hours, during which CryD replaces WcoA to up-regulate *carB* and *carRA*, seemingly post-transcriptionally rather than transcriptionally, explaining the slow induction of carotenoids after illumination in the absence of WcoA and the slower response after several hours of illumination in the absence of CryD. In this stage VvdA up-regulates CryD while it keeps WcoA partially inactivated. However, although at a lower rate, WcoA would also participate upon prolonged incubation under light, since carotenoid production is not totally prevented in *ΔCryD* mutants during long-term illumination. Finally, the data also suggest the participation of the only phytochrome in the *F. fujikuroi* proteome, that we shall call here PhyA. Tentatively, PhyA could act as an accessory red-light absorbing pigment that would transfer the signal to the putative WcoA/WcoB complex, which would be the only specific transcriptional activator in this scheme. As already stated, the participation of PhyA is just speculative, and remains to be experimentally demonstrated in future works.

In summary, the regulatory system in *F. fujikuroi* is similar to that of *N. crassa* in that the expression of the structural genes of the carotenoid pathway is controlled by a WC complex, susceptible to be activated by light, which in turn is modulated by a VVD protein. However, *F. fujikuroi* exhibits a more sophisticated regulation with some distinctive features: WcoA mediates a basal transcription level in the dark, allowing a detectable carotenoid biosynthesis under these conditions, and other photoreceptors add to WcoA to stimulate the synthesis in reponse to light, as CryD and probably also PhyA.

Confirmation of this model will require further experimentation. The model predicts protein-protein interactions that will be very interesting to analyze in depth, as formerly done for WC-1 and VVD in *N. crassa* (Hunt et al., 2010). The analysis of protein levels and subcellular localizations by specific detection techniques will be also a future valuable tool. Moreover, post-transcriptional modifications as those described for WC-1 could also play a relevant role (Arpaia et al., 1999; Schafmeier et al., 2005). The work in this Thesis achieved attempts of western blot analyses with antibodies raised against WcoA and VvdA peptides, but unfortunately the results were not reliable. The analysis of double mutants was also an evident complementary approach. However, as described in Chapter IV, the different attempts to make the double Δ*wcoA*/Δ*cryD* were not successful. In conclusion, the experiments described in this Thesis have settled the basis for future experiments for a more complete understanding of the molecular mechanisms that controls photocarotenogenesis in this fungus.

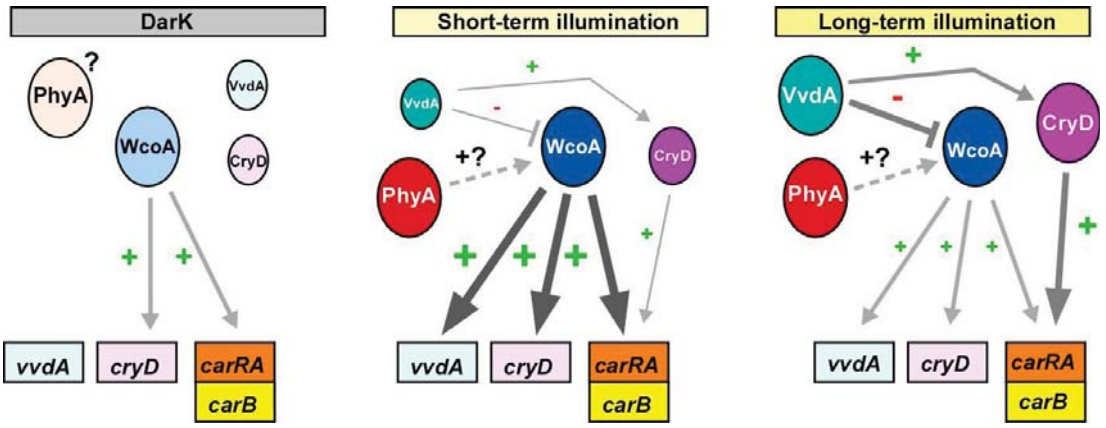

Fig. D-1. Model for carotenid regulation by light. Light circles correspond to proteins and squares to genes. The size of the circles represents the amount of protein in those conditions. Inactive proteins are indicated in black letters and those proteins activated by light are white. The thickness of the lines represent the intensity of the participation in the expression, while positive and negative signs (arrows and truncated lines) make reference to induction or repression.

CONCLUSIONES

1. Se han caracterizado los genes *cryD* y *vvdA* de *F. fujikuroi*, que determinan un criptocromo de la familia DASH y una pequeña flavoproteína ortóloga a VIVID de *Neurospora crassa*, respectivamente. La expresión de ambos genes es fuertemente estimulada por la luz a través de la proteína WcoA, de la familia White Collar.

2. La mutación dirigida del gen *cryD* produce diferentes alteraciones fenotípicas en condiciones de iluminación pero no en la oscuridad, demostrando la asociación de CryD con la regulación por luz en este hongo. Tales alteraciones incluyen cambios en la morfología, la producción de conidios o la producción de metabolitos secundarios, como bikaverinas y giberelinas, indicando una alta diversificación funcional.

3. El efecto de la mutación del gen *cryD* es especialmente llamativo en el caso de la producción de bikaverinas y más sutil en el caso de las giberelinas, pero los cambios fenotípicos no se correlacionan con cambios en los patrones de ARNm de genes estructurales relevantes de ambas rutas, sugiriendo la participación de CryD en mecanismos de regulación post-transcripcional.

4. La proteína CryD se ha expresado en *E. coli* y su purificación ha permitido determinar su capacidad para unirse a los dos cofactores característicos de esta familia de proteínas, dinucleotido de flavina-adenina (FAD) y N^5,N^{10}-metenil-tetrahidrofolato (MTHF).

5. Experimentos de fotorreducción y fotorreparación *in vitro* han confirmado que CryD posee actividad de reparación de daños inducidos en el ADN por radiación UV. Además, los experimentos de retraso de bandas han demostrado que CryD es capaz de unirse *in vitro* a moléculas de ADN, con independencia de la presencia o no de daños en dichas moléculas. Sin embargo, los mutantes del gen *cryD* no muestran cambios en su sensibilidad a radiación UV en la luz, lo que indica que la fotorreactivación es fundamentalmente llevada a cabo *in vivo* por la fotoliasa del hongo.

6. La mutación dirigida del gen *vvdA* produce en la luz una pigmentación más pálida que en la estirpe silvestre debido a una menor acumulación de carotenoides, indicando la participación de VvdA en esta fotorrespuesta. Los mutantes muestran además otras alteraciones fenotípicas bajo iluminación, como una menor producción

de conidios y un desarrollo diferente del micelio sobre agar, sugiriendo de nuevo una alta diversidad funcional.

7. La menor acumulación de carotenoides en los mutantes del gen *vvdA* no es acompañada por cambios detectables en la fotoinducción de los niveles de ARNm de los genes de la carotenogénesis, incluyendo la bajada posterior tras exposiciones más largas a la luz. Este último dato sugiere que, al contrario que su ortólogo VVD en *N. crassa*, VvdA no es responsable de la fotoadaptación transcripcional de dichos genes.

8. La iluminación de colonias de *F. fujikuroi* en agar muestra una cinética de síntesis de carotenoides en dos fases. En las primeras 6 horas se produce una rápida acumulación de carotenoides, seguida de una pausa y una acumulación más lenta a partir de las 12 horas. Los mutantes carentes de alelos funcionales de los genes *wcoA*, *cryD* y *vvdA* muestran alteraciones específicas en las distintas fases de síntesis, lo que indica su participación como fotorreceptoresco funciones diferentes en un mecanismo coordinado de regulación.

9. Las cinéticas de síntesis de los mutantes y sus respuestas a distintas intensidades de luz indican que WcoA es un fotorreceptor de alta sensibilidad responsable de la primera fase de la cinética, mientras que CryD es un fotorreceptor de baja sensibilidad responsable de la segunda fase de la cinética. Por su parte, VvdA se comporta como regulador negativo de WcoA y positivo de CryD.

10. Los análisis de expresión de los genes de la carotenogénesis en los citados mutantes sugieren que WcoA actúa esencialmente a nivel transcripcional, mientras que CryD y VvdA ejercen sus efectos de regulación principalmente a nivel postranscripcional o de interacción proteína/proteína.

11. La iluminación con luz roja produce una significativa inducción de la expresión de varios genes fotorregulados, como *vvdA, cryD* y el gen de la carotenogénesis *carRA*. Esta fotoinducción es dependiente de WcoA, y da lugar a una sensible fotoinducción de la síntesis de carotenoides, sugiriendo la participación de un fitocromo en el sistema fotosensorial que regula esta ruta en *F. fujikuroi*.

CONCLUSIONS

1. We have characterized the genes *cryD* and *vvdA* of *F. fujikuroi*, which encode a DASH-cryptochrome and a small flavoprotein otrholog of the *Neuropora crassa* VVD, respectively. The expression of both genes is strongly induced by the WcoA protein of the white collar family.

2. Site-directed mutation of the *cryD* gene produces different phenotypic alterations under light conditions but not under darkness, confirming the link of CryD with light regulation in this fungus. Such alterations include changes in morphology, conidia or production of secondary metabolites, like bikaverins and gibberellins, indicating a high functional diversification.

3. The effect of the *cryD* gene mutation is especially remarkable in the case of bikaverins production and more subtle for that of gibberellins, but the phenotyic changes do not correlate with changes in the mRNA pattern of relevant structural genes of the pathway, suggesting the participation of CryD in post-transcriptional regulatory mechanism.

4. CryD protein has been expressed in *E. coli* and its purification has allowed to determine its capacity to bind the two cofactors characteristic of this protein family, flavin-adenin-dinucleotide (FAD) and N^5,N^{10}-methenyl-tetrahidrofolate (MTHF).

5. Photoreduction and photorepair *in vitro* experiments have confirmed that CryD has repair activity on UV-induced damaged DNA. Moreover, electrophoretic mobility shift assays have proven that CryD is able to bind *in vitro* to DNA molecules, irrespective of the presence of UV-lesions. However, the mutants in the *cryD* gene do not show changes in their sensitivity to UV radiation, what indicates that photoreactivation is mainly achieved *in vivo* by the fungal photolyase in this fungus.

6. Site-directed mutation of *vvdA* gene produces under light a paler pigmentation than that of the wild type strain, due to a lower carotenoid accumulation, indicating that VvdA participates in this photoresponse. Additionally, the mutants show other phenotypic alterations under illumination, such lower conidia production and different mycelia development on agar surfaces, suggesting again a high functional diversification.

7. The lower carotenoid accumulation in the *vvdA* mutants is not accompanied by detectable changes in the photoinduction of mRNA levels of the genes for carotenogenesis, including the decrease upon longer light expositions. This result suggests that, in contrast to its ortholog VVD in *N. crassa*, VvdA is not responsible for the transcriptional photoadaptation of the carotenogenic genes.

8. The illumination of *F. fujikuroi* colonies on agar plates revealed a two-phase kinetics of carotenoid synthesis. In the first 6 hours a rapid carotenoid accumulation is produced, followed by a pause, and a slower accumulation after 12 hours. The mutants lacking functional alleles of the genes *wcoA*, *cryD* and *vvdA* show specific alterations in the different biosynthetic phases, indicating their participation as photoreceptors with different functions in a coordinated regulatory mechanism.

9. Time-course synthesis experiments in the mutants and their responses to different light intensities indicate that WcoA is a high sensitive photoreceptor responsible for the first induction phase, while CryD is a low sensitive photoreceptor responsible for the second phase. Regarding VvdA, it behaves as a negative regulator for WcoA and a positive regulator for CryD.

10. The expression analyses of the carotenogenic genes in the aforementioned mutants suggests that WcoA acts mainly at transcriptional level, while CryD and VvdA exert their regulatory functions at post-transcriptional level or through protein/protein interactions.

11. Red light illumination produces a significant induction of the expression of several photoregulated genes, such as *vvdA*, *cryD*, and the carotenogenic gen *carRA*. This photoinduction is dependent on WcoA, and leads to a minor photoinduction of carotenoid synthesis, suggesting the participation of a phytochrome in the photosensory system that regulates this pathway in *F. fujikuroi*.

MATERIALS AND METHODS

1.Organisms

1.1. Bacteria strains

Two *E. coli* strains were used for different purposes:

- DH5α (*sup*E44 Δ *lac*U169 [Ø80 lacZ ΔM15] *hsd*R17 *recA1 end*A1 *gyr*A96 *thi-1 relA1*) was employed for transformation and plasmids replication (Hanahan, 1983b).

- BL21(DE3) (*F⁻ ompT gal dcm lon hsdSB(r_B^- m_B^-) λ(DE 3[lacI lacUV5-T7 gene 1 ind1 sam7 nin5],* Promega, Mannheim, Germany*)* was chosen for heterologous protein expression and purification (Studier and Moffatt, 1986) in Chapter II.

1.2. *Fusarium* strains

The *Fusarium fujikuroi* wild-type strain was FKMC1995, kindly provided by Dr. J.F. Leslie from the Kansas State University, EEUU. All mutant strains, listed in Table MM1, were obtained from FKMC1995.

Table MM1. *Fusarium fujikuroi* strains used in this Thesis.

Strain	Origin	Genotype/Phenotype	Reference/Chapter
FKMC1995		Wild type	Kansas state university (USA)
SF226 and SF229	FKMC1995 (gene disruption)	*ΔwcoA*	Estrada and Avalos 2008
SF236 and SF237	FKMC1995 (gene deletion)	*ΔcryD*	Chapter I
SF262-267	*ΔcryD* SF236 (integration)	*ΔcryD* complementation	Chapter I
SF268	*ΔcryD* SF237 (chlorate resistance)	*ΔcryD niaD⁻*	Chapter I
SF256, SF257 and SF258	FKMC1995 (gene deletion)	*ΔvvdA*	Chapter III
SF259, SF260 and SF261	*ΔvvdA* SF258 (integration)	Silvestre: *ΔvvdA* complemented	Chapter III

2. Plasmids

2.1. Plasmids not constructed in the Thesis

- pGEMT-easy (Promega, Mannheim, Germany). Commercial vector used for cloning of PCR products. This 3Kb plasmid contains the β-lactamase gene (*bla*) which confers resistance to the antibiotic ampicillin. It also includes the β-galactosidase gene (*lacZ*) interrupted by a multiple cloning site (MCS) for detection of right clones by colour screening through β-galactosidase activity on X-gal (5-bromo-4-cloro-3-indolil-β-galactopiranoside) upon IPTG (isopropil- β-D-1-tiogalactopiranoside) induction. The plasmid is provided as a *Eco*RV-digested linear form, with a 3'-thymidine overhang to facilitate PCR product ligation.
- pAN7-1 (Punt et al., 1987). A plasmid containing the *bla* ampicillin resistance gene and the hygromycin resistance cassette consisting of *E. coli hphB* gene under control of the *A. nidulans* glyceraldehyde-3-phosphate dehydrogenase (*gdpA*) promoter and the tryptophan C terminator (*trpC*).
- pHJA2 (7Kb) (Fernández-Martín et al., 2000). Derived from pBluescript®II KS+ (Stratagene). The 4.06 Kb hygromycin resistance cassette was removed from pAN7-1, obtained by complete *Xba*I and partial *Eco*RI digestions, end-filled by treatement with Klenow and cloned in the NaeI site of pBluescript®II KS+.
- pNTP2 (kindly provided by A. Adám). This 4.8 Kb vector contains a geneticin resistance cassette consisting on the neomycin phosphotransferase II gene (*nptII*) under control of a duplicated cauliflower mosaic virus 35S promoter (CaMV). Used as a plasmid with an alternative selection marker.
- pET51+b (Novagen). A 5.2 Kb plasmid carrying an N-terminal Strep-tag II and a C-terminal His-tag to facilitate protein purification. It also has the ampicillin resistance gene (*bla*) and a *lacI* promoter region to induce expression after IPTG addition.
- pALEX7 (Estrada and Avalos, 2008): 11 Kb pGEMT-easy-based vector containing the *F. fujikuroi wcoA* gene including 0.56 Kb upstream and 0.65 Kb downstream sequences, interrupted by the hygromycin resistance cassette obtained from pHJA2.

2.2. Plasmids constructed in the Thesis

Cloning strategies and primer sequences are detailed in following sections (14, 15, 16 and Annex 1 and 2).

- pDcryD. A 9.9 Kb pGemT-based plasmid constructed to obtain the targeted disruption of gene *cryD*. It contains the hygromycin resistance cassette from pAN7-1 flanked by the 5' upstream non coding region of cryD and a partial segment of the 3' coding region.

- pCcry: A 8.5 Kb pNTP2-derived plasmid created for *ΔcryD* complementation. The *cryD* coding region and 0.7 and 0.9 Kb of the upstream and downstream regulatory region was cloned in the *Eco*RI site of pNTP2.
- pDvvd (9.9Kb): A 9.9 Kb plasmid constructed to generate the targeted deletion of gene *vvdA*. The coding region of *vvdA* was replaced by the hygromycin resistance cassette from pHJA2. 1.4 Kb of upstream and downstream sequences were left for double homologous recombination.
- pCvvd. A 9.8 Kb pNTP2-derived plasmid created for Δ*vvdA* complementation. A 5 Kb fragment containing the *vvdA* coding sequence and 2.3 and 2.0 Kb of the upstream and downstrema regulatory regions were cloned in the *Not*I site of pNTP2.
- pDMWC. A 10.8 Kb pALEX7-derived plasmid created to obtain a double Δ*wcoA* Δ*cryD* mutant from a single Δ*cryD* strain*,* using the *niaD* gene as alternative selection marker. The hygromycin resistance cassette (*hphB*) from pALEX7 was replaced by the *niaD* gene of *F. fujikuroi*.
- pDwc2. A 7.8 Kb pALEX7-derived plasmid created to obtain a double Δ*wcoA* Δ*cryD* mutant from a single Δ*cryD* strain using the *nptII* gene as alternative selection marker. The hygromycin resistance cassette (*hphB*) from pALEX7 was replaced by neomycin phosphotransferase cassette from plasmid pNTP2.
- pGcry7. A 7.5 Kb pDcry-derived plasmid created to obtain a double Δ*wcoA* Δ*cryD* mutant from a single Δ*wcoA* strain using the *nptII* cassette as alternative selection marker. The cassette was flanked by the 5' upstream region and 3' *cryD* coding region from pDcry.

3. Solutions and culture media

3.1. *E. coli* culture media and solutions

- LB media: LB (Luria Bertani) is a rich medium for enterobacteria, whose components are the following: 5 g L^{-1} of yeast extract, 10 g L^{-1} of peptone and 10 g L^{-1} of NaCl. For solid media, 20 g L^{-1} of agar are added (Sambrook and Russell, 2001). Final pH is adjusted to 7-7.5 if required.
- SOB media: used to generate *E. coli* competent cells for transformation (Inoue et al., 1990). The composition is: 5 g L^{-1} of yeast extract, 20 g L^{-1} of tryptone, 0,5 g L^{-1} of NaCl and 10 ml L^{-1} of a KCl 250 mM solution. Once autoclaved, $MgCl_2$ is added to a final concentration of 10 mM.
- SOC: SOB medium to which glucose is added at a final 20 mM concentration after sterilization.
- Antibiotics and other medium supplements: to select transformant colonies, ampicillin was added to LB media at 100 mg L^{-1}. To detect insertions in the multiple cloning site of plasmids and to induce the production of proteins in the

expression vectors, X-gal and IPTG were added at 40 mg L^{-1} and 20 mg L^{-1} respectively.

- Sorensen's phosphate buffer A and B: for *E. coli* lysis, the buffer A contained Na_2HPO_4 200 mM and buffer B NaH_2PO_4 200 mM. Concentrations indicated hereafter for this buffer refer to final phosphate concentration after mixture of A and B.
- *E. coli* Lysis buffer 2X: Sorensen's phosphate 100 mM pH 7.5 (42 ml of A and 8 ml of B), NaCl 600 mM, glycerol 20% (v/v), triton x-100 1% (v/v), and imidazole 20 mM.
- No-imidazole buffer: used for nickel affinity chromatography. The composition is Sorensen's phosphate A and B 50 mM pH 7.5 (21 ml of A and 4ml of B), NaCl 200 mM, glycerol 10% (v/v), and β-mercaptoethanol 10 mM.
- High imidazole buffer: used for nickel affinity chromatography. The composition is Sorensen's phosphate A and B 50 mM pH 7.5 (21 ml of A and 4ml of B), NaCl 200 mM, glycerol 10% (v/v), imidazole 500 mM and β-mercaptoethanol 10 mM.
- No-NaCl buffer: used for heparin chromatography: The composition is Sorensen's phosphate A and B 50 mM pH 7.5 (21 ml of A and 4ml of B), glycerol 10% (v/v) and β-mercaptoethanol 10 mM.
- High NaCl buffer: for heparin chromatography: The composition is Sorensen's phosphate A and B 50 mM pH 7.5 (21 ml of A and 4ml of B), glycerol 10% (v/v), NaCl 2 M and β-mercaptoethanol 10 mM.

3.2. *Fusarium* culture media and solutions

F. fujikuroi was grown either in liquid or solid media. Solid media were prepared by adding 16 g L^{-1} of agar to the composition listed below.

- DG minimal medium: standard medium used for *F. fujikuroi* growth for routine laboratory manipulations. The composition is 30 g L^{-1} of glucose, 3 g L^{-1} of $NaNO_3$, 1 g L^{-1} of KH_2PO_4, 0.5 g L^{-1} of KCl, 0.5 g L^{-1} of $MgSO_4$-$7H_2O$ and 2 ml L^{-1} of a microelements solution (Avalos et al., 1985a).
- DG microelements solution. Per 100 ml: 0.5 mg of H_3BO_3, 5 mg of $CuSO_4$, 10 mg of $FeCl_3$, 1 mg of $NaMoO_4$, 1 mg of $MnCl_2$ and 100 mg of $ZnSO_4$ (Avalos et al., 1985a).
- DG asparagine (DGasn): DG minimal medium in which the 3 g L^{-1} of $NaNO_3$ are replaced by 3 g L^{-1} of L-asparagine.
- Low nitrogen DG or DGasn: the concentration of $NaNO_3$ and asparagine was reduced to 0.625 g L^{-1}.
- ICI medium: used for excess nitrogen conditions in experiment of production of secondary metabolites. It contains 80 g L^{-1} of glucose, 4.8 g L^{-1} of NH_4NO_3, 5 g L^{-1} of

KH_2PO_4, 1 g L^{-1} of $MgSO_4$-$7H_2O$ and 2 ml L^{-1} of a microlements solution (Geissman et al., 1966).

- 10%ICI medium: ICI medium with 10% of nitrogen source (0.48 g L^{-1} of NH_4NO_3).
- ICI microelements solution. Per 100 ml: 100 mg of $FeSO_4$-$7H_2O$, 15 mg of $CuSO_4$-$5H_2O$, 161 mg of $ZnSO_4$-$7H_2O$, 10 mg of $MnSO_4$-$7H_2O$ and 10 mg of $(NH4)_6Mo_7O_{24}$-$4H_2O$) (Geissman et al., 1966).
- DGasn chlorate: medium used to obtain spontaneous mutants unable to use nitrate as nitrogen source. Its composition is the same as DGAsn but with the addition of 15 g L^{-1} $KClO_3$.
- Medium for *niaD*$^-$ mutants screening: to select those colonies with a spontaneous mutation in the *niaD* gene, the chlorate resistant strains were transferred to DG with 0.2 g L^{-1} of hypoxanthin, 1 g L^{-1} of asparagine, 0.5 g L^{-1} of $NaNO_2$ or 3 g L^{-1} of $NaNO_3$ as nitrogen source. Those specifically affected in the nitrate reductase gene (*niaD*) were identified through their ability to grow with asparagine, nitrite or hypoxanthin, but not with nitrate, as nitrogen sources (Klittich and Leslie, 1988).
- Top-agar: 4 1 g L^{-1} of agarose.
- YPED-2G: used for conidia germination in the *F. fujikuroi* protoplasts formation protocol. Composition: 3 g L^{-1} of yeast extract, 10 g L^{-1} of peptone and 20 g L^{-1} of glucose.
- Enzymatic lysis solution: used for cell wall digestion in the protoplast formation protocol. It is a mixture of degrading enzymes from different organisms (Sigma-Aldrich): 10 g L^{-1} of lytic enzymes from *Trichoderma harzianum,* 25 g L^{-1} of driselase from basidiomycetes and 50 mg L^{-1} of quitinase from *Streptomyces grisea.* These compounds are dissolved in 200 ml 0.7 M NaCl, centrifuged (1300 rpm 10 min), filtered through a 0.2 Millipore filter attached to a vacuum system and stored at -80° C.
- STC 1X: sorbitol 1.2 M, Tris-HCl 10 mM pH8, $CaCl_2$ 50 mM.
- STC 2X: sorbitol 2.4 M, Tris-HCl 20 mM pH8, $CaCl_2$ 100 mM.
- PEG 30%: PEG 8000 30%, Tris-HCl 10 mM pH8, $CaCl_2$ 50 mM.
- Regeneration medium 2X: a rich medium used for protoplast regeneration after the transformation protocol. The composition is 2 g L^{-1} of yeast extract, 2 g L^{-1} of casein (N-Z aminoacids, Sigma) and 32 g L^{-1} of agar. This medium is mixed with sucrose 1.6 M in equal volumes to obtain regeneration medium 1X.
- Top-agar for regeneration medium 2X: 2 g L^{-1} of yeast extract, 2 g L^{-1} of N-Z amino acids and 20 g L^{-1} of agarose. This medium is mixed with sucrose 1.6 M in equal volumes to obtain regeneration medium 1X. In the case of antibiotic selection, 50 mg L^{-1} of hygromycin or 150 mg L^{-1} geneticin were added to the medium and to top agar.

- Selective medium: DG or DGasn were supplemented with 100 mg L^{-1} of hygromycin B (Roche) or 250 mg L^{-1} geneticin (G-418 disulphate salt, Sigma).

4. Culture conditions

4.1. *E. coli* culture conditions

E. coli was grown in LB at 37°C for 12-16h. For liquid culture, 10 ml-tubes were incubated in a shaker at 200 rpm. When required, antibiotics and/or inducers were added to the medium.

4.2. *F. fujikuroi* culture conditions

Unless otherwise indicated, *F. fujikuroi* was incubated in petri-dishes either at 22°C or 30°C. For liquid cultures, 500 ml Erlenmeyer flasks with 250 ml of medium were shaked at 150 rpm at 30°C. To check the effects of light on *F. fujikuroi* strains, dark and continuous illuminated cultures were assayed. Total darkness was achieved by incubating the plates in closed boxes or wrapping the flasks with aluminum foil surrounded by black plastic bags.

Standard incubation times either in solid or liquid cultures were 7 days, after which mycelia samples were collected.

4.2.1. Illumination conditions

A set of fluorescent tubes Sylvania Standard F36/154-t8 were used to get a luminous flux of 7 W m^{-2}. The flux was measured with a silicon photodiode PIN-10DP/SB (United Detector Technology, Hawthorne, California, EEUU) connected to 485 picoameter (Keithley Instruments, Cleveland, Ohio, EEUU). When illumination was restricted to a specific range of wavelengths, light was filtered with commercial cellophane sheets. In this case, with the blue filter the light intensity was 1.7 W m^{-2} and with the red filter it was 1.5 W m^{-2}. Parallel transparent cellophane sheets were used as a control (6 W m^{-2}). Lower intensities of white light were reduced in an exponential manner by using grey commercial plastic sheets. 3 plastic sheets caused a light reduction of 10%, from 7 W m^{-2} to 0.7 W m^{-2}, and the addition of 3 additional plastic filters reduced the light intensity to 1% (0.07 W m^{-2}).

4.2.2 *F. fujikuroi* DNA extraction

250 ml Erlenmeyer flasks with 100 ml of liquid DGasn medium were inoculated with 10^5 conidia and shaked at 200 rpm at 30°C for 5 days at under indirect illumination. The whole volume was filtered through a vacuum device and the mycelia were frozen at -20°C.

4.2.3. Expression analyses

Petri dishes of 15 cm of diameter (Ø) with 80 ml of DGasn liquid medium were inoculated with 10^6 fresh spores. The plates were incubated in total darkness for 3 days to obtain young mycelia samples. After this period, the thin mycelia layer formed at the bottom of the plate was exposed to different illumination (7 W m^{-2}) times (15,

30, 60, 120, 240 minutes). Samples were collected and immediately frozen in liquid nitrogen for -80°C storage.

4.2.4. Carotenoid and conidiation analyses

For carotenoids determination, petri dishes with 25 ml of solid DG or DGasn media were incubated for 7 days either at 22°C or 30°C. Conidiation was analyzed under the same conditions at 22°C. Strains were plated in seven separated inoculation points and kept in darkness or illuminated during the 7 days incubation. Carotenoid samples were preserved from light until extraction.

4.2.5. Bikaverin and gibberellin production

The production of these compounds was assayed in ICI and 10%ICI liquid media. 500-ml Erlenmeyer flasks with 250 ml of medium were incubated in a rotary shaker at 150 rpm for 7 days at 30°C in darkness or under continuous illumination. Each flask was inoculated with 10^6 fresh conidia. After 1 week, cultures were filtered and separate mycelia and medium samples were stored at -20°C

5. Nucleic acids extraction

5.1. Small-scale plasmid preparations (miniprep)

Adapted from the alkaline lysis protocol (Sambrook and Russell, 2001; Stephen et al., 1990), this protocol is used to obtained DNA amounts under 10 µg. 1.5 ml from a 3-ml *E. coli* overnight culture at 37°C was centrifuged at maximum speed (13,200 rpm) for 1 min. The cell pellet was resuspended and mixed in 200 µl of cold solution I (Tris 50 mM pH 7.5, EDTA 10 mM and 10 mg L^{-1} RNase). 200 µl of fresh solution II (NaOH 0.2 M and 10 g L^{-1} SDS) were added to the sample and carefully inverted to clear up the cell suspension, and kept in ice. To neutralize the lysis process, 150 µl of cold solution III (Potassium acetate 3 M, glacial acetic acid 11.5%, pH 4.8) were added and vortexed. The mixture was centrifuged for 10 min at 13,200 rpm and the supernatant was poured in a clean 1.5 ml tube. For DNA precipitation the sample was mixed with 500 µl of isopropanol and centrifuged again for 5 min at maximum speed. The supernatant was discarded and the pellet was washed with ethanol 70%. After 5 min of centrifugation, the precipitated DNA was resuspended in 20-30 µl of H_2Odd (bidistilled water).

5.2. Large scale plasmid preparations (maxiprep)

The maxiprep protocol yields DNA amounts over 500 µg, with average concentrations between 1 and 3 µg $µl^{-1}$. The initial overnight culture has a volume of 50 ml and the centrifugation steps are done at 4°C and 4,500 rpm. All the steps were carried out in 50-ml Falcon tubes. The pellet obtained from the 50 ml LB-grown *E. coli* was resuspended in 1.6 ml of solution I and kept in ice for 5 min. 3.2 ml and 2.4 ml of solution II and III respectively were added proceeding as above and the lysed suspensions was centrifuged for 10 min. The supernatant was filtered through a sterile gauze and 6.4 ml of a mixture of phenol: chloroform: isoamilic alcohol (25:24:1) were added, mixed, and centrifuged for 10 min. Afterwards, the supernatant was

transferred to a clean 50 ml tube and precipitated with 2 volumes of ethanol 96% at -80 °C for 10 min. The sample was centrifuged for 10 min and the pellet was washed with 3.2 ml of ethanol 70%. A final centrifugation step was performed to remove the ethanol and the pellet was dried at 37°C. The plasmidic DNA was finally resuspended in 0.5-1 ml of H_2Odd.

5.3. *F. fujikuroi* nucleic acids extraction

5.3.1. Genomic DNA

For genomic DNA isolation three procedures were followed. All of them required fine powder as the starting sample, obtained by grinding an appropriate mycelia amount with liquid nitrogen in a mortar with a pestle.

- Small DNA amounts for PCR tests were obtained with the GenElute Plant Genomic DNA Miniprep kit (Sigma-Aldrich, USA) according with manufacturer's instructions.
- Larger DNA quantities for Southern Blot analyses were performed as described (Weinkove et al., 1998): 7 ml of an extraction solution (Tris-HCl 50 mM, EDTA 20 mM, pH 7.5) were added to the fine powder and resuspended carefully on ice. Afterwards the sample was incubated at 65°C for 30 min with 0.5 ml of SDS 10%. The sample was cooled for 30-60 min in ice and 2 ml of neutralizing solution (Potassium acetate 5 M) were added prior to centrifugation at 4°C and 14,000 rpm for 10 min. The supernatant was transferred to a new 50 ml tube and precipitated with 2 volumes of ethanol 96% at -80°C for 1h. After this time, the sample was centrifuged for 20 min at 14,000 rpm (4°C) and the pellet was washed with 1 volume of ethanol 70% and centrifuged again. Finally, the pellet was dried and resuspended in 1 ml of TE. RNase treatment (Ribonuclease A 10 µg/ml, Sigma) was carried out for 30 min at 37°C, followed by enzyme inactivation at 65°C.
- In some cases, for PCR amplifications it was used an adaptation of the above protocol. 350 µl of DNA extraction solution were added to grinded mycelia and mixed. Then, the sample was incubated for 20 minutes at 65°C with 25 µl of SDS 10%. Then, 100 µl of neutralization solution were added, the mixture was incubated for another 20 minutes in ice, and centrifuged for 10 min at 13,200 rpm. The supernatant was transferred to a new tube, precipitated with 2 volumes of 100% ethanol at -20°C and centrifuged again. The pellet was washed twice with 70% ethanol, centrifuged for 5 min at 13,200 rpm and finally dissolved in 100 µl of H_2Odd.

5.3.2. RNA extraction

Total RNA was isolated from frozen samples. Mycelia were ground with the FAST-PREP24 (Biomedicals, LLC Europe, France) disruption system and extraction was achieved with the RNeasy mini Kit (Quiagen) according to the manufacturer's protocol.

5.4. Nucleic acids quantification

Plasmid, DNA and RNA concentratiosn were calculated spectrophotometrically with a Nanodrop 3.0.1 equipment (Coleman Technologies Inc., Orlando, Florida, EEUU).

Samples with low amount of DNA were visualized in an agarose gel electrophoresis by ethidium bromide staining. To estimate their concentrations, the samples were run in parallel with a known concentration of size markers consisting on Lambda DNA (Roche) digested with *Hin*dIII.

6. Nucleic acids manipulation

6.1. Enzymatic treatments

6.1.1. DNA digestions

Restriction enzymes were purchased either to New England Biolabs (Ipswich, MA, USA) or to Takara (Shiga, Japan). The enzymes were supplied at concentrations ranging from 10 to 20 U μl^{-1}, and with specific reaction buffers (10X). Plasmidic DNA and PCR fragments were digested in a total volume of 10-20 µl using 0.2 µl of the enzyme. Incubation temperatures varied according to the manufacturer`s instruction for each enzyme, and incubations time were usually of at least 1h 30 min. When required, digestions were followed by enzyme inactivation at high temperature (65-80°C).

For southern Blot analyses, due to the larger DNA amount needed, more enzymatic units and longer incubation times were used. Usually, two-step digestions were performed. About 10 µg of genomic DNA were first treated with 10 units of the corresponding enzyme for 1 h, and then another 10 units were added for an overnight incubation. The digested sample was finally precipitated at -80°C for 1h with 0.1 volume of sodium acetate and 2 volumes of ethanol 96%. After centrifugation at 13,200 rpm for 10 min, the DNA pellet was washed with 2 volumes of ethanol 70%, centrifuged and dried. The sample was resuspended in an appropriate volume of TE (20-40 µl) and loaded in an agarose gel.

6.1.2. End-filling

Some PCR polymerases and most restriction enzymes yield DNA products with overhang/cohesive ends. To generate blunt ends, the products were treated with DNA Klenow polymerase (Roche), which fills-in 5' overhang ends or removes 3'overhangs ends. Klenow reactions were performed with 1 U μg^{-1} DNA and incubated with 1 mM dNTPs (Bioline) at 37 °C for 30 min followed by heat inactivation at 65°C.

6.1.3. Dephosphorylation

When a vector was linearized with a restriction enzyme to be ligated with a DNA fragment digested with the same enzyme, the monophosphate group of the 5' end of the vector was removed to avoid recircularization and increase the efficiency of the ligation. 1 U of Alkaline Phospahatase (Roche) was incubated with DNA at 37°C for 15 min followed by heat inactivation at 65 °C.

6.1.4. Ligation

DNA ligations were performed with T4 DNA ligase (Roche). Final reaction volume was 15 µl using 1U of the enzyme and suitable DNA amounts of each fragment. 10x

buffer (including ATP) was provided by the supplier. Sticky-end ligations were incubated at 16°C overnight, and blunt-end ligation 25°C.

6.1.5. DNase treatment

RNA samples were treated with rDNAse I, RNAse-free (USB, Affymetrix) to ensure no traces of DNA in the samples. 2.5 µg of RNA were incubated with 10 U of DNAse at 25°C for 15 min. 10x buffer was provided by the supplier. To inactivate the enzyme, 1 µl of STOP solution (EDTA 50 mM, pH8) was added and incubated at 65°C for 10 min.

6.2. Nucleic acids synthesis and expression analyses

6.2.1. PCR

PCR amplifications from genomic or plasmidic DNA were done with different enzymes: for standard reactions EcoTaq polymerase (Ecogen, Barcelona) or BIOTAQ^{TM} DNA polymerase (London, UK) were used; for high fidelity reactions, such as those used for cloning or sequencing purposes, the Expand High Fidelity PCR system (Roche) was chosen because of its lower mutation rate. PCR mixtures contained 50 ng of template DNA, 0.2 mM of dNTPS, 1 µM of forward and reverse primers, 1X reaction buffer, 1.75 mM of $MgCl_2$, and 1U of polymerase in a final volume of 20 µl. PCR conditions varied according to the primers sequences and the length of the synthesized DNA. An initial denaturalization step at 94 °C for 2 min was followed by 35 cycles of DNA amplification, consisting on strand denaturalization (94 °C, 20s), primers hybridization (50-60°C, 30s), and polymerase elongation (68°C for fragments > 3Kb or 72°C for fragments < 3Kb, 1 min Kb^{-1}). Last step was a final polymerization cycle at 72 °C for 5-10 min.

6.2.2. cDNA synthesis

cDNA was obtained from DNase-treated RNA samples using the Transcriptor First Strand cDNA Synthesis Kit (Roche) and following the manufacturer's protocol: 2.5 µg of RNA were incubated with 2.5 µM anchored oligo $(dT)_{18}$ primers at 65°C for 10 min. Reversed transcription was performed at 25°C for 10 min followed by 30 min at 55°C with 1X Transcriptor RT reaction buffer, 20 U of RNase inhibitors, 1 mM dNTPs and 10 U of reverse transcriptase. Finally, the enzyme was inactivated at 85°C for 5 min. Assuming a reverse transcriptase efficiency of 70%, samples were diluted to 25 ng μl^{-1}.

6.2.3. Real time PCR

Quantitative PCR was performed with the two-step system of Roche. cDNA synthesis was as described above and mRNA quantification was made in a Light Cycler 480 device (Roche) by using the Light Cycler 480 SYBR Green Master I kit. Reaction samples contained 50 ng of RNA (2 µl at 25 ng μl^{-1}), 0.4 µM of forward and reverse primers (0.4 µl of 10 µM stock), 5 µl of 1X SYBR Green I Master (hot start PCR mix), which includes FastStart Taq DNa Polymerase, reaction buffer, dNTPs mix (dUTP instead of dTTP), SYBR Green I Dye and $MgCl_2$. The final volume in each well was 10 µl. The program used for cDNA amplification and quantification was as described in the supplier's manual, and consists of:

- Pre-incubation: 95°C, 5 min.

- Amplification (45 cycles) and quantification analyses comprise three steps: 1) 95°C 10 s, 2) 60°C 10 s, 3) 72°C 10 s with single acquisition mode.

- Melting curve to check the specificity of the product. Amplification includes a step at 95°C 5s, 65°C 1 min and 97°C for continuous acquisition.

- Cooling: 40 °C 30 s.

Primer sets used in the RT-PCR expression analyses are described in Annex 1.

7. DNA electrophoresis and purification

7.1. Electrophoresis

Agarose gels were prepared in TAE buffer with low electroendosmosis agarose (low D1 EEO agarose, Pronadisa) at a concentration of 8 g L^{-1} supplemented with an appropriate concentration of ethidium bromide. Electrophoreses were run in horizontal cells (Ecogen, Barcelona) filled with TAE and connected to a power supply (Pharmacia Biotech EPS 200 or Bio-rad PowerPac™ Basic Power Supply). Samples were loaded in the gel mixed with 1X loading buffer (1% SDS, 50% glycerol and 0.05% bromophenol blue, Takara) and run in parallel with commercial 1Kb size markers (Invitrogen™ Life Technologies, Aberdeen, Washington, USA) or concentration/size markers (Lambda DNA digested with *Hin*dIII). DNA was visualized in the gels by UV radiation with a transilluminator equipment (UVP). Pictures were taken and printed with a ImageStore 5000 (UVP) equipment coupled to a UP-895MD/LE printer (Sony).

7.2. DNA purification from agarose gels

To avoid UV-induced mutations in DNA fragments used for sequencing or cloning, DNA was visualized with an UV hand-lamp (312 nm). DNA bands were carefully cut out from the agarose gels with a blade and extracted with the GFX PCR DNA and Gel Band Purification Kit (GE, Healthcare) following manufacturer's instructions.

8. Transformation procedures

8.1. *E. coli* transformation

8.1.1. Competent *E. coli* cells

E. coli DH5α competent cells were produced according to a published protocol (Inoue et al., 1990). *E. coli* BL21 DE3 competent cells were kindly provided by Professor Alfred Batschauer group.

A 1-L Erlenmeyer flask containing 200 ml of SOC medium was inoculated with 1 ml of an *E. coli* preculture in stationary phase and incubated at 22°C. When the optical density reached 0.5, the culture was cooled down in ice for 10 minutes and centrifuged at 4°C for 10 min at 2,500 g. The pellet was resuspended in 80 ml of cold TB buffer (PIPES 10 mM, $CaCl_2$-$2H_2O$ 15 mM, KCl 250 mM and $MnCl_2$-$6H_2O$ 55 mM, pH 6.7) and incubated for 10 min in ice. The sample was centrifuged as described above and

resuspended in a volume of 20 ml of TB. To preserve cells from freezing, 1.5 ml of DMSO was added and left 10 min in ice. The cells were then distributed in 0.2 ml aliquots in sterile 1.5 ml tubes and frozen immediately in liquid nitrogen.

8.1.2. *E. coli* transformation

0.1 ml of competent cells were thawed on ice and mixed with 1 µl of a plasmid sample or 5 µl of a ligation mixture. The samples were incubated in ice for 30 min, subjected to a heat shock at 42°C for 45 s and cooled in ice for 2 min. Afterwards, 0.8 ml of LB medium was added to the transformation mixture and incubated at 37°C for 1h. Finally, the cells were plated on ampicillin-supplemented LB medium with appropriate dilutions to ensure the formation of isolated colonies. The typical procedure consisted in plating 10 µl, 100 µl and the rest of the sample after centrifugation. Plates were incubated at 37°C for 12-16h.

8.2. *F. fujikuroi* transformation

8.2.1. Protoplasts formation

$5x10^8$ fresh conidia were inoculated in 250 ml flask containing 100 ml of YPED-2G and incubated at 25°C for 12h. After this time the germinating spores (germinules) reached a size about 5-7 fold that of the conidium, and the culture was filtered using a vacuum system consisting of a Kitasato or side-arm flask attached to a funnel. The filter was first moistened in NaCl 0.7 M and the spores were discarded, while the germinules were retained. Then, the germinules were collected with a spatula, resuspended on a petri dish in 5 ml of enzymatic lysis solution and transferred to a 125 ml sterile empty Erlenmeyer flask. This step was repeated three times and the 15 ml were incubated at 30°C for 75 min in a waving shaker at 40 rpm. This was the estimated time for optimal formation of protoplasts in the sample, but their formation was anyhow checked every 20 min under microscope. Protoplasts were then subjected to a double filtration through a borosilicate filter crucibles of 50 ml volume and 40 mm of diameter (Robu,Hatter, Germany) and moistened in NaCl 0.7 M. First, a filter of porosity 0 was used and subsequently, one of porosity 1. Filtered protoplasts were collected in a sterile 50 ml Falcon tube, filled with NaCl 0.7 M to complete the volume and centrifuged at 20°C for 10 min at 1,500 rpm. NaCl solution supernantant was sucked out with a Pasteur pipette connected to a vacuum pump and the step repeated twice. The third centrifugation was made in STC 1X solution and the pellet was finally resuspended in 200 µl of STC 1X. Protoplasts concentration was estimated in hemocytometer and diluted aliquots of $2x10^8$ protoplast were frozen in a solution with 0.1% of PEG 30% and 0.01% (v/v) of DMSO.

8.2.2. Protoplasts transformation

The protocol is basically as described (Proctor et al., 1997). A transformation and a control tube were prepared in parallel. 100 µl of protoplast suspension were added to two 1.5 ml sterile tubes with cut tips, one for transformation and the second as a control. 50 µl of STC 2X and 30 µg of plasmid (circular or linearized) were added to the

first tube and filled up to 200 µl with H_2O. In parallel, 100 µl of STC 1X were added to the second tube. The tubes were gently inverted, 50 µl of PEG 30% were added followed by 20 min incubation at room temperature. The samples were transferred then to 10 ml sterile tubes, 2 ml of PEG 30% were added again and mixed by inversion. After 5 min incubation at room temperature, 4 ml of STC 1X were added, carefully mixed, and the tubes were centrifuged for 5 min at 1,500 rpm. The supernatants were suck out with a Pasteur pipette and the pellets were resuspended in 200 µl of STC 1X.

During the incubations described above, 10 ml tubes with 5 ml of top agar to be added to regeneration medium were prepared and kept in a bath at 50°C. In each experiment 4 tubes were required, two for the transformation and two for the control reaction.

100 µl of the transformation tube were added to a 5 ml top-agar tube, inverted and plated on regeneration medium. The procedure was repeated with the remaining 100 µl of the transformation tube. The same procedure was followed with the control tubes, dividing the 200 µl volume in 100 µl aliquots and plating them separately on regeneration medium. These plates were incubated at 30°C for 10 h to allow protoplast regeneration and the expression of the antibiotic resistance cassette. Then, 140 µl of hygromycin B (50 mg ml^{-1}) or 30 µl of G418 (150 mg ml^{-1}) were added to 3 top agar tubes, which were carefully laid over the two transformation plates and one of the control plates (negative control). The remaining control plate served as a regeneration control and only 5 ml of top agar were added. All the plates were then incubated at 30 °C for 7-10 days.

The colonies grown on the transformation plates were subcultured in 6 cm Ø Petri dishes with antibiotic-supplemented DGasn medium. Conidia were collected from each transformant and plated at an appropriate dilution to obtain isolate colonies. To ensure homokaryosis, this step was repeated at least three times.

9. DNA hybridization protocol: Southern Blot

9.1. Radioactive labeling of the DNA probe

For hybridization, 100 ng (15 µl) of purified probe were labeled with [α-32P]dCTP (Perkin-Elmer, Boston, MA). In parallel, 100 ng of Lambda phage DNA (5 µl) were also labeled. The sample and the ladder were heated at 100°C for 10 min and stored on ice. Labeling was performed adding 2 µl of a pool of dATP, dGTP and dTT (0.5 mM), 2 µl [α-32P] dCTP (3000 Ci $mmol^{-1}$), 2 µl of random hexanucleotides 10X (Roche) and 2 U of Klenow enzyme (Roche). The volume reaction was completed to 20 µl with H_2O, and the mixture was incubated at 37°C for 3-4 h. Finally, the radioactive probe and markers were purified with the GFX DNA purification kit (GE, Healthcare).

9.2. Membrane DNA transfer

The digested genomic DNA was run in 0.8% agarose electrophoresis. 5-10 µg of the DNA were loaded in the gel and run for 4 h at 60V. Afterwards, the gel was submerged 10 min in HCl 0.25 M and washed with water. It was followed by two 15 min washing

steps in denaturing solution (NaCl 1.5 M and NaOH 0.5 M) and two subsequent washing steps in neutralization solution (Tris-HCl pH 7.5 0.5 M and NaCl 3 M). Transfer was performed by capillarity in SSC 20X (NaCl 3 M and Na_3citrate 300 mM) as described (Sambrook and Russell, 2001). A piece of Hybond-N nylon membrane (Amersham Biosciences) was cut with a size to fit the gel dimensions and the same procedure was followed to cut two pieces of Whatman paper 3MM and several pieces of standard filter paper. The gel was placed at the bottom of a container filled with SSC 20X and the membrane, Whatman and filter papers were placed over in this order and left overnight. After transfer, the membrane was washed in SSC 2X, dried and exposed to 700 J m^{-2} in a crosslinker RPN 2500 (Amersham) for DNA linking.

9.3. Probe hybridization

The procedure was as described (Sambrook and Russell, 2001). The membrane was incubated in an oven (HB-100 Hybridizer, UVP) at 65°C for 30 min in a hybridization tube with 20 ml of pre-heated hybridization solution (Na_2HPO_4 pH7 0.5 M and SDS 7%). Then, the solution was replaced by another 20 ml and the probe was heated at 100°C for 5 min prior to addition to the hybridization tube. The radioactive probe was incubated with the DNA overnight.

The hybridization solution was discarded safely as radioactive waste, and the membrane was washed with 40 ml of 65°C pre-heated washing solution (SSPE 0.1%, SDSD 0.5% and EDTA 5 mM) for 5 min to eliminate non-bound probe. Another washing step was repeated for 1 h at 65°C. The solution was discarded and the radioactive membrane was covered with transparent film, placed between two acetate sheets and stored in a exposing cassette.

9.4. DNA detection

Bound probe was detected by using a photographic Kodak Biomax MS film, (Scientific Imaging Film, Kodak). The film was placed over the membrane and kept at -80°C for 30 min. Afterwards, the film was developed, fixed and checked for radioactive signals. If exposure time was not enough for reliable signals, new films were placed in the cassette until suitable band visualization.

10. Analysis of secondary metabolites

10.1. Total carotenoids extraction and estimation

50 mg of freeze-dried mycelial samples were grinded in hermetic 2 ml tubes with sea sand and 1 ml of acetone in a FAST-PREP®-24 device (Biomedicals, Irvine, CA). Two disruption pulses of 30 s at 6.5 m s^{-1} were performed in every extraction step. Samples were centrifuged 1 min at 13,200 rpm and the carotenoid-containing supernatant was transferred to a new 2 ml tube. The extraction step were repeated up to total bleaching of the sample and collected into the same tube. For dark samples, 3 extractions were enough for total bleaching of the mycelia, but for illuminated samples 4-6 extractions were required. Then, the samples were centrifuged to eliminate cellular and sand debris, and supernantants were dried in a concentrator device

(Concentrator plus, Eppendorf) at 45°C. Carotenoids were analyzed spectrophotometrically in a Shimadzu UV spectrophotometer 1800. Samples were resuspended in n-hexane and the spectra were measured in the range of 350 and 650 nm. Concentrations of total carotenoids were estimated from the maximal absorbance of the peak (usually ca. 479-482 nm), considering an average molar extinction coefficient of 200 mg L^{-1} cm after correction with the dry weight of the samples and dilution factor of the dissolved carotenoids.

10.1.1. Neutral and polar carotenoids separation

Separations were achieved in 1 ml blue tips internally plugged with a piece of cellulose paper to allow Al_2O_3 addition. In each tip, the paper was soaked with petroleum ether and a layer 0.5 cm of Al_2O_3 was added in petroleum ether. Then, the carotenoid samples formerly used for total carotenoid analysis were vacuum dried, resuspended in *ca.* 200 µl of n-hexane. Each sample was applied to a column and the flow-through was collected in a 2 ml tube. Neutral carotenoids were eluted from the column by adding 0.5 ml of diethyl ether, collected in the same tube, vacuum-dried and finally resuspended in the same volume in which the total carotenoids were estimated. The polar carotenoids remain absorbed to the Al_2O_3 top layer. Spectra measurements of neutral carotenoids were performed as above except that their concentrations were estimated assuming an average molar extinction coefficient of 250 mg L^{-1} cm.

Polar carotenoids spectra were obtained by subtracting the neutral spectra from the their corresponding total spectra, and concentrations were estimated according to an average molar extinction coefficient of 171 mg L^{-1} cm.

10.2. Bikaverin extraction

Bikaverins are accumulated in the mycelia and excreted to the media. Two different protocols were used depending on the type of sample.

To estimate the amount of bikaverins in the mycelia, extractions were performed as described for carotenoids but using chloroform as solvent instead of acetone. After total color extraction, the samples were vacuum-dried, resuspended in an appropriate volume of chloroform and measured in the spectrophotometer.

For secreted bikaverins, samples of 1 ml of filtered cultures were acidified to pH 2.5 with HCl 10 M. Equal volumes of chloroform were added and mixed in a vortex. Samples were centrifuged and the chloroform fraction was collected in a new tube. The step was repeated up to total color extraction and the collected chloroform sample was vacuum dried and measured in the spectrophotometer.

Bikaverins were estimated according to the maximal absorbance at 521 nm and a molar extinction coefficient of 8.400 M^{-1} cm^{-1}.

10.2.1. Bikaverin separation from carotenoids

In samples with a significant bikaverin content, the spectrum of this pigment partially overlaps with that of carotenoids. In this case, a protocol was used to

separate bikaverins from carotenoids by precipitation. The extracted pigments were resuspended in 500 µl of acetone and 50 µl of NaOH 10 M were added to raise the pH and precipitate bikaverins. Samples were vortexed and centrifuged for 2 min at 13,000 rpm, supernatants were transferred to new 2 ml tube and dried in the concentrator device for further measurements as already described. When required, precipitated bikaverins were resuspended again in 500 µl of chloroform and 200 µl of HCl to lower the pH. The samples were vortexed, centrifuged for 2 min at 13,000 rpm and the chloroform fractions were transferred to a clean tube and measured as described for bikaverin quantification.

10.3. Gibberellin extraction and determination

Gibberellins were extracted from the filtered culture media. The filtrates were acidified to pH 2.5 with HCl 10 M and 500 µl were used for gibberellins extraction. 2 volumes of ethyl-acetate were added, mixed and centrifuged for 1 min at 13,000 rpm. The ethyl-acetate fractions were transferred to a clean 2 ml tube and the procedure was repeated 2-3 times with 1 volume (500 µl) of ethyl-acetate. Anhydrous sodium sulphate was added to the eppendorf up to the 0.25 ml mark to remove water. Samples were centrifuged for 1 min, passed through a Millipore 0.22-µm pore filter and dried in the concentrator device.

Gibberellin determinations were done by thin layer chromatography (TLC). Dried samples were resuspended in 6 µl of acetonitrile and loaded on a Silica gel 60 TLC plastic sheet (Merck, Darmstadt, Germany) in parallel to a GA3 (Sigma) standard (1.25 µg, 2.5 µg, 5 µg, 10 µg). Benzene:n-butyl alcohol:acetic acid (60:30:10) was used as the mobil phase. After five minutes run, the TLC sheet was air-dried, sprayed with a mixture of ethanol and concentrated sulfuric acid (95:5) and incubated 5 minutes at 80°C. Developed spots of gibberellic acid were photographed under 302 nm UV. Relative GA3 production was estimated by densitometry analysis of the spots with the ImageJ 1.42q program (Wayne Rasband, NIH, Bethesda, MD; http://rsb.info.nih.gov/ij).

11. Conidiation

11.1. Conidia collection

Conidia were collected from 7-day old plates incubated under indirect illumination in a 22°C chamber. Plates were scrapped with 5-10 ml of sterile distilled H_2O and filtered through a borosilicate filter crucible of size pore 1 (30 ml vol. and 30 mm Ø, Robu, Hatter, Germany) attached to a 100 ml flask. The scrapping was repeated, filtered and collected in the same flask. The content of each flask was poured into a 50 ml Falcon tube, centrifuged for 10 min at 2,000 rpm and the supernatant was discarded. Two washing steps with 5 ml of sterile H_2O were done and the conidia pellets were resuspended in 1 ml of sterile H_2O and transferred to a sterile 1.5 ml eppendorf tube. Conidia concentrations were calculated in a hemocytometer using a LEICA DM1000 microscope (400x). Depending on conidia concentrations, dilutions were required before counting.

11.2. Conidiation assays

For quantitative conidia determinations, the colonies of the Petri dish surfaces were scrapped with 12 ml of glycerol 15% and collected in a 50 ml Falcon tube. Afterwards mycelia were washed twice with 8 ml of distilled water and collected to the same tube. Aliquots were taken to calculate conidia concentration in a hemocytometer as described in 12.1. Total amount of conidia was calculated from the total volume of the collected sample.

When indicated, microconidia and macroconidia were counted in the same sample and annotated separately for independent calculations.

12. Miscellaneous phenotypic assays

12.1 Cellulose degrading assays

Two approaches were used to check the cellulose degrading ability.

- A round piece of sterile cellulose filter paper (73 g m^{-2}, RM13054252, Filtros Anoia, Barcelona, Spain) was placed on DG medium devoid of glucose.
- A sterile cellophane discs (Scotch, Cergy Pontoise, France) was laid on DG agar surface. To prevent cellophane for drying, the sheets were moistened before covering the plates.

In both cases, the plates were inoculated with a 5 mm Ø mycelial plug on the middle of the cellulose or cellophane material, and theu were incubated either in the dark or under white light illumination (7 W m^{-2}) at 30°C for 7 days.

12.2. UV sensitivity assays

Fresh collected microconidia of the wild type and Δ*cryD* strains SF236 and SF237 were inoculated on DGasn agar and irradiated with a prewarmed UV lamp Philips TUV 15W/G15T8 (Holland) at a distance of *ca.* 60 cm. Plates were exposed for 30, 60, 90, 120 and 150 seconds and immediately preserved from light. Then, they were incubated for 3 days at 30°C under darkness or 5 W m^{-2} white light to test photorepair activity *in vivo*. Controls with non-irradiated conidia were done in parallel. Survival rates were expressed as the percentage of the number of colonies grown at different irradiation times and the total colonies grown in the non-irradiated control.

13. Biochemical analyses of CryD

13.1. Recombinant protein expression

13.1.1. CryD cloning and expression in *E. coli*

The whole *cryD* coding region was amplified by PCR from cDNA, obtained from a wild type FKMC1995 culture grown for three days in the dark and illuminated for 1 h, using primer set B1 (containing *Kpn*I and *Not*I restriction sites), and cloned in pGEM-T. The correctness of the PCR product was verified by sequencing. The insert was cut out using the above mentioned enzymes and cloned into the corresponding sites in

pET51b(+) in-frame with both the N-terminal Strep-tag and the C-terminal His_{10}-tag encoded by the vector. The plasmid was then introduced in *E. coli* BL21(DE3) by transformation to express CryD.

13.1.2. Small-scale production

E. coli BL21 (DE3) transformed with pET51b+cryD was incubated in LB medium supplemented with ampicillin (final concentration 100 µg ml^{-1}) at 37°C for 16h at 200 rpm (New Brunswick Scientific G25 Shaker Incubator). 50 ml of LB were inoculated with 1 ml of the preculture and incubated in the same conditions up to 0.6 optical density. Then, two 1 ml-samples were collected, centrifuged 10 min at 5,000 rpm at 4°C and the cells pellet was frozen. Induction of expression was achieved by addition of 50 µl of IPTG 1 M (final concentration 1 mM). Every two hours (at 2h, 4 h, 6h, 8h, 16h and 24h), two 1 ml samples were collected and stored as described.

13.1.3. Large-scale production

10 ml tubes containing 3 ml of LB were inoculated with an *E. coli* colony for 3 h in the aforementioned conditions. 50 ml of LB were inoculated with 1 ml of the preculture and incubated overnight (12h). The 50 ml culture was then transferred to 1.5 L of LB and the optical density was monitored in a UV-1202 UV-VIS spectrophotometer (Shimadzu). When the optical density reached 0.6, IPTG was added at a final concentration of 1 mM and incubated for 6h at 30°C.

The culture was then vacuum-centrifuged in 500 ml tubes at 5,000 rpm for 30 min at 4°C. The centrifugation step was repeated three times in the same 500 ml tube to pellet the whole volume. The pellet was resuspended in PBS 1X (NaCl 137 mM, KCl 2.7 mM, Na_2HPO_4 8 mM, and KH_2PO_4 2 mM), transferred to a 50 ml Falcon tube and centrifuged again 30 min at 4,500 rpm at 4 °C. Pellet was weighted and frozen in liquid nitrogen.

13.2. Protein extraction and quantification

13.2.1. Total protein extraction

100 µl of SDS 1X buffer (Tris-HCl 45 mM pH 6.8, dithiothreitiol 50 mM, SDS 1%, glycerol 10% and bromophenol blue 0.01%) were added to the *E. coli* pellet. Samples were boiled at 95°C at 800 rpm for 10 min in an Eppendorf Thermomixer comfort. Samples were cooled down and centrifuged to eliminate cellular debris.

13.2.2. Soluble protein extraction

A cold mixture of *E. coli* lysis buffer 2X and proteases inhibitors was prepared. Per ml of lysis buffer 100 µl of Benzamidine 200 mM, 33 µl of E-64 0.8 mM, 12 µl of Pepstatine A 1.5 M, 90 µl of PMSF 100 mM, 1 µl of β-mercaptoethanol 14.5 M and 200 µl of lysozyme 1% w/v were added and filled up to 2 ml with milliQ water. Final concentrations were: lysis buffer 1X, benzamidine 10 mM, E-64 14 µM, pepstatine A 8.8 µM, PMSF 4.5 mM, β-mercaptoethanol 10 mM and lysozyme 0.1% w/v. 80 µl of the

mixture were added to each sample and incubated on ice at 100 rpm for 1h in a GFL 3005 shaker. Then the samples were sonicated five times for 5 min in an ultrasonic bath (Bandelin sonorex TK 52) and centrifuged 10 min at 14,000 rpm at 4°C. The supernatant was transferred to a new tube and 20 µl of SDS 5X buffer (Tris-HCl 225 mM pH 6.8, dithiothreitiol 250 mM, SDS 5%, glycerol 50% and bromophenol blue 0.05%) were added per 80 µl of sample.

When protein was expressed for further purification, the lysis procotol was slightly modified and manipulations were done under red light and cold conditions to avoid changes in the oxidative state of the protein. The pellets were resuspended in ice in the mixture of *E. coli* lysis buffer and protease inhibitors without lysozyme. When the sample was homogeneous, 3 ml of lysozyme were added under red light and the sample was protected from white light. Under safe red light, cells were disrupted by using a French Press (3 x 1000 psig) and the processed samples were transferred to 50 ml Falcon tubes, centrifuged at 18,000 rpm for 30 min (4°C) and filtered through a 0.45 µm pore size filter.

13.2.3. Protein quantification

Protein estimation was done with the Amido black method. First a calibration curve was prepared from a stock solution of bovine serum albumin (BSA) 0.1% w/v with the following quantities: 1, 5, 10, 15, 20, 25, and 50 µm of BSA in a final volume of 200 µl of water. Another 10 µl of the sample of interest were prepared in the same volume. Then, 800 µl of amido black solution (amido black in acetic acid 10% and methanol 90%) were added to the samples and mixed in a vortex. After centrifugation at maximum speed for 12 min at room temperature, the supernatant was discarded and the pellet was washed with 1 ml of washing solution (acetic acid 10% and methanol 90%). Samples were vortexed, centrifuged as above and dried for 15 min in a fume hood. Finally, the pellets were dissolved in 1 ml of dissolving solution (NaOH 0.2 M). Absorbance of the samples was measured at 615 nm in a UV-2410 PC UV-VIS recording spectrophotometer (Shimadzu). The calibration curve was plotted and a linear fit was added to estimate the protein amount in the rest of the samples.

13.3. Protein purification

An ÄKTA purifier device (Amersham Biosciences, Buckinghamshire, UK) was used for CryD purification in two steps. Purifications were performed under red light in a 4°C chamber.

13.3.1. Nickel affinity chromatography

In the first step the lysate sample was injected into a HisTrap FF crude column of 1 ml (GE Healthcare) consisting of tetradentate nitrilotriacetic acid charged with nickel, which mediates the interaction with the imidazole ring of histidines. Buffers were filtered through a 0.2 µm membrane, stirred in vacuum to avoid air in the paths system and stored at 4°C. The system was washed with ethanol FPLC-grade H_2O (NaN_3 0.02% w/v) at a flow rate of 5 ml min^{-1}, and then it was washed with high-imidazole buffer 2% at a flow rate of 5 ml min^{-1}. The sample path and pumps were washed with

equilibration buffer (high-imidazole buffer 2%, imidazole 10 mM) at the same rate flow. Flow restrictor between the sample pump and the injection valve was removed during sample loading and replaced once finished.

Different wavelengths were chosen to monitor the absorbance during the purification step: absorbance at 280 nm was used as an indicator of protein presence, absorbance at 384 nm served for methenyl-tetrahydrofolate (MTHF) detection, and absorbance at 450 nm was used for oxidized flavin forms.

Program details:

- Equilibration step: high-imidazole buffer 2% (10 mM), 5 column volumes (CV).

- Washing step: high-imidazole buffer 8% (40 mM), 3 CV.

- Elution: linear gradient from 0% to 100% high imidazole buffer, 20 CV.

- Gradient delay: 100% high imidazole buffer (500 mM), 10 CV.

- Re-equilibration: high-imidazole buffer 2% (10 mM), 3CV.

The system was programmed to collect 0.5 ml fractions but the flow-through fraction with non-bound proteins was also collected before washing the system.

Once the program was finished, the whole system, column, pumps and paths were washed with FPLC-grade H_2O. The column was stored in FPLC-grade 20% ethanol (NaN_3 20% w/v).

The fraction(s) with high absorbance at 280, 384 and 450 nm were pooled for heparin purification. 100 µl of the flow-through and the different collected peaks were saved for protein determination before the second step purification. Peaks were diluted 1:1 to decrease the imidazole concentration in the sample prior to heparin purification.

13.3.2. Heparin chromatography

The CryD containing fractions of the HisTrap purification were then subjected to heparin affinity purification. The column (heparin HP 1 ml, Ge Healthcare) consisted of heparine molecules bound to a sepharose matrix. The biochemical properties of the heparin, a highly sulfated (negatively charged) glucosaminoglycan which mimics DNA structure, confer the suitable characteristics for DNA-binding proteins purification. As in nickel affinity chromatography, prior to the operation the system paths and column were washed with FPLC-grade H_2O (5 ml min^{-1}) and equilibrated with high-NaCl buffer 10% (equilibration buffer) (5 ml min^{-1}). In this case the sample was injected manually through a superloop™. A different run was done for each peak and followed by absorbance at 280 nm, 384 nm and 450 nm.

Program details:

- Equilibration step: high-NaCl buffer 10% (200 mM), 3 column volumes (CV).

- Washing step: high-NaCl buffer 15% (200 mM), 5 CV.

- Elution: linear gradient 15% to 100% high imidazole buffer, 10 CV.

- Gradient delay: 100% high imidazole buffer (500 mM), 10 CV.

- Re-equilibration: high-imidazole buffer 10% (200 mM), 5CV.

The system was programmed to collect 1 ml fractions but the flow-through fraction with non-bound proteins was also collected before washing system.

Once the purification program ended, it was proceeded in the same way that for HisTrap purification. The paths, pumps and columns were washed with FPLC-H_2O and the column was stored in FPLC-ethanol. Fractions enriched in protein and cofactors were pooled and saved together with 100 µl of the flow-through.

13.3.3 Protein concentration

For further analyses the samples were concentrated and the salt content was diluted. For this purpose a protocol based on membrane concentrators (Amicon Ultra-15 Centrifugal Filter Device 30K NMWL, Millipore) was used. Concentrators were equilibrated with 5 ml of equilibration buffer, centrifuged 10 min at 4,500 g (4°C) and the flow-through discarded. The eluted peaks from the purification were applied to individual concentrators (under red light) and centrifuged for 1 h at 4,500 g (4°C). Concentrators were checked to have an approximated volume of 1-2 ml and the samples were diluted 1:5 with no-NaCl buffer to obtain a NaCl concentration of 0.2 M (corresponding to the equilibration buffer concentration). A similar centrifugation step was performed and a final volume of 500 µl was collected from the concentrators, frozen in liquid nitrogen and stored preserved from light.

13.4. Protein electrophoresis

For proteins visualization and identification, a SDS-PAGE separation method based on the charge/mass ratio was used. To dissociate any interaction between proteins, we made the electrophoresis in denaturing conditions, and for greater resolution we chose a discontinuous system (a gel with two components).

13.4.1. Gel preparation

Polyacrylamide gels were prepared from a mixture of acrylamide:bisacrylamide (Rotipherose Gel 40, Carl-Roth, Karlsruhe) with the following components:

- Resolving gel 10%: 5 ml Rotipherose Gel 40 (1:1 diluted stock in H_2Odd), 2.5 ml of resolving gel buffer (Tris-HCl 1.5 M pH 8.8), 100 µl of SDS 10%, 40 µl of APS (10% w/v), 6 µl of TEMED and 2.5 ml of H_2Odd.

- Stacking gel 5%: 1.25 ml of Rotipherose Gel 40 (1:1 diluted), 1.25 ml of stacking gel buffer (Tris-HCl 0.5 pH 6.8), 100 µl of SDS 10%, 37.5 µl of APS (10% w/v), 2.5 µl of TEMED and 2.45 ml of H_2Odd.

The glass plates were placed at a distance of 1 mm and 1 ml of quick polymerization resolving gel (sealing mixture: 1 ml resolving gel + 16 µl of APS + 2.4 µl of TEMED) was added to the bottom. Once polymerized, 8 ml of resolving gel were added and overlaid

with 1 ml of isopropanol. Once polymerized (about 1h), isopropanol was removed and 1 ml of the stacking gel was poured and a 10 well-comb was inserted.

13.4.2. Sample preparation

For protein loading, 10 µg of protein sample from the induction kinetic experiments and 5 µg of the purified peaks and flow-through were used. 5 µl of "5X reducing sample buffer" (Tris-HCl 45 mM pH 6.8, dithiothreitiol 50 mM, SDS 1%, glycerol 10% and bromophenol blue 0.01%) were added to the samples for a 1X final concentration. Prior to loading, the samples were heated at 95°C for 5 min. 3 µl of a protein marker (PageRuler Pre-stained Molecular Weights Standards, Fermentas) were treated and loaded in parallel as a reference of protein molecular mass.

13.5. Electrophoresis and proteins staining

Electrophoresis was run in Laemmli buffer 1X (Tris-HCl 25 mM, glycine 192 mM and SDS 0.1%) in an Integra Biosciences equipment at a constant current of 30 mA per gel (voltage limit 300 V).

Once the electrophoresis finished, the gel was disassembled from the gel holder and placed in a plastic container. The gel was overlaid with Coomassie staining solution (Coomassie Brilliant Blue CBB R-250 0.05%, isopropanol 25% and acetic acid 10%) and heated in a microwave for 30 s. After 30-60 min of shaking, the Coomassie solution was replaced by destaining solution (acetic acid 10%), heated again and destained for 30-60 min. After this period, new destaining solution was added and shaked until the gel background became transparent.

13.6. Protein immunodetection (Western Blot)

13.6.1. Protein transfer

The proteins separated in the electrophoresis were transferred (blotted) to a membrane. Two different blotting systems were used depending on the amount of buffer required for transfer. The wet blotting system requires higher volumes of transfer buffer than the semi-dry blotting system. Irrespective of the system used, gel and membrane preparation were carried out in the same way.

Two pieces of blot paper (Biorad) and a piece of NCP (nitrocellulose Porablot) of the same size of the gel were cut and equilibrated in transfer buffer (Tris-Hcl 48 mM, glycine 39 mM, SDS 0.0375% w/v and methanol 20%), as well as the gel. Once equilibrated, a transfer sandwich (blot paper/membrane/gel/blot paper) was assembled avoiding bubbles between the layers. For the wet blotting the power supply (Integra Biosciences) was set during 60-90 min to 100 V (constant voltage) and the current was limited to 350 mA. In the case of the semi-dry system (Trans-Blot SD semidry transfer cell, Biorad) the transfer was done at a constant voltage of 21V.

After transfer, the membrane was soaked in transfer buffer to remove possible rests of the gel.

13.6.2. Immunodetection

Mouse monoclonal antibody against the 6×His-tag (Clontech-Takara Bio Europe) was used as primary antibody, and the IRDye 800CW donkey-anti-mouse IgG (Li-Cor Biosciences, Lincoln, NE, USA) was used as secondary antibody.

All inmunodetection steps were incubated by gently shaking. To prevent unspecific interactions, the membrane was first blocked with 20 ml of blocking solution (BSA 3% and NaN_3 0.02%) prepared in TS buffer (Tris-HCl 20 mM, NaCl 150 mM) for 1 h at room temperature or overnight at 4°C. Afterwards, the membrane was washed with 20 ml of TST (Tris-HCl 20 mM, NaCl 150 mM, Tween 20 0.1%) for 5 min, and a primary antibody incubation (dilution 1:5000) was performed for 1 h. This was followed by 3 washing steps of 10 min with TST buffer. The secondary antibody was then applied at 1:10000 dilution, prepared in TST buffer containing milk powder 5 % (1g milk powder/20 ml TST), and incubated for 45 min. Finally, the membrane was again washed three times with TST and visualized in the Odysey® Infrared Imaging System scanner (Li-Cor Biosciences, Lincoln, NE, USA) by using the 800 channel.

13.7. Cofactors characterization

13.7.1. Cofactor release

For fluorescence measurements and HPLC analyses, the protein was precipitated in 7.2% of TCA (tricholoacetic acid) in ice for 1 h at 100 rpm. The sample was centrifuged at 4°C for 10 min and the supernatant contained the cofactors. During all the steps, the sample was preserved from light. Finally TCA in the sample was neutralized with the same amount of NaOH 5 M.

13.7.2. Spectophotometric determinations

- UV-visible absorption spectra of purified CryD were recorded in a 2-channel UV-2401 PC spectrophotometer (Shimadzu, Kyoto). No-NaCl buffer was used to make the baseline spectra in three-window quartz cuvettes (Quartz Suprasil fluorescence cuvette, Hellma GmbH & Co. KG). The volume of the cuvette was 125 µl. Spectra were measured in the range of 220-700 nm, and for a detailed analysis in the UV-region the range was 200-340 nm.

- Excitation and emission spectra of the released cofactors were recorded in a RF-5301 PC spectrofluorophotometer (Shimadzu) in the aforementioned cuvettes by using an excitation wavelength of 450 nm. Fluorescence emission was recorded in the range of 470-700 nm. Spectra were measured at acidic and neutral pH to characterize the flavin cofactor. For this purpose, an acidic and a neutral buffer were prepared. The acidic

buffer consisted on 112.5 µl of phosphate citrate buffer (PCB) pH 2.5 and 12.5 µl of NaOH 1.2 M (final concentration 0.4 M), while the neutral buffer composition was 112.5 µl of Tris-HCl buffer pH 7.5 and 12.5 µl of NaOH 1.35 M (final concentration 0.45 M). These buffers were used as a baseline for measurements. Standards of flavin-adenine-dinuceotide (FAD) and flavin-mononucleotide (FMN) were measured at a final concentration of 1 µM in PCB and Tris-HCl buffers. 100 µl of the released cofactors were mixed with 50 µl of NaOH 1.2 M or NaOH 1.35 M to obtain acidic and neutral samples and measured as above in PCB and Tris-HCl respectively (112.5 µl of PCB + 12.5 µl of acidic sample and 112.5 µl of Tris + 12.5 µl of neutral sample).

13.7.3. HPLC analysis

Released cofactors were separated by reverse phase chromatography on a Nucleosil 100-10 C18 column connected to the ÄKTA purifier and pre-equilibrated with a 9:1 mixture of phosphate citrate buffer pH 2.5 (Na_2HPO_4 10 mM and citric acid 45 mM) and methanol. 1 ml of the sample was filtered through a 0.2 µm pore and injected into the column. The sample contained 100 µl of released cofactors, 10 µl of TCA 72%, 10 µl of NaOH 5 M (to neutralize TCA), 800 µl of PCB and 100 µl of methanol. In parallel a mixture containing 20 µM of each standard was also analyzed: MTHF-Cl (Schircks Laboratories), FAD (Sigma), FMN (Sigma) and riboflavin (Duchefa Biochemie). Separation and elution was performed with a linear gradient of methanol (60-80%) and absorbance was monitored at 360 nm (MTHF and oxidized flavins) and 450 nm (oxidized flavins)

13.7.4. *In silico* modeling and determinations

Absorption cross-section spectra (Song et al., 2006) were used in plots. Multi-component simulations of the spectra were done by PhotochemCAD 2.1 software (Dixon et al., 2005) using the reference spectra of all relevant species (CryD apoprotein, methenyl-THF, methylene-THF, FAD_{ox} and $FADH^-$) in their protein-bound states. The reference spectrum of CryD apoprotein was constructed based on the primary sequence of the expressed protein with 33 Phe, 31 Tyr and 19 Trp residues (no cysteine was considered). Reference spectra for Phe, Tyr and Trp were taken from the master database provided by the PhotochemCAD software (Dixon et al., 2005). Methenyl-THF (MTHF) and methylene-THF reference spectra were described (Tyagi et al., 2009) and the former one was upshifted 20 nm as typical for its protein-bound state. The reference spectra for FAD_{ox} and $FADH^-$ were also described (Song et al., 2006). Again, for the FAD_{ox} spectrum, a slight downshift of 4 nm was applied and the typical protein-bound feature, *i.e.* the "head and shoulders" resonance structure of the 450 and 375 nm peaks, was imprinted on both peaks using the spectrum of the MTHF-free E149A *cry3* mutant of *A. thaliana* (Klar et al., 2007) as a template.

13.8. Photoreduction assays

Reduction of the oxidized forms of FAD was done by blue light illumination with an intensity of 100 µ mol m^{-2} s^{-1} of 450 nm photons obtained with a slide projector and a

xenon burner. Interference filters (Schott, Mainz, Germany) were used for monochromatic blue radiation. All the steps were done in a cold atmosphere (10°C), controlling sample and light temperature. The sample was placed in a black box to avoid other undesirable light sources and illuminated through one of the cuvette windows. Spectra were recorded from 200 to 700 nm at different illumination times: 0, 1, 2, 5, 10, and 20 min. Finally the kinetics of the absorbance peak at 450 nm was plotted and fitted by mono-exponential decay curves.

Purified CryD sample (peak 3 of the HiHep purification) was diluted to 1:1 with equilibration buffer (NaCl 10%). DTT (dithiothreitol) was used at a final concentration of 10 mM as an external reductant agent. Baseline was made with 123.75 µl of equilibration buffer and 1.25 µl of DTT, and 62.5 µl of sample was diluted 1:1 with 61.25 µl of equilibration buffer and 1.25 µl of DTT. The purified fraction peak 2 was also used to photoreduced the flavin cofactor. To make comparable the assay (same absorbance at 380 nm), this peak was diluted 1:0.25 using 95 µl of the sample, 28.75 µl of the equilibration buffer and 1.25 µl of DTT.

To test the stability of the fully reduced CryD, a dark recovery assay was performed by placing the sample in a black box without any external illumination source. Spectra were recorded at different times: 0, 10, 20, 30, 45, 60, 120, 180, 240 and 300 min. The absorbance at 450 nm was plotted against time.

13.9. Repair of UV-induced lesions in DNA

13.9.1. Probe preparation

A stock of 100 µM of oligo $(dT)^{18}$ in TE buffer (Tris-HCl 10 mM, EDTA 1 mM pH 7.5) was heated at 95°C and filtered to ensure no DNAse presence. Thymine dimers (T<>T) were induced by using a UV-transilluminator (6x15 W, TF-20M, Vilber Lourmat) in cold conditions. The sample was placed in the dark in a Quartz Suprasil cuvette and argon was bubbled inside for 30 min to obtain anaerobic conditions and avoid oxidative DNA cleavages. Then, 3 cycles of 3 minutes of UV-irradiation separated by 3 minutes of cooling on ice were carried out.

Spectra of 5 µM oligo$(dT)_{18}$ before and after UV-irradiation (undamaged *vs* damaged) were recorded from 200 to 340 nm. Estimation of T<>T levels was done according to the decrease in 265 nm absorbance and assuming a difference in the molar absorption coefficient of 19,000 M^{-1} cm^{-1} between normal T-T and T<>T. An average of one CPD-lesions per molecule of oligonucleotide were produced.

13.9.2. Photorepair assay

Repair of pyrimidine dimers was performed by incubation of the damaged probe with photoreduced CryD and illuminated with UV-A irradiation (73 µmol m^{-2} s^{-1} of 365 nm UV-A) in a Quartz Suprasil cuvette placed in a dark box. The assay was carried out in photorepair buffer (Tris-HCl 50 mM pH 7.5, NaCl 200 mM, glycerol 10%) with 10 mM of DTT, 100 nM of CryD and 5 µM of damaged oligo$(dt)_{18}$. The mixture was incubated

in ice for 10 min and latter irradiated with UV-A for 5, 10, 20, 30, 45, 60 and 120 minutes.

Spectra at these times were recorded from 200 to 340 nm and the absorbance at 265 nm was plotted against time. Increase in absorbance was indicative of damage repair. The amount of repaired T<>T was calculated from the difference at the given time and time zero considering the molar absorption coefficient and the volume of the reaction:

$$\mu mol\ T<>T = (A_{tx}-A_{t0})/19000 * V$$

The number of repaired T<>T plotted against time followed a linear tendency and the slope of the linear fit represented the mols of T<>T repair per minute. To calculate the repair rate of CryD, the T<>T repair per minute value was divided by the amount of CryD used in the assay (C * V):

$$mol\ T<>T * mol\ CryD^{-1} * min^{-1} = slope\ (mol\ min^{-1}) * mol\ cryD^{-1}$$

The assay was performed twice with 100 nM of CryD and a dark control was done in parallel. A ten-fold dilution of CryD (10 nM) was used to ensure no saturation of the repair.

13.10. Electrophoretic mobility shift assays (EMSA)

To check the ability of CryD to bind to DNA and its binding specificity to damaged or undamaged probes, different EMSA assays were performed. The probes used for this assays were labeled with IRDye700 in the 5' region and they consisted of 50 mer oligonucleotides named LAMRA (**L**eft**A**rm - **M**iddle - **R**ight**A**rm). The external arms were constituted by 15 mer and the middle one by 20 mer. Two LAMRA versions differing in the presence or not of a single T<>T in the central region were used. When indicated, double stranded probes of the LAMRA oligonucleotide were also used. The protocol for synthesis for these probes has been described (Pokorny et al., 2008), and the sequences in 5'-3' direction are detailed below:

LAMRA*: AAAATGCTGGATGTC - GAGGTGTAATTAATGTGGAG - CTGTAGGTCGTAAAA

LAMRA^*: AAAATGCTGGATGTC - GAGGTGTAAT<>TAATGTGGAG - CTGTAGGTCGTAAAA

The same separation method was used for the two binding assays described in the next section. 5% polyacrylamide non-denaturing gels were run in TBE in the dark at 4°C to separate the bound products. Gel composition was: 10 ml of rotipherose gel A (AA 30%), 4 ml of rotipherose gel B (bisAA 2%), 1.5 ml of TBE 10X (final concentration 0.25X: Tris-HCl 25 mM, borate 25 mM, EDTA 0.6 mM, pH 8.4), 0.66 ml of APS 10%, 60 µl of TEMED and up to 60 ml of milliQ H_2O. The gel was covered with TBE and kept at 4°C overnight. Then TBE buffer was replaced by new cold TBE and the gel was pre-run at 4°C for 1-2 h at 200 V (without samples). The wells were rinsed with TBE and sample loading was done under red light, as well as the running for 2h.

Once the run finished, the gel was scanned in the Odyssey infrared Imaging system with excitation in the 700 channel. Percentage of bound probe for each condition was

expressed as the ratio between the intensity of the shifted band and the sum of the intensities of shifted and free probe bands. The estimated percentages were plotted against CryD concentration and a Hill equation was fitted to calculate the K_D of the interaction.

$$y = Vmax * x^n / (k^n+x^n)$$

13.10.1 Competition assays

In this experiment the affinity of CryD for a damaged probe was tested in the presence of a competitor or inhibitor (non-labeled and non-damaged). The competitor was the LA region of the LAMRA oligonucleotide at different concentrations. The reactions were performed in a final volume of 10 µl. Each reaction contained:

- 1 µl of LAMRA*/ LAMRA*^ (stock 200 nM)
- 1 µl of CryD (stock 1 µM)/ 1 µl of Equilibration buffer in the control
- 1 µl of competitor (final concentrations 200, 100, 40, 20, 10, 4, or 2 nM)
- 2 µl of binding buffer 5X (Tris-HCl 50 mM pH 7.5, glycerol 45%)
- 0.05 µl of BSA (stock 10 mg ml^{-1})
- 0.05 µl of DTT (stock 1M)
- 4.9 µl of H_2O.

The LAMRA* oligonucleotides are sensitive to light and they must be handled under green light. On the other hand, CryD is sensitive to blue light and it required to work under red light. For this reason, competitor stocks were prepared separately (non-sensitive), and added to the premix without CryD. Finally, LAMRA were added under green light, CryD was added under red light and mixture was incubated for 30 min in the dark to favour CryD-DNA interactions.

13.10.2. Non-competition assays

In this case only LAMRA* oligonucleotides were used as probes, but with varying concentrations of CryD. The concentrations tested were 0, 2, 5, 10, 20, 50, 100, 200, 500 and 1000 nM. The reaction composition was:

- 0.1 µl of LAMRA*/ LAMRA*^ (stock 200 nM)
- 1 µl of CryD stock / 1 µl of Equilibration buffer in the control
- 2 µl of binding buffer 5X (Tris-HCl 50 mM pH 7.5, glycerol 45%)
- 0.05 µl of BSA (stock 10 mg ml^{-1})
- 0.05 µl of DTT (stock 1M)
- 6.8 µl of H_2O.

The same assays was carried out with double stranded DNA probes (LAMRA* and LAMRA*^). In this cases 2 µl of a 100 nM LAMRA stock were used instead of 1 µl of a 200 nM stock.

13.11. Identification of CryD-bound nucleic acid

The purified protein with a shift in the absorbance peak from 280 nm to 260 nm was used to characterize the bound nucleic acids. For that purpose the protein was precipitated by heating (95°C 10 min), the sample was centrifuged at 4° C for 10 min at 14,000 rpm and the supernatant containing the nucleic acids was incubated with 1 U μl^{-1} DNAse I (Fermentas) or 10 mg ml^{-1} Ribonuclease A (Roth). The reactions were performed in DNAse buffer 1X (Tris-HCl 10 mM pH 7.5, $MgCl_2$ 2.5 mM, $CaCl_2$ 0.1 mM). 1U of Ribolock RNase inhibitor (Thermo Scientific) was added to control and DNase treatments. The reaction mixtures described below were incubated for 20 min at 37°C.

Control	DNAse treatment	RNAse treatment
5 µl nucleic acids	5 µl nucleic acids	5 µl nucleic acids
1 µl DNase buffer 10X	1 µl DNase buffer 10X	1 µl DNase buffer 10X
0.25 µl Ribolock	0.25 µl Ribolock	---
---	1 µl DNaseI	---
---	---	3.4 µl RNase
3.75 µl H_2O	2.75 µl H_2O	0.6 µl H_2O

The digested samples were run in a 6% polyacrylamide gel with urea to obtain a better resolution of small fragments, and the presence of nucleic acids was visualized by SYBR Green dye. Gel composition was 4.2 g of urea, 1 ml of TBE 10X, 1.6 ml of Rotipherose gel 40, 100 µl of APS, 10 µl of TEMED, and up to 10 ml of H_2O. Formamide loading buffer (formamide 95%, bromophenol blue 0.025%, xylene cianol 0.025%, and EDTA 5 mM pH 8), which helped to RNA separation and destabilization of secondary structures, was mixed 1:2 with the samples and heated for 5 min at 75°C. 5 µl of DNA marker (GeneRuler Ultra Low Range DNA ladder ready-to-use, Fermentas) were loaded in one of wells and the gel was run at a constant voltage of 70 V.

14. Molecular genetics of *F. fujikuroi cryD*

14.1. Cloning of *cryD* and generation of Δ*cryD* mutants

The cry-DASH protein sequence for *Fusarium fujikuroi* was submitted to EMBL under accession no. HE650104. To generate Δ*cryD* mutants, a plasmid was constructed with a hygromycin resistance (Hyg^R) cassette, containing the *Escherichia coli* hygromycin phosphotransferase gene *hph* under the control of *Aspergillus nidulans* regulatory sequences. For this purpose, a 4.2 kb region containing the whole *cryD* gene was obtained by PCR with primer set A1 (these and other primers described in Annex 2) and cloned in pGEM-T-easy. The resulting plasmid was used as the template for reverse PCR amplification with primer set A2. The resulting amplification product is the linearized vector lacking 1.3 kb in the 5' region of the *cryD* gene. The deleted region was replaced with the Hyg^R cassette, obtained from plasmid pAN7-1 (Punt et al., 1987), resulting in plasmid pDCry. Transformation of *F. fujikuroi* was done as described with a mixture of 30 µg of plasmid pDCryD previously linearized with *Not*I and 10 µg of

undigested plasmid. For Southern blot analysis, genomic DNA from the wild type and three transformants was extracted as described previously and digested with *Eco*RI, *Bam*HI, or *Dra*I. DNA was quantified and the same amount of digested DNA was loaded per lane on a 0.8% agarose gel. The probe used for hybridization consisted on a 1.3 kb *cryD* internal fragment. A 1.6 kb product was amplified by PCR with primer set A3 and digested with *Nco*I.

To check the replacement of an internal region of the *cryD* gene by the Hyg^R cassette, genomic DNA samples from the investigated strains were used as the substrate for PCR amplifications. Primer set A4 was used to detect the *hph* gene (expected 1.02 kb product), and primer set A5 (forward primer 1.25 kb upstream of the *cryD* coding sequence; reverse primer from the *cryD* coding sequence, positioned 787 bp upstream of the stop codon) was used to detect the *cryD* gene (2.7 kb product expected for the wild-type allele and 5.3 kb product for the mutant allele).

14.2. Complementation of *ΔcryD* mutants

The wild-type *cryD* gene, including 680 bp and 870 bp of upstream and downstream regulatory sequences, was amplified from FKMC1995 genomic DNA with primer set A6 and cloned in pGEM-T easy. The gene was removed from the resulting plasmid by *Eco*RI digestion and cloned into the *Eco*RI site of pNTP2, to yield plasmid pCcryD. For complementation, 40 µg of pCcryD were used to transform strain SF236 and selected in geneticin cointaining medium (final concentration 150 mg l^{-1}). Genomic DNA samples were obtained from the transformants and used to check by PCR the occurrence of the *hph* gene (primer set A1, former section), the *nptII* gene (primer set A9), and total or partial sequences of the *cryD* gene (primer sets A7 and A8, respectively). To confirm complementation of the *ΔcryD* mutants, occurrence of wild-type *cryD* transcript was assayed by PCR amplification with primer set A10 on cDNA samples from 3-day-old mycelia of the transformants incubated for 60 min under white light.

15. Molecular genetics of *F. fujikuroi vvdA*

15.1. *vvdA* identification

The *Fusarium* orthologs of *vvd* of *N. crassa* were identified by Blast analysis. The *F. fujikuroi* sequence was identified in its draft genome in two separate contigs (Ffuj 01148 and Ffuj 01338), each one containing a part of the *vvdA* sequence (271 and 123 nucleotides of the coding sequence, respectively). The intercontig region was sequenced with primer set C3 to obtain the complete coding sequence of 702 pb. The sequence was later confirmed from the complete genome sequence recently available (Wiemann et al., 2013).

15.2. Generation of Δ*vvdA* mutants

To obtain Δ*vvd* mutants, a disruption plasmid was constructed to replace the coding region of *vvdA* with the hygromycin resistance cassette (Hyg^R) by double homologous

recombination. For this purpose, the HygR cassette was flanked by upstream and downstream regions of the *vvdA* gene. To construct the plasmid, the whole *vvdA* gene including *ca.* 2.3 kb of the 5' region and *ca.* 2 kb of the 3' region was amplified from genomic DNA with primer set C1. This 5 Kb fragment was cloned in pGEMT-easy and the resulting plasmid was used as DNA template for reverse PCR amplification with primer set C2, which was modified to include *Hin*dIII restriction sites. The PCR product lacked the coding sequence of *vvdA* but contained 1.4 Kb of upstream and downstream *vvdA* regions. In parallel, a 4.1 kb Hyg^R cassette was obtained by PCR from plasmid pHJA2 (Fernández-Martín et al., 2000) with primer set C4, also modified to include *Hin*dIII restriction sites. The two PCR products were digested with this enzyme and ligated to yield plasmid pDvvd (9.9 Kb). 30 µg of *Spe*I-linearized pDvvd were used to transform 10^8 protoplasts of the wild type strain of *F. fujikuroi*, obtained as described.

To check the occurrence of the *vvdA* coding region, primer set C3 was used to amplify a 1.4 Kb fragment, expected only in the wild type or in ectopic transformants. The presence of the Hyg^R cassette was confirmed with primer set C5, which amplifies 1.02 Kb of the *hph* gene. Homologous recombination and correct replacement in the transformants was detected with primer set C6, which results in a of 2.2 Kb DNA product from a wild type *vvdA* allele and a 4.2 Kb from the disrupted *vvdA* allele.

15.3. Δ*vvdA* complementation

The complementation plasmid pCvvd, containing the *vvdA* coding sequence surrounded by 2.3 Kb upstream and 2.0 Kb downstream *vvdA* regulatory sequences, and a geneticin resistance cassette (neomycin phosphotransferase II gene, *nptII,* (Castrillo et al., 2013) as selective marker, was constructed to reintroduce *vvdA* in the SF258 strain. The *vvdA* 5 Kb fragment obtained with primer set C1 was cloned in pGEM®-T Easy (Promega, Mannheim, Germany) as described above and the resulting plasmid was digested with *Not*I (two restriction sites surrounding the cloning site of the commercial vector). The *Not*I fragment containing the *vvdA* gene was cloned in the unique *Not*I site of pNTP2 (Castrillo et al., 2013) to yield the 9.8 Kb plasmid pCvvd. 30 µg of undigested pCvvd were used to transform 3 x 10^8 protoplasts of the T6 mutant strain. To check the integration of the whole *vvdA* gene in the transformants, primer sets C3 and C7 were used to amplify by PCR 1.4 Kb of coding and flanking *vvdA* regions, and 0.8 Kb of the *nptII* coding region of the resistance cassette, respectively.

16. Search of Δ*wcoA* Δ*cryD* double mutants

16.1. *niaD* gene as a second selectable marker

A new plasmid derived from pALEX7 was constructed in which the hygR cassette was replaced by the *niaD* wild-type sequence. pALEX7 was used as a template for reverse-PCR amplification with primer set D1 (modified to include a *Hin*dIII restriction site). The 6 KbPCR product, which includes 1 Kb of the 5' and 3' coding region, was digested with *Hin*dIII and dephosphorylated (section 6.1.3). The *niaD* gene was amplified from FKMC1995 genomic DNA with primers D2 (containing a *Hin*dIII site), and the 4.8 Kb

PCR product was digested with *Hin*dIII and ligated to the pALEX7 fragment. The resulting vector was called pDMWC.

As recipient strains, *niaD*$^{-}$ mutants, unable to assimilate nitrate as nitrogen source, were generated by growing the *ΔcryD* strains SF237 in DG media supplemented with $KClO_3$ (section 3.2). After 7 days incubation at 30°C, small sectors started to emerge from the mycelial fragments. To further confirm the specific mutation of the *niaD* gene, the sectors were plated in different nitrogen sources: hypoxanthin, asparagine, $NaNO_2$ and $NaNO_3$. Mutant SF268unable to grow on $NaNO_3$ and with a similar aspect to SF236 and SF237, was chosen as recipient strain for transformation with plasmid pDMWC by a biolistic method (one attempt) and by the protoplast method (two attempts). Selection was made in DG nitrate medium.

16.2. Genetecin as second selectable marker

Plasmid pDwc2 was constructed by replacement of the central region of the *wcoA* ORF and hygR cassette by the neomycin resistance cassette. A 6.2 Kb of pALEX7 was reverse-amplified with primers D3 (containing *Hin*dIII) and the 1.6 Kb neomycin resistance cassette was amplified with primers D4, also containing *Hin*dIII restriction sites. Both PCR products were digested with *Hin*dIII and ligated to yield a 7.8 Kb plasmid named pDwc2. Five transformations were performed with either *Bam*HI or *Spe*I-linearized vector on *ΔcryD* protoplasts (1 attempt with strain SF237 and 4 attempts with strain SF236).

Plasmid pGcry7 was obtained by replacement of the HygR resistance cassette by the neomycin resistance cassette. For this purpose, pDcry was reverse-amplified by PCR with primers D5 (1R modified to include a *Hin*dIII restriction site) to obtain a 5.9 Kb product. As for pDwc2 construction, the PCR product was digested with *Hin*dIII and ligated to the 5.9 Kb vector to yield a plasmid of 7.5 Kb. This plasmid was linearized with *Sca*I and used to transform SF226 (Δ*wcoA*) protoplasts.

16.3. Mutagenesis

As an attempt to obtain *wcoA*/*cryD* double mutants, random mutagenesis experiments were performed.

16.3.1 UV-mutagenesis

Ultraviolet radiation was used to induce mutations in the SF237 strain. 1,000 spores were inoculated on 80 plates of DGasn medium and exposed to 45 seconds of UV-radiation. This exposure time reduced viability to a 50% upon darkness incubation (no photoreactivation). After three days of growth at 30°C, petri dishes were screened for colonies with Δ*wcoA* phenotype.

16.3.2. N-methyl-N'nitro-N-nitrosoguanidine mutagenesis

Two mutagenesis tubes were prepared together with two control tubes. 1 ml with 10^7 fresh conidia from SF236 were treated with 50 µl of a N-methyl-N'nitro-N-nitroso-guanidine stock of 2 mg ml^{-1} and incubated 30 min in the dark. Control tubes without the mutagen were incubated in parallel. The tubes were centrifuged and washed twice

with sterile H_2O and 50-100 dilutions were plated in DGasn and incubated for 3 days in the dark at 30°C and screened for colonies with Δ*wcoA* phenotype.

17. Bioinformatic analyses

17.1. Identification of DNA sequences

The genomes of three species of the genus *Fusarium*, *F. oxysporum*, *F. verticllioides* and *F. graminearum*, are available through the web server of the Broad Institute (www.broadinstitute.org, Cambridge, Massachusets, USA). The *Fusarium* Comparative Database includes the draft genomes of *F. verticllioides* 7600*, F. graminearum* PH-1, *F. oxysporum* 4287 and many other *F. oxysporym* strains. The high sequence conservation between *F. fujikuroi* and these species facilitated gene identifications by sequence comparisons. In some cases, *Neurospora crassa* sequences obtained from the same server were also used.

At a late stage of the Thesis, a draft genome of *F. fujikuroi* IMI58289 was obtained by shotgun with a Roche 454 Genome Sequencing System (454 Life Sciences Corporation, Branford, CT, USA) by the Genomic Unit (CCiT) of the University of Barcelona). Genome assembly was done by S. Beltrán (Bioinformatics Unit, Scientific-Technical Service of the University of Barcelona) based on 339 Mb of total reads, with an average read size of 287 bp. Later, a more complete draft of the genome from the same *F. fujikuroi* strain was developed and made publicly available (Wiemann et al., 2013).

17.2. Sequence analyses

Sequence comparisons (nucleic acid or protein) to determine conserved positions among genes from related species or strains were done with the program ClustalW2 (European Bioinformatics Institute of the European Molecular Biology Laboratory, EMBL-EBI, Cambridgeshire, UK). BLAST analyses were done through the servers of either the Broad Institute or the NCBI (National Center of Biotechnoloy and Informatics, Maryland, USA, www.ncbi.nlm.nih.gov/BLAST/). Phylogenetic trees were constructed with the Clustal 1.83 program and reliability of clusters was evaluated by bootstrapping with 1000 replicates.

Protein domains were determined with the SMART architecture research online tool (http://smart.embl.de/).

Restriction maps and *in silico* plasmid constructions were made with the programs Vector NTI® (Invitrogen) and GENtle (GENtle v1.9.4, Magnus Manske, University of Cologne, released under GPL 2003).

17.3. Primer design

To calculate physical properties of oligonucleotides, such as G+C content, melting temperature, self-complementarity or hairpin formation, the online tool OligoCalc (version 3.26, http://www.basic.northwestern.edu/biotools/oligocalc.html, North-

western University©) was used. In the case of RT-PCR primers, the oligonucleotides were designed with the PrimerExpress™ V2.0.0 (Applied Biosystems) program. Primers synthesis was ordered either to StabVida (Oeiras, Portugal) or to Integrated DNA Technologies (https://www.idtdna.com)

ANNEX 1. Primers used in RT-PCR expression analyses

Gene	Forward primer (5'->3')	Reverse primer (5'->3')
bik1	CTCGTCACCGACGCTCTAGTC	TGGGCATTGACCGGTATCA
bik2	CGAAGCTAGGCTCGGGAAGT	CAACAAGAACACCACCACATTGA
bik3	GGCCGAAGATATCCGAATTTT	CCTCCGATTTCTGCGTGTTT
gibB	TGTCAGCGAATCTGCTCCAA	GACGCATAACGGATGAAATGAG
gibD	GCCTTCCGTGCAGTAGAAGAA	GGCATGAACCACTGGACTACAG
gibG	GCTCGCCCCTCCTTATCC	TGGCTTCCCTTTCCTTGCT
carRA	CAGAAGCTGTTCCCGAAGACA	TGCGATGCCCATTTCTTGA
carB	TCGGTGTCGAGTACCGTCTCT	TGCCTTGCCGGTTGCTT
carT	CGGCACCAACACCAGACA	TGGACTAGGAATGGCAAGGACTT
carX	GCCGCCCATGAGGATACA	TCAGCTTCAACACCGTCGAA
carO	TGGGCAACGCAGTGACAT	TGCGCAGACAGCCCAGTA
phlA	TGGCAAGGCATTCGAAGTC	CGCCGGTGTGGAGTTCTC
wcoA	TGAGATTGTCGGCCAGAATTG	GAGCCCGCTTCGACTTTG
cryD	CGGGACTACATGCGATTGTG	CTTGAAAAGACGTGAGCCAAACT
vvdA	GCACCACCAGGGCATGA	GCGGTGTGAAGCGACCTT
β-tubulin	CCGGTGCTGGAAACAACTG	CGAGGACCTGGTCGACAAGT

ANNEX 2. Other primers used in the Thesis

Primer set (objective)	Primer names	Forward primer(5'→3')	Reverse primer (5'→3')
A1 (*cryD* cloning)	cry4F-2R	TAGACCTGGACAAATCGGAG	CTGCTGGAACGGGGCTACAG
A2 (*cryD* reverse PCR)	cry2F-3R	TAGACGAGGAGTTTATTCCCAGCC	CGGCTACACCTCGAACCGAG
A3 *(cryD* probe)	cry6F-4R	TCTGACAGCGTCTCCGCC	CATTCAGCTCCGTAGCGC
A4 (*hph* detection)	hph1F-1R	TGCCTGAACTCACCGCGACG	TATTCCTTTGCCCTCGGACG
A5 (*cryD* detection)	cry4F-4R	TAGACCTGGACAAATCGGAG	CATTCAGCTCCGTAGCGC
A6 (*cryD* complementation)	cry8F-6R	CACGGGATATCTGGCCAGGA	TTTCGAGATATCCGCAAAGGAG
A7 (*cryD* detection 2)	cry9F-7R	GCTTGTTCCCCATCCATCTA	GAAAGACAGGAGGAAGATGG
A8 (*cryD* detection 3)	cry9F-8R	GCTTGTTCCCCATCCATCTA	AGGGTTGAAGATGCGTGCGT
A9 (*nptII* detection)	neo3F-4R	GAACAAGATGGATTGCACGC	CGCTCAGAAGAACTCGTCAA
A10 (*cryD* cDNA detection)	RTcry1F-cry8R	CAGAAGCTGTTCCCGAAGACA	AGGGTTGAAGATGCGTGCGT
B1 (CryD recombinant expression)	cryrec1F-1R	GGTACCTGGGAATAAGCTCCTCGTCTATC	GCGGCCGCATGGGGTCCAAGGTGAGGAGG
C1 (*vvdA* cloning)	vvd1F-1R	CTACTCCATACCTACCTTAGG	CACATCAAGTGCTATTCCTACC
C2 (*vvdA* reverse PCR)	vvd2F-2R	CTGGAAATCAAGCTTGGGCT	TCTCGAGACACAAGCTTGGT
C3 *(vvdA* internal sequencing)	vvd3F-3R	CTCCTCGTTTACCTGCCAGT	CCTTGAAGTGCTTCTCCTGC
C4 (*hph* cassette cloning)	hph5F-5R	TTTCTCGCAAGCTTCGCCAA	CCGATTTTAAGCTTGACGGG

C5 (*hph* detection)	hph1F-1R	TGCCTGAACTCACCGCGACG	TATTCCTTTGCCCTCGGACG
C6 (*vvdA* replacement)	vvd5F-5R	CAATCTGACAGGTCGTTCCTT	GAAAAGGTCTTTTCCCAACCC
C7 (*nptII* detection)	neo3F-4R	GAACAAGATGGATTGCACGC	CGCTCAGAAGAACTCGTCAA
D1 (pLAEX reverse PCR)	pALEX1F-1R	CTACTCCATACCTACCTTAGG	CACATCAAGTGCTATTCCTACC
D2 (*niaD* cloning)	niaD1F-1R	CTGGAAATCAAGCTTGGGCT	TCTCGAGACACAAGCTTGGT
D3 (pLAEX reverse PCR2)	pALEX2F-1R	CTCCTCGTTTACCTGCCAGT	CCTTGAAGTGCTTCTCCTGC
D4 (*nptII* cassette cloning)	neo1F-1R	TTTCTCGCAAGCTTCGCCAA	CCGATTTTAAGCTTGACGGG
D5 (pDcry reverse PCR)	pDcry1F-R	CAATCTGACAGGTCGTTCCTT	GAAAAGGTCTTTTCCCAACCC

BIBLIOGRAFÍA

Adám, A.L., García-Martínez, J., Szucs, E.P., Avalos, J., and Hornok, L. (2011). The MAT1-2-1 mating-type gene upregulates photo-inducible carotenoid biosynthesis in *Fusarium verticillioides*. FEMS Microbiol Lett *318*, 76-83.

Ahmad, M., and Cashmore, A.R. (1993). HY4 gene of *A. thaliana* encodes a protein with characteristics of a blue-light photoreceptor. Nature *366*, 162-166.

Ahmad, M., Lin, C., and Cashmore, A.R. (1995). Mutations throughout an *Arabidopsis* blue-light photoreceptor impair blue-light-responsive anthocyanin accumulation and inhibition of hypocotyl elongation. Plant J *8*, 653-658.

Alejandre-Durán, E., Roldán-Arjona, T., Ariza, R.R., and Ruiz-Rubio, M. (2003). The photolyase gene from the plant pathogen *Fusarium oxysporum f. sp. lycopersici* is induced by visible light and alpha-tomatine from tomato plant. Fungal Genet Biol *40*, 159-165.

Álvarez, V., Rodríguez-Sáiz, M., de la Fuente, J.L., Gudiña, E.J., Godio, R.P., Martín, J.F., and Barredo, J.L. (2006). The *crtS* gene of *Xanthophyllomyces dendrorhous* encodes a novel cytochrome-P450 hydroxylase involved in the conversion of β-carotene into astaxanthin and other xanthophylls. Fungal Genet Biol *43*, 261-272.

Amoah, B.K., Rezanoor, H.N., Nicholson, P., and MacDonald, M.V. (1995). Variation in the *Fusarium* section *Liseola*:pathogenicity and genetic studies of *Fusarium moniliforme* Sheldon from different hosts in Ghana. . Plant Pathol *44*.

Armstrong, G.A. (1997). Genetics of eubacterial carotenoid biosynthesis: a colorful tale. Annu Rev Microbiol *51*, 629-659.

Arpaia, G., Cerri, F., Baima, S., and Macino, G. (1999). Involvement of protein kinase C in the response of *Neurospora crassa* to blue light. Mol Gen Genet *262*, 314-322.

Arrach, N., Fernández-Martín, R., Cerdá-Olmedo, E., and Avalos, J. (2001). A single gene for lycopene cyclase, phytoene synthase, and regulation of carotene biosynthesis in *Phycomyces*. Proceedings of the National Academy of Sciences *98*, 1687-1692.

Aubert, C., Vos, M.H., Mathis, P., Eker, A.P., and Brettel, K. (2000). Intraprotein radical transfer during photoactivation of DNA photolyase. Nature *405*, 586-590.

Austin, D.J., Bu'Lock, J.D., and Drake, D. (1970). The biosynthesis of trisporic acids from β-carotene via retinal and trisporol. Experientia *26*, 348-349.

Austwick, P.K.C. (1984). Fusarium infections in man and animals. In The applied Mycology of *Fusarium* Cambridge University Press (M O Moss and J E Smith) *London*, 129-140.

Avalos, A., Díaz-Sánchez, V., García-Martínez, J., Castrillo, M., Ruger-Herreros, M., and Limón, M.C. (2014). Biosynthesis and Molecular Genetics of Fungal Secondary Metabolites. In Carotenoids, e.a. J. F. Martín, Eds., ed. (Springer).

Avalos, J., Bejarano, E.R., and Cerdá-Olmedo, E. (1993). Photoinduction of carotenoid biosynthesis. In Methods in Enzymology, P. Lester, ed. (Academic Press), pp. 283-294.

Avalos, J., Casadesús, J., and Cerdá-Olmedo, E. (1985a). *Gibberella fujikuro*i mutants obtained with UV radiation and N-methyl-N'-nitro-N-nitrosoguanidine. Appl Environ Microbiol *49*, 187-191.

Avalos, J., Casadesús, J., and Cerdá-Olmedo, E. (1985b). *Gibberella fujikuroi* mutants obtained with UV radiation and N-methyl-N'-nitro-N-nitrosoguanidine. *Appl Environ Microbiol 49*, 187-191.

Avalos, J., and Cerdá-Olmedo, E. (1986). Chemical modification of carotenogenesis in *Gibberella fujikuroi*. Phytochemistry *25*, 1837-1841.

Avalos, J., and Cerdá-Olmedo, E. (1987). Carotenoid mutants of *Gibberella fujikuroi*. Curr Genet *11*, 505-511.

Avalos, J., and Cerdá-Olmedo, E. (2004). Fungal carotenoids production. In Handbook of fungal biotechnology Arora, DK (ed) New York, Marcel Dekker, Inc, 367-378.

Avalos, J., Cerdá-Olmedo, E., Reyes, F., and Barrero, A.F. (2007). Gibberellins and Other Metabolites of *Fusarium fujikuroi* and Related Fungi *Curr Org Chem 11*, 721-737.

Avalos, J., and Estrada, A.F. (2010). Regulation by light in *Fusarium*. Fungal Genet Biol *47*, 930-938.

Avalos, J., Prado-Cabrero, A., and Estrada, A.F. (2012). Neurosporaxanthin production by *Neurospora* and *Fusarium*. Methods Mol Biol *898*, 263-274.

Avalos, J., and Schrott, E.L. (1990). Photoinduction of carotenoid biosynthesis in *Gibberella fujikuroi*. FEMS Microbiol Lett *66*, 295-298.

Bacon, C.W., Porter, J.K., Norred, W.P., and Leslie, J.F. (1996). Production of fusaric acid by *Fusarium* species. Applied and Environmental Microbiology *62*, 4039-4043.

Baima, S., Macino, G., and Morelli, G. (1991). Photoregulation of the *albino-3* gene in *Neurospora crassa*. J Photochem Photobiol B *11*, 107-115.

Balan, J., Fuska, J., Kuhr, I., and Kuhrová, V. (1970). Bikaverin, an antibiotic from *Gibberella fujikuroi*, effective against *Leishmania brasiliensis*. Folia Microbiol *15*, 479-484.

Balland, V., Byrdin, M., Eker, A.P., Ahmad, M., and Brettel, K. (2009). What makes the difference between a cryptochrome and DNA photolyase? A spectroelectrochemical comparison of the flavin redox transitions. J Am Chem Soc *131*, 426-427.

Ballario, P., and Macino, G. (1997). White collar proteins: PASsing the light signal in *Neurospora crassa*. Trends Microbiol *5*, 458-462.

Ballario, P., Vittorioso, P., Magrelli, A., Talora, C., Cabibbo, A., and Macino, G. (1996). White collar-1, a central regulator of blue light responses in *Neurospora*, is a zinc finger protein. EMBO J *15*, 1650-1657.

Banerjee, R., Schleicher, E., Meier, S., Viana, R.M., Pokorny, R., Ahmad, M., Bittl, R., and Batschauer, A. (2007). The signaling state of *Arabidopsis* cryptochrome 2 contains flavin semiquinone. J Biol Chem *282*, 14916-14922.

Barnett, H.L., Lilly, V.G., and Krause, R.F. (1956). Increased production of carotene by mixed + and - cultures of *Choanephora cucurbitarum*. Science *123*, 141-142.

Barrero, A.F., Sánchez, J.F., Oltra, J.E., Tamayo, N., Cerdá-Olmedo, E., Candau, R., and Avalos, J. (1991). Fusarin C and 8Z-fusarin C from *Gibberella fujikuroi*. *Phytochemistry 30*, 2259-2263.

Bayram, O., Biesemann, C., Krappmann, S., Galland, P., and Braus, G.H. (2008a). More than a repair enzyme: *Aspergillus nidulans* photolyase-like CryA is a regulator of sexual development. Mol Biol Cell *19*, 3254-3262.

Bejarano, E.R., Avalos, J., Lipson, E.D., and Cerdá-Olmedo, E. (1991). Photoinduced accumulation of carotene in *Phycomyces*. Planta *183*, 1-9.

Bell, A.A., Wheeler, M.H., Liu, J., Stipanovic, R.D., Puckhaber, L.S., and Orta, H. (2003). United States Department of Agriculture-Agricultural Research Service studies on polyketide toxins of Fusarium oxysporum f sp vasinfectum: potential targets for disease control. Pest Manag Sci *59*, 736-747.

Berrocal-Tito, G., Sametz-Baron, L., Eichenberg, K., Horwitz, B.A., and Herrera-Estrella, A. (1999). Rapid blue light regulation of a *Trichoderma harzianum* photolyase gene. J Biol Chem *274*, 14288-14294.

Berrocal-Tito, G.M., Esquivel-Naranjo, E.U., Horwitz, B.A., and Herrera-Estrella, A. (2007). *Trichoderma atroviride* PHR1, a fungal photolyase responsible for DNA repair, autoregulates its own photoinduction. Eukaryot Cell *6*, 1682-1692.

Bieszke, J.A., Braun, E.L., Bean, L.E., Kang, S., Natvig, D.O., and Borkovich, K.A. (1999). The *nop-1* gene of *Neurospora crassa* encodes a seven transmembrane helix retinal-binding protein homologous to archaeal rhodopsins. Proc Natl Acad Sci U S A *96*, 8034-8039.

Bieszke, J.A., Li, L., and Borkovich, K.A. (2007). The fungal opsin gene *nop-1* is negatively-regulated by a component of the blue light sensing pathway and influences conidiation-specific gene expression in *Neurospora crassa*. Curr Genet *52*, 149-157.

Bindl, E., Lang, W., and Rau, W. (1970). Untersuchungen über die lichtabhängige Carotinoidsynthese. VI. Zeitlicher Verlauf der Synthese der einzelnen Carotinoide bei *Fusarium aquaeductuum* unter verschiedenen Induktionsbedingungen. Planta, 156-174.

Bluhm, B.H., and Dunkle, L.D. (2008a). PHL1 of *Cercospora zeae-maydis* encodes a member of the photolyase/cryptochrome family involved in UV protection and fungal development. Fungal Genet Biol *45*, 1364-1372.

Blumenstein, A., Vienken, K., Tasler, R., Purschwitz, J., Veith, D., Frankenberg-Dinkel, N., and Fischer, R. (2005). The *Aspergillus nidulans* phytochrome FphA represses sexual development in red light. Curr Biol *15*, 1833-1838.

Bohnert, H.U., Fudal, I., Dioh, W., Tharreau, D., Notteghem, J.L., and Lebrun, M.H. (2004). A putative polyketide synthase/peptide synthetase from *Magnaporthe grisea* signals pathogen attack to resistant rice. Plant Cell *16*, 2499-2513.

Bok, J.W., and Keller, N.P. (2004). LaeA, a Regulator of Secondary Metabolism in *Aspergillus* spp. Eukaryotic Cell *3*, 527-535.

Booth C. (1971). The genus *Fusarium*. Commonwealth Mycological Institute *Kew*.

Borrow, A., Brown, S., Jefferys, E.G., Kessell, R.H., Lloyd, E.C., Lloyd, P.B., Rothwell, A., Rothwell, B., and Swait, J.C. (1964). The kinetics of metabolism of *Gibberella fujikuro*i in stirred culture. Can J Microbiol *10*, 407-444.

Brakhage, A.A. (1998). Molecular regulation of beta-lactam biosynthesis in filamentous fungi. Microbiol Mol Biol Rev *62*, 547-585.

Brakhage, A.A., Sprote, P., Al-Abdallah, Q., Gehrke, A., Plattner, H., and Tuncher, A. (2004). Regulation of penicillin biosynthesis in filamentous fungi. Adv Biochem Eng Biotechnol *88*, 45-90.

Brandt, S., von Stetten, D., Gunther, M., Hildebrandt, P., and Frankenberg-Dinkel, N. (2008). The fungal phytochrome FphA from *Aspergillus nidulans*. J Biol Chem *283*, 34605-34614.

Brautigam, C.A., Smith, B.S., Ma, Z., Palnitkar, M., Tomchick, D.R., Machius, M., and Deisenhofer, J. (2004). Structure of the photolyase-like domain of cryptochrome 1 from *Arabidopsis thaliana*. Proc Natl Acad Sci U S A *101*, 12142-12147.

Briggs, W.R., and Spudich, J.L. (2005). Handbook of photosensory receptors (Weinheim).

Britton, G., Liaaen-Jensen, S., and Pfander, H. (1998). Carotenoids. *Birkhäuser Verlag, Basel.*

Brown, D.W., Butchko, R.A., Busman, M., and Proctor, R.H. (2007). The *Fusarium verticillioides* FUM gene cluster encodes a Zn(II)2Cys6 protein that affects FUM gene expression and fumonisin production. Eukaryot Cell *6*, 1210-1218.

Brown, L.S. (2004). Fungal rhodopsins and opsin-related proteins: eukaryotic homologues of bacteriorhodopsin with unknown functions. Photochem Photobiol Sci *3*, 555-565.

Brudler, R., Hitomi, K., Daiyasu, H., Toh, H., Kucho, K., Ishiura, M., Kanehisa, M., Roberts, V.A., Todo, T., Tainer, J.A.*, et al.* (2003). Identification of a new cryptochrome class. Structure, function, and evolution. Mol Cell *11*, 59-67.

Brunner, M., and Kaldi, K. (2008). Interlocked feedback loops of the circadian clock of *Neurospora crassa*. Mol Microbiol *68*, 255-262.

Bunning, E., and Moser, I. (1973). Light-induced phase shifts of circadian leaf movements of *phaseolus*: comparison with the effects of potassium and of ethyl alcohol. Proc Natl Acad Sci U S A *70*, 3387-3389.

Butchko, R.A., Adams, T.H., and Keller, N.P. (1999). *Aspergillus nidulans* mutants defective in stc gene cluster regulation. Genetics *153*, 715-720.

Caldwell, R.W., Tuite, J., Stob, M., and Baldwin, R. (1970). Zearalenone production by *Fusarium* species. Applied Microbiology *20*, 31-34.

Calvo, A.M., Wilson, R.A., Bok, J.W., and Keller, N.P. (2002). Relationship between secondary metabolism and fungal development. Microbiology and Molecular Biology Reviews *66*, 447-459.

Candau, R., Avalos, J., and Cerda-Olmedo, E. (1992). Regulation of gibberellin biosynthesis in *Gibberella fujikuroi*. Plant Physiol *100*, 1184-1188.

Canessa, P., Schumacher, J., Hevia, M.A., Tudzynski, P., and Larrondo, L.F. (2013). Assessing the effects of light on differentiation and virulence of the plant pathogen *Botrytis cinerea*: characterization of the White Collar complex. PLoS One *8*, e84223.

Casas-Flores, S., Ríos-Momberg, M., Bibbins, M., Ponce-Noyola, P., and Herrera-Estrella, A. (2004). BLR-1 and BLR-2, key regulatory elements of photoconidiation and mycelial growth in *Trichoderma atroviride*. Microbiology *150*, 3561-3569.

Casas-Flores, S., Ríos-Momberg, M., Rosales-Saavedra, T., Martínez-Hernández, P., Olmedo-Monfil, V., and Herrera-Estrella, A. (2006). Cross talk between a fungal blue-light perception system and the cyclic AMP signaling pathway. Eukaryot Cell *5*, 499-506.

Cashmore, A.R., Jarillo, J.A., Wu, Y.J., and Liu, D. (1999). Cryptochromes: blue light receptors for plants and animals. Science *284*, 760-765.

Castellanos, F., Schmoll, M., Martínez, P., Tisch, D., Kubicek, C.P., Herrera-Estrella, A., and Esquivel-Naranjo, E.U. (2010). Crucial factors of the light perception machinery and their impact on growth and cellulase gene transcription in *Trichoderma reesei*. Fungal Genet Biol *47*, 468-476.

Castillo, R., Fernández, J.A., and Gómez-Gómez, L. (2005). Implications of carotenoid biosynthetic genes in apocarotenoid formation during the stigma development of *Crocus sativus* and its closer relatives. Plant Physiology *139*, 674-689.

Castrillo, M., García-Martínez, J., and Avalos, J. (2013). Light-dependent functions of the *Fusarium fujikuroi* CryD DASH cryptochrome in development and secondary metabolism. Appl Environ Microbiol *79*, 2777-2788.

Čonková, E., Laciaková, A., Kováč, G., and Seidel, H. (2003). Fusarial Toxins and their Role in Animal Diseases. The Veterinary Journal *165*, 214-220.

Cornforth, J.W., Ryback, G., Robinson, P.M., and Park, D. (1971). Isolation and characterization of a fungal vacuolation factor (bikaverin). J Chem Soc Perkin 1 *16*, 2786-2788.

Corrochano, L.M. (2007). Fungal photoreceptors: sensory molecules for fungal development and behaviour. Photochem Photobiol Sci *6*, 725-736.

Corrochano, L.M., and Garre, V. (2010). Photobiology in the Zygomycota: multiple photoreceptor genes for complex responses to light. Fungal Genet Biol *47*, 893-899.

Crawford, J.M., Dancy, B.C., Hill, E.A., Udwary, D.W., and Townsend, C.A. (2006). Identification of a starter unit acyl-carrier protein transacylase domain in an iterative type I polyketide synthase. Proc Natl Acad Sci U S A *103*, 16728-16733.

Crawford, J.M., Korman, T.P., Labonte, J.W., Vagstad, A.L., Hill, E.A., Kamari-Bidkorpeh, O., Tsai, S.C., and Townsend, C.A. (2009). Structural basis for biosynthetic programming of fungal aromatic polyketide cyclization. Nature *461*, 1139-1143.

Crosthwaite, S.K., Loros, J.J., and Dunlap, J.C. (1995). Light-induced resetting of a circadian clock is mediated by a rapid increase in frequency transcript. Cell *81*, 1003-1012.

Cuttriss, A.J., and Pogson, B.J. (2006). In The structure and function of plastids. (Wise RR and Hoober JK eds), Springer, Dordrecht, The Netherlands.

Chaves, I., Pokorny, R., Byrdin, M., Hoang, N., Ritz, T., Brettel, K., Essen, L.O., van der Horst, G.T., Batschauer, A., and Ahmad, M. (2011). The cryptochromes: blue light photoreceptors in plants and animals. Annu Rev Plant Biol *62*, 335-364.

Chen, C.H., DeMay, B.S., Gladfelter, A.S., Dunlap, J.C., and Loros, J.J. (2010). Physical interaction between VIVID and white collar complex regulates photoadaptation in *Neurospora*. Proc Natl Acad Sci U S A *107*, 16715-16720.

Chen, C.H., and Loros, J.J. (2009b). *Neurospora* sees the light: light signaling components in a model system. Commun Integr Biol *2*, 448-451.

Chen, C.H., Ringelberg, C.S., Gross, R.H., Dunlap, J.C., and Loros, J.J. (2009a). Genome-wide analysis of light-inducible responses reveals hierarchical light signalling in *Neurospora*. EMBO J *28*, 1029-1042.

Cheng, P., He, Q., Yang, Y., Wang, L., and Liu, Y. (2003a). Functional conservation of light, oxygen, or voltage domains in light sensing. Proc Natl Acad Sci U S A *100*, 5938-5943.

Cheng, P., Yang, Y., Gardner, K.H., and Liu, Y. (2002). PAS domain-mediated WC-1/WC-2 interaction is essential for maintaining the steady-state level of WC-1 and the function of both proteins in circadian clock and light responses of *Neurospora*. Mol Cell Biol *22*, 517-524.

Cheng, P., Yang, Y., Wang, L., He, Q., and Liu, Y. (2003b). WHITE COLLAR-1, a multifunctional *neurospora* protein involved in the circadian feedback loops, light sensing, and transcription repression of *wc-2*. J Biol Chem *278*, 3801-3808.

Cheng, S.J., Jiang, Y.Z., Li, M.H., and Lo, H.Z. (1985). A mutagenic metabolite produced by *Fusarium moniliforme* isolated from Linxian county, China Carcinogenesis *6*, 903-905.

Chiang, Y.M., Oakley, B.R., Keller, N.P., and Wang, C.C. (2010). Unraveling polyketide synthesis in members of the genus *Aspergillus*. Appl Microbiol Biotechnol *86*, 1719-1736.

Daiyasu, H., Ishikawa, T., Kuma, K., Iwai, S., Todo, T., and Toh, H. (2004). Identification of cryptochrome DASH from vertebrates. Genes Cells *9*, 479-495.

Daub, M.E., Herrero, S., and Chung, K.R. (2005). Photoactivated perylenequinone toxins in fungal pathogenesis of plants. FEMS Microbiol Lett *252*, 197-206.

Daub, M.E., and Payne, G.A. (1989). The role of carotenoids in resistance of fungi to cercosporin. Phytopathology *79*, 180-185.

Degli-Innocenti, F., Chambers, J.A., and Russo, V.E. (1984b). Conidia induce the formation of protoperithecia in *Neurospora crassa*: further characterization of white collar mutants. J Bacteriol *159*, 808-810.

Degli-Innocenti, F., and Russo, V.E. (1984a). Isolation of new white collar mutants of *Neurospora crassa* and studies on their behavior in the blue light-induced formation of protoperithecia. J Bacteriol *159*, 757-761.

Delbrück, M., Katzir, A., and Presti, D. (1976). Responses of *Phycomyces* indicating optical excitation of the lowest triplet state of riboflavin. Proc Natl Acad Sci U S A *73*, 1969-1973.

Demerec, M., Adelberg, E.A., Clark, A.J., and Hartman, P.E. (1966). A proposal for a uniform nomenclature in bacterial genetics. Genetics *54*, 61-76.

Desjardins, A.E., and Busman, M. (2006). Mycotoxins in developing countries: A case study of maize in Nepal. Mycotoxin Res *22*, 92-95.

Desjardins, A.E., Hohn, T.M., and McCormick, S.P. (1993). Trichothecene biosynthesis in *Fusarium* species: chemistry, genetics, and significance. Microbiological Reviews *57*, 595-604.

Desjardins, A.E., Manandhar, H.K., Plattner, R.D., Manandhar, G.G., Poling, S.M., and Maragos, C.M. (2000). *Fusarium* species from nepalese rice and production of mycotoxins and gibberellic acid by selected species. Appl Environ Microbiol *66*, 1020-1025.

Desjardins, A.E., Plattner, R.D., and Nelson, P.E. (1997). Production of fumonisin B(inf1) and moniliformin by *Gibberella fujikuroi* from rice from various geographic areas. Appl Environ Microbiol *63*, 1838-1842.

Desjardins, A.E., and Proctor, R.H. (2007a). Molecular biology of *Fusarium* mycotoxins. Int J Food Microbiol *119*, 47-50.

Devlin, P.F. (2002). Signs of the time: environmental input to the circadian clock. J Exp Bot *53*, 1535-1550.

Díaz-Sánchez, V. (2013). Enzimas fúngicas implicadas en la síntesis y modificación de compuestos de interés. In Departmento de Genética (Sevilla, Universidad de Sevilla).

Díaz-Sánchez, V., Avalos, J., and Limón, M.C. (2012). Identification and regulation of *fusA*, the polyketide synthase gene responsible for fusarin production in *Fusarium fujikuroi*. Appl Environ Microbiol *78*, 7258-7266.

Díaz-Sánchez, V., Estrada, A.F., Trautmann, D., Al-Babili, S., and Avalos, J. (2011a). The gene *carD* encodes the aldehyde dehydrogenase responsible for neurosporaxanthin biosynthesis in *Fusarium fujikuroi*. FEBS J *278*, 3164-3176.

Dixon, J.M., Taniguchi, M., and Lindsey, J.S. (2005). PhotochemCAD 2: a refined program with accompanying spectral databases for photochemical calculations. Photochem Photobiol *81*, 212-213.

Domenech, C.E., Giordano, W., Avalos, J., and Cerdá-olmedo, E. (1996). Separate compartments for the production of sterols, carotenoids and gibberellins in *Gibberella fujikuroi.* European Journal of Biochemistry *239*, 720-725.

Dong, W., Tang, X., Yu, Y., Nilsen, R., Kim, R., Griffith, J., Arnold, J., and Schuttler, H.B. (2008). Systems biology of the clock in *Neurospora crassa*. PLoS One *3*, e3105.

Dong, Z.Y., and Zhan, Y.H. (1987). Inhibitory effect of a mycotoxin, fusarin C, on macrophage activation and macrophage mediated cytotoxicity to tumor cells in mice. J Exp Clin Cancer Res *6*, 31-38.

Dowzer, C.A., and Kelly, J. (1989). Cloning of the *creA* gene from *Aspergillus nidulans*: a gene involved in carbon catabolite repression. Curr Genet *15*, 457-459.

Drössler, P., Holzer, W., Penzkofer, A., and Hegemann, P. (2002). pH dependence of the absorption and emission behaviour of riboflavin in aqueous solution. Chemical Physics *282*, 429-439.

Dufour, N., and Rao, R.P. (2011). Secondary metabolites and other small molecules as intercellular pathogenic signals. FEMS Microbiol Lett *314*, 10-17.

Dunlap, J.C., and Loros, J.J. (2004). The *Neurospora* circadian system. J Biol Rhythms *19*, 414-424.

Dunlap, J.C., Loros, J.J., Colot, H.V., Mehra, A., Belden, W.J., Shi, M., Hong, C.I., Larrondo, L.F., Baker, C.L., Chen, C.H*., et al.* (2007). A circadian clock in *Neurospora*: how genes and proteins cooperate to produce a sustained, entrainable, and compensated biological oscillator with a period of about a day. Cold Spring Harb Symp Quant Biol *72*, 57-68.

Edge, R., McGarvey, D.J., and Truscott, T.G. (1997). The carotenoids as anti-oxidants — a review. Journal of Photochemistry and Photobiology B: Biology *41*, 189-200.

Elvin, M., Loros, J.J., Dunlap, J.C., and Heintzen, C. (2005). The PAS/LOV protein VIVID supports a rapidly dampened daytime oscillator that facilitates entrainment of the *Neurospora* circadian clock. Genes Dev *19*, 2593-2605.

Emery, P., So, W.V., Kaneko, M., Hall, J.C., and Rosbash, M. (1998). CRY, a *Drosophila* clock and light-regulated cryptochrome, is a major contributor to circadian rhythm resetting and photosensitivity. Cell *95*, 669-679.

Espagne, A., Byrdin, M., Eker, A.P., and Brettel, K. (2009). Very fast product release and catalytic turnover of DNA photolyase. Chembiochem *10*, 1777-1780.

Espeso, E.A., Tilburn, J., Arst, H.N., Jr., and Peñalva, M.A. (1993). pH regulation is a major determinant in expression of a fungal penicillin biosynthetic gene. EMBO J *12*, 3947-3956.

Espeso, E.A., Tilburn, J., Sánchez-Pulido, L., Brown, C.V., Valencia, A., Arst, H.N., Jr., and Peñalva, M.A. (1997). Specific DNA recognition by the *Aspergillus nidulans* three zinc finger transcription factor PacC. J Mol Biol *274*, 466-480.

Esquivel-Naranjo, E.U., and Herrera-Estrella, A. (2007). Enhanced responsiveness and sensitivity to blue light by *blr-2* overexpression in *Trichoderma atroviride*. Microbiology *153*, 3909-3922.

Essen, L.O. (2006). Photolyases and cryptochromes: common mechanisms of DNA repair and light-driven signaling? Curr Opin Struct Biol *16*, 51-59.

Estrada, A.F., and Avalos, J. (2008). The White Collar protein WcoA of *Fusarium fujikuroi* is not essential for photocarotenogenesis, but is involved in the regulation of secondary metabolism and conidiation. Fungal Genet Biol *45*, 705-718.

Estrada, A.F., and Avalos, J. (2009a). Regulation and targeted mutation of *opsA*, coding for the NOP-1 opsin orthologue in *Fusarium fujikuroi*. J Mol Biol *387*, 59-73.

Estrada, A.F., Brefort, T., Mengel, C., Díaz-Sánchez, V., Alder, A., Al-Babili, S., and Avalos, J. (2009b). *Ustilago maydis* accumulates beta-carotene at levels determined by a retinal-forming carotenoid oxygenase. Fungal Genet Biol *46*, 803-813.

Estrada, A.F., Youssar, L., Scherzinger, D., Al-Babili, S., and Avalos, J. (2008b). The *ylo-1* gene encodes an aldehyde dehydrogenase responsible for the last reaction in the *Neurospora* carotenoid pathway. Mol Microbiol *69*, 1207-1220.

Facella, P., Lopez, L., Chiappetta, A., Bitonti, M.B., Giuliano, G., and Perrotta, G. (2006). CRY-DASH gene expression is under the control of the circadian clock machinery in tomato. FEBS Lett *580*, 4618-4624.

Fang, S., Lorick, K.L., Jensen, J.P., and Weissman, A.M. (2003). RING finger ubiquitin protein ligases: implications for tumorigenesis, metastasis and for molecular targets in cancer. Semin Cancer Biol *13*, 5-14.

Fernández-Martín, R., Cerdá-Olmedo, E., and Avalos, J. (2000). Homologous recombination and allele replacement in transformants of *Fusarium fujikuroi*. Molecular and General Genetics *263*, 838-845.

Flaherty, J.E., Pirttila, A.M., Bluhm, B.H., and Woloshuk, C.P. (2003). *PAC1*, a pH-regulatory gene from *Fusarium verticillioides*. Appl Environ Microbiol *69*, 5222-5227.

Franchi, L., Fulci, V., and Macino, G. (2005). Protein kinase C modulates light responses in *Neurospora* by regulating the blue light photoreceptor WC-1. Mol Microbiol *56*, 334-345.

Froehlich, A.C., Chen, C.H., Belden, W.J., Madeti, C., Roenneberg, T., Merrow, M., Loros, J.J., and Dunlap, J.C. (2010). Genetic and molecular characterization of a cryptochrome from the filamentous fungus *Neurospora crassa*. Eukaryot Cell *9*, 738-750.

Froehlich, A.C., Liu, Y., Loros, J.J., and Dunlap, J.C. (2002). White Collar-1, a circadian blue light photoreceptor, binding to the frequency promoter. Science *297*, 815-819.

Froehlich, A.C., Noh, B., Vierstra, R.D., Loros, J., and Dunlap, J.C. (2005). Genetic and molecular analysis of phytochromes from the filamentous fungus *Neurospora crassa*. Eukaryot Cell *4*, 2140-2152.

Geissman, T.A., Verbiscar, A.J., Phinney, B.O., and Cragg, G. (1966). Studies on the biosynthesis of gibberellins from (-)-kaurenoid acid in cultures of *Gibberella fujikuroi*. Phytochemistry *5*, 933-947.

Gelderblom, W.C., Jaskiewicz, K., Marasas, W.F., Thiel, P.G., Horak, R.M., Vleggaar, R., and Kriek, N.P. (1988). Fumonisins-novel mycotoxins with cancer-promoting activity produced by *Fusarium moniliforme*. Appl Environ Microbiol *54*, 1806-1811.

Gelderblom, W.C.A., Thiel, P.G., van der Merwe, K.J., Marasas, W.F.O., and Spies, H.S.C. (1983). A mutagen produced by *Fusarium moniliforme.* Toxicon *21*, 467-473.

Georgiou, C.D., Tairis, N., and Polycratis, A. (2001). Production of β-carotene by *Sclerotinia sclerotiorum* and its role in sclerotium differentiation. Mycol Res *105*, 1110-1115.

Gin, E., Diernfellner, A.C., Brunner, M., and Hofer, T. (2013). The *Neurospora* photoreceptor VIVID exerts negative and positive control on light sensing to achieve adaptation. Mol Syst Biol *9*, 667.

Giordano, W., Avalos, J., Cerdá-Olmedo, E., and Domenech, C.E. (1999). Nitrogen availability and production of bikaverin and gibberellins in *Gibberella fujikuroi*. FEMS Microbiology Letters *173*, 389-393.

Giovani, B., Byrdin, M., Ahmad, M., and Brettel, K. (2003). Light-induced electron transfer in a cryptochrome blue-light photoreceptor. Nat Struct Biol *10*, 489-490.

Godin, K.S., and Varani, G. (2007). How arginine-rich domains coordinate mRNA maturation events. RNA Biol *4*, 69-75.

Goodwin, T.W., and Lijinski, W. (1952). Studies in carotenogenesis: 3. Identification of the minor polyene components of the fungus *Phycomyces blakesleeanus* an a study of their synthesis under various cultural conditions. Biochem J *50*, 550-558.

Govind, N.S., and Cerda-Olmedo, E. (1986). Sexual activation of carotenogenesis in *Phycomyces blakesleeanus*. J Gen Microbiol *132*.

Greene, A.V., Keller, N., Haas, H., and Bell-Pedersen, D. (2003). A circadian oscillator in *Aspergillus spp*. regulates daily development and gene expression. Eukaryot Cell *2*, 231-237.

Hadley, C.W., Miller, E.C., Schwartz, S.J., and Clinton, S.K. (2002). Tomatoes, lycopene, and prostate cancer: progress and promise. Experimental Biology and Medicine *227*, 869-880.

Haldi, M., Ton, C., Seng, W.L., and McGrath, P. (2006). Human melanoma cells transplanted into zebrafish proliferate, migrate, produce melanin, form masses and stimulate angiogenesis in zebrafish. Angiogenesis *9*, 139-151.

Hanahan, D. (1983b). Studies on transformation of Escherichia coli with plasmids. J Mol Biol *166*, 557-580.

Harding, R.W., and Melles, S. (1983). Genetic analysis of phototropism of *Neurospora crassa* perithecial beaks using *white collar* and *albino* mutants. Plant Physiol *72*, 996-1000.

Harding, R.W., and Turner, R.V. (1981). Photoregulation of the carotenoid biosynthetic pathway in *albino* and *white collar* mutants of *Neurospora crassa*. Plant Physiol *68*, 745-749.

Hargrave, P.A., McDowell, J.H., Feldmann, R.J., Atkinson, P.H., Rao, J.K., and Argos, P. (1984). Rhodopsin's protein and carbohydrate structure: selected aspects. Vision Res *24*, 1487-1499.

He, Q., Cheng, P., Yang, Y., Wang, L., Gardner, K.H., and Liu, Y. (2002). White collar-1, a DNA binding transcription factor and a light sensor. Science *297*, 840-843.

He, Q., and Liu, Y. (2005). Molecular mechanism of light responses in *Neurospora*: from light-induced transcription to photoadaptation. Genes Dev *19*, 2888-2899.

Hedden, P., MacMillan, J., and Phinney, B.O. (1974). Fungal products. Part XII. Gibberellin A14 aldehyde, an intermediate in gibberellin biosynthesis in *Gibberella fujikuroi*. J Chem Soc Perkin Trans I, 58: 7-592 *1*, 587-592.

Hedden, P., Phillips, A.L., Rojas, M.C., Carrera, E., and Tudzynski, B. (2001). Gibberellin Biosynthesis in Plants and Fungi: A Case of Convergent Evolution? J Plant Growth Regul *20*, 319-331.

Heijde, M., Zabulon, G., Corellou, F., Ishikawa, T., Brazard, J., Usman, A., Sanchez, F., Plaza, P., Martin, M., Falciatore, A*., et al.* (2010). Characterization of two members of the cryptochrome/photolyase family from *Ostreococcus tauri* provides insights into the origin and evolution of cryptochromes. Plant Cell Environ *33*, 1614-1626.

Heintzen, C., and Liu, Y. (2007). The *Neurospora crassa* circadian clock. Adv Genet *58*, 25-66.

Heintzen, C., Loros, J.J., and Dunlap, J.C. (2001). The PAS protein VIVID defines a clock-associated feedback loop that represses light input, modulates gating, and regulates clock resetting. Cell *104*, 453-464.

Hendrischk, A.K., Fruhwirth, S.W., Moldt, J., Pokorny, R., Metz, S., Kaiser, G., Jager, A., Batschauer, A., and Klug, G. (2009). A cryptochrome-like protein is involved in the regulation of photosynthesis genes in *Rhodobacter sphaeroides*. Mol Microbiol *74*, 990-1003.

Herrera-Estrella, A., and Horwitz, B.A. (2007). Looking through the eyes of fungi: molecular genetics of photoreception. Mol Microbiol *64*, 5-15.

Hitomi, K., Okamoto, K., Daiyasu, H., Miyashita, H., Iwai, S., Toh, H., Ishiura, M., and Todo, T. (2000). Bacterial cryptochrome and photolyase: characterization of two photolyase-like genes of *Synechocystis sp*. PCC6803. Nucleic Acids Res *28*, 2353-2362.

Hoffmeister, D., and Keller, N.P. (2007). Natural products of filamentous fungi: enzymes, genes, and their regulation. Natural Product Reports *24*, 393-416.

Hsu, D.S., Zhao, X., Zhao, S., Kazantsev, A., Wang, R.P., Todo, T., Wei, Y.F., and Sancar, A. (1996). Putative human blue-light photoreceptors hCRY1 and hCRY2 are flavoproteins. Biochemistry *35*, 13871-13877.

Huang, W., Ramsey, K.M., Marcheva, B., and Bass, J. (2011). Circadian rhythms, sleep, and metabolism. J Clin Invest *121*, 2133-2141.

Hunt, S.M., Thompson, S., Elvin, M., and Heintzen, C. (2010). VIVID interacts with the WHITE COLLAR complex and FREQUENCY-interacting RNA helicase to alter light and clock responses in *Neurospora*. Proc Natl Acad Sci U S A *107*, 16709-16714.

Hynes, M.J. (1975). Studies on the role of the are a gene in the regulation of nitrogen catabolism in *Aspergillus nidulans.* Australian Journal of Biological Sciences *28*, 301-314.

Idnurm, A., and Heitman, J. (2005). Light controls growth and development via a conserved pathway in the fungal kingdom. PLoS Biol *3*, e95.

Idnurm, A., and Heitman, J. (2010). Ferrochelatase is a conserved downstream target of the blue light-sensing White collar complex in fungi. Microbiology *156*, 2393-2407.

Idnurm, A., and Howlett, B.J. (2001). Characterization of an opsin gene from the ascomycete *Leptosphaeria maculans*. Genome *44*, 167-171.

Idnurm, A., Rodriguez-Romero, J., Corrochano, L.M., Sanz, C., Iturriaga, E.A., Eslava, A.P., and Heitman, J. (2006). The *Phycomyces madA* gene encodes a blue-light photoreceptor for phototropism and other light responses. Proc Natl Acad Sci U S A *103*, 4546-4551.

Idnurm, A., Verma, S., and Corrochano, L.M. (2010). A glimpse into the basis of vision in the kingdom Mycota. Fungal Genet Biol *47*, 881-892.

Inoue, H., Nojima, H., and Okayama, H. (1990). High efficiency transformation of *Escherichia coli* with plasmids. Gene *96*, 23-28.

Islam, M.S., Susdorf, T., Penzkofer, A., and Hegemann, P. (2003). Fluorescence quenching of flavin adenine dinucleotide in aqueous solution by pH dependent isomerisation and photo-induced electron transfer. Chemical Physics *295*, 137-149.

Jestoi, M. (2008). Emerging *Fusarium* Mycotoxins Fusaproliferin, Beauvericin, Enniatins, And Moniliformin—A Review. Critical Reviews in Food Science and Nutrition *48*, 21-49.

Johnson, S.W., and Coolbaugh, R.C. (1990). Light-stimulated gibberellin biosynthesis in *Gibberella fujikuroi*. Plant Physiol *94*, 1696-1701.

Jyonouchi, H., Zhang, L., and Tomita, Y. (1993). Studies of immunomodulating actions of carotenoids. II. Astaxanthin enhances in vitro antibody production to T-dependent antigens without facilitating polyclonal B-cell activation. Nutr Cancer *19*, 269-280.

Kale, S.P., Milde, L., Trapp, M.K., Frisvad, J.C., Keller, N.P., and Bok, J.W. (2008). Requirement of LaeA for secondary metabolism and sclerotial production in *Aspergillus flavus*. Fungal Genet Biol *45*, 1422-1429.

Kam, R.K., Deng, Y., Chen, Y., and Zhao, H. (2012). Retinoic acid synthesis and functions in early embryonic development. Cell Biosci *2*, 11.

Kami, C., Lorrain, S., Hornitschek, P., and Fankhauser, C. (2010). Light-regulated plant growth and development. Curr Top Dev Biol *91*, 29-66.

Kao, Y.T., Saxena, C., Wang, L., Sancar, A., and Zhong, D. (2005). Direct observation of thymine dimer repair in DNA by photolyase. Proc Natl Acad Sci U S A *102*, 16128-16132.

Kao, Y.T., Tan, C., Song, S.H., Ozturk, N., Li, J., Wang, L., Sancar, A., and Zhong, D. (2008). Ultrafast dynamics and anionic active states of the flavin cofactor in cryptochrome and photolyase. J Am Chem Soc *130*, 7695-7701.

Kato, M. (2005). An overview of the CCAAT-box binding factor in filamentous fungi: assembly, nuclear translocation, and transcriptional enhancement. Biosci Biotechnol Biochem *69*, 663-672.

Kato, T., Jr., Todo, T., Ayaki, H., Ishizaki, K., Morita, T., Mitra, S., and Ikenaga, M. (1994). Cloning of a marsupial DNA photolyase gene and the lack of related nucleotide sequences in placental mammals. Nucleic Acids Res *22*, 4119-4124.

Kawaide, H. (2006). Biochemical and molecular analyses of gibberellin biosynthesis in fungi. Biosci Biotechnol Biochem *70*, 583-590.

Kawaide, H., Imai, R., Sassa, T., and Kamiya, Y. (1997). Ent-kaurene synthase from the fungus *Phaeosphaeria* sp. L487. cDNA isolation, characterization, and bacterial expression of a bifunctional diterpene cyclase in fungal gibberellin biosynthesis. J Biol Chem *272*, 21706-21712.

Kelber, A., and Lind, O. (2010). Limits of colour vision in dim light. Ophthalmic Physiol Opt *30*, 454-459.

Keller, N.P., and Hohn, T.M. (1997). Metabolic Pathway Gene Clusters in Filamentous Fungi. Fungal Genetics and Biology *21*, 17-29.

Keller, N.P., Turner, G., and Bennett, J.W. (2005). Fungal secondary metabolism - from biochemistry to genomics. Nat Rev Micro *3*, 937-947.

Kennis, J.T., Crosson, S., Gauden, M., van Stokkum, I.H., Moffat, K., and van Grondelle, R. (2003). Primary reactions of the LOV2 domain of phototropin, a plant blue-light photoreceptor. Biochemistry *42*, 3385-3392.

Kihara, J., Moriwaki, A., Matsuo, N., Arase, S., and Honda, Y. (2004). Cloning, functional characterization, and near-ultraviolet radiation-enhanced expression of a photolyase gene (PHR1) from the phytopathogenic fungus *Bipolaris oryzae*. Curr Genet *46*, 37-46.

Kim, H., Son, H., and Lee, Y.W. (2013b). Effects of light on secondary metabolism and fungal development of *Fusarium graminearum*. J Appl Microbiol.

Kim, S.T., and Sancar, A. (1991a). Effect of base, pentose, and phosphodiester backbone structures on binding and repair of pyrimidine dimers by *Escherichia coli* DNA photolyase. Biochemistry *30*, 8623-8630.

Kiontke, S., Geisselbrecht, Y., Pokorny, R., Carell, T., Batschauer, A., and Essen, L.O. (2011). Crystal structures of an archaeal class II DNA photolyase and its complex with UV-damaged duplex DNA. EMBO J *30*, 4437-4449.

Klar, T., Pokorny, R., Moldt, J., Batschauer, A., and Essen, L.O. (2007). Cryptochrome 3 from *Arabidopsis thaliana*: structural and functional analysis of its complex with a folate light antenna. J Mol Biol *366*, 954-964.

Klein, R.M. (1992). Effects of green light on biological systems. Biol Rev Camb Philos Soc *67*, 199-284.

Kleine, T., Lockhart, P., and Batschauer, A. (2003). An *Arabidopsis* protein closely related to *Synechocystis* cryptochrome is targeted to organelles. Plant J *35*, 93-103.

Klittich, C., and Leslie, J.F. (1988). Nitrate reduction mutants of *Fusarium moniliforme* (*Gibberella fujikuroi*). Genetics *118*, 417-423.

Koelblin, R.I., Brückner, B., Blechschmidt, D., and Fischer, W. (1990). Activity of mutagens in the fungus *Gibberella fujikuroi.* Journal of Basic Microbiology *30*, 675-677.

Kosalkova, K., Garcia-Estrada, C., Ullan, R.V., Godio, R.P., Feltrer, R., Teijeira, F., Mauriz, E., and Martin, J.F. (2009). The global regulator LaeA controls penicillin biosynthesis, pigmentation and sporulation, but not roquefortine C synthesis in *Penicillium chrysogenum*. Biochimie *91*, 214-225.

Kuhlman, E.G. (1983). Varieties of *Gibberella fujikuroi* with anamorphs in *Fusarium* section *Liseola*. Mycologia *74*.

Kumagai, T. (1989). Temperature and mycochrome system in near-UV light inducible and blue light reversible photoinduction of conidiation in *Alternaria tomato*. Photochemistry and photobiology
50, 793-798.

Kuzina, V., and Cerdá-Olmedo, E. (2007). Ubiquinone and carotene production in the Mucorales *Blakeslea* and *Phycomyces*. Appl Microbiol Biotechnol *76*, 991-999.

Kwon, H.R., Son, S.W., Han, H.R., Choi, G.J., Jang, K.S., Choi, Y.H., Lee, S., Sung, N.D., and Kim, J.C. (2007). Nematicidal activity of bikaverin and fusaric acid isolated from *Fusarium oxysporum* against pine wood nematode *Bursaphelenchus xylophilus*. Plant Pathology Journal
23, 318-323.

Lee, C.T., Malzahn, E., Brunner, M., and Mayer, M.P. (2014). Light-induced differences in conformational dynamics of the circadian clock regulator VIVID. J Mol Biol *426*, 601-610.

Lee, K., Loros, J.J., and Dunlap, J.C. (2000). Interconnected feedback loops in the *Neurospora* circadian system. Science *289*, 107-110.

Lee, K., Singh, P., Chung, W.C., Ash, J., Kim, T.S., Hang, L., and Park, S. (2006). Light regulation of asexual development in the rice blast fungus, *Magnaporthe oryzae*. Fungal Genet Biol *43*, 694-706.

Leslie, J.F. (1991). Mating population in *Gibberella fujikuroi* (*Fusarium* Section *Liseola*). Phytopathology *81*, 1058-1060.

Leslie, J.F., and Summerell, B.A. (2006). The *Fusarium* laboratory manual. Blackwell Professional, Ames, IA.

Leslie, J.F., Summerell, B.A., Bullock, S., and Doe, F.J. (2005). Description of *Gibberella sacchari* and neotypification of its anamorph *Fusarium sacchari*. Mycologia *97*, 718-724.

Lewis, Z.A., Correa, A., Schwerdtfeger, C., Link, K.L., Xie, X., Gomer, R.H., Thomas, T., Ebbole, D.J., and Bell-Pedersen, D. (2002). Overexpression of White Collar-1 (WC-1) activates circadian clock-associated genes, but is not sufficient to induce most light-regulated gene expression in *Neurospora crassa*. Mol Microbiol *45*, 917-931.

Li, Q.H., and Yang, H.Q. (2007). Cryptochrome signaling in plants. Photochem Photobiol *83*, 94-101.

Liedvogel, M., and Mouritsen, H. (2010). Cryptochromes--a potential magnetoreceptor: what do we know and what do we want to know? J R Soc Interface *7 Suppl 2*, S147-162.

Limón, M.C., Rodríguez-Ortiz, R., and Avalos, J. (2010). Bikaverin production and applications. Applied Microbiology and Biotechnology *87*, 21-29.

Lin, C. (2002). Blue light receptors and signal transduction. Plant Cell *14 Suppl*, S207-225.

Lin, C., and Todo, T. (2005). The cryptochromes. Genome Biol *6*, 220.

Linden, H., and Macino, G. (1997). White collar 2, a partner in blue-light signal transduction, controlling expression of light-regulated genes in *Neurospora crassa*. EMBO J *16*, 98-109.

Linnemannstöns, P., Prado, M.M., Fernández-Martín, R., Tudzynski, B., and Avalos, J. (2002b). A carotenoid biosynthesis gene cluster in *Fusarium fujikuroi*: the genes *carB* and *carRA*. Mol Genet Genomics *267*, 593-602.

Linnemannstöns, P., Schulte, J., Prado, M.M., Proctor, R.H., Avalos, J., and Tudzynski, B. (2002). The polyketide synthase gene *pks4* from *Gibberella fujikuroi* encodes a key enzyme in the biosynthesis of the red pigment bikaverin. Fungal Genet Biol *37*, 134-148.

Liu, B., Liu, H., Zhong, D., and Lin, C. (2010). Searching for a photocycle of the cryptochrome photoreceptors. Curr Opin Plant Biol *13*, 578-586.

Liu, H., Liu, B., Zhao, C., Pepper, M., and Lin, C. (2011). The action mechanisms of plant cryptochromes. Trends Plant Sci *16*, 684-691.

Liu, Y., He, Q., and Cheng, P. (2003). Photoreception in *Neurospora*: a tale of two White Collar proteins. Cell Mol Life Sci *60*, 2131-2138.

Lombardi, L.M., and Brody, S. (2005). Circadian rhythms in *Neurospora crassa*: clock gene homologues in fungi. Fungal Genet Biol *42*, 887-892.

Lopez-Diaz, I., and Cerda-Olmedo, E. (1980). Relationship of photocarotenogenesis to other behavioural and regulatory responses in *Phycomyces*. Planta *150*, 134-139.

Lorca-Pascual, J.M., Murcia-Flores, L., Garre, V., Torres-Martinez, S., and Ruiz-Vazquez, R.M. (2004). The RING-finger domain of the fungal repressor crgA is essential for accurate light regulation of carotenogenesis. Mol Microbiol *52*, 1463-1474.

MacMillan, J. (1997). Biosynthesis of the gibberellin plant hormones. Natural Product Reports *14*, 221-244.

Malz, S., Grell, M.N., Thrane, C., Maier, F.J., Rosager, P., Felk, A., Albertsen, K.S., Salomon, S., Bohn, L., Schafer, W*., et al.* (2005). Identification of a gene cluster responsible for the biosynthesis of aurofusarin in the *Fusarium graminearum* species complex. Fungal Genet Biol *42*, 420-433.

Malzahn, E., Ciprianidis, S., Kaldi, K., Schafmeier, T., and Brunner, M. (2010). Photoadaptation in *Neurospora* by competitive interaction of activating and inhibitory LOV domains. Cell *142*, 762-772.

Mapari, S.A.S., Nielsen, K.F., Larsen, T.O., Frisvad, J.C., Meyer, A.S., and Thrane, U. (2005). Exploring fungal biodiversity for the production of water-soluble pigments as potential natural food colorants. Current Opinion in Biotechnology *16*, 231-238.

Marasas, W.F., Thiel, P.G., Rabie, C.J., Nelson, P.E., and Tousson, T.A. (1986). Moniliformin production in *Fusarium* section *Liseola*. Mycologia *78*, 242-247.

Marzluf, G.A. (1997). Genetic regulation of nitrogen metabolism in the fungi. Microbiology and Molecular Biology Reviews *61*, 17-32.

Mende, K., Homann, V., and Tudzynski, B. (1997). The geranylgeranyl diphosphate synthase gene of *Gibberella fujikuroi*: isolation and expression. Mol Gen Genet *255*, 96-105.

Menon, S.T., Han, M., and Sakmar, T.P. (2001). Rhodopsin: structural basis of molecular physiology. Physiol Rev *81*, 1659-1688.

Menzella, H.G., Reid, R., Carney, J.R., Chandran, S.S., Reisinger, S.J., Patel, K.G., Hopwood, D.A., and Santi, D.V. (2005). Combinatorial polyketide biosynthesis by de novo design and rearrangement of modular polyketide synthase genes. Nat Biotech *23*, 1171-1176.

Mertz, D., and Henson, W. (1967). Light stimulated biosynthesis of gibberellins in *Fusarium moniliforme*. Nature *214*, 844-846.

Mihlan, M., Homann, V., Liu, T.D., and Tudzynski, B. (2003). AREA directly mediates nitrogen regulation of gibberellin biosynthesis in *Gibberella fujikuroi*, but its activity is not affected by NMR. Molecular Microbiology *47*, 975-991.

Moldt, J., Pokorny, R., Orth, C., Linne, U., Geisselbrecht, Y., Marahiel, M.A., Essen, L.O., and Batschauer, A. (2009). Photoreduction of the folate cofactor in members of the photolyase family. J Biol Chem *284*, 21670-21683.

Moline, M., Libkind, D., Dieguez Mdel, C., and van Broock, M. (2009). Photoprotective role of carotenoids in yeasts: Response to UV-B of pigmented and naturally-occurring albino strains. J Photochem Photobiol B *95*, 156-161.

Mooney, J.L., and Yager, L.N. (1990a). Light is required for conidiation in *Aspergillus nidulans*. Genes Dev *4*, 1473-1482.

Moran, N.A., and Jarvik, T. (2010). Lateral transfer of genes from fungi underlies carotenoid production in aphids. Science *328*, 624-627.

Moretti, A., Mule, G., Ritieni, A., and Logrieco, A. (2007). Further data on the production of beauvericin, enniatins and fusaproliferin and toxicity to *Artemia salina* by *Fusarium* species of *Gibberella fujikuroi* species complex. International Journal of Food Microbiology *118*, 158.163.

Müller, M., and Carell, T. (2009). Structural biology of DNA photolyases and cryptochromes. Curr Opin Struct Biol *19*, 277-285.

Muñoz, G.A., and Agosín, E. (1993). Glutamine involvement in nitrogen control of gibberellic acid production in *Gibberella fujikuroi*. Applied and Environmental Microbiology *59*, 4317-4322.

Nanou, K., and Roukas, T. (2011). Stimulation of the biosynthesis of carotenes by oxidative stress in *Blakeslea trispora* induced by elevated dissolved oxygen levels in the culture medium. Bioresour Technol *102*, 8159-8164.

Navarro-Sampedro, L., Yanofsky, C., and Corrochano, L.M. (2008). A genetic selection for *Neurospora crassa* mutants altered in their light regulation of transcription. Genetics *178*, 171-183.

Nicolas-Molina, F.E., Navarro, E., and Ruiz-Vazquez, R.M. (2008). Lycopene over-accumulation by disruption of the negative regulator gene crgA in Mucor circinelloides. Appl Microbiol Biotechnol *78*, 131-137.

Niehaus, E.M., Kleigrewe, K., Wiemann, P., Studt, L., Sieber, C.M., Connolly, L.R., Freitag, M., Güldener, U., Tudzynski, B., and Humpf, H.U. (2013). Genetic manipulation of the *Fusarium fujikuroi* fusarin gene cluster yields insight into the complex regulation and fusarin biosynthetic pathway. Chem Biol *20*, 1055-1066.

O'Donnell, K., Cigelnik, E., and Nirenberg, H.I. (1998). Molecular systematics and phylography of the *Gibberella fujikuroi* complex. Mycologia *90*, 465-493.

Oberpichler, I., Pierik, A.J., Wesslowski, J., Pokorny, R., Rosen, R., Vugman, M., Zhang, F., Neubauer, O., Ron, E.Z., Batschauer, A*., et al.* (2011). A photolyase-like protein from *Agrobacterium tumefaciens* with an iron-sulfur cluster. PLoS One *6*, e26775.

Ojima, K., Breitenbach, J., Visser, H., Setoguchi, Y., Tabata, K., Hoshino, T., Berg, J., and Sandmann, G. (2006). Cloning of the astaxanthin synthase gene from *Xanthophyllomyces dendrorhous* (*Phaffia rhodozyma*) and its assignment as a β-carotene 3-hydroxylase/4-ketolase. Mol Gen Genet *275*, 148-158.

Olmedo, M., Ruger-Herreros, C., Luque, E.M., and Corrochano, L.M. (2010). A complex photoreceptor system mediates the regulation by light of the conidiation genes con-10 and con-6 in *Neurospora crassa*. Fungal Genet Biol *47*, 352-363.

Olson, J.A., and Krinsky, N.I. (1995). Introduction: the colorful, fascinating world of the carotenoids: important physiologic modulators. The FASEB Journal *9*, 1547-1550.

Osbourn, A. (2010). Secondary metabolic gene clusters: evolutionary toolkits for chemical innovation. Trends Genet *26*, 449-457.

Ou, S.H. (10987). Rice diseases (CAB International).

Ozgür, S., and Sancar, A. (2003). Purification and properties of human blue-light photoreceptor cryptochrome 2. Biochemistry *42*, 2926-2932.

Oztürk, N., Kao, Y.T., Selby, C.P., Kavakli, I.H., Partch, C.L., Zhong, D., and Sancar, A. (2008). Purification and characterization of a type III photolyase from *Caulobacter crescentus*. Biochemistry *47*, 10255-10261.

Oztürk, N., Selby, C.P., Annayev, Y., Zhong, D., and Sancar, A. (2011). Reaction mechanism of *Drosophila* cryptochrome. Proc Natl Acad Sci U S A *108*, 516-521.

Palmer, J.M., and Keller, N.P. (2010). Secondary metabolism in fungi: does chromosomal location matter? Current Opinion in Microbiology *13*, 431-436.

Park, H.W., Kim, S.T., Sancar, A., and Deisenhofer, J. (1995). Crystal structure of DNA photolyase from *Escherichia coli*. Science *268*, 1866-1872.

Partch, C.L., Clarkson, M.W., Ozgur, S., Lee, A.L., and Sancar, A. (2005). Role of structural plasticity in signal transduction by the cryptochrome blue-light photoreceptor. Biochemistry *44*, 3795-3805.

Pokorny, R., Klar, T., Hennecke, U., Carell, T., Batschauer, A., and Essen, L.O. (2008). Recognition and repair of UV lesions in loop structures of duplex DNA by DASH-type cryptochrome. Proc Natl Acad Sci U S A *105*, 21023-21027.

Polaino, S., Herrador, M.M., Cerdá-Olmedo, E., and Barrero, A.F. (2010). Splitting of β-carotene in the sexual interaction of *Phycomyces*. Organic & Biomolecular Chemistry *8*, 4229-4231.

Porter, J.W., and Lincoln, R.E. (1950). Lycopersicon selections containing a high content of carotenes and colorless polyenes; the mechanism of carotene biosynthesis. Arch Biochem *27*, 390-403.

Prado-Cabrero, A., Estrada, A.F., Al-Babili, S., and Avalos, J. (2007b). Identification and biochemical characterization of a novel carotenoid oxygenase: elucidation of the cleavage step in the *Fusarium* carotenoid pathway. Molecular Microbiology *64*, 448-460.

Prado-Cabrero, A., Schaub, P., Díaz-Sánchez, V., Estrada, A.F., Al-Babili, S., and Avalos, J. (2009). Deviation of the neurosporaxanthin pathway towards beta-carotene biosynthesis in *Fusarium fujikuroi* by a point mutation in the phytoene desaturase gene. FEBS J *276*, 4582-4597.

Prado-Cabrero, A., Scherzinger, D., Avalos, J., and Al-Babili, S. (2007a). Retinal Biosynthesis in Fungi: Characterization of the carotenoid oxygenase CarX from *Fusarium fujikuroi*. Eukaryotic Cell *6*, 650-657.

Prado, M.M., Prado-Cabrero, A., Fernández-Martín, R.l., and Avalos, J. (2004). A gene of the opsin family in the carotenoid gene cluster of *Fusarium fujikuroi*. Curr Genet *46*, 47-58.

Proctor, R.H., Hohn, T.M., and McCormick, S.P. (1997). Restoration of wild-type virulence to *Tri5* disruption mutants of *Gibberella zeae* via gene reversion and mutant complementation. Microbiology *143 (Pt 8)*, 2583-2591.

Puhalla, J.E., and Spieth, P.T. (1983). Heterokaryosis in *Fusarium moniliforme*. Experimental Mycology *7*, 328-335.

Puhalla, J.E., and Spieth, P.T. (1985). A comparison of heterokaryosis and vegetative incompatibility among varieties of *Gibberella fujikuroi* (*Fusarium moniliforme*). Experimental Mycology *9*, 39-47.

Punt, P.J., Oliver, R.P., Dingemanse, M.A., Pouwels, P.H., and van den Hondel, C.A. (1987). Transformation of *Aspergillus* based on the hygromycin B resistance marker from *Escherichia coli*. Gene *56*, 117-124.

Purschwitz, J., Müller, S., Kastner, C., and Fischer, R. (2006). Seeing the rainbow: light sensing in fungi. Curr Opin Microbiol *9*, 566-571.

Purschwitz, J., Müller, S., Kastner, C., Schoser, M., Haas, H., Espeso, E.A., Atoui, A., Calvo, A.M., and Fischer, R. (2008). Functional and physical interaction of blue- and red-light sensors in *Aspergillus nidulans*. Curr Biol *18*, 255-259.

Rademacher, W. (1997). Gibberellins. In Fungal Biotechnology, *I.*A. T, ed. (Chapman & Hall), pp. 193-205.

Rau, W. (1967a). Untersuchungen über die lichtabhängige Carotinoidsynthese. I. Das Wirkungsspektrum von *Fusarium aquaeductuum*. Planta *72*, 14-28.

Rau, W. (1967b). Untersuchungen über die lichtabhängige Carotinoidsynthese. II. Ersatz der Lichtinduktion durch Mercuribenzoat. Planta *74*, 263-277.

Rau, W. (1969). Untersuchungen über die lichtabhängige Carotinoidsynthese. IV. Die Rolle des Sauerstoffs bei der Lichtinduktion. Planta *84*, 30-42.

Rau, W., Feuser, B., and Rau-Hund, A. (1967c). Substitution of p-chloro- or p-hydroxymercuribenzoate for light in carotenoid synthesis by *Fusarium aquaeductuum*. Biochim Biophys Acta *136*, 589-590.

Rau, W., Lindemann, I., and Rau-Hund, A. (1968). Untersuchungen über die lichtabhängige Carotinoidsynthese. III. Die Farbstoffbildung von *Neurospora crassa* in Submerskultur Planta *80*, 309-316.

Rhinn, M., and Dolle, P. (2012). Retinoic acid signalling during development. Development *139*, 843-858.

Rockwell, N.C., and Lagarias, J.C. (2006a). The structure of phytochrome: a picture is worth a thousand spectra. Plant Cell *18*, 4-14.

Rockwell, N.C., Su, Y.S., and Lagarias, J.C. (2006b). Phytochrome structure and signaling mechanisms. Annu Rev Plant Biol *57*, 837-858.

Rodrigues, A.P., Carvalho, A.S., Santos, A.S., Alves, C.N., do Nascimento, J.L., and Silva, E.O. (2011). Kojic acid, a secondary metabolite from *Aspergillus sp*., acts as an inducer of macrophage activation. Cell Biol Int *35*, 335-343.

Rodríguez-Ortiz, R. (2012). Análisis genético y molecular del fenotipo *carS* en *Fusarium*. In Departamento de Genética (Sevilla, Universidad de Sevilla).

Rodríguez-Ortiz, R., Limón, M.C., and Avalos, J. (2009). Regulation of carotenogenesis and secondary metabolism by nitrogen in wild-type *Fusarium fujikuroi* and carotenoid-overproducing mutants. Applied and Environmental Microbiology *75*, 405-413.

Rodríguez-Ortiz, R., Limón, M.C., and Avalos, J. (2013). Functional analysis of the *carS* gene of *Fusarium fujikuroi*. Mol Genet Genomics *288*, 157-173.

Rodríguez-Ortiz, R., Mehta, B.J., Avalos, J., and Limón, M.C. (2010). Stimulation of bikaverin production by sucrose and by salt starvation in *Fusarium fujikuroi*. Appl Microbiol Biotechnol *85*, 1991-2000.

Rodríguez-Ortiz, R., Michielse, C., Rep, M., Limón, M.C., and Avalos, J. (2012). Genetic basis of carotenoid overproduction in *Fusarium oxysporum*. Fungal Genet Biol *49*, 684-696.

Rodríguez-Romero, J., Hedtke, M., Kastner, C., Müller, S., and Fischer, R. (2010). Fungi, hidden in soil or up in the air: light makes a difference. Annu Rev Microbiol *64*, 585-610.

Rohlfs, M., Albert, M., Keller, N.P., and Kempken, F. (2007). Secondary chemicals protect mould from fungivory. Biol Lett *3*, 523-525.

Rohlfs, M., and Churchill, A.C. (2011). Fungal secondary metabolites as modulators of interactions with insects and other arthropods. Fungal Genet Biol *48*, 23-34.

Rohmer, M., Knani, M., Simonin, P., Sutter, B., and Sahm, H. (1993). Isoprenoid biosynthesis in bacteria: a novel pathway for the early steps leading to isopentenyl diphosphate. Biochem J *295*, 517-524.

Rosales-Saavedra, T., Esquivel-Naranjo, E.U., Casas-Flores, S., Martínez-Hernández, P., Ibarra-Laclette, E., Cortés-Penagos, C., and Herrera-Estrella, A. (2006). Novel light-regulated genes in *Trichoderma atroviride*: a dissection by cDNA microarrays. Microbiology *152*, 3305-3317.

Ruger-Herreros, C., Rodríguez-Romero, J., Fernández-Barranco, R., Olmedo, M., Fischer, R., Corrochano, L.M., and Cánovas, D. (2011). Regulation of conidiation by light in *Aspergillus nidulans*. Genetics *188*, 809-822.

Ruiz-Hidalgo, M.J., Benito, E.P., Sandmann, G., and Eslava, A.P. (1997). The phytoene dehydrogenase gene of *Phycomyces* : regulation of its expression by blue light and vitamin A. Molecular and General Genetics *253*, 734-744.

Ruiz-Roldán, M.C., Garre, V., Guarro, J., Marine, M., and Roncero, M.I. (2008). Role of the white collar 1 photoreceptor in carotenogenesis, UV resistance, hydrophobicity, and virulence of *Fusarium oxysporum*. Eukaryot Cell *7*, 1227-1230.

Saelices, L., Youssar, L., Holdermann, I., Al-Babili, S., and Avalos, J. (2007). Identification of the gene responsible for torulene cleavage in the *Neurospora* carotenoid pathway. Mol Genet Genomics *278*, 527-537.

Salgado, L.M., Avalos, J., Bejarano, E.R., and Cerdá-Olmedo, E. (1991). Correlation between in vivo and in vitro carotenogenesis in *Phycomyces*. Phytochemistry *30*, 2587-2591.

Sambrook, R., and Russell, D.W. (2001). Molecular cloning: a laboratory manual, 3rd edn (New York, NY, Cold Spring Harbor Laboratory Press).

Sancar, A. (1994). Structure and function of DNA photolyase. Biochemistry *33*, 2-9.

Sancar, A. (2003). Structure and function of DNA photolyase and cryptochrome blue-light photoreceptors. Chem Rev *103*, 2203-2237.

Sancar, A. (2004). Photolyase and cryptochrome blue-light photoreceptors. Adv Protein Chem *69*, 73-100.

Sancar, G.B. (1990). DNA photolyases: physical properties, action mechanism, and roles in dark repair. Mutat Res *236*, 147-160.

Sandmann, G., and Misawa, N. (2002). Fungal carotenoids. In The Mycota X Industrial Applications *(Osiewacz HD ed.)* 247-262.

Sanz, C., Rodríguez-Romero, J., Idnurm, A., Christie, J.M., Heitman, J., Corrochano, L.M., and Eslava, A.P. (2009). *Phycomyces* MADB interacts with MADA to form the primary photoreceptor complex for fungal phototropism. Proc Natl Acad Sci U S A *106*, 7095-7100.

Sargent, M.L., and Briggs, W.R. (1967). The effects of light on a circadian rhythm of conidiation in *Neurospora*. Plant Physiol *42*, 1504-1510.

Schafmeier, T., and Diernfellner, A.C. (2011). Light input and processing in the circadian clock of *Neurospora*. FEBS Lett *585*, 1467-1473.

Schafmeier, T., Haase, A., Kaldi, K., Scholz, J., Fuchs, M., and Brunner, M. (2005). Transcriptional feedback of *Neurospora* circadian clock gene by phosphorylation-dependent inactivation of its transcription factor. Cell *122*, 235-246.

Schafmeier, T., Kaldi, K., Diernfellner, A., Mohr, C., and Brunner, M. (2006). Phosphorylation-dependent maturation of *Neurospora* circadian clock protein from a nuclear repressor toward a cytoplasmic activator. Genes Dev *20*, 297-306.

Schmidhauser, T.J., Lauter, F.R., Russo, V.E., and Yanofsky, C. (1990). Cloning, sequence, and photoregulation of *al-1*, a carotenoid biosynthetic gene of *Neurospora crassa*. Molecular and Cellular Biology *10*, 5064-5070.

Schmidhauser, T.J., Lauter, F.R., Schumacher, M., Zhou, W., Russo, V.E., and Yanofsky, C. (1994). Characterization of *al-2*, the phytoene synthase gene of *Neurospora crassa*. Cloning, sequence analysis, and photoregulation. Journal of Biological Chemistry *269*, 12060-12066.

Schmoll, M. (2011). Assessing the relevance of light for fungi: Implications and insights into the network of signal transmission. Adv Appl Microbiol *76*, 27-78.

Schmoll, M., Esquivel-Naranjo, E.U., and Herrera-Estrella, A. (2010a). *Trichoderma* in the light of day: physiology and development. Fungal Genet Biol *47*, 909-916.

Schmoll, M., Franchi, L., and Kubicek, C.P. (2005b). Envoy, a PAS/LOV domain protein of *Hypocrea jecorina* (Anamorph *Trichoderma reesei*), modulates cellulase gene transcription in response to light. Eukaryot Cell *4*, 1998-2007.

Schmoll, M., Schuster, A., Silva Rdo, N., and Kubicek, C.P. (2009). The G-alpha protein GNA3 of *Hypocrea jecorina* (Anamorph *Trichoderma reesei*) regulates cellulase gene expression in the presence of light. Eukaryot Cell *8*, 410-420.

Schmoll, M., Zeilinger, S., Mach, R.L., and Kubicek, C.P. (2004). Cloning of genes expressed early during cellulase induction in *Hypocrea jecorina* by a rapid subtraction hybridization approach. Fungal Genet Biol *41*, 877-887.

Schönig, B., Brown, D.W., Oeser, B., and Tudzynski, B. (2008). Cross-species hybridization with *Fusarium verticillioides* microarrays reveals new insights into *Fusarium fujikuroi* nitrogen regulation and the role of AreA and NMR. Eukaryot Cell *7*, 1831-1846.

Schönig, B., Vogel, S., and Tudzynski, B. (2009). Cpc1 mediates cross-pathway control independently of Mbf1 in *Fusarium fujikuroi*. Fungal Genet Biol *46*, 898-908.

Schroeder, W.A., and Johnson, E.A. (1995). Singlet oxygen and peroxyl radicals regulate carotenoid biosynthesis in *Phaffia rhodozyma*. Journal of Biological Chemistry *270*, 18374-18379.

Schrott, E.L. (1980). Fluence response relationship of carotenogenesis in *Neurospora crassa*. Planta *150*, 174-179.

Schrott, E.L., Hubber-Willer, A., and Rau, W. (1982). Is phytochrome involved in the light-mediated carotenogenesis in *Fusarium aquaeductuum* and *Neurospora crassa*? . Photochemistry and photobiology *35*, 213-216.

Schuster, A., Kubicek, C.P., Friedl, M.A., Druzhinina, I.S., and Schmoll, M. (2007). Impact of light on *Hypocrea jecorina* and the multiple cellular roles of ENVOY in this process. BMC Genomics *8*, 449.

Schwerdtfeger, C., and Linden, H. (2000). Localization and light-dependent phosphorylation of white collar 1 and 2, the two central components of blue light signaling in *Neurospora crassa*. Eur J Biochem *267*, 414-422.

Schwerdtfeger, C., and Linden, H. (2001). Blue light adaptation and desensitization of light signal transduction in *Neurospora crassa*. Mol Microbiol *39*, 1080-1087.

Schwerdtfeger, C., and Linden, H. (2003). VIVID is a flavoprotein and serves as a fungal blue light photoreceptor for photoadaptation. EMBO J *22*, 4846-4855.

Seibel, C., Gremel, G., do Nascimento Silva, R., Schuster, A., Kubicek, C.P., and Schmoll, M. (2009). Light-dependent roles of the G-protein alpha subunit GNA1 of *Hypocrea jecorina* (anamorph *Trichoderma reesei*). BMC Biol *7*, 58.

Seibel, C., Tisch, D., Kubicek, C.P., and Schmoll, M. (2012). ENVOY is a major determinant in regulation of sexual development in *Hypocrea jecorina* (*Trichoderma reesei*). Eukaryot Cell *11*, 885-895.

Selby, C.P., and Sancar, A. (2006). A cryptochrome/photolyase class of enzymes with single-stranded DNA-specific photolyase activity. Proc Natl Acad Sci U S A *103*, 17696-17700.

Sharma, A.K., Spudich, J.L., and Doolittle, W.F. (2006). Microbial rhodopsins: functional versatility and genetic mobility. Trends Microbiol *14*, 463-469.

Shibata, S., Morishita, E., Takeda, T., and Sakata, K. (1966). The structure of aurofusarin. Tetrahedron Lett *7*, 4855-4860.

Shrode, L.B., Lewis, Z.A., White, L.D., Bell-Pedersen, D., and Ebbole, D.J. (2001). VVD is required for light adaptation of conidiation-specific genes of *Neurospora crassa*, but not circadian conidiation. Fungal Genet Biol *32*, 169-181.

Sidhu, G.S. (1983). Genetics of *Gibberella fujikuroi*. III. Significance of heterokaryosis in naturally occurring corn isolates. Canadian Journal of Botany *61*, 3320-3325.

Silva, F., Navarro, E., Penaranda, A., Murcia-Flores, L., Torres-Martinez, S., and Garre, V. (2008). A RING-finger protein regulates carotenogenesis via proteolysis-independent ubiquitylation of a white collar-1-like activator. Mol Microbiol *70*, 1026-1036.

Silva, F., Torres-Martínez, S., and Garre, V. (2006). Distinct *white collar-1* genes control specific light responses in *Mucor circinelloides*. Mol Microbiol *61*, 1023-1037.

Smith, K.M., Sancar, G., Dekhang, R., Sullivan, C.M., Li, S., Tag, A.G., Sancar, C., Bredeweg, E.L., Priest, H.D., McCormick, R.F*., et al.* (2010). Transcription factors in light and circadian clock signaling networks revealed by genomewide mapping of direct targets for *Neurospora* white collar complex. Eukaryot Cell *9*, 1549-1556.

Sokolowsky, K., Newton, M., Lucero, C., Wertheim, B., Freedman, J., Cortazar, F., Czochor, J., Schelvis, J.P., and Gindt, Y.M. (2010). Spectroscopic and thermodynamic comparisons of *Escherichia coli* DNA photolyase and *Vibrio cholerae* cryptochrome 1. J Phys Chem B *114*, 7121-7130.

Sommer, T., Chambers, J.A., Eberle, J., Lauter, F.R., and Russo, V.E. (1989). Fast light-regulated genes of *Neurospora crassa*. Nucleic Acids Res *17*, 5713-5723.

Son, S.W., Kim, H.Y., Choi, G.J., Lim, H.K., Jang, K.S., Lee, S.O., Lee, S., Sung, N.D., and Kim, J.C. (2008). Bikaverin and fusaric acid from *Fusarium oxysporum* show antioomycete activity against *Phytophthora infestans.* J Appl Microbiol *104*, 692-698.

Song, S.H., Dick, B., Penzkofer, A., Pokorny, R., Batschauer, A., and Essen, L.O. (2006). Absorption and fluorescence spectroscopic characterization of cryptochrome 3 from *Arabidopsis thaliana*. J Photochem Photobiol B *85*, 1-16.

Spudich, J.L., Yang, C.S., Jung, K.H., and Spudich, E.N. (2000b). Retinylidene proteins: structures and functions from archaea to humans. Annu Rev Cell Dev Biol *16*, 365-392.

Staunton, J., and Weissman, K.J. (2001). Polyketide biosynthesis: a millennium review. Natural Product Reports *18*, 380-416.

Steenkamp, E.T., Wingfield, B.D., Coutinho, T.A., Keller, K.A., Wingfield, M.J., O'Marasas, W.F., and Leslie, J.F. (2000). PCR-based identification of MAT-1 and MAT-2 in the *Gibberella fujikuroi* species complex. Appl Environ Microbiol *66*, 4378-4382.

Stephen, D., Jones, C., and Schofield, J.P. (1990). A rapid method for isolating high quality plasmid DNA suitable for DNA sequencing. Nucleic Acids Res *18*, 7463-7464.

Studier, F.W., and Moffatt, B.A. (1986). Use of bacteriophage T7 RNA polymerase to direct selective high-level expression of cloned genes. J Mol Biol *189*, 113-130.

Studt, L., Wiemann, P., Kleigrewe, K., Humpf, H.U., and Tudzynski, B. (2012). Biosynthesis of fusarubins accounts for pigmentation of *Fusarium fujikuroi* perithecia. Applied and Environmental Microbiology *78*, 4468-4480.

Sutter, R.P. (1975). Mutations affecting sexual development in *Phycomyces blakesleeanus*. Proceedings of the National Academy of Sciences *72*, 127-130.

Talora, C., Franchi, L., Linden, H., Ballario, P., and Macino, G. (1999). Role of a white collar-1-white collar-2 complex in blue-light signal transduction. EMBO J *18*, 4961-4968.

Tan, Y., Merrow, M., and Roenneberg, T. (2004). Photoperiodism in *Neurospora crassa*. J Biol Rhythms *19*, 135-143.

Teichert, S., Rutherford, J.C., Wottawa, M., Heitman, J., and Tudzynski, B. (2008). Impact of ammonium permeases mepA, mepB, and mepC on nitrogen-regulated secondary metabolism in *Fusarium fujikuroi*. Eukaryot Cell *7*, 187-201.

Teichert, S., Schönig, B., Richter, S., and Tudzynski, B. (2004). Deletion of the *Gibberella fujikuroi* glutamine synthetase gene has significant impact on transcriptional control of primary and secondary metabolism. Molecular Microbiology *53*, 1661-1675.

Teichert, S., Wottawa, M., Schonig, B., and Tudzynski, B. (2006). Role of the *Fusarium fujikuroi* TOR kinase in nitrogen regulation and secondary metabolism. Eukaryot Cell *5*, 1807-1819.

Terashima, K., Yuki, K., Muraguchi, H., Akiyama, M., and Kamada, T. (2005). The *dst1* gene involved in mushroom photomorphogenesis of *Coprinus cinereus* encodes a putative photoreceptor for blue light. Genetics *171*, 101-108.

Theimer, R.R., and Rau, W. (1970). Light dependent carotenoid synthesis : V. Extinction of the photoinduction by reducing substances and substitution of hydrogen peroxide for light. Planta *92*, 129-137.

Thewes, S., Prado-Cabrero, A., Prado, M.M., Tudzynski, B., and Avalos, J. (2005). Characterization of a gene in the *car* cluster of *Fusarium fujikuroi* that codes for a protein of the carotenoid oxygenase family. Molecular Genetics and Genomics *274*, 217-228.

Tilburn, J., Sarkar, S., Widdick, D.A., Espeso, E.A., Orejas, M., Mungroo, J., Peñalva, M.A., and Arst , H.N.J. (1995). The *Aspergillus* PacC zinc finger transcription factor mediates regulation of both acid- and alkaline-expressed genes by ambient pH. EMBO J *14*, 779-790.

Tisch, D., Kubicek, C.P., and Schmoll, M. (2011). New insights into the mechanism of light modulated signaling by heterotrimeric G-proteins: ENVOY acts on gna1 and gna3 and adjusts cAMP levels in *Trichoderma reesei* (*Hypocrea jecorina*). Fungal Genet Biol *48*, 631-640.

Tisch, D., and Schmoll, M. (2010). Light regulation of metabolic pathways in fungi. Appl Microbiol Biotechnol *85*, 1259-1277.

Todo, T. (1999). Functional diversity of the DNA photolyase/blue light receptor family. Mutat Res *434*, 89-97.

Todo, T., Ryo, H., Takemori, H., Toh, H., Nomura, T., and Kondo, S. (1994). High-level expression of the photorepair gene in *Drosophila* ovary and its evolutionary implications. Mutat Res *315*, 213-228.

Todo, T., Ryo, H., Yamamoto, K., Toh, H., Inui, T., Ayaki, H., Nomura, T., and Ikenaga, M. (1996). Similarity among the *Drosophila* (6-4)photolyase, a human photolyase homolog, and the DNA photolyase-blue-light photoreceptor family. Science *272*, 109-112.

Trapp, S.C., Hohn, T.M., McCormick, S., and Jarvis, B.B. (1998). Characterization of the gene cluster for biosynthesis of macrocyclic trichothecenes in *Myrothecium roridum*. Mol Gen Genet *257*, 421-432.

Troncoso, C., Gonzalez, X., Bomke, C., Tudzynski, B., Gong, F., Hedden, P., and Rojas, M.C. (2010). Gibberellin biosynthesis and gibberellin oxidase activities in *Fusarium sacchari*, *Fusarium konzum* and *Fusarium subglutinans* strains. Phytochemistry *71*, 1322-1331.

Tudzynski, B. (1999). Biosynthesis of gibberellins in *Gibberella fujikuroi*: biomolecular aspects. Appl Microbiol Biotechnol *52*, 298-310.

Tudzynski, B. (2005). Gibberellin biosynthesis in fungi: genes, enzymes, evolution, and impact on biotechnology. Appl Microbiol Biotechnol *66*, 597-611.

Tudzynski, B., and Holter, K. (1998a). Gibberellin biosynthetic pathway in Gibberella fujikuroi: evidence for a gene cluster. Fungal Genet Biol *25*, 157-170.

Tudzynski, B., Kawaide, H., and Kamiya, Y. (1998b). Gibberellin biosynthesis in *Gibberella fujikuroi*: cloning and characterization of the copalyl diphosphate synthase gene. Curr Genet *34*, 234-240.

Tyagi, A., Penzkofer, A., Batschauer, A., and Wolf, E. (2009). Fluorescence behaviour of 5,10-Methenyltetrahydrofolate, 10-Formyltetrahydrofolate, 10-Formyldihydrofolate, and 10-Formylfolate in aqueous solution at pH 8. Chem Phys *358*, 132-136.

Urrutia, O., Hedden, P., and Rojas, M.C. (2001). Monooxygenases involved in GA12 and GA14 synthesis in *Gibberella fujikuroi*. Phytochemistry *56*, 505-511.

Valadon, L., Osman, M., and Mummery, R.S. (1979). Phytochrome mediated carotenoid synthesis in the fungus *Verticillium agaricinum*. Photochem Photobiol *29*, 605-607.

van den Berg, M.A. (2011). Impact of the *Penicillium chrysogenum* genome on industrial production of metabolites. Appl Microbiol Biotechnol *92*, 45-53.

van der Horst, G.T., Muijtjens, M., Kobayashi, K., Takano, R., Kanno, S., Takao, M., de Wit, J., Verkerk, A., Eker, A.P., van Leenen, D.*, et al.* (1999). Mammalian Cry1 and Cry2 are essential for maintenance of circadian rhythms. Nature *398*, 627-630.

Velayos, A., Blasco, J.L., Alvarez, M.I., Iturriaga, E.A., and Eslava, A.P. (2000b). Blue-light regulation of phytoene dehydrogenase (*carB*) gene expression in *Mucor circinelloides*. Planta *210*, 938-946.

Velayos, A., Eslava, A.P., and Iturriaga, E.A. (2000a). A bifunctional enzyme with lycopene cyclase and phytoene synthase activities is encoded by the *carRP* gene of *Mucor circinelloides*. European Journal of Biochemistry *267*, 5509-5519.

Veluchamy, S., and Rollins, J.A. (2008). A CRY-DASH-type photolyase/cryptochrome from *Sclerotinia sclerotiorum* mediates minor UV-A-specific effects on development. Fungal Genet Biol *45*, 1265-1276.

Verdoes, J.C., Krubasik, P., Sandmann, G., and van Ooyen, A.J.J. (1999b). Isolation and functional characterisation of a novel type of carotenoid biosynthetic gene from *Xanthophyllomyces dendrorhous*. Molecular and General Genetics *262*, 453-461.

Verdoes, J.C., Misawa, N., and van Ooyen, A.J.J. (1999a). Cloning and characterization of the astaxanthin biosynthetic gene encoding phytoene desaturase of *Xanthophyllomyces dendrorhous*. Biotechnology and Bioengineering *63*, 750-755.

Voigt, K., Schleier, S., and Brückner, B. (1995). Genetic variability in *Gibberella fujikuroi* and some related species of the genus *Fusarium* based on random amplification of polymorphic DNA (RAPD). Curr Genet *27*, 528-535.

von Lintig, J. (2010). Colors with functions: elucidating the biochemical and molecular basis of carotenoid metabolism. Annual Review of Nutrition *30*, 35-56.

Wagner, D., Schmeinck, A., Mos, M., Morozov, I.Y., Caddick, M.X., and Tudzynski, B. (2010). The bZIP transcription factor MeaB mediates nitrogen metabolite repression at specific loci. Eukaryot Cell *9*, 1588-1601.

Wang, H., Ma, L.G., Li, J.M., Zhao, H.Y., and Deng, X.W. (2001). Direct interaction of *Arabidopsis* cryptochromes with COP1 in light control development. Science *294*, 154-158.

Waschuk, S.A., Bezerra, A.G., Jr., Shi, L., and Brown, L.S. (2005). *Leptosphaeria* rhodopsin: bacteriorhodopsin-like proton pump from a eukaryote. Proc Natl Acad Sci U S A *102*, 6879-6883.

Weinkove, D., Poyatos, J.A., Greiner, H., Oltra, E., Avalos, J., Fukshansky, L., Barrero, A.F., and Cerdá-Olmedo, E. (1998). Mutants of *Phycomyces* with decreased gallic acid content. Fungal Genet Biol *25*, 196-203.

Wiebe, L.A., and Bjeldanes, L.F. (1981). Fusarin C, a mutagen from *Fusarium Moniliforme* grown on corn. J Food Sci *46*, 1424–1426.

Wiemann, P., Brown, D.W., Kleigrewe, K., Bok, J.W., Keller, N.P., Humpf, H.U., and Tudzynski, B. (2010). FfVel1 and FfLae1, components of a velvet-like complex in *Fusarium fujikuroi*, affect differentiation, secondary metabolism and virulence. Molecular Microbiology *77*, 972-994.

Wiemann, P., Sieber, C.M., von Bargen, K.W., Studt, L., Niehaus, E.M., Espino, J.J., Huss, K., Michielse, C.B., Albermann, S., Wagner, D.*, et al.* (2013). Deciphering the cryptic genome: genome-wide analyses of the rice pathogen *Fusarium fujikuroi* reveal complex regulation of secondary metabolism and novel metabolites. PLoS Pathog *9*, e1003475.

Wiemann, P., Willmann, A., Straeten, M., Kleigrewe, K., Beyer, M., Humpf, H.U., and Tudzynski, B. (2009). Biosynthesis of the red pigment bikaverin in *Fusarium fujikuroi*: genes, their function and regulation. Molecular Microbiology *72*, 931-946.

Wollenweber, H.W., and Reinking, O.A. (1935). Die fusarien, ihre eschreibung, schadwirkung und bekämpfung. Berlin, Alemania, Ed Parey, P.

Worthington, E.N., Kavakli, I.H., Berrocal-Tito, G., Bondo, B.E., and Sancar, A. (2003). Purification and characterization of three members of the photolyase/cryptochrome family blue-light photoreceptors from *Vibrio cholerae*. J Biol Chem *278*, 39143-39154.

Yamaguchi, S. (2008). Gibberellin metabolism and its regulation. Annu Rev Plant Biol *59*, 225-251.

Yang, H.Q., Wu, Y.J., Tang, R.H., Liu, D., Liu, Y., and Cashmore, A.R. (2000). The C termini of *Arabidopsis* cryptochromes mediate a constitutive light response. Cell *103*, 815-827.

Yasui, A., Eker, A.P., Yasuhira, S., Yajima, H., Kobayashi, T., Takao, M., and Oikawa, A. (1994). A new class of DNA photolyases present in various organisms including aplacental mammals. EMBO J *13*, 6143-6151.

Yin, W., and Keller, N.P. (2011). Transcriptional regulatory elements in fungal secondary metabolism. J Microbiol *49*, 329-339.

Youssar, L., Schmidhauser, T.J., and Avalos, J. (2005). The *Neurospora crassa* gene responsible for the cut and ovc phenotypes encodes a protein of the haloacid dehalogenase family. Mol Microbiol *55*, 828-838.

Zhu, H., and Green, C.B. (2001). A putative flavin electron transport pathway is differentially utilized in *Xenopus* CRY1 and CRY2. Curr Biol *11*, 1945-1949.

Zoltowski, B.D., and Crane, B.R. (2008). Light activation of the LOV protein vivid generates a rapidly exchanging dimer. Biochemistry *47*, 7012-7019.